Understanding the biosynthesis of fabclavines in entomopathogenic bacteria

Dissertation
zur Erlangung des Doktorgrades
der Naturwissenschaften

vorgelegt beim Fachbereich für Biowissenschaften (15)
der Johann Wolfgang Goethe-Universität
in Frankfurt am Main

von
Sebastian Leonhard Wenski

Frankfurt am Main 2020
(D30)

vom Fachbereich für Biowissenschaften (15) der
Johann Wolfgang Goethe-Universität als Dissertation angenommen.

Dekan:	Prof. Dr. Sven Klimpel
Gutachter:	Prof. Dr. Helge B. Bode
Zweitgutachter:	Juniorprof. Dr. Eugen Proschak
Datum der Disputation:	

Table of contents

Table of contents I

Abbreviations IV

Zusammenfassung V

Summary X

1 Introduction 1

1.1 Thiotemplate-based metabolite biosynthesis 3

1.2 Non-ribosomal peptide biosynthesis 4

1.2.1 Basic NRPS reaction mechanisms 4

1.2.2 NRPS engineering 7

1.3 Polyketide biosynthesis 9

1.3.1 Basic PKS reaction mechanisms 9

1.3.2 PKS engineering 11

1.4 Fatty acid biosynthesis 13

1.5 Polyunsaturated fatty acid biosynthesis 16

1.6 Lifecycle of *Xenorhabdus* and *Photorhabdus* 20

1.7 Fabclavines and structural related specialized metabolites 21

1.8 Aims of this work 24

2 Publications and manuscripts 27

2.1 Fabclavine biosynthesis in *X. szentirmaii*: shortened derivatives and characterization of the thioester reductase FclG and the condensation domain-like protein FclL 27

2.2 Fabclavine diversity in *Xenorhabdus* bacteria 28

2.3 Nematode-Associated Bacteria: Production of Antimicrobial Agent as a Presumptive Nominee for Curing Endodontic Infections Caused by *Enterococcus faecalis* 29

2.4 Structure and biosynthesis of deoxy-polyamine in *X. bovienii* 30

3 Additional results: Engineering the fabclavine biosynthesis 31

3.1 Elucidation of the biosynthesis: Heterologous complementation of FclD..... 32

3.2 Engineering of the PKS pathway: Heterologous complementation of FclK 34

3.3 Engineering of the NRPS pathway: Heterologous complementation of FclJ 36

3.4 Engineering of the NRPS pathway: Generation of chimeric NRPS 38

4 Discussion 41

4.1 Mode of action of fabclavines and related compounds..... 42

4.2 Natural function of fabclavines – more than a general defense mechanism?... 47

4.3 Possible applications of fabclavines 49

4.4 DH_{PKS} domain of *X. bovienii* 50

4.5 Further research opportunities 51

4.5.1 Detailed elucidation of the polyamine biosynthesis..... 52

4.5.2 Fabclavines in the genus *Photorhabdus* 53

4.5.3 NRPS-NRPS-PKS interaction analyis..... 55

5 References..... 59

6 Attachments 79

6.1 Fabclavine biosynthesis in *X. szentirmaii*: shortened derivatives and characterization of the thioester reductase FclG and the condensation domain-like protein FclL 79

6.2 Fabclavine diversity in *Xenorhabdus* bacteria 112

6.3 Nematode-Associated Bacteria: Production of Antimicrobial Agent as a Presumptive Nominee for Curing Endodontic Infections Caused by *Enterococcus faecalis* 167

6.4 Structure and biosynthesis of deoxy-polyamine in *X. bovienii* 184

6.5 Additional results 224

6.5.1 Material and methods 224

6.5.2 Supplementary informations 229

7 List of publications and manuscripts 235

8 Conference participation 236

9 Danksagung 237

10 Erklärung und Versicherung 238

11 Curriculum vitae 239

Abbreviations

A	adenylation
ACP	acyl-carrier-protein
AMP	antimicrobial peptide
AMT	aminotransferase
AT	acyl transferase
ATP	adenosine triphosphate
BCA	biological pest control agent
BGC	biosynthesis gene cluster
C	condensation
CLF	chain length factor
CoA	coenzyme A
COM	communication-mediating
DD	docking domain
DEET	N,N-diethyl-3-methylbenzamide
DH	dehydratase
DHA	docosahexaenoic acid
DPA	docosapentaenoic acid
E	epimerization
EPA	eicosapentaenoic acid
ER	enoylreductase
et al.	*et alii*
FAS	fatty acid biosynthesis
Hy	hydrolase
IJ	infective juvenile
KAS	β-ketoacylsynthase
KR	keto reductase
KS	β-ketoacylsynthase
LB	lysogeny broth
MALDI	matrix-assisted laser desorption/ionization
MAT	malonyl CoA transacylase
MS	mass spectrometry
MS^2	tandem mass spectrometry
MT	methylation
NADH	nicotinamide adenine dinucleotide
NADPH	nicotinamide adenine dinucleotide phosphate
Nit	nitrilase
NMR	nuclear magnetic resonance
NRP	non-ribosomal peptide
NRPS	non-ribosomal peptide biosynthesis
Ox	2-nitropropane dioxygenase
PCP	peptidyl-carrier-protein
PK	polyketide
PKS	polyketide biosynthesis
PPTase	4-phosphopantetheinyl transferase
PUFA	poly-unsaturated fatty acid
RT	room temperature
SM	specialized metabolites
T	thiolation
TE	thioesterase
TP	transport
TR	thioester reductase
Xlt	Xenorhabdus lipoprotein toxin
XU	exchange unit
XUC	exchange unit condensation domain

Zusammenfassung

Während der „goldenen Ära“ der Naturstoffe ab den 1940ern wurden viele Stoffklassen entdeckt, die noch heute in unterschiedlichsten Therapien Anwendung finden. Danach verflachte das kommerzielle Interesse, da die gleichen Stoffklassen immer wieder entdeckt wurden. Eine mögliche Lösung sind neue mikrobielle Quellen, beispielsweise Bakterien der Gattungen *Xenorhabdus* und *Photorhabdus*. Diese leben in Symbiose mit Nematoden, die wiederum Insekten befallen. Dem daraus resultierenden Wechsel zwischen mutualistischen und pathogenen Lebensstil begegnen die Bakterien mit der Biosynthese einer Vielzahl an Naturstoffen. Diese tragen unter Anderem dazu bei, die Immunantwort des Insekts zu unterdrücken, es anschließend zu töten und diese „Nahrungsquelle“ gegen mikrobielle Fressfeinde zu verteidigen.

Die Stoffklasse der Fabclavine wurde 2014 für die Stämme *Xenorhabdus budapestenesis* und *X. szentirmaii* beschrieben. Dabei konnte ein Derivat erfolgreich isoliert und dessen Struktur mittels Kernspinresonanzspektroskopie (Nuclear Magnetic Resonance, NMR) bestimmt werden. Mithilfe massenspektroskopischer Analysen in Verbindung mit Isotopenmarkierungsexperimenten konnten weitere Derivate aufgeklärt werden. Chemisch betrachtet bestehen Fabclavine aus einem Hexapeptid, welches über ein oder mehrere partiell reduzierte Polyketid-Einheiten mit einem ungewöhnlichen Polyamin verbunden ist. Eine nahezu identische Struktur weisen (Pre-)Zeamine auf, welche für die Stämme *Serratia plymuthica* und *Dickeya zeae* beschrieben sind. Weiterführende Analysen zeigten, dass Fabclavine gegen viele unterschiedliche Organismen (Gram-negative und Gram-positive Bakterien, Hefen und Protozoen) aber auch eukaryotische Zellkullturlinien bioaktiv sind. Darüber hinaus konnte das entsprechende Biosynthese Gencluster (BGC) identifiziert und *in silico* analysiert werden. Dieses besitzt eine Größe von etwa 50.000 Basenpaaren und kodiert für Enzyme unterschiedlicher Naturstoff-Biosynthesewege. Darunter zählen zwei nicht-ribosomale Peptidsynthetasen (non-ribosomal peptide synthetase, NRPS), eine Polyketid-Synthase (polyketide synthase, PKS) sowie Homologe der mehrfach ungesättigten Fettsäurebiosynthese (polyunsaturated fatty acid synthase, PUFA). Basierend auf Homologien von bekannten katalytischen Domänen in Kombination mit

der Bildung der Zeamine, konnte ein möglicher Biosyntheseweg der Fabclavine postuliert werden.

Eines der Ziele der vorliegenden Arbeit war die Aufklärung beziehungsweise Bestätigung der bereits vorgeschlagenen Biosynthese der Fabclavine. Um einzelne Proteinfunktionen zu analysieren, wurden die entsprechenden Gene in dem Stamm *X. szentirmaii* deletiert und der resultierende Phänotyp im Vergleich zum Wildtyp analysiert. Hierzu wurde Matrix-unterstützte Laser-Desorption/Ionisation Massenspektrometrie (Matrix Assisted Laser Desorption Ionization, MALDI) verwendet. Während der Mutationsanalyse wurden fast alle Gene des Fabclavin BGC einzeln deletiert, wodurch die bereits postulierte Biosynthese bestätigt und ergänzt werden konnte. Diese startet mit der Bildung eines Tetrapeptids, katalysiert durch die erste NRPS FclI, welches durch die zweite NRPS FclJ mit zwei weiteren Aminosäuren zu einem Hexapeptid erweitert wird. Die Analyse der Δ*fclI* Mutante zeigte darüber hinaus die Bildung weiterer Fabclavin-assoziierter aber noch unbekannter Produkte. Massenspektrometrische Fragmentierungsexperimente bestätigten, dass es sich ebenfalls um Fabclavin Derivate handelte. Diese verkürzten Derivate besaßen statt eines Hexa- nur ein Dipeptid und konnten ebenfalls im Wildtyp nachgewiesen werden. Dementsprechend kann die zweite NRPS FclJ als alternativer Start der Biosynthese agieren. Die gebildeten Peptide werden anschließend von FclJ auf die iterative Typ I PKS FclK transferiert. Diese katalysiert die Elongation mit ein oder mehreren partiell reduzierten Polyketid-Einheiten. Das NRPS-PKS-basierte Intermediat bleibt im Anschluss Enzym-gebunden an der phosphopantetheinylierten Acyl-Carrier-Protein (ACP) Domäne. Parallel und unabhängig dazu erfolgt die Biosynthese des ungewöhnlichen Polyamins. In einem Zusammenspiel der PUFA-Homologe FclC, FclD und FclE zusammen mit FclF, FclG und FclH werden einfache Acyl-Coenzym A (CoA) Bausteine wie Acetyl- und Malonyl-CoA analog zur PKS- oder Fettsäurebiosynthese mittels decarboxylierender Claisen-Thioester-Kondensation miteinander verknüpft. Die β-Keto-Gruppen des entstehenden Polyketids werden dabei entweder vollständig reduziert oder transaminiert, was zu einem regelmäßigen Aufbau aus Amin-Einheiten führt. Die β-Keto-Gruppe der letzten Elongationseinheit wird zu einer Hydroxy-Gruppe reduziert. Während des Kettenaufbaus und der β-Gruppen-Prozessierung bleiben die Intermediate an der ACP Domäne gebunden. Die letztliche Freisetzung als Aldehyd wird

durch die Thioester Reduktase FclG katalysiert. Diese Reaktion wurde *in vitro* bestätigt. Acyl-CoA Derivate, welche das natürliche Phosphopantethein-gebundene Polyamin Intermediat imitieren sollten, wurden mit heterolog produziertem und gereinigtem FclG und NADPH inkubiert. Die Katalyse führt zur Oxidation von NADPH, welche spektrometrisch nachgewiesen werden konnte. Auch die Bildung des erwarteten Aldehyds konnte mittels Gaschromatographie-gekoppelter Massenspektrometrie (Gas Chromatography, GC) bestätigt werden. Dabei wurde für FclG eine Promiskuität inklusive einer erhöhten Selektivität von Acyl-CoA Derivaten ab einer Kettenlänge von 10 Kohlenstoffen beobachtet. In der Fabclavin Biosynthese wird der Polyamin-Aldehyd nach der Freisetzung erneut transaminiert. Die zentrale Schnittstelle zwischen der Biosynthese des NRPS-PKS-Hybrids und des Polyamins ist das Kondensations Domänen-ähnliche Protein FclL. Dieses katalysiert die Verknüpfung des Polyamins mit dem Enzym-gebundenen Peptid-Polyketid-Intermediat, was schließlich zur Freisetzung des finalen Fabclavins führt. Diese Reaktion wurde näher *in vivo* analysiert, um zu ermitteln, ob FclL aus *X. szentirmaii* auch nicht-native Polyamine als Substrat akzeptiert. Hierbei ist zu beachten, dass *X. budapestensis* im Vergleich zu *X. szentirmaii* ein um eine Amin-Einheit verlängertes Polyamin produziert. Eine Polyamin-defiziente *X. szentirmaii* Mutante wurde mit dem Überstand eines *X. budapestensis* Polyamin-Überproduzenten inkubiert. Anschließende Analysen bestätigten, dass das längere Polyamin erfolgreich in die Fabclavin Biosynthese von *X. szentirmaii* integriert werden konnte. Die beobachtete, verminderte Substratspezifität von FclL kann für weitere Manipulationen der Fabclavin Biosynthese genutzt werden. Detaillierte Ergebnisse sind in der ersten Publikation „*Fabclavine biosynthesis in X. szentirmaii: shortened derivatives and characterization of the thioester reductase FclG and the condensation domain-like protein FclL*", *J Ind Microbiol Biotechnol* (Erst-Autor) beschrieben.

Fabclavin BGCs kommen in einer Vielzahl von *Xenorhabdus* aber auch *Photorhabdus* Stämmen vor. In der Gattung *Xenorhabdus* sind sowohl die Struktur des Clusters als auch die Homologie der einzelnen Proteine äußerst konserviert. Die Fabclavin BGCs der Gattung *Photorhabdus* beinhalten ausschließlich die drei PUFA-homologen Gene *fclC*, *fclD* und *fclE*. Darüber hinaus zeigen Fabclavin und Zeamin BGCs große Ähnlichkeit bezüglich des Aufbaus und der Homologie. Großer Unterschied hier ist jedoch eine zusätzliche Acyl-Peptid-Hydrolase, welche für die Prozessierung von

Prezeamin zu Zeamin verantwortlich ist. Nach der Aufklärung der Biosynthese in *X. szentirmaii* rückten die weiteren *Xenorhabdus* und *Photorhabdus* Stämme mit Fabclavin BGCs in den Vordergrund. Um die zugehörigen Fabclavine näher zu charakterisieren, wurden Promotoraustausch-Mutanten mit einer chemisch induzierbaren Promotorkassette vor dem ersten essentiellen Biosynthese-Gen erzeugt. Die Induktion des künstlichen Promotors führt zu einer Überproduktion während die nicht-Induktion nachfolgende Gene inaktiviert, was die Identifizierung entsprechender Produkte erleichtert. Die Analyse der erzeugten Mutanten zeigte, dass die verschiedenen Stämme eine Vielzahl an Derivaten produzieren. Insgesamt konnten 22 bisher unbekannte Derivate beschrieben werden, was zu einer Gesamtzahl von 32 führt. Dabei zeichnete sich ab, dass der grundsätzliche Aufbau der Fabclavine identisch bleibt und nur einzelne Bausteine variabel sind. Diese Variablen sind die zweite und sechste Aminosäure, die Anzahl der eingebauten Polyketid-Einheiten sowie die Anzahl der eingebauten Amin-Einheiten des Polyamins. In Verbindung mit der aufgeklärten Biosynthese konnten die entsprechenden Proteine oder katalytische Domänen für die Diversifizierung bestimmt werden. Insgesamt betrachtet zeigte sich, dass die einzelnen Stämme individuelle Gruppen von Derivaten produzieren, welche nur leicht überlappen. Ausnahmen bilden taxonomisch eng verwandte Stämme, welche größtenteils identische Derivate produzieren. Analysen der Überstände der erzeugten Promotoraustausch-Mutanten zeigten, dass in den jeweiligen Stämmen die Fabclavine die hauptverantwortlichen Komponenten der Bioaktivität waren. Aufgrund der Komplexität der Proben konnte jedoch nicht unterschieden werden, ob die einzelnen Derivate eine vergleichbare oder unterschiedliche Bioaktivität besaßen und inwiefern synergistische Effekte eine Rolle spielten. Detaillierte Ergebnisse sind in der zweiten Publikation „*Fabclavine diversity in Xenorhabdus bacteria*“, *Beilstein J Org Chem* (Erst-Autor) beschrieben.

Aufgrund der bereits beschriebenen Bioaktivität der Fabclavine wurden mögliche Anwendungsgebiete dieser Stoffklasse analysiert. In Zusammenarbeit mit unserem Kooperationspartner Prof. Selcuk Hazir konnte nach einem Vergleich mehrerer Stämme eine potente Bioaktivität von *X. cabanillasii* gegen das humanpathogene Bakterium *Enterococcus faecalis* festgestellt werden. Dieses wird oftmals mit Entzündungen von Zahnwurzelkanälen in Verbindung gebracht. Mit Hilfe ausführlicher Analysen konnte

gezeigt werden, dass die beschriebene Bioaktivität auf die Fabclavine zurückzuführen ist. Darüber hinaus zeigten Anwendungs-orientierte Experimente ebenfalls eine höhere Effizienz der Fabclavine im Gegensatz zu Referenzen wie Calciumhydroxid. Detaillierte Ergebnisse sind in der dritten Publikation „*Nematode-Associated Bacteria: Production of Antimicrobial Agent as a Presumptive Nominee for Curing Endodontic Infections Caused by Enterococcus faecalis*", *Front Microbiol* (Co-Autor) beschrieben.

Im Vergleich mit anderen Stämmen besitzt *X. bovienii* eine Sonderstellung in der Gattung *Xenorhabdus*, da dessen NRPS- und PKS-verantwortliche Gene im Fabclavin BGC entweder fehlen oder stark verkürzt sind. Wie aufgrund des BGC Aufbaus zu erwarten war, produzierte dieser Stamm statt Fabclavinen lediglich ein Polyamin mit vier Amin-Einheiten, welches bereits aus weiteren Stämmen bekannt war. Darüber hinaus konnte ein zweites Produkt beobachtet werden, das sich um 16 Dalton unterschied. Analysen von Isotopenmarkierungsexperimenten bestätigten, dass es sich hierbei um das Desoxy-Derivat des bereits identifizierten Polyamins handelte. In der Regel befindet sich im Fabclavin BGC von *Xenorhabdus* Stämmen eine FabA-verwandte Dehydratase (DH)-Domäne in FclD. Detailierte Analysen zeigten jedoch, dass *X. bovienii* eine zusätzliche, PKS-verwandte DH-Domäne in FclC besitzt. Heterologe Expression der Gene, die für die Polyamin-Bildung verantwortlich sind sowie die Deletion der PKS-verwandten DH-Domäne wurden durchgeführt, um dessen Einfluß auf die Biosynthese zu ermitteln. Analysen mittels Flüssigchromatographie gekoppelt mit Massenspektrometrie (Liquid Chromatography, LC) offenbarten, dass diese zusätzliche Domäne für die Bildung des Desoxy-Derivats verantwortlich ist. Darüber hinaus konnte die PKS-verwandte DH-Domäne auch erfolgreich in die Polyamin Biosynthese weiterer Stämme, welche im natürlichen Zustand keine Desoxy-Derivate produzieren, eingeführt werden. Unabhängig davon, ob die DH-Domäne *in cis* oder *in trans* integriert wurde, konnten Desoxy-Derivate der natürlich vorkommenden Polyamine produziert werden. Diese zusätzliche DH-Domäne stellt damit eine weitere Diversifizierungsmöglichkeit neben den bereits bekannten Elementen der Fabclavin Biosynthese dar. Des Weiteren konnte nicht nur für Fabclavine sondern auch für Intermediate der Biosynthese wie dem Polyamin-Teil eine Bioaktivität nachgewiesen werden. Detaillierte Ergebnisse sind im beigefügten Manuskript „*Structure and biosynthesis of deoxy-polyamine in X. bovienii*" (Erst-Autor) beschrieben.

Summary

The compound class of the fabclavines was described as secondary or specialized metabolites (SM) for *Xenorhabdus budapestensis* and *X. szentirmaii*. Their corresponding structure was elucidated by NMR and further derivatives could be identified in both strains. Biochemically, fabclavines are hybrid SMs derived from two non-ribosomal-peptide-synthetases (NRPS), one type I polyketide-synthase (PKS) and polyunsaturated fatty acid (PUFA) synthases. In detail, a hexapeptide is connected via partially reduced polyketide units to an unsual polyamine. Structurally, they are related to the (pre-)zeamines, described for *Serratia plymuthica* and *Dickeya zeae*. Fabclavines exhibit a broad-spectrum bioactivity against a variety of different organisms like Gram-positive and Gram-negative bacteria, fungi, protozoa but also against eukaryotic cell-lines.

In this work, the fabclavine biosynthesis was elucidated and assigned to two independently working assembly lines. The NRPS-PKS-pathway is initiated by the first NRPS FclI via generation of a tetrapeptide, which is elongated by the second NRPS FclJ, leading to a hexapeptide. Alternatively, FclJ can also act as direct start of the biosynthesis, resulting in the final formation of shortened fabclavine derivatives with a di- instead of a hexapeptide. In both cases, the peptide moiety is transferred to the iterative type I PKS FclK, leading to an elongation with partially reduced polyketide units. The resulting NRPS-PKS-intermediate is still enzyme-bound. The PUFA-homologues FclC, FclD and FclE in combination with FclF, FclG and FclH belong to the polyamine-forming pathway. Briefly, repeating decarboxylative Claisen thioester condensation reactions of acyl-coenzym A building blocks lead to the generation of an acyl chain in a PKS- or fatty acid biosynthesis-like manner. The corresponding β-keto-groups are either completely reduced or transaminated in a specific and repetitive way, resulting in the concatenation of so-called amine-units. The final β-keto-group is reduced to a hydroxy-group and the intermediate is reductively released by the thioester reductase FclG. A subsequent transamination step leads to the final polyamine. The NRPS-PKS- as well as the polyamine-pathway are connected by FclL. This condensation domain-like protein catalyzes the condensation of the polyamine with the NRPS-PKS-part, which results in

the release of the final fabclavine. The results are described in detail in the first publication (first author).

Fabclavine biosynthesis gene cluster (BGC) are widely spread among the genus *Xenorhabdus* and *Photorhabdus*. In *Xenorhabdus* strains a high degree of conservation regarding the BGC synteny as well as the identity of single proteins can be observed. However, *Photorhabdus* strains harbor only the PUFA-homologues. While in *Photorhabdus* no product could be detected, our analysis revealed that the *Xenorhabdus* strains produce a large chemical diversity of different derivatives. Briefly, the general backbone of the fabclavines is conserved and only four chemical moieties are variable: The second and last amino acids of the NRPS-part, the number of incorporated polyketide units as well as the number of amine units in the polyamine. In combination with the elucidated biosynthesis, these variables could be assigned to single biosynthesis components as diversity mechanisms. Together with the 10 already described derivatives, a total of 32 derivatives could be detected. Interestingly, except for taxonomic closely related strains, all analyzed strains produce their own set of derivatives. Finally, we could confirm that the fabclavines are the major bioactive compound class in the analyzed strains under laboratory conditions. The results are described in detail in the second publication (first author).

Together with our collaboration partner Prof. Selcuk Hazir a potent bioactivity against *Enterococcus faecalis*, which is associated with endodontic infections, could be contributed to *X. cabanillasii*. Here, we could confirm that this bioactivity can be assigned to the fabclavines. The results are described in detail in the third publication (co-author).

Among the genus *Xenorhabdus*, *X. bovienii* represents an exception as its NRPS and PKS genes of the fabclavine BGC are missing or truncated, resulting in the exclusive production of polyamines. Furthermore, its PUFA-homologue FclC harbors an additional dehydratase (DH) domain. Upon extensive analysis a yet unknown deoxy-polyamine was identified and assigned to this additional domain. Finally, the DH domain was transferred into other polyamine pathways. Regardless of an *in cis* or *in trans* integration, the chimeric pathways produced deoxy-derivatives of its naturally occurring polyamines, suggesting that this represents another diversification mechanism. The results are described in detail in the attached manuscript (first author).

.

1 Introduction

Microorganisms show great adaptability to withstand and survive many different environmental conditions [1,2]. On the one hand, they prefer certain habitats with its physical and chemical factors, most impressively demonstrated by extremophiles [3]. On the other hand, there is the fast adaption to changing abiotic but also biotic factors inside a formerly preferred habitat [1,4]. For example, a temperature decrease as abiotic stress factor is counteracted by changes in membrane fluidity, RNA metabolism or translation of cold-inducible proteins [2]. Hence, the stress response is more or less tolerated and mainly affects the primary metabolism, responsible for catabolism as well as biosynthesis of complex structures required for growth and reproduction [5]. Biotic stress factors for microorganism include competitors for nutrients and habitats [6]. Microorganisms release toxic chemicals to inhibit or even kill competitors [4,6]. These chemicals are derived from the secondary metabolism and often called secondary or specialized metabolites (SMs) or natural products [4,7,8].

The secondary metabolism involves biosynthesis pathways, which are not or only partially required for maintaining life or reproduction. However, primary and secondary metabolism can not completely be separated from one another, as they contribute to each other [9]. For instance, the primary metabolism provides building blocks like amino acids to generate SMs [10], while SMs like siderophores can directly support the primary metabolism via iron acquisition [11]. Regarding their natural function, several SMs are described as attractant or deterrent [12], as inhibiting or toxic defense factor or as signaling molecules [13]. These properties lead to advantages during competition in ecological niches.

Beside investigations of their natural function, the commercial interest on SMs mainly relies on their pharmaceutical potential or utilization as agrochemical. The probably most prominent example is penicillin, a β-lactam antibiotic (Figure 1) [14–16]. In the 1940s, the so-called “golden era” of antibiotic research started with the discovery of aminoglycosides, tetracyclines, chloramphenicols and Macrolides [14]. The success of this era can be assigned to the innovative discovery platform by Selman Waksman,

enabling large screening approaches mainly with soil microbes as sources [17]. Beside the identification of new antibiotics, SMs were also used as source for further applications like antitumor drugs (Bleomycin) [18], immunosuppressants (Rapamycin) [19] or proherbicides (Bialaphos) [20] (Figure 1).

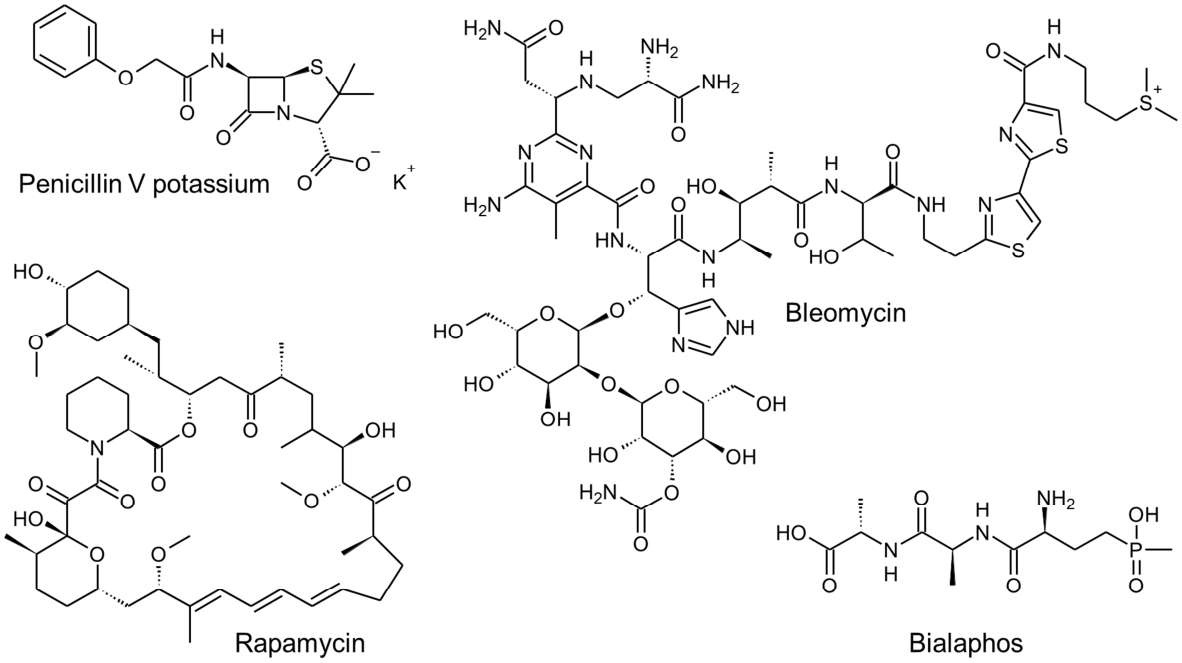

Figure 1. Specialized metabolites used in pharmaceutical or agricultural applications. Shown are the antibiotic penicillin [15,16], the antitumor drug bleomycin [18], the immunosuppressant rapamycin [19] and the proherbicide bialaphos [20].

However, this era ended due to the constant rediscovery of SM classes, resulting in decreased ouputs of screening approaches [21]. Multiple strategies are postulated like establishing new microbial sources, utilization of synthetic biology to improve combinatorial biosynthesis as well as genome-mining in large genome organisms to revitalize the “golden era” [21]. The decreasing costs for genome sequencing in combination with the development of *in silico* platforms to identify SM encoding genes could lead to a renaissance of SM identification [22,23]. These encoding regions can be classified into different biosynthesis pathways like non-ribosomal peptide synthetases (NRPS), polyketide synthases (PKS), poly-unsaturated fatty acid (PUFA) biosynthesis, terpene biosynthesis or ribosomally synthesized and post-translationally modified peptides.

1.1 Thiotemplate-based metabolite biosynthesis

SM pathways like NRPS, PKS and PUFA but also fatty acid biosynthesis (FAS) have in common that they include thiolation proteins or domains, respectively [24–26]. In accordance to their substrate, these small proteins are also called peptidyl-carrier-protein (PCP) for aminoacyl-moieties or acyl-carrier-proteins (ACP) for acyl-moieties. Except for the region adjacent to the cofactor binding site the overall sequence homology of PCP and ACP proteins is low [24]. However, the overall structure as well as the function is conserved [25].

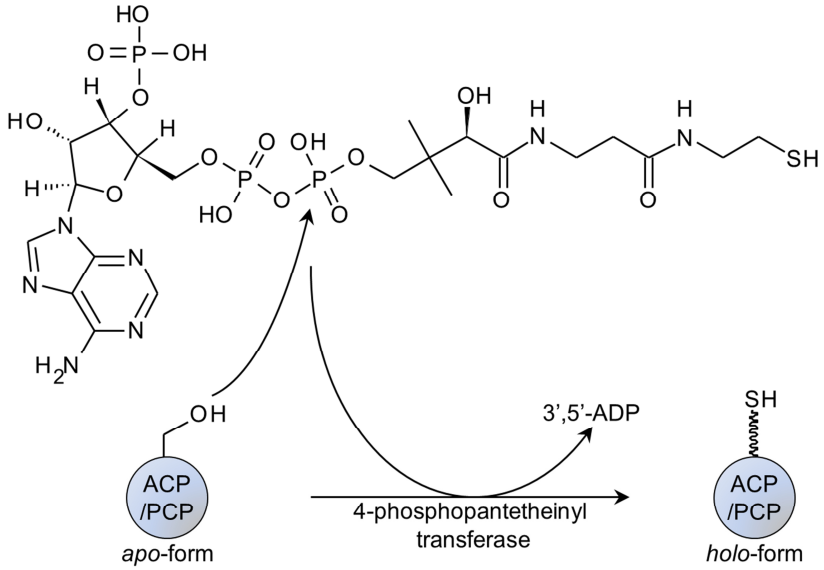

Figure 2. Conversion of the acyl-carrier-protein (ACP) or peptidyl-carrier-protein (PCP) from *apo*- to *holo*-form (Figure was adapted and modified from [24]).

PCPs as well as ACPs are translated in their *apo*-form [25]. The subsequent conversion into their functional *holo*-form requires a posttranslational modification by a 4-phosphopantetheinyl transferase (PPTase) [25]. This enzyme is responsible for the transfer of the 4-phosphopantetheine moiety from coenzyme A to the conserved serine residue of the thiolation protein (Figure 2) [25]. The attached 4-phosphopantetheine moiety ends with a thiol moiety, which can be loaded with substrates by pathway specific enzymes via thioester formation. Generally, during NRPS, PKS, FAS and PUFA-

biosynthesis substrates and intermediates stay enzyme-bound on these carrier-proteins/domains until the end of the biosynthesis, determined by product release.
In general, the PPTase superfamily can be categorized into the Sfp-like type, responsible for NRPS and PKS modification, and the AcpS-like type, responsible for FAS modification [27–29]. The responsible PPTase for PUFA biosynthesis is a Sfp-like type, but differs in some structural elements [30,31].

1.2 Non-ribosomal peptide biosynthesis

Generally, in primary metabolism peptides and proteins are generated by ribosomes in an mRNA-templated biosynthesis, called translation. In secondary metabolism peptides can also be generated by NRPS. Here, resulting peptides are derived from a multiple carrier thiotemplate-mechanism [32]. As the incorporated building blocks are not determined by an mRNA, more than the commonly 20 proteinogenic amino can be utilized, which are selected or processed by specific enzymes or domains. These include D-amino acids, glycosylated moieties, N-, C- and O-methylated residues, N-formylated residues, fatty acids and heterocyclic elements [10,33]. These highly specialized features enable the generation of compounds with remarkable physicochemical and biological properties.

1.2.1 Basic NRPS reaction mechanisms

In general, NRPS are large mega-enzymes composed of repeating modules and domains. A canonical/minimal-NRPS module is responsible for one elongation step and harbors an adenylation (A), a condensation (C) and a PCP domain, the so-called core domains [33]. These are responsible for the activation, transfer and condensation reactions, required for the elongation of one building block (Figure 3). The A domain recognizes a specific substrate and activates it as an amino acyl adenylate (Figure 3, I). Respective substrate specificites are based upon certain amino acids in the binding pocket [34]. These residues, denoted as Stachelhaus code, can be identified *in silico* to predict the specificities [34,35]. The activated amino acid is transferred onto the 4-phosphopantetheine moiety of the PCP domain as thioester, while adenosine

monophosphate is released (Figure 3, II). The 4-phosphopantetheine moiety transfers the bound amino acid between the catalytic centers, leading to the multiple carrier thiotemplate-mechanism [32]. Finally, the C domain catalyzes the condensation reaction of two PCP-tethered amino acyl building blocks via nucleophilic attack of the imino group of the downstream amino acyl moiety on the carboxy carbon of the upstream amino acyl or peptidyl moiety (Figure 3, III) [36].

Based on the module arrangement and utilization, NRPS systems can be classified into type A (linear), B (iterative) and C (nonlinear) [33]. This work focusses on type A NRPS with the module structure C-A-PCP (Figure 3) [33]. As one module elongates the intermediate with one building block and transfers it onto the adjacent module, the final product is determined by the NRPS enzyme structure with its concatenated modules and their specificity [33]. This collinearity between the NRPS domain organization and the resulting peptide-product is essential for the *in silico* predication of the product on the basis on sequence data of the corresponding biosynthesis gene cluster.

The final product can be released by diverse mechanisms depending on the final domain at the *C*-terminal end of a NRPS. The most common domains are thioesterase (TE) domains, which catalyze a hydrolyzation or cyclization, leading to carboxylic acid or lacton/ lactam as products [37,38]. Moreover, products can be released by reductase domains, performing a reduction of the thioester, leading to an aldehyde [37]. Finally, *C*-terminal C domains can catalyze a nucleophilic attack by an amine onto the thioester bond [37]. The required nucleophile can either be intramolecular like the *N*-terminal amino moiety, which leads to a macrolactam as product, or intermolecular using a small amine, leading to a C-terminal amide [37,39].

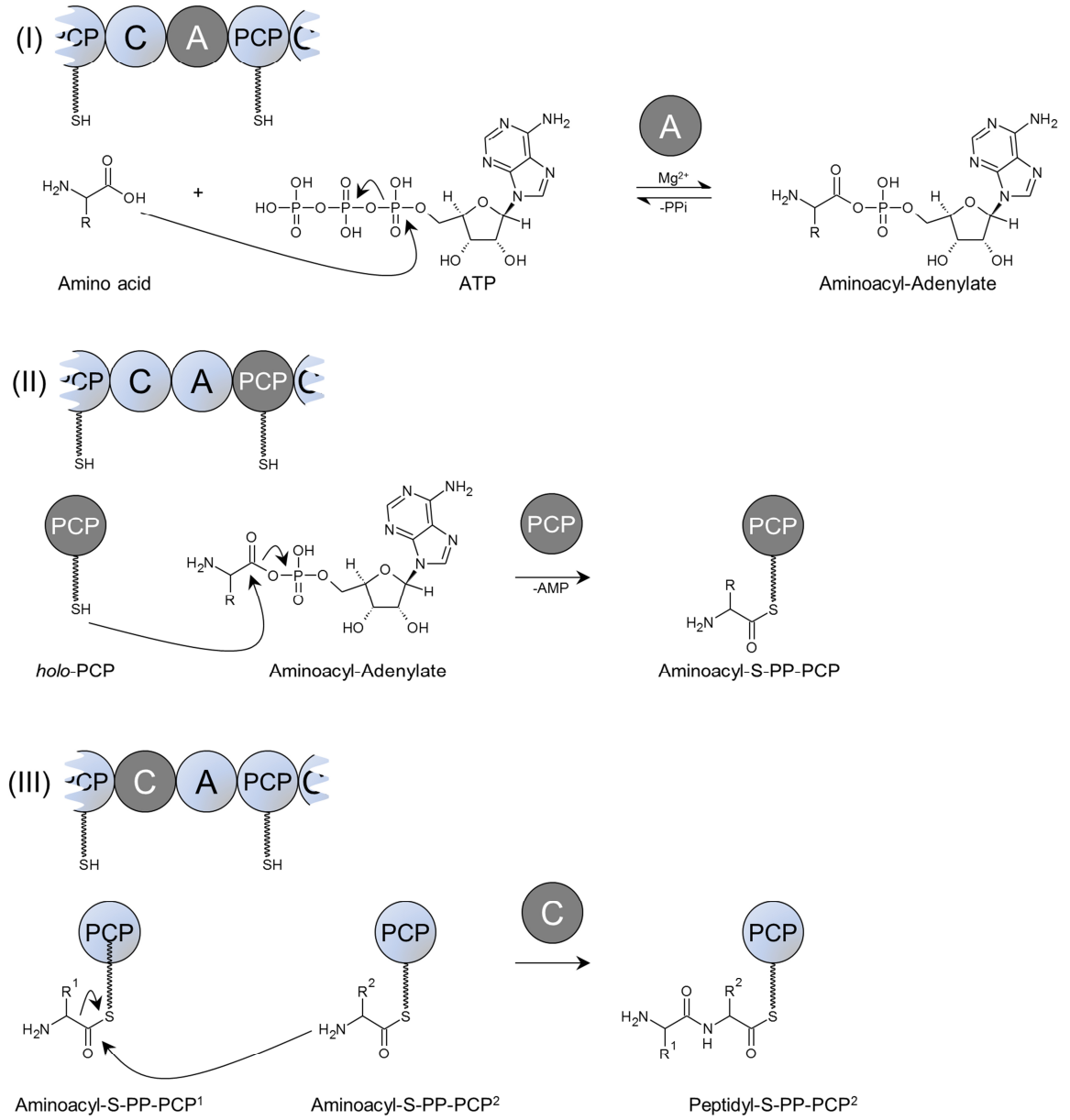

Figure 3. Mechanisms of the core domains in non-ribosomal peptide biosynthesis. (I) Activation of an amino acyl adenylate by the A domain. (II) Transfer of the amino acyl adenylate onto the PCP domain. (III) C domain catalyzed condensation. Abbreviations: A: Adenylation domain; PCP: Peptidyl-carrier-protein domain; C: Condensation domain (Figure was adapted and modified from [40]).

Certain chemical moieties can be introduced in the non-ribosomal peptides (NRPs) in two ways. The first involves the variation of the building blocks, determined by the A domains and their specificity. These include the proteinogenic and nonprotenogenic amino acids [41,42].

The second way involves the modification of incorporated building blocks. As example, a common way to introduce D-amino acids is the epimerization of an already incorporated L-amino acid, catalyzed by an epimerization (E) domain [43]. E domains can occur upstream of a C domain or as a combination of both (dual E/C domains) [43]. Furthermore, optional *N*-terminal (starter) C domains are able to acylate the first amino acid with a (β-hydroxy) carboxylic acid [43]. Instead of a starter C domain the initiation module can also harbor a *N*-terminal formylation domain, catalyzing a formylation of the first amino acid [44]. Elongating C domains can also be substituted by the structural related heterocyclization domains, performing beside the peptide bond formation also a cyclization reaction of cysteine, serine and threonine [10,43]. Methylation reactions can be performed either by N-, C- or O-methylation (MT) domains [45–47].

1.2.2 NRPS engineering

NRPS, especially type A, are promising targets for rational engineering due to their modularity and the utilized multiple carrier thiotemplate-mechanism. Both are contributing to the collinearity between the NRPS enzyme structure and the resulting peptide-product [32,48]. Despite of the conserved structure of these mega-enzymes the success rate of engineering approaches was low, except for some few systems, which did not allow general conclusions [49,50]. In the past, the main strategies to alter the product structure focused on A domains due to their initial role of building block selection [51]. Therefore, either the A domain specificity was manipulated by mutagenesis of the substrate binding pocket or the whole A domain was exchanged either alone or in combination with other domains (A, A-PCP, C-A or C-A-PCP) [51].
Two recently published methods by Bozhüyük *et al*. revitalized the hope for general and applicable NRPS engineering. In 2018, the first method classified the NRPS not into modules with the domain order C-A-PCP, but into exchange units (XU) with the order A-PCP-C (Figure 4). Thereby, a flexible loop inside the C-A didomain linker region (32 amino acids) was determined as fusion point as it does not interrupt domain interactions [49].

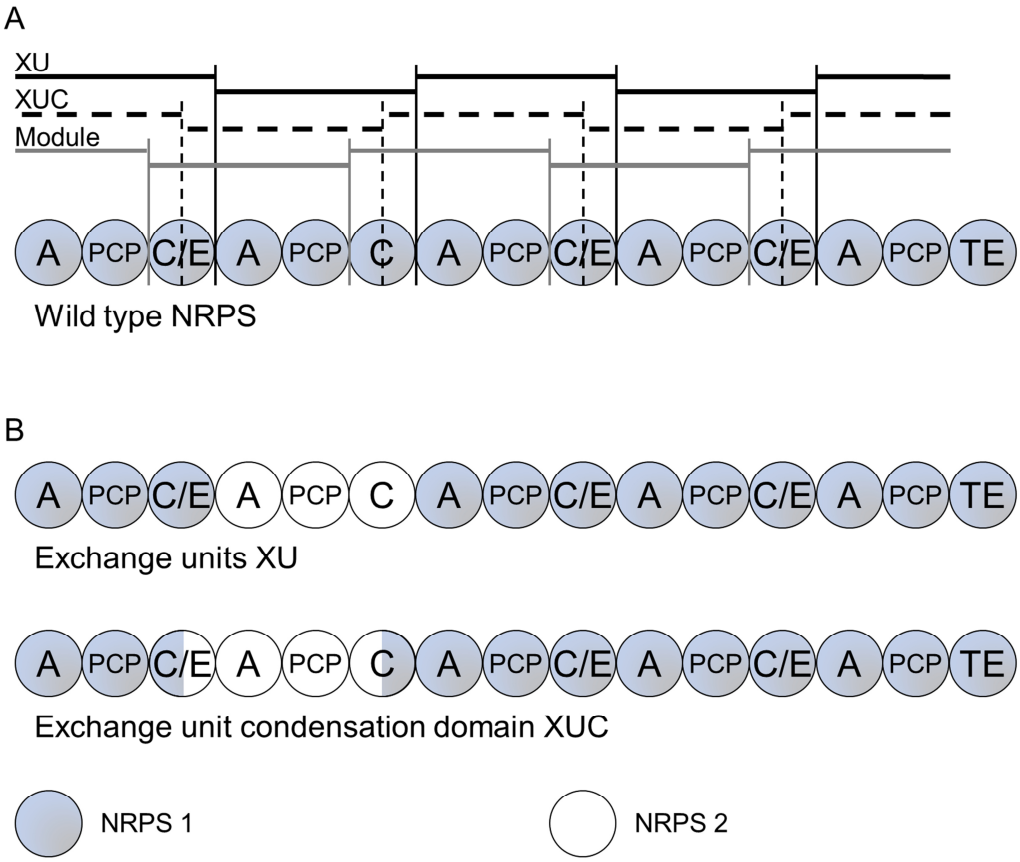

Figure 4. NRPS engineering strategies. (A) Classification of a NRPS according to exchange unit (XU) concept, exchange unit condensation domain (XUC) concept and classic modules. (B) Examples for engineered NRPS systems using the XU and the XUC concept (Figure was adapted and modified from [52]).

However, this method is restricted by the specificity of the downstream C domain [49]. Nevertheless, XUs could be swapped between NRPS of the genera *Xenorhabdus*, *Photorhabdus* and *Bacillus* and artificial peptides could be generated *de novo* [49]. In 2019, the second method re-classified the NRPS again into exchange unit condensation domains (XUC) with the domain order $^{C}/_{2}$-A-PCP-$^{C}/_{2}$ (Figure 4) [52]. Here, the C domain is divided into an acceptor and a donor site, connected by a flexible linker region, which is used as fusion point [52]. While this method avoids the specificity of the downstream C domain, C/E and C domains cannot be combined using XUC [52]. Fortunately, both XU and the XUC methods can be combined, offering a great potential for NRPS engineering [52].

1.3 Polyketide biosynthesis

Polyketides (PKs) represent another important class of SMs [53], which can be generated by large mega-enzymes [54] as well as by distinct monofunctional proteins [55]. Although the set of utilized building blocks is much lower in comparison to NRPS, they exhibit a high structural diversity. In general, acyl-coenzyme A (CoA) derivatives like acetyl- or (methyl) malonyl-CoA are incorporated, which are derived from the primary metabolism [56]. However, alternatives like ethylmalonyl-CoA [57] or ACP-bound methoxymalonyl- [57], aminomalonyl- and hydroxymalonyl-moieties [58] are also possible [53].

1.3.1 Basic PKS reaction mechanisms

Basically, a β-ketoacylsynthase (KS) domain, an acyl transferase (AT) domain and a ACP domain represent a minimal module and are the PKS core domains with analogous function like the C, A and PCP domain, described for NRPS (Figure 5) [53]. Regarding the utilized building blocks and the corresponding reaction mechanism to connect them, PKS systems are comparable to FAS [53]. The polyketide-backbone is generated in a successive manner via multiple decarboxylative Claisen thioester condensations [53]. Therefore, the AT domains select and transfer the as CoA-thioester activated acyl moieties onto the ACP domains of the upstream and downstream module (Figure 5). The starter acyl moiety is transferred onto a conserved cysteine of the KS domain. Simultaneously, the elongation acyl moiety is decarboxylated, catalyzed by the KS domain. The resulting ester-enolat performs a nucleophilic attack on the starter acyl moiety, leading to the formation of a C-C bond, including the transfer onto the downstream ACP (Figure 5) [56].

PKS systems can be subdivided into three types that differ in their enzyme structures and reaction mechanisms: Type I PKS are multimodular mega-enzymes with KS domains either performing one (non-iterative) or multiple (iterative) condensation reactions. While the non-iterative type I PKS can be further distinguished into *cis* or *trans* AT-PKS according to the nature of their AT domains [53,59], the iterative type can be

classified into non, partially or highly reducing PKS following their activity of the β-processing domains [53].

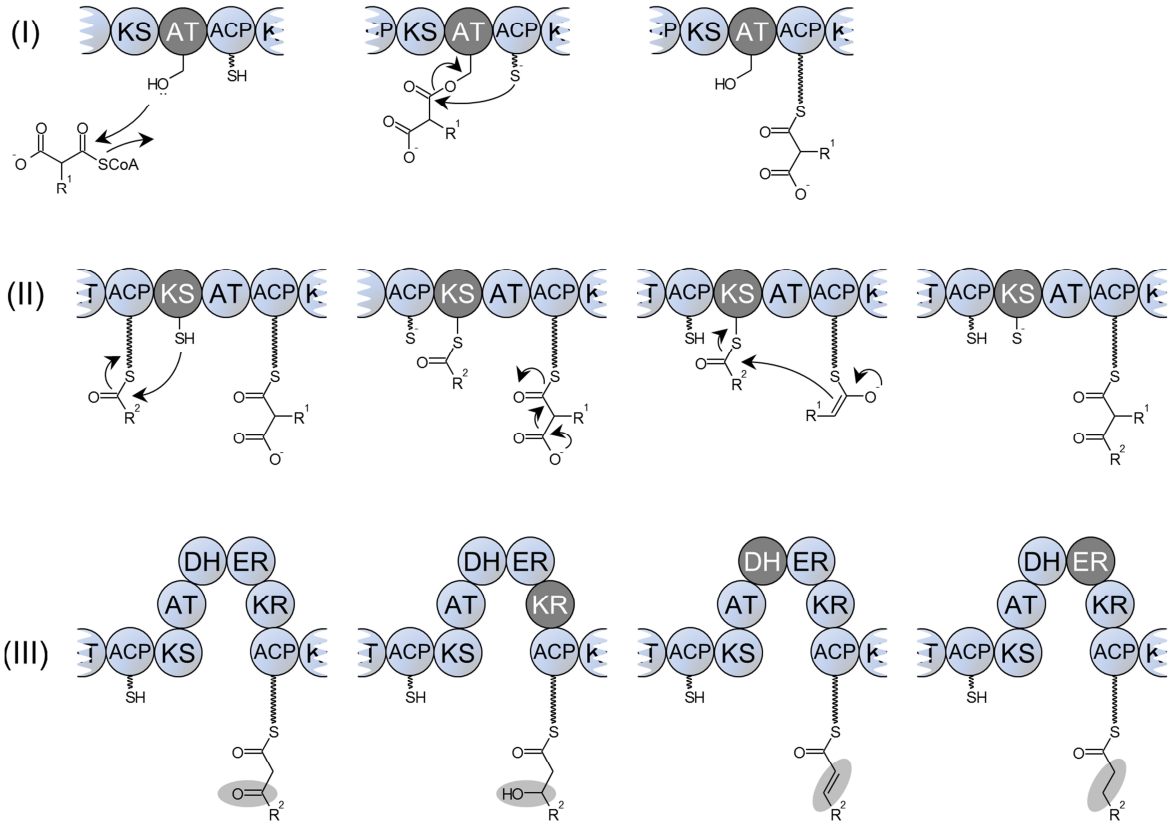

Figure 5. General PKS biosynthesis steps. (I) The AT domain selects the substrate, releases the coenzyme A to bind the acyl moiety and transfers it onto the ACP domain. (II) The upstream ACP-bound acyl moiety is transferred to the KS domain, which simultaneously catalysis the decarboxylation of the extender moiety. The nucleophilic attack by the resulting enolate led to the formation of a C-C bond bound on the downstream ACP. (III) The KR domain reduces the β-keto group to a hydroxyl-group, which is reduced by the DH domain to an α,β-enoyl group. The ER domain finally converts it to a saturated CH_2-CH_2 bond (Figure was adapted and modified from [56]).

Type II PKS systems consist of monomodular iteratively working single enzymes. Here, the minimal module is extended by an additional KS domain, acting as chain-length-factor [53]. Type III PKS are commonly found in plants (chalcone/stilbene synthases) but also in bacteria. Since these systems directly use coenzyme A-derivatives as building blocks, ACP domains are not required [60]. Furthermore, there can be hybrids of different PKS types or mixed with NRPS or FAS [53].

Subsequently, the β-keto group of the intermediate is optionally reduced by a keto reductase (KR) domain to a β-hydroxy group. Thereby, the configuration of the resulting stereo center is determined by the KR domain [61,62]. Further reductions can be performed by a dehydratase (DH) domain, leading to an α,β-enoyl group, or by a enoylreductase (ER) domain, leading to a completely saturated CH_2-CH_2 bond (Figure 5) [56]. MT domains can modify the α-position with a methyl-group in a *S*-adenosylmethionine-dependent manner and are embedded between the β-processing domains [63].

In non-iterative Type I cis-AT PKS a minimal module harbors a KS, AT and ACP domain and after each elongation the acyl-intermediate is transferred to the adjacent module. This leads to a collinearity between the PKS architecture and the corresponding product, as observed for type A NRPS systems [53]. Furthermore, the optional occurrence and activity of β-processing domains corresponds with the reduction state of the β-keto-groups [53]. Both correlations enable the prediction of the resulting PKS product. Nevertheless, inactive or missing as well as skipped or iteratively utilized domains lead to the loss of this collinearity in such systems [53,56].

In general, the full-length polyketide is finally released by a *C*-terminal TE domain, either as linear or circular product [53]. Thereby, the polyketide intermediate is transferred onto the active site serine, attacked by an external nucleophile like water for hydrolysis or by an internal carbonyl for macrocyclization [64]. Finally, the synthesized polyketide can be modified by additional tailoring enzymes, as example, P-450 monooxygenases introduce additional hydroxyl moieties [56,65] and glycosyltransferase attach sugars, as it can be observed for the erythromycin biosynthesis [66].

1.3.2 PKS engineering

Type I PKS are preferred systems for engineering due to their collinearity. Here, the generation of “unnatural” PKs mainly focused on the variation of starting or elongating building blocks, reduction patterns and stereochemistry [67]. Successful engineering strategies include the exchange of whole modules [68] or individual domains to generate chimeric PKS systems [67].

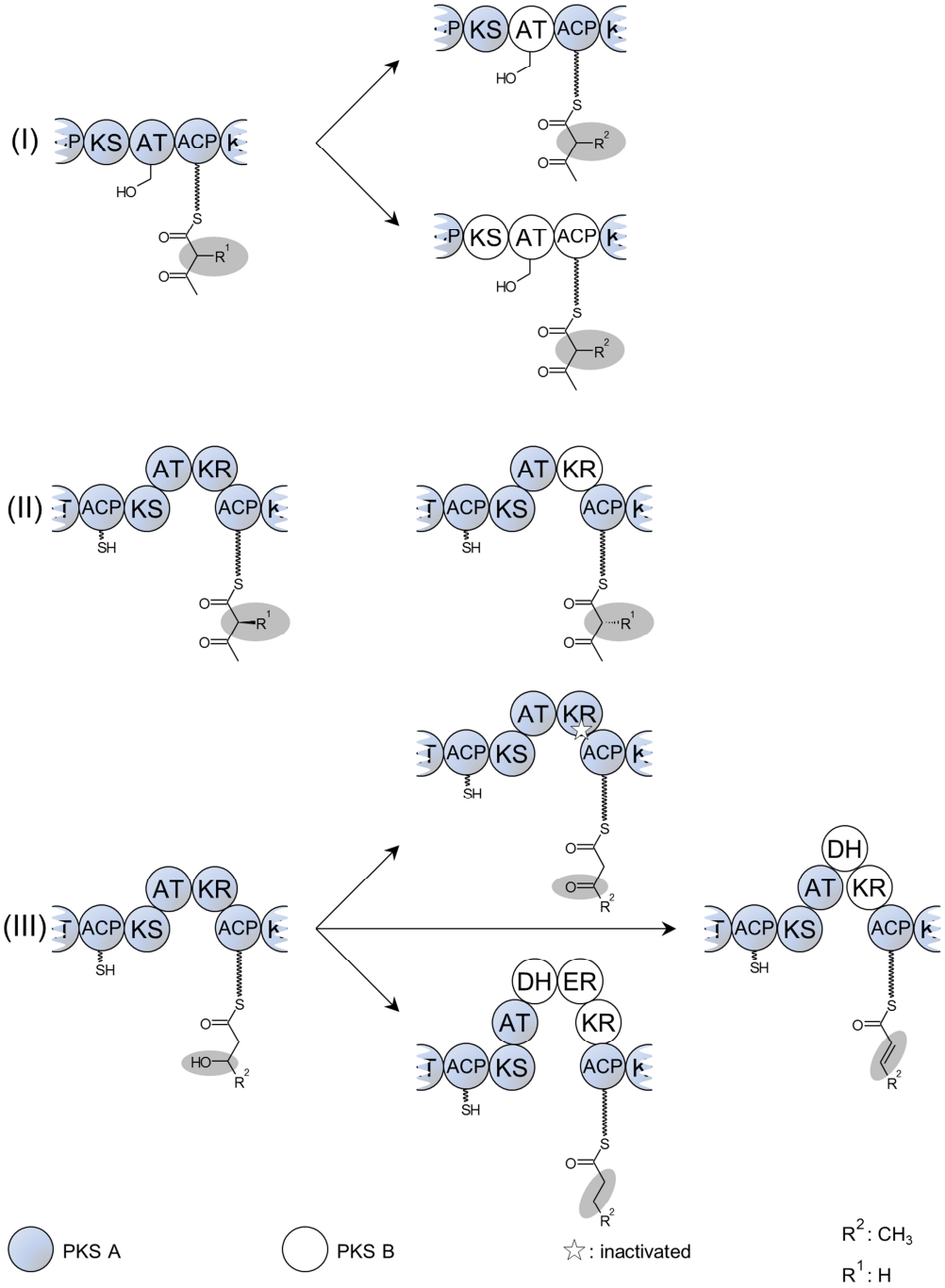

Figure 6. PKS engineering strategies. (I) Altering the building blocks at specific position by exchanging the AT domain or whole modules. (II) Altering the stereochemistry by exchanging the KR domain. (III) Altering the reduction state by inactivation of β-processing domains or exchange of reductive loops (Figure was adapted and modified from [69]).

Promising targets to alter chemical moieties at a specific position are AT domains in starter (together with the downstream ACP domain) [70] or extender modules [71]

(Figure 6, I). Furthermore, the KR domain can be substituted to change the stereochemistry, inactivated or exchanged with a di- (KR-DH) or tridomain (KR-DH-ER) to alter the reduction state (Figure 6, II-III) [67,69,71,72]. Limited proteolysis experiments and structural data indicate that these β-processing domains or so-called “reductive loops” appear as integral units, which facilitate engineering approaches due to decreased interaction with other domains [72–75].

1.4 Fatty acid biosynthesis

In contrast to NRPS and PKS, FAS is assigned to the primary metabolism, as the products are further incorporated into membranes in form of lipids [76,77]. Similar to PKS the decarboxylative Claisen thioester condensation reactions as well as a similar setup of enzymes/domains, including KS, ACP, KR, DH and ER domains are applied [55,78]. In contrast, FAS building blocks are more restricted to acetyl- and malonyl-CoA and each elongation cycle is followed by complete reduction of the β-keto group. Furthermore, the FAS machinery can be extended by the heterotetramer AccABCD, responsible for the conversion of acetyl- to malonyl-CoA and thus providing the required building blocks for chain elongation [79].

FASs can also be classified into different types, like PKSs in accordance to their architecture. Type I FASs harbor all required domains, being translated as one polypeptide chain, and occur generally in eukaryotes and rarely in prokaryotes [25,80]. These large mega-enzymes associate to generate a reaction chamber and the single domains are used iteratively [78,81]. FAS type I can be further subdivided into mammalian, fungal or bacterial FAS, differing in their domain organization, number of associated units, inserted scaffolding elements and the occurrence of an intramolecular PPTase [78]. Furthermore, the ACP-loading in FAS type I is catalyzed by a malonyl-acetyl-transferase (mammalian), by a malonyl-palmitoyl-transferase (fungal) or by a malonyl-acyl-transferase (bacterial). While the two latter are also able to unload the ACP, in mammals an additional TE domain is required [78].

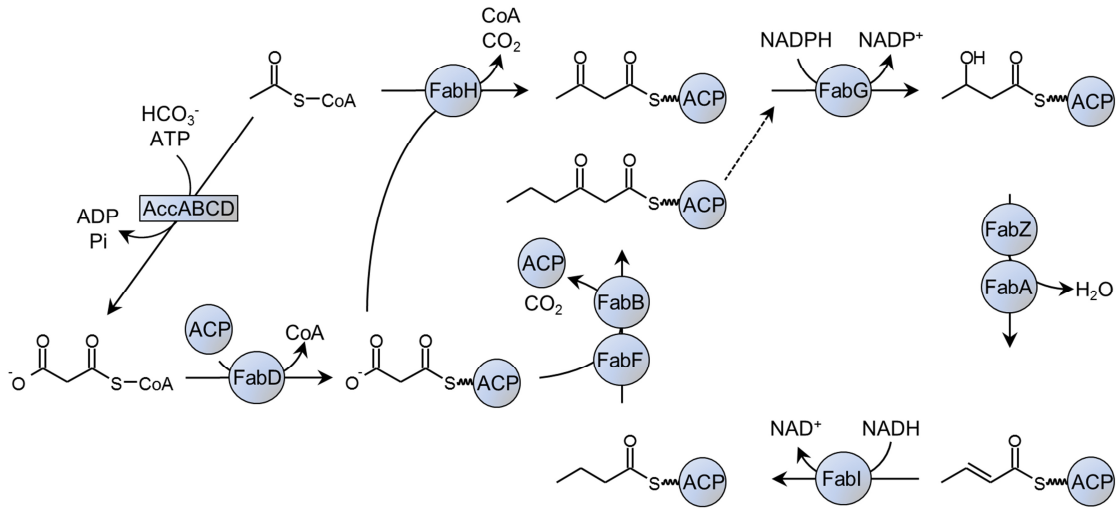

Figure 7. Fatty acid biosynthesis in *Escherichia coli* (model system for FAS II). Catalytic activities: AccABCD: acetyl-CoA carboxylase; FabD: malonyl-CoA:ACP transacylase; FabG: ketoreductase; FabA/FabZ: dehydratase; FabI: enoylreductase; FabB, FabF, FabH: β-ketoacyl synthase (KAS I, II, III). (Figure was adapted and modified from [82])

Type II FAS can be found in prokaryotes and their characterization was mainly performed in the model organism *Escherichia coli* (Figure 7) [25,83]. Identical to type II PKS all required catalytic steps are performed by iteratively working, monofunctional enzymes [83]. Strikingly, FASs type II differ from type I by using two or more enzymes for an identical catalytic step. For instance, FabH, one of three KS enzymes, is responsible for the first condensation reaction of ACP-bound malonyl moiety with acetyl-CoA, leading to the ACP-bound acetocetyl moiety (Figure 7) [82,83]. Thereby, FabH is able to diversify the fatty acid type by using different starter building blocks. Beside acetyl-CoA also iso- and anteiso-branched-chain acyl-CoA derivatives can be incorporated, leading to branched chain fatty acids, as it occurs in *Bacillus subtilis* [84]. The other two KSs FabB and FabF are responsible for the elongation (Figure 7) [85]. Furthermore, the dehydration of β-hydroxy-intermediates can be performed by FabZ as well as by FabA. While both dehydratases show overlapping substrate specificities, the FabZ activity is increased with saturated short chain acyl-ACPs, while FabA prefers medium chain lengths [86]. Furthermore, FabA is almost inactive using unsaturated acyl-ACP as substrate, but in contrast to FabZ shows isomerization activity [86]. Beside saturated fatty acids, FAS type II generate also monounsaturated fatty acids. Therefore, FabA isomerizes *trans*-2-decenoyl-ACP to *cis*-3-decenoyl-ACP, which is directly

elongated by FabB without the usual enoylreduction by FabI [55]. Nevertheless, the final condensation reaction is catalyzed by FabF [55]. These monounsaturated fatty acids are important for the regulation of the membrane viscosity during homeoviscous adaptation [87,88].

Finally, the ACP-bound acyl-moiety can be used for the formation of phosphatidic acid, a precursor for phospholipids, either by the PlsB/PlsC or the PlsX/PlsY/PlsC acyltransferase pathway [89].

1.5 Polyunsaturated fatty acid biosynthesis

In general, PUFA products contain more than two double bonds (Figure 8) [90]. In eukaryotes the aerobic biosynthesis of omega-3 and omega-6 fatty acids like eicosapentaenoic acid (EPA, C20:5 ω3) or docosapentaenoic acid (DPA, C22:5 ω6) starts with saturated stearic acid (18:0) or palmitic acid (16:0), which are further processed by desaturases and elongases [91]. In contrast to lower eukaryotes, plants and animals, mammals including humans lack most of the required enzymes [91–94]. Therefore, these essential fatty acids or precursors like linoleic acid and α-linolenic acid have to be part of the diet, as they have an important impact on human health [90,91].
The anaerobic biosynthesis of PUFAs can be seen as mixed type I FAS or PKS system due to the homology of single domains [95–97]. However, three to four discrete proteins/subunits harbor the catalytic domains instead of one large mega-enzyme (Figure 8) [95,96]. Similar to FAS, all required domains for chain elongation and β-processing, including KS, MAT, AT, ACP, KR, DH, and ER domains are included (Figure 8). Furthermore, the biosynthesis of PUFAs requires a PPTase, either encoded within the corresponding BGC or at a separate region [30,31,97,98]. Generally, during PUFA biosynthesis an acetyl moiety is elongated by repeating decarboxylative Claisen thioester condensation reactions with malonate units [97]. In contrast to FAS, the resulting β-keto groups are either completely reduced or multiple isolated double bonds are formed in a specific pattern (Figure 8) [97].

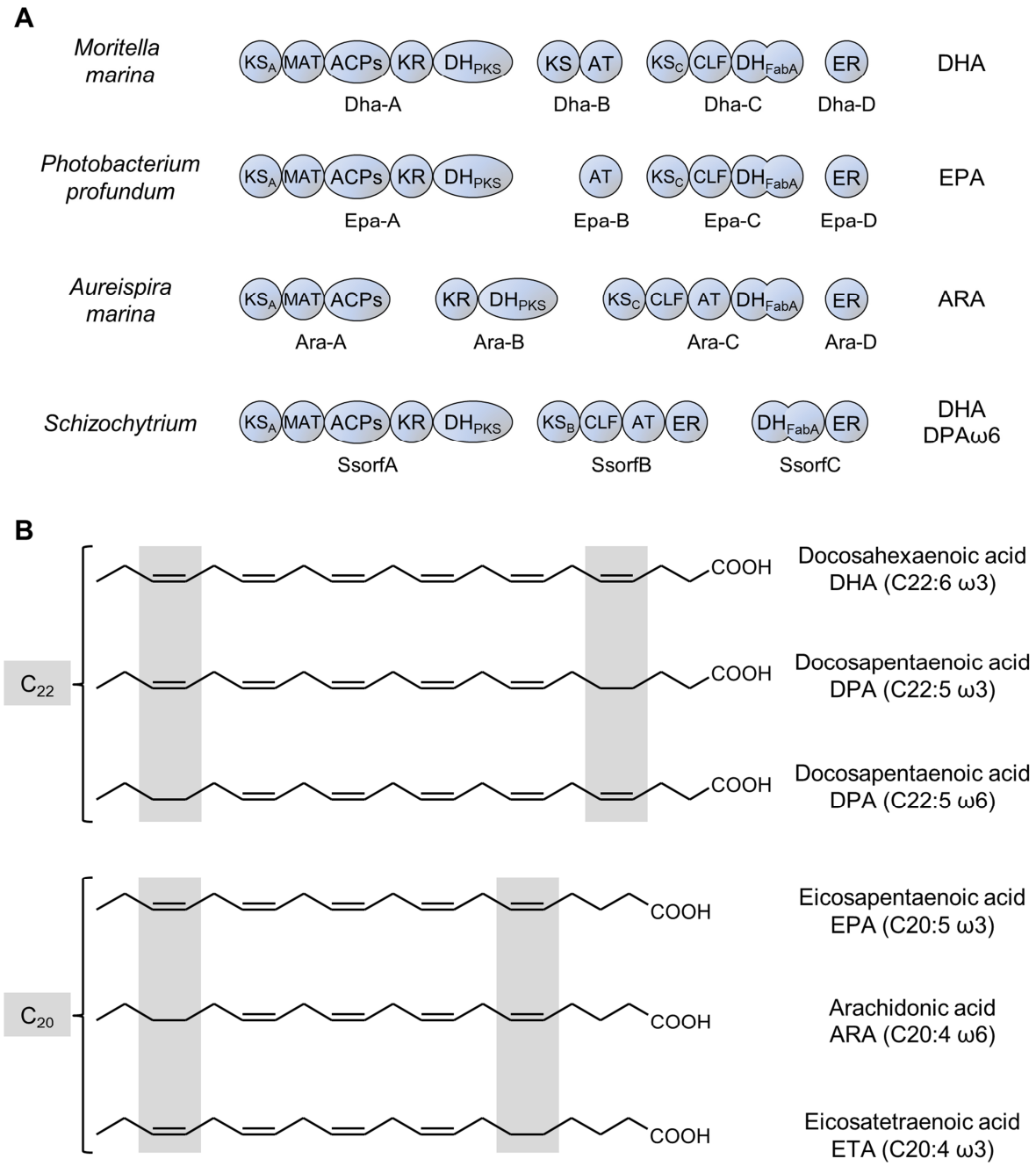

Figure 8. Domain distribution of enzymes in different PUFA producers (**A**) and chemical structures of PUFAs (**B**). Abbreviations for domains: KS: ketosynthase, MAT: malonyl CoA transacylase, ACP: acyl carrier protein, KR: ketoreductase, DH_{PKS}: PKS-like dehydratase, AT: acyltransferase, CLF: chain length factor domain, DH_{FabA}: FabA-like dehydratase, ER: enoyl reductase (Figure was adapted and modified from [95]).

Corresponding genes can be found in multiple genera like the marine bacteria *Shewanella*, *Moritella*, *Colwellia* [99], *Photobacterium* [100] or *Aureispira* [101] but also in the marine fungus-like *Schizochytrium* [102,103] or terrestrial myxobacterial strains [97]. Between the different organisms the number of domains and their distribution among the subunits can differ (Figure 8). While the basic mechanisms of chain elongation and β-processing steps were known, single reaction mechanisms during the iterative cycles could not be assigned to single catalytic domains as the PUFA biosynthesis harbors multiple catalytic domains of the same type (ACP, KS, DH domains) (Figure 8). Nevertheless, recently published studies elucidated their function, mainly by dissecting the PUFA mega-enzymes into single components or successful engineering [95,104,105]. In contrast to PKS/FAS systems the number of natural occurring ACP domains can differ from four to nine [104]. Studies of engineered PUFAs with additional or inactivated ACP domains revealed, that the number of ACP domains influences production titers without changing product profiles [26,104]. Two recently published studies revealed the function of the two KS (KS_A and KS_C) and DH domains (DH_{PKS} and DH_{FabA}), and a detailed biosynthesis pathway for PUFAs was postulated, shown in Figure 9 [95,105]. Both studies are based on gene exchange experiments in combination with *in vitro* characterizations. One study compared the biosynthesis of the C_{20}-PUFAs EPA with arachidonic acid (ARA), both differing only in the ω3 double bond (Figure 8). Here, the catalytic activity of the DH_{PKS} domain is followed by an enoyl-reduction, leading to a complete saturation of the intermediate. In contrast, the DH_{FabA} domain catalyzes both dehydration and isomerization, followed by chain elongation and resulting in a cis-double bond [105]. Thereby, the DH_{PKS} and DH_{FabA} domains from EPA and ARA biosynthesis showed different specificities concerning the chain-length of their substrate. In summary, the different patterns of double bonds is based on the catalytic activities of the DH_{PKS} and DH_{FabA} domains in combination with their chain length specificities, which differ between EPA and ARA biosynthesis [105]. The other study analyzed the biosynthesis of EPA and docosahexaenoic acid (DHA, C22:6 ω3), both differing only in their chain length (Figure 9). Briefly, the KS_A domain prefers substrates with short- and medium-chain lengths, while the KS_C domain utilizes long chain substrates [95]. Nevertheless, the condensation reaction from C_{18} to C_{20} (last elongation in EPA-biosynthesis) is performed by the KS_A domain and C_{20} to C_{22} conversion is

performed by the KS_C domain (last elongation in DHA-biosynthesis) [95]. This confirmed the KS_C domain as chain length determining factor.

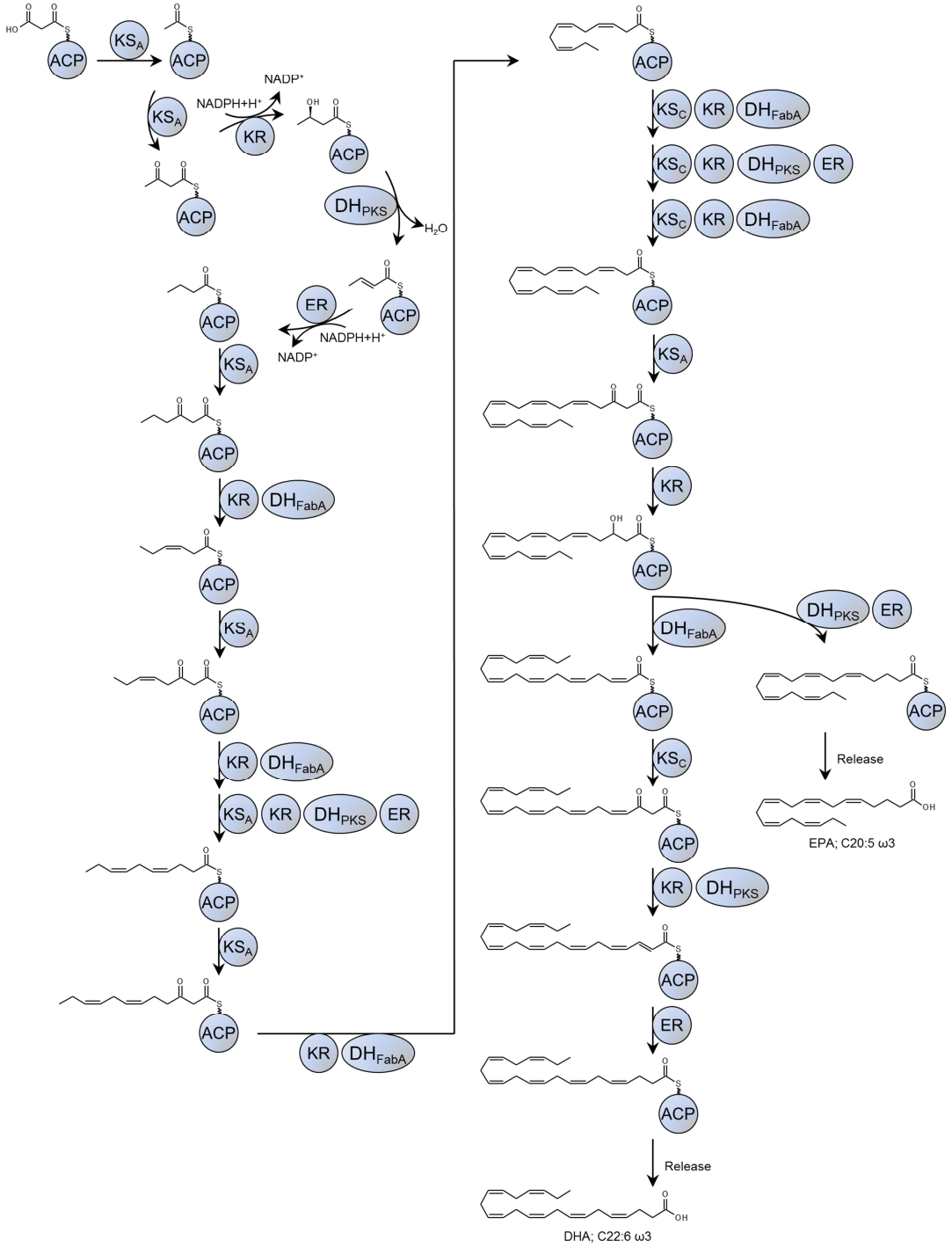

Figure 9. Postulated EPA and DHA biosynthesis. Abbreviations for domains: KS_A/KS_C: ketosynthases from different subunits (Figure 8), MAT: malonyl CoA transacylase, ACP: acyl carrier protein, KR: ketoreductase, DH_{PKS}: PKS-like dehydratase, AT: acyltransferase, DH_{FabA}: FabA-like dehydratase, ER: enoyl reductase (Figure was adapted and modified from [95]).

The final PUFA product can be released by multiple mechanisms: In *Photobacterium profundum* a TE-encoding gene could be identified next to the PUFA biosynthesis gene cluster (BGC), and *in vitro* studies revealed a TE activity with preference for saturated and unsaturated long-chain CoA derivatives [106]. In BGCs of the genera *Sorangium* or *Aetherobacter* a 1-acylglycerol-3-phosphate O-acyltransferase is part of the last PUFA subunit, presumable performing a direct transfer into lipids [97]. Furthermore, the heterologous expression of a *Schizochytrium* PUFA-synthase in *E. coli* led to the accumulation of free fatty acids, indicating an internal release mechanism [102].

1.6 Lifecycle of *Xenorhabdus* and *Photorhabdus*

In the past, main sources for the discovery of SMs like NRPs or PKs were microbes like actinomycetes and fungi [21]. As the rediscovery of SM classes increased, new microbial sources have to be established in order to increase diversity [21]. Here, potential, new genera are *Burkholderia*, *Paenibacillus*, *Pseudomonas*, *Photorhabdus* and *Xenorhabdus* [21]. For instance, in *Photorhabdus luminescens* about 6.5% of the genome is associated with secondary metabolism [107].

Our group is mainly focused on the enterobacteriaceae *Xenorhabdus* and *Photorhabdus*, which live in mutualistic symbiosis with the nematodes of the genus *Steinernema* and *Heterorhabditis* [107]. As infective juveniles (IJ) the nematodes host the bacteria in their anterior intestine [108]. While in *Heterorhabditis* the bacteria stay in close contact to the gut epithelia [109], *Steinernema* contains vesicles with specialized substructures called intravesicular structure [110]. In soil, the colonized nematodes wait for or actively search for a potential prey like an insect larvae and infect it by entering it through the spinacles, mouth or anus (Figure 10) [107,108,111]. After the nematode migrates to the hemocoel, the bacteria are released into the hemolymph. Without the protective environment of the nematode they are exposed to several threats like the insect immune system, microbes from the insect itself or from the soil [107].

Nevertheless, *Xenorhabdus* and *Photorhabdus* bacteria reproduce and overwhelm these threats by a change from a mutualistic to a pathogenic lifestyle. They start producing SMs as well as protein toxins to inhibit the immune response of the insect, kill the insect prey and to protect the insect cadaver against food competitors [13].

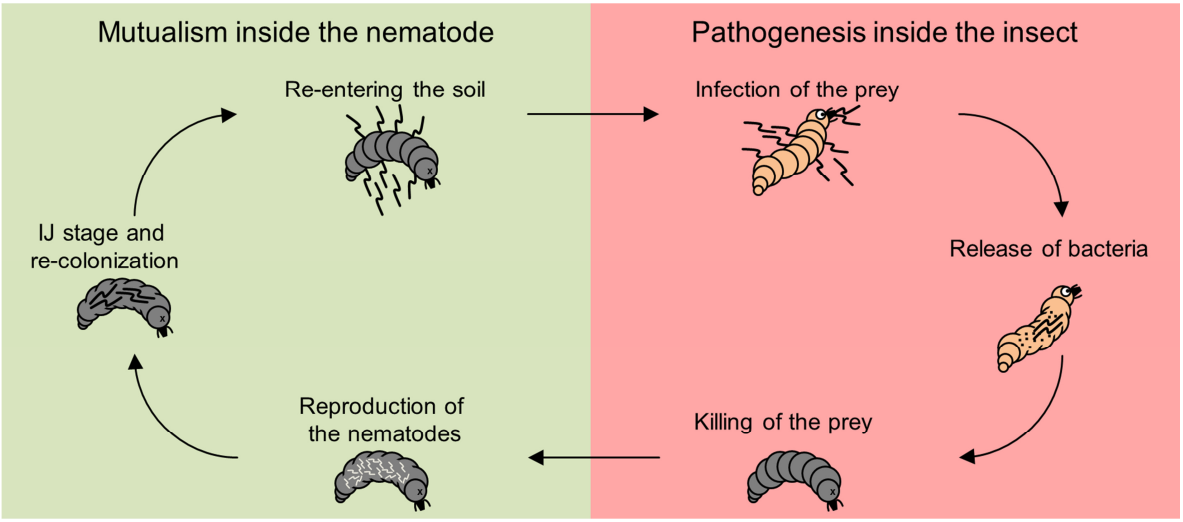

Figure 10. Lifecycle of *Xenorhabdus* and *Photorhabdus* bacteria (Figure was adapted and modified from [108]).

Furthermore, they convert the carcass into a more accessible nutrient source via exo-enzymes to support the reproduction of the nematodes (Figure 10) [112]. After several generations, the nematodes receive signals to develop into IJs and are re-colonized by the bacteria in a process called *endotokia matricida*. This includes that the juveniles hatch inside of the parent nematodes and use them as nutrient source [108]. Thereby, a small number of bacteria are received, which reproduce inside the nematode towards a mature population [108]. About several hundred thousands of the nematodes then leave the exploited carcass and the life cycle restarts in the soil (Figure 10) [108].

1.7 Fabclavines and structural related specialized metabolites

In 2014, a study revealed the occurrence of the fabclavine SMs in *Xenorhabdus budapestensis* and *X. szentirmaii* [113]. These compounds are of particular interest due to their broad-spectrum bioactivity against a variety of different organisms, including important pathogens like *Plasmodium falciparum*, responsible for malaria [113]. Also a bioactivity against eukaryotic cell lines was detected, decreasing its potential as pharmaceutical application [113]. The corresponding biosynthesis could be assigned to a 50 kb BGC (Figure 11) [113].

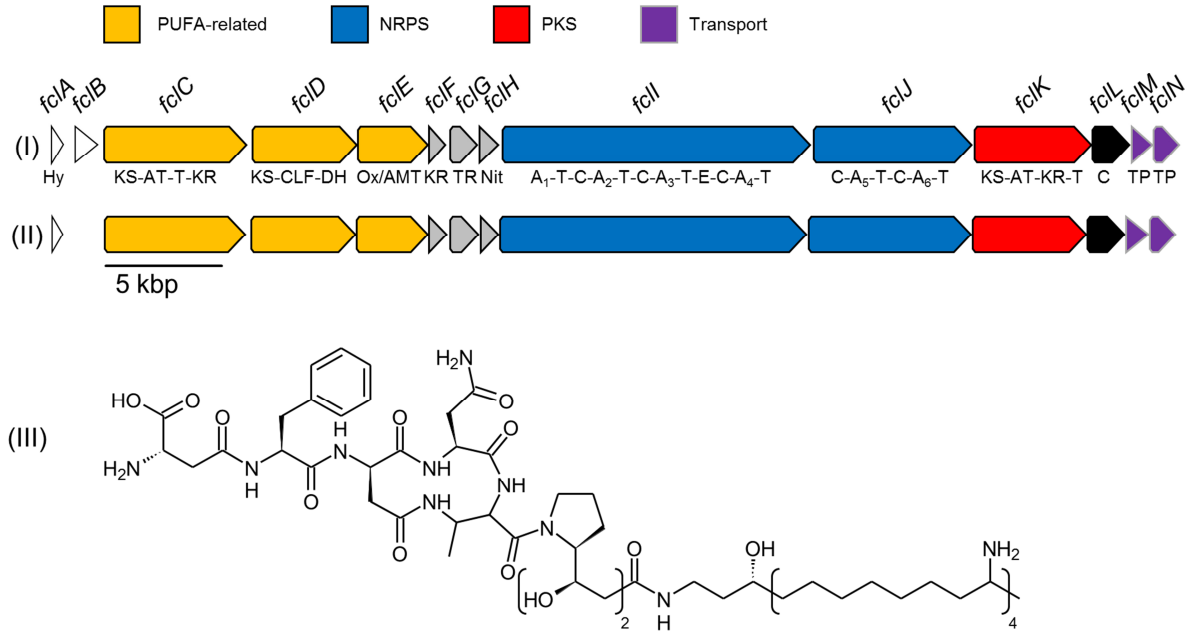

Figure 11. Fabclavine (*fcl*) BGCs in *X. budapestensis* (I) and *X. szentirmaii* (II) and the NMR-solved structure of fabclavine Ia (III). Abbreviations: Hy: hydrolase, KS: ketosynthase, AT: acyltransferase, T: thiolation domain, KR: ketoreductase, CLF: chain length factor domain, DH: dehydratase, Ox: 2-nitropropane dioxygenase (enoyl reductase), AMT: aminotransferase, TR: thioester reductase, Nit: nitrilase, A: adenylation, C: condensation, E: epimerization, TP: transport (Figure was adapted and modified from [113] in accordance to 2.2 and 2.4).

Strikingly, the postulated biosynthesis includes three PUFA-homologues FclC, FclD and FclE, two NRPS FclI and FclJ and one type I PKS FclK, indicating a highly specialized hybrid pathway (Figure 11) [113]. Derivate Ia from *X. budapestensis* was isolated and its structure elucidated by nuclear magnetic resonance (NMR) and the advanced Marfey's method (Figure 11) [113]. Biochemically, an unusual polyamine is connected by one or multiple partially reduced polyketide units to a hexapeptide (Figure 11) [113].

The (pre-)zeamines, described for *Serratia plymuthica* and *Dickeya zeae*, share multiple similarities with fabclavines regarding their biosynthesis, biochemical structure and bioactivity (Figure 12) [114–116]. Like *Xenorhabdus* zeamine producers are Gram-negative bacteria, but live in different habitats. While *S. plymuthica* is associated with the rhizosphere of different plants with a potential role as fungal control agent [117], *D. zeae* is a plant pathogen, responsible for rice and maize diseases [118].

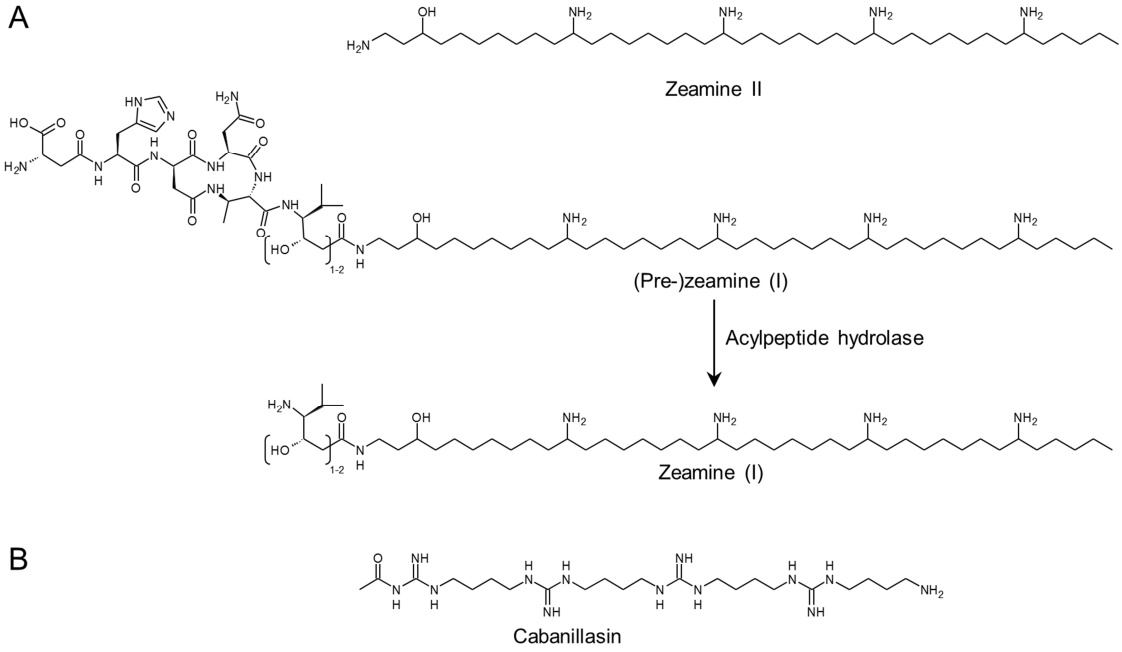

Figure 12. Structural fabclavine-related SMs. (A) The polyamine-intermediate zeamine II, as well as the cleavage of (pre-)zeamine (I) to zeamine (I) by an acylpeptide hydrolase (adapted and modified from [116]). (B) The polyagmatine cabanillasin from *X. cabanillasii* (adapted and modified from [119]).

Despite all similarities between fabclavines and zeamines the biosynthesis of the latter differs in an additional catalytic step [116]. Thereby, the prezeamines, which share the highest similarities with the fabclavines, are cleaved by an acylpeptide hydrolase (Zmn22), generating a pentapeptide and the final zeamine product (Figure 12) [116]. These resulting zeamines exhibit an increased bioactivity compared to prezeamines [116]. A corresponding acylpeptide hydrolase homologue could not be detected in the fabclavine (*fcl*) BGC [116]. Another related compound is cabanillasin, described for *X. cabanillasii* in 2013 [119]. The elucidated polyagmatine structure resembles the structure of the polyamine part of the fabclavines (Figure 12, B) [119]. While the corresponding biosynthetic gene cluster remains unknown, the repeating guanidino groups indicate the utilization of agmatine or arginine as building blocks. Bioactivity analysis of cabanillasin revealed an antifungal activity against different strains of the genus *Candida*, but no complete inhibition of *Candia albicans* was observed. *C. albicans* is a fungal pathogen, responsible for nosocomial infections in hospitals [120]. Beside its antifungal activity, cabanillasin could further act as nitrogen storage, comparable to the multi-L-arginyl-poly-L-aspartate polymer cyanophycin from cyanobacteria [121].

1.8 Aims of this work

Present work is focused on the SM class of fabclavines. Although a pharmaceutical application seems unlikely due to their cytotoxicity, the project was structured with regard to the identification of a lead compound. The schematic overview of the project aims is shown in Figure 13 on the basis of a theoretical SM. The aims include the detection of a potential compound, followed by elucidation of the biosynthesis and the identification of homologous BGCs as well as related compounds. Thereby, the elucidation and identification steps are the foundation for the next step, as they provide detailed insights into the biosynthesis. After identifying possible starting points for engineering, the next step is the modification of the biosynthesis to generate compounds with more preferable properties. Finally, the focus lay on the identification of possible ares of application.

As the initial description of the fabclavines was performed prior to this work the detection aim is not part of this present thesis (Figure 13) [113]. However, the elucidated structure as well as the postulated biosynthesis in combination with the corresponding BGC laid the foundation for the here presented work [113].

Consequently, the first aim of this study was the elucidation of the corresponding biosynthesis of the fabclavines (Figure 13). As a knock-out of the condensation domain-like protein FclL resulted in the production of the polyamine and not in a complete collapse of the biosynthesis, we suggested, that polyamine and the NRPS-PKS pathway can work independently [113]. Therefore, the elucidation of biosynthesis was based on a mutational analysis in *X. szentirmaii*, followed by the identification of intermediates. Furthermore, selected enzymes of interest, responsible for the reductive release of the polyamine or its condensation with the NRPS-PKS-part, were characterized either *in vitro* or *in vivo* (2.1) [122].

While elucidating respective biosynthesis, *in silico* analysis revealed that *fcl* BGCs are widely distributed among the genera *Xenorhabdus* as well as *Photorhabdus* [122]. Furthermore, the first essential biosynthesis gene could be determined, which was essential for further analysis. Consequently, the second aim of this thesis includes the identification of unknown fabclavine derivatives in further strains via introduction of an artificial promoter to chemically activate or inactivate the biosynthesis (Figure 13) [123].

Subsequent comparisons revealed a high diversity of former unknown derivatives (2.2) [124].

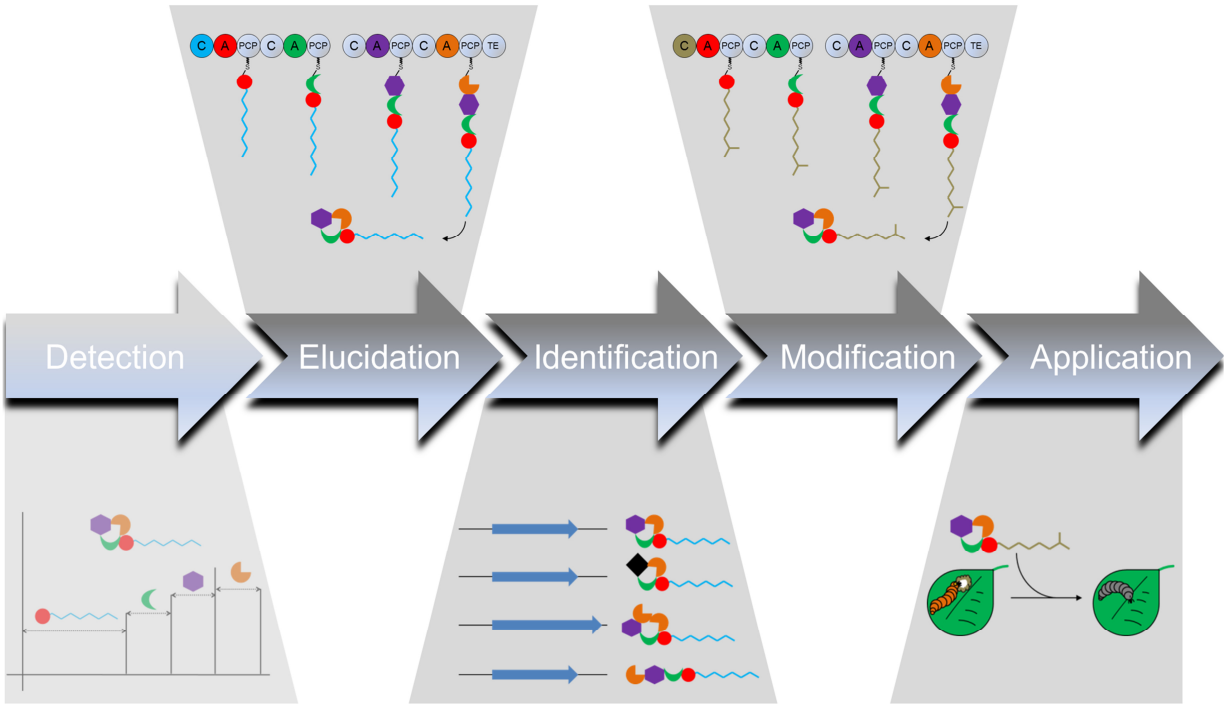

Figure 13. Schematic overview of the project aims on the basis of a theoretical SM.

In combination with the elucidated biosynthesis, specific chemical moieties could be assigned to enzymes or even single domains. This leads to the third aim of this thesis, the modification of the biosynthesis in order to expand the natural diversity by artificial derivatives (Figure 13). Therefore, gene exchange experiments were performed to recombine chemical moieties derived from the different fabclavine pathways (PUFA, NRPS, PKS) (3). Furthermore, the NRPS pathway was manipulated to change the product spectra (3.4).

Detailed *in silico* analysis revealed that in *X. bovienii* the *fcl* BGC differs from other *Xenorhabdus* strains in the presence of the NRPS and PKS genes as well as in an additional domain during the polyamine fabclavine biosynthesis. Here, a novel polyamine-derivate could be identified and its biosynthesis assigned to the additional domain. This domain was classified as another modification mechanism and therefore integrated into further polyamine pathways to generate artificial derivatives (Figure 13) (2.4).

Finally, the elucidation of the biosynthesis, the identification and characterization of homologous BGCs and the modification of single pathways led to a high number of different intermediates and derivatives. For the fourth aim these fabclavine derivatives were analyzed in order to determine possible applications (Figure 13). Therefore, bioactivity analyses were performed in our laboratory but also in collaboration with other working groups (2.3) [125].

2 Publications and manuscripts

2.1 Fabclavine biosynthesis in *X. szentirmaii*: shortened derivatives and characterization of the thioester reductase FclG and the condensation domain-like protein FclL

Authors:

Sebastian L. Wenski[1] · Diana Kolbert[1] · Gina L. C. Grammbitter[1] · Helge B. Bode[1,2*]

[1] Molekulare Biotechnologie, Fachbereich Biowissenschaften, Goethe Universität Frankfurt, 60438 Frankfurt, Germany

[2] Buchmann Institute for Molecular Life Sciences (BMLS), Goethe Universität Frankfurt, 60438 Frankfurt, Germany

Published in:

Journal of Industrial Microbiology & Biotechnology 46 (2019) 565–572

doi: 10.1007/s10295-018-02124-8

Online access: https://link.springer.com/article/10.1007/s10295-018-02124-8

Reprinted with permission, licence number: 4865230936460

Attachements:

Declaration on the contribution of the authors and the publication.

2.2 Fabclavine diversity in *Xenorhabdus* bacteria

Authors:

Sebastian L. Wenski[1], Harun Cimen[2], Natalie Berghaus[1], Sebastian W. Fuchs[1], Selcuk Hazir[2] and Helge B. Bode[1,3,4*]

[1] Molekulare Biotechnologie, Fachbereich Biowissenschaften, Goethe Universität Frankfurt, Max-von-Laue-Str. 9, 60438 Frankfurt, Germany and

[2] Adnan Menderes University, Faculty of Arts and Sciences, Department of Biology, 09010 Aydin, TURKEY and

[3] Buchmann Institute for Molecular Life Sciences (BMLS), Goethe Universität Frankfurt, Max-von-Laue-Str. 15, 60438 Frankfurt, Germany and

[4] Senckenberg Gesellschaft für Naturforschung, Senckenberganlage 25, 60325 Frankfurt, Germany

Published in:

Beilstein Journal of Organic Chemistry 16 (2020) 956–965

doi: 10.3762/bjoc.16.84

Online access: https://www.beilstein-journals.org/bjoc/articles/16/84

© 2020 Wenski et al.; licensee Beilstein-Institut.

This is an Open Access article under the terms of the Creative Commons Attribution License (http://creativecommons.org/licenses/by/4.0). Please note that the reuse, redistribution and reproduction in particular requires that the authors and source are credited.

Attachements:

Declaration on the contribution of the authors and the publication.

2.3 Nematode-Associated Bacteria: Production of Antimicrobial Agent as a Presumptive Nominee for Curing Endodontic Infections Caused by *Enterococcus faecalis*

Authors:

Hicran Donmez Ozkan[1]*, Harun Cimen[2], Derya Ulug[2], Sebastian Wenski[3], Senem Yigit Ozer[1], Murat Telli[4], Neriman Aydin[4], Helge B. Bode[3] and Selcuk Hazir[2]*

[1] Department of Endodontics, Faculty of Dentistry, Adnan Menderes University, Aydin, Turkey

[2] Department of Biology, Faculty of Arts and Sciences, Adnan Menderes University, Aydin, Turkey

[3] Molekulare Biotechnologie, Fachbereich Biowissenschaften, Buchmann Institute for Molecular Life Sciences (BMLS), Goethe Universität Frankfurt Biozentrum, Frankfurt am Main, Germany

[4] Department of Microbiology, Faculty of Medicine, Adnan Menderes University, Aydin, Turkey

Published in:

Frontiers in Microbiology 10 (2019) 2672

doi: 10.3389/fmicb.2019.02672

Online access: https://www.frontiersin.org/articles/10.3389/fmicb.2019.02672/full

Copyright © 2019 Donmez Ozkan, Cimen, Ulug, Wenski, Yigit Ozer, Telli, Aydin, Bode and Hazir. This is an open-access article distributed under the terms of the Creative Commons Attribution License (CC BY). The use, distribution or reproduction in other forums is permitted, provided the original author(s) and the copyright owner(s) are credited and that the original publication in this journal is cited, in accordance with accepted academic practice. No use, distribution or reproduction is permitted which does not comply with these terms.

Attachements:

Declaration on the contribution of the authors and the publication.

2.4 Structure and biosynthesis of deoxy-polyamine in *X. bovienii*

Authors:

Sebastian L. Wenski[1], Natalie Berghaus[1], Nadine Keller[1], Helge B. Bode[1,2,3,*]

[1] Molekulare Biotechnologie, Fachbereich Biowissenschaften, Goethe Universität Frankfurt, 60438 Frankfurt, Germany. Telephone number: +49 69 798-29557
E-mail: h.bode@bio.uni-frankfurt.de
[2] Buchmann Institute for Molecular Life Sciences (BMLS), Goethe Universität Frankfurt, 60438 Frankfurt, Germany.
[3] Senckenberg Gesellschaft für Naturforschung, 60325 Frankfurt, Germany

Status:

Submitted manuscript.

Attachements:

Declaration on the contribution of the authors and the manuscript.

3 Additional results: Engineering the fabclavine biosynthesis

Fabclavines are hybrid SMs and their biosynthesis can be devided into a PKS, a NRPS and a PUFA-like pathway. The fabclavine biosynthesis in *X. szentirmaii* was elucidated and analysis of further *Xenorhabdus* strains revealed a wide variety of fabclavine derivatives (2.1, 2.2 and 2.4). In the following, the results of gene exchange experiments are described in order to understand the biosynthesis in detail and to extend the naturally occurring diversity by artificial derivatives. Thereby, the three sections can be thematically classified into further elucidation of the polyamine biosynthesis as well as the engineering of the PKS and the NRPS pathways.

The first part (3.1) describes the continuation of the work of section 2.1 and 2.4 [122]. In detail, a *X. szentirmaii* mutant with a deletion in *fclD* was heterologously complemented to determine the role of FclD during the polyamine formation.

In the course of the analysis of multiple *Xenorhabdus* strains with *fcl* BGCs, fabclavine derivatives with three polyketide units could be observed in *X. stockiae*, KJ12.1 and KK7.4 [124]. As this represents a unique feature during biosynthesis, we were interested if this special moiety could be integrated in other fabclavine producers by manipulating the PKS pathway (3.2).

Finally, the last two parts (3.3 and 3.4) describes NRPS engineering experiments. Gene exchange experiments were performed in the *X. szentirmaii* fabclavine biosynthesis in order to vary the incorporated amino acids. Furthermore, chimeric NRPS were generated in accordance to the recently published XU concept [49].

3.1 Elucidation of the biosynthesis: Heterologous complementation of FclD

All polyamine-forming enzymes FclC, FclD, FclE, FclF and FclG are essential for the biosynthesis, as the deletion of their encoding regions leads to a complete loss of polyamine and fabclavine production (2.1) [122]. Furthermore, *fclH* influences the biosynthesis as its deletion leads to decreased titers (2.4).

Consequently, the biosynthesis is mainly based on *in silico* analysis of the domain functions in comparison with the zeamine and PUFA biosynthesis [96,114]. Two recently published studies, analyzing the PUFA biosynthesis with gene exchange experiments, inspired us to identify the chain length determining factor among the polyamine biosynthesis [95,105].

Thereby, we focused on FclD, as it contains a CLF domain, a known factor for chain length determination [126]. For the analysis, a *X. szentirmaii* Δ*fclD* mutant was heterologously complemented with FclD from and *X. hominickii*, *X. budapestensis*, *X. bovienii*, KJ12.1 and *X. szentirmaii* as control. Naturally, the selected strains produce polyamines, which differ in the number of integrated amine units (*X. szentirmaii*: 3, *X. hominickii*: 5, *X. budapestensis*: 3 or 4, *X. bovienii*: 4, KJ12.1: 4) (2.2 and 2.4) [124]. In case of a functional integration of FclD, we expected that it determines the number of incorporated amine units. Consequently, the *X. szentirmaii* gene exchange mutants produce different polyamines dependent of the origin of FclD. As the condensation domain-like protein FclL is promiscuous concerning its amine substrate, the conjugation of polyamines of different lengths to the NRPS-Part should be possible, which can be easily detected by matrix-assisted laser desorption/ionization-mass spectrometry (MALDI-MS) (Figure 14) (2.1 and 2.4) [122].

The subsequent analysis of induced and non-induced production cultures revealed, that in all gene exchange mutants fabclavine derivatives could be detected (Figure 14). This confirmed that heterologous FclD can be functionally integrated in the fabclavine biosynthesis of *X. szentirmaii*. However, none of the mutants showed the production of polyamines, differing in the number of amine units as it was proposed (Figure 14).

(I)

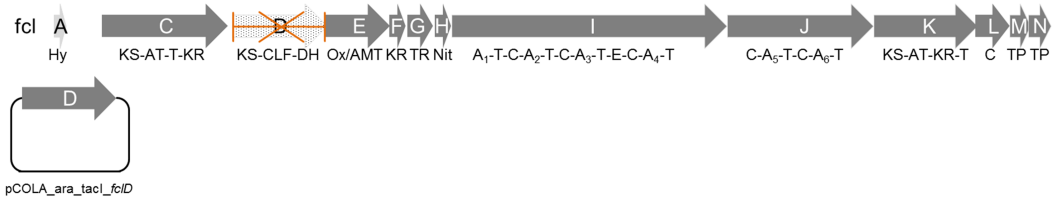

(II)

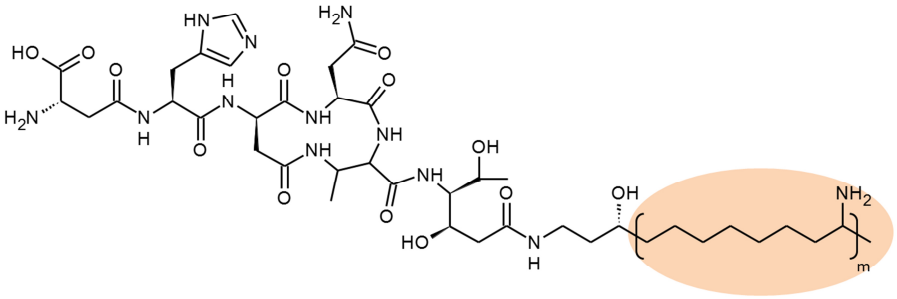

(III)

	FclD origin	Detected products		
		m = 3	m = 4	m = 5
a	*X. szentirmaii*	+++	-	-
b	*X. hominickii*	+	-	-
c	*X. budapestensis*	+++	-	-
d	*X. bovienii*	+	-	-
e	KJ12.1	++	-	-

Figure 14. Gene exchange experiments in *X. szentirmaii* Δ*fclD* mutant and resulting product spectra. (I) The *X. szentirmaii* Δ*fclD* mutant was complemented with *fclD* homologues, encoded on a plasmid. (II) The corresponding production cultures were analyzed by MALDI-MS for the shown fabclavine scaffold (Figure S1). (III) The origin of the exchanged FclD and corresponding phenotypes are shown concerning the variable polyamine lengths [124]. The numbers of + correlates with the signal intensities (- : not detectable) (Figure S1).

Surprisingly, all mutants including the control produced derivatives with three amine units, which can also be observed for the *X. szentirmaii* wild type [124]. Although the performed MALDI-MS experiments can not be used for quantification, we compared the signal intensities of single derivatives like described previously (2.1) [122]. This revealed strongly decreased intensities for mutants with FclD from *X. hominickii* or *X. bovienii* in comparison to the control *X. szentirmaii* (Figure 14). In contrast, gene exchange mutants with FclD from *X. budapestensis* or KJ12.1 showed similar signal intensities.

3.2 Engineering of the PKS pathway: Heterologous complementation of FclK

The PKS part of the majority of fabclavine derivatives consists of one or two partially reduced polyketide units (2.2) [124]. However, additional derivatives were observed in the strains KJ12.1, KK7.4 and *X. stockiae* with up to three polyketide units (2.2) [124]. As the type I PKS FclK catalyzes this reaction step in an iterative manner, we were interested if such moieties can be introduced into other strains via gene exchange of *fclK* [122].

(I)

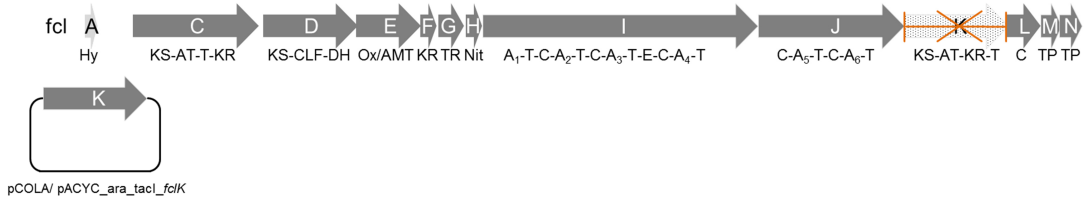

(II)

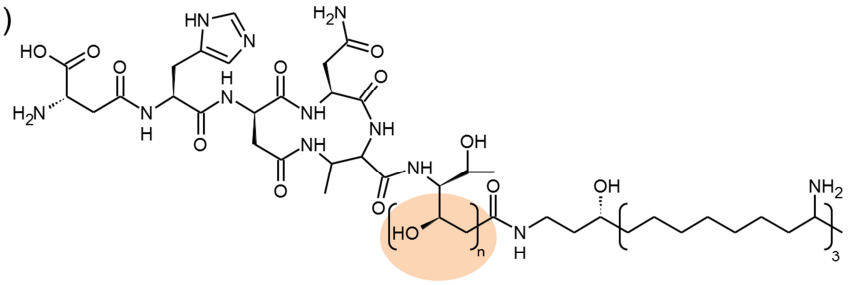

(III)

	FclK origin	Detected products		
		n = 1	n = 2	n = 3
a	*X. szentirmaii*	+++	+++	+
b	KJ12.1	++	++	++
c	*X. budapestensis*	++	+++	+
d	*X. hominickii*	++	++	+

Figure 15. Gene exchange experiments in *X. szentirmaii* Δ*fclK* mutant and resulting product spectra. (I) The *X. szentirmaii* Δ*fclK* mutant was complemented with *fclK* homologues, encoded on a plasmid. (II) The corresponding production cultures were analyzed by MALDI-MS for the shown fabclavine scaffold. (III) The origin of the exchanged FclK and corresponding phenotypes are shown concerning the variable numbers of incorporated malonate units (Figure S2) [124]. The numbers of + correlates with the signal intensities (- : not detectable).

Therefore, a *X. szentirmaii* Δ*fclK* mutant was complemented with FclK from KJ12.1, *X. budapestensis*, *X. hominickii* and *X. szentirmaii* (control) encoded on a plasmid. Subsequently, production cultures of the gene exchange mutants were analyzed concerning the production of certain fabclavine derivatives (Figure 15).

MALDI-MS experiments revealed, that in all mutants fabclavine derivatives could be detected, confirming the succesfull incorporation of FclK-homologues into the biosynthesis of *X. szentirmaii* (Figure 15). As expected the mutant with FclK from KJ12.1 is able to produce derivatives with one, two or three polyketide units (Figure 15 b). Mutants with FclK from *X. budapestensis*, *X. hominickii* or *X. szentirmaii* (control) showed the production of one or two polyketide unit derivatives (Figure 15 a, c, d). Surprisingly, further signals could be detected in these mutants, corresponding to a three polyketide unit derivate (Figure 15). However, the intensities of the the signals are too low for a confirmation by further experiments like MALDI-MS^2 (Figure S2).

3.3 Engineering of the NRPS pathway: Heterologous complementation of FclJ

Generally, full-length fabclavine derivatives differ in four chemical moieties: the polyamine and the PKS-part, as well as the second and last amino acid of the NRPS-part (2.2) [124]. The succesfull gene exchanges for *fclK* confirmed that the interaction of FclJ with heterologous FclK is still functional, as fabclavine production could be observed. Thus, we were interested if the other way around was also possible via heterologous complementation of *fclJ*. Here, heterologous FclJ has to interact with FclK but also with FclI for the formation of full-length fabclavines. Furthermore, we expected that succesfull gene exchanges lead to divergent NRPS-parts, as FclJ is responsible for the incorporation of the last two amino acids in the full-length derivatives. Based on the identified fabclavine derivatives, the natural specificity of the A6 domain in FclJ could be determined for *X. szentirmaii* (Thr or Val), *X. budapestensis* (Pro) and *X. hominickii* (Pro or Val) (2.2) [124]. Moreover, minor derivatives could be observed for *X. szentirmaii*, harboring also a proline at the sixth position (2.2) [124].

To prove our hypothesis the deletion mutant *X. szentirmaii* Δ*fclJ* was complemented with *fclJ* from *X. budapestensis*, *X. hominickii* and *X. szentirmaii* (control) encoded on plasmids. Subsequent MALDI-MS analysis of induced and non-induced production cultures revealed, that all gene exchange mutants produce full-length derivatives, confirming that heterologous FclJ interacts with the downstream FclK and upstream FclI (Figure 16). The control mutant with *fclJ* from *X. szentirmaii* showed the expected production of the valine and the threonine derivatives but none with proline (Figure 16 a).

Surprisingly, the gene exchange mutants with *fclJ* from *X. budapestensis* and *X. hominickii* show only the production of the valine derivate (Figure 16 b and c). Here, neither the expected proline- nor the threonine derivatives could be detected (Figure 16 b and c).

(I)

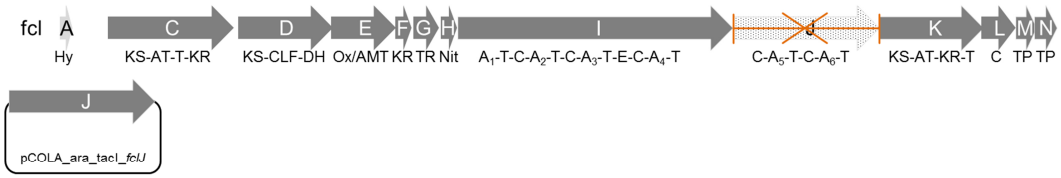

(II)

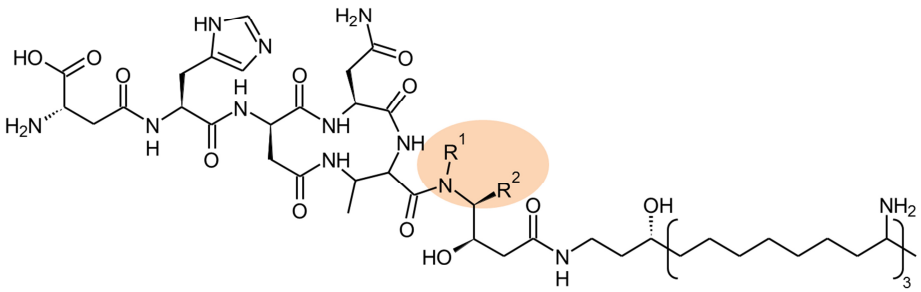

(III)

		FclJ origin	Products			
		R^1/R^2	R^1	R^2	R^1	R^2
			H		H	
a	*X. szentirmaii*	-	++		+++	
b	*X. budapestensis*	-	++		-	
c	*X. hominickii*	-	++		-	

Figure 16. Heterologous complementation of *X. szentirmaii* Δ*fclJ* and resulting product spectra. (I) The *X. szentirmaii* Δ*fclJ* mutant was complemented with *fclJ* homologues, encoded on a plasmid. (II) The corresponding production cultures were analyzed by MALDI-MS for the shown fabclavine scaffold. (III) The origin of the exchanged FclJ and corresponding phenotypes are shown concerning the variable sixth amino acid (Figure S3) [124]. The numbers of + correlates with the signal intensities (- : not detectable).

3.4 Engineering of the NRPS pathway: Generation of chimeric NRPS

After the succesfull gene exchange in *X. szentirmaii* Δ*fclJ*, an identical approach was performed in *X. szentirmaii* Δ*fclIJ*. Due to the addtitional deletion of *fclI* the complemented mutants produce only the shortened derivatives (2.1) [122]. The absence of full-length derivatives leads to smaller derivate sets, which facilitate the detection and comparison. Nevertheless, the specificity of FclJ, responsible for the first and second amino acid in the shortened derivatives, can still be analyzed. Here, experiments with FclJ, originating from *X. szentirmaii* (Thr or Val), *X. budapestensis* (Pro) and *X. hominickii* (Pro or Val), were performed (Figure 17 a-c and Figure S4) (2.2) [124].
In a second step, the recently described XU concept was used to separate FclJ in an *N*-terminal and a *C*-terminal part between the C domain of module five and the A domain of module six (Figure S5) [49]. The recombination of these two parts from *X. szentirmaii*, *X. budapestensis* and *X. hominickii* resulted in six chimeric NRPS (Figure 17 d-i and Figure S6). Identical to the gene exchange experiments this chimeric NRPS were used to complement *X. szentirmaii* Δ*fclIJ*.
MALDI-MS analysis for the gene exchange mutants of *fclJ* in *X. szentirmaii* Δ*fclIJ* revealed comparable results like the complementation in *X. szentirmaii* Δ*fclJ* (3.3). As expected, the control mutant with *fclJ* from *X. szentirmaii* produced shortened derivatives with an incorporated valine or threonine, but none with proline (Figure 17 a). In the mutant with *fclJ* from *X. budapestensis* mainly derivatives with a valine were detected beside threonine and proline derivatives (Figure 17 b). Finally, the *fclJ* *X. hominickii*-complemented mutant produced only valine, but no proline or threonine derivatives (Figure 17 c).
Surprisingly, all mutants, harboring the chimeric constructs, produced the valine and the proline derivatives. While mutants with an *N*-terminal part from *X. hominickii* showed no production of the threonine-derivate (Figure 17 e and g), constructs with an N-terminal part from *X. szentirmaii* or *X. budapestensis* (Figure 17 d, f, h, i) showed signals, corresponding to the threonine derivate.

(I)

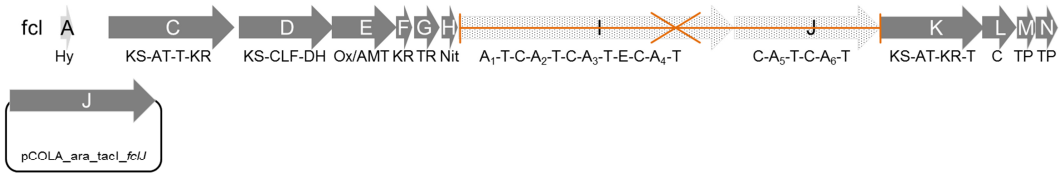

(II)

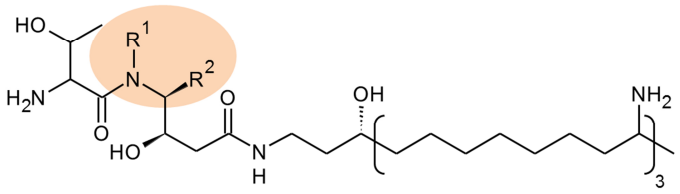

(III)

	FclJ composition	Products		
		R^1 H, R^2	R^1 H, R^2	R^1/R^2
a	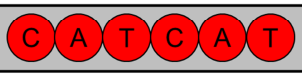	++	+++	-
b		+++	+	+
c	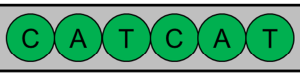	++	-	-
d		++	+	+
e	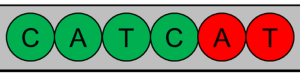	++	-	+
f		++	++	+
g	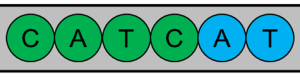	++	-	+
h		++	+++	+
i	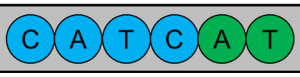	++	++	+

X. szentirmaii *X. budapestensis* *X. hominickii*

Figure 17. NPRS-engineering in *X. szentirmaii* Δ*fclIJ* mutant and resulting product spectra. (I) The *X. szentirmaii* Δ*fclIJ* mutant was complemented with *fclJ* homologues (a-c) and the chimeric pDD-constructs (d-i), encoded on a plasmid. (II) The corresponding production cultures were analyzed by MALDI-MS for the shown fabclavine scaffold. (III) The analyzed constructs and their corresponding phenotypes are shown concerning the variable amino acid (Figure S4 and Figure S6) [124]. The numbers of + correlates with the signal intensities (- : not detectable).

4 Discussion

In 2014, the fabclavines were described for the first time as hybrid SMs, produced by *X. budapestensis* and *X. szentirmaii* [113]. In this work, the respective biosynthesis in *X. szentirmaii* was elucidated, revealing the occurrence of three types: the full-length and shortened derivatives as well as the polyamine (Figure 18) (2.1) [122]. Biochemically, a NRPS-derived peptide is connected via one or multiple polyketide units to a polyamine (2.1) [122]. Subsequently, *in silico* analysis showed that homologous *fcl* BGCs are widely distributed among the genus *Xenorhabdus* (2.2) [124]. In detail, the BGC synteny as well as the identity on single protein level is highly conserved (2.1 and 2.2) [122,124]. The subsequent analysis of the corresponding strains led to the identification of a large chemical diversity of derivatives (2.2) [124]. While the general scaffold is conserved, the diversity is associated with four chemical moieties and could be assigned to responsible pathways, enzymes and catalytic domains (2.2) [124]. The *fcl* BGC of *X. bovienii* is an exception, as the NRPS and PKS genes are non-existent or truncated and as there is an additional PKS-like DH domain in the type I PKS FclC (2.2 and 2.4) [124]. The emergence of the additional domain is restricted to *X. bovienii* regarding the genus *Xenorhabdus* and it is responsible for the formation of a unique deoxy-polyamine (2.4). The integration of this domain into homologous polyamine pathways resulted in the formation of deoxy-derivatives beside the naturally occurring polyamines (2.4). Thus, the domain function can be seen as further diversification mechanism. The elucidation of the biosynthesis as well as the identification of promiscous catalytic activities was utilized in multiple engineering approaches, leading to the production of artificial derivatives (3). Analysis of purified full-length fabclavines as well as culture supernatants from different *Xenorhabdus* strains showed, that these SMs exhibit wide range of bioactivity (2.2 and 2.4) [113,124]. Furthermore, this bioactivity is not restricted to the full-length derivatives, but can also be observed for the shortened fabclavines and the polyamine (2.4). Thus, these SMs were analyzed for different potential applications, revealing a potent bioactivitiy of the *X. cabanillasii* fabclavines

against *Enterococcus faecalis*, a human pathogen associated with endodontic infections (2.3) [125].

4.1 Mode of action of fabclavines and related compounds

Fabclavines are structurally related to other compound classes like zeamine and cabanillasin (Figure 12) (2.1) [116,119]. Moreover, the recently described Xenorhabdus lipoprotein toxin (Xlt) from *X. innexi* was postulated as fabclavine-like [127]. As there is no published structure for Xlt, it is not possible to confirm this relationship. However, the analysis of *X. innexi* revealed the production of fabclavines, suggesting that Xlt and fabclavines are the same compounds [124].

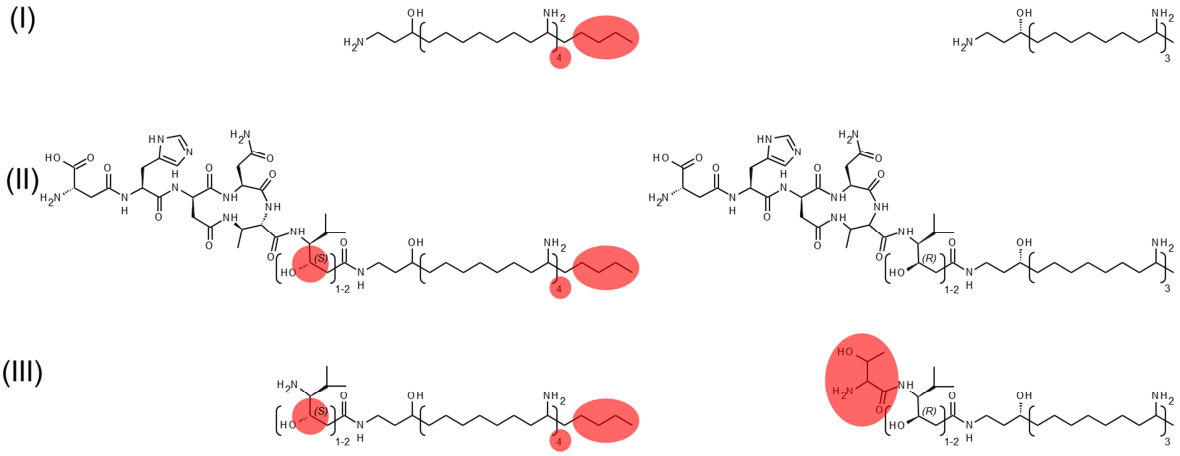

Figure 18. Structural comparison of the compound classes zeamine (left) and fabclavine (right). Marked in red are structural differences between the polyamines (I), the prezeamines/ fabclavines as full-length derivatives (II) and the zeamines/ shortened fabclavines as shortened derivatives (III) (adapted and modified from [116,122]).

A comparison of the zeamines and fabclavines from *X. szentirmaii* confirms that the corresponding peptide part of multiple derivatives is identical to the prezeamines (Figure 18) [116]. Principally, both compound classes can be classified into three similar types: the polyamine moiety, the full-length and the shortened derivatives [116,122]. In both compound classes the polyamines consist of a primary amine with a β-hydroxy group, followed by amine units of the same size (Figure 18). Zeamine II contains four amine

units, while the fabclavine-polyamine can differ from three to five amine units (three in *X. szentirmaii*) (Figure 18) [124]. While in zeamine II the last amine unit is connected to a butyl group, in the fabclavine class it is a methyl group (Figure 18). Additional to the described differences the prezeamines differ from the full-length fabclavines only in the configuration of the hydroxy group in the polyketide, connecting the polyamine with the NRPS-part (Figure 18). Finally, the shortened fabclavines can be distinguished from zeamine (I) as they harbor an additional threonyl group. While the proteolytic cleavage of prezeamine (I) leads to the formation of zeamine (I) [116], the shortened fabclavines are generated by the alternative biosynthesis starting unit FclJ [122]. In summary, fabclavines and zeamines are structurally almost identical.

The *fcl* BGCs are widely distributed among the genus *Xenorhabdus* and the chemical diversity is high (2.2) [124]. Zeamine BGCs can be found in subspecies of *Serratia plymuthica* as well as in multiple strains of the genus *Dickeya* [128]. Here, the question remains to be answered if these strains produce all the same zeamine derivatives or whether there is an uncovered fabclavine-like diversity. Nevertheless, the bioactivity of the different zeamine types is well described: Masschelein *et al*. demonstrated that the prezeamines have a higher bioactivity than zeamine II but less than the processed zeamines against the test organism *E. coli* and *Staphylococcus aureus* [116]. Surprisingly, our results showed that mixtures containing all fabclavine types are the most bioactive in comparison to mixtures of the shortened fabclavines with the polyamine or the polyamine alone (2.4). However, the concentration of single components in the mixtures was not determined, preventing a detailed comparison (2.4). Furthermore, the firstly described broad-spectrum bioactivity was based on assays with the purified full-length fabclavines Ia and Ib [113]. Future work will include the purification of shortened fabclavines and the polyamine to determine their bioactivity in comparison to the full-length derivate.

Based on the high structural similarity it seems possible that zeamines and fabclavines share a common mode of action. Detailed analysis with a zeamine mixture (zeamine, zeamine I and zeamine II) revealed that the bioactivity is based on direct membrane interactions without participating proteins [129]. Thereby, the membrane gets nonspecifically permeabilized, leading to a subsequent inhibition of the primary metabolism or to cell lysis in a dose-dependent manner [129]. The composition of the

membranes seems to be important as stronger effects on bacterial than on eukaryotic model membranes could be observed [129]. Experiments with zeamine II alone led to similar results albeit higher doses were required [129]. This is in accordance with its previously observed, reduced antibacterial bioactivity [116,129]. Furthermore, it is likely that all three zeamine types contribute to the overall bioactivity, as they can be detected in the supernatant of wild type cultures [116]. Regarding the bioactivity, it is also important, how the producing organism protects itself. For *S. plymuthica* it was postulated, that some of the transport related genes, located in the zeamine BGC, are responsible for the transport and/or the resistance [114]. In contrast, the ABC-transporter system of *D. zeae*, encoded in the zeamine BGC, is not relevant for resistance [130]. Nevertheless, adjacent to the BGC further transporter genes were identified and a mutation drastically decreased the zeamine resistance [130]. Surprisingly, corresponding homologues were not found in proximity to the zeamine BGC in *S. plymuthica* but in further strains of the genus *Dickeya*, although they are not harboring the zeamine responsible genes [130].

The mode of action of the zeamines was mainly analyzed with artificial model membranes as well as bacterial strains [129]. Detailed studies were also performed for the compound Xlt with a special focus on insect toxicity [131]. Here, an insecticidal activity against the larvae stage of three mosquito species was observed, while most other insect species stayed unaffected [131]. In detail, Xlt induced apoptosis to mosquito cell lines of *Aedes aegypti* while no acute cytotoxicity on *Drosophila melanogaster* or *Manduca sexta* cell lines could be observed [131]. Furthermore, human cell lines were also affected at higher concentrations of Xlt [131]. Detailed analysis of mosquito larvae revealed a pH change and apoptosis in the anterior gut after Xlt treatment [131].

Antimicrobial peptides (AMPs) are not directly related to fabclavines, but both could share a common mode of action, especially concerning the cationic structural elements like the polyamine part [113,132]. AMPs are ribosomally synthesized, small-sized peptides with an overall positive charge while harboring also hydrophobic moieties [132,133]. They are widely distributed among nearly all living organism [132,133]. While the cationic character of AMPs initiates the interaction with bacterial membranes, the hydrophobic character leads to the insertion [133,134]. Thereby, the selectivity for bacterial membranes is higher than for eukaryotic due to its negatively charged surface,

generated by phospholipids, lipopolysaccharide or teichoic acids [134,135]. Regarding Gram-negative bacteria, AMPs use a process, called “self-promoted uptake”, to overcome the outer and reach the cytoplasmic membrane [134]. Subsequently, transient pore/channel-formation, disruption of or translocation through the cytoplasmic membrane occurs [134]. Here, it is important to mention, that almost all cationic amphiphilic peptides are able to disturb membranes in a concentration dependent manner [136]. Nevertheless, the permeabilization of the membrane is not necessarily the final target of the AMPs to kill the microbes. As example, minimal inhibitory concentrations of some peptides lead to the inhibition of RNA biosynthesis, but a 10-fold increase completely disrupts the membrane [136]. Further modes of action include the inhibition of essential processes like nucleic acid, protein and cell wall biosynthesis or of specific enzymes [134,135].

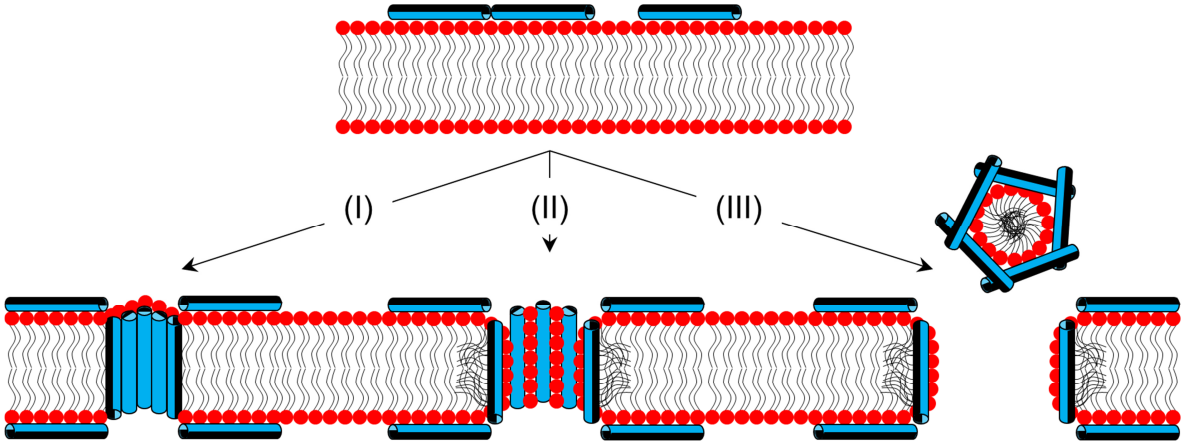

Figure 19. Schematic models for modes of action of AMPs. (I) Barrel-stave-model, (II) Toroidal model, (III) Carpet model. The barrels represent the AMPs with a hydrophilic part in blue and a hydrophobic part in black (adapted and modified from [134]).

For AMPs several models are described, illustrating possible modes of action to permeabilize the membrane (Figure 19) [137]. In the barrel stave model, the peptides locally accumulate and induce membrane thinning by moving the polar headgroups aside [137]. Afterwards, the hydrophobic part is inserted as staves inside of the membrane to finally form the barrel [137]. In contrast, in the toroidal model the hydrophilic parts of the AMPs are still associated with the polar headgroups after the perforation, which requires a bending of the membrane [137]. The carpet model

describes a detergent-like mechanism. Here, the AMPs cover the membrane, perforate it and ultimately form micelles, leading to a dispersive-like disruption [137].

Based on the reported bioactivities and modes of action for zeamines and Xlt, we assume that one of the three described models for AMPs can also fit to the fabclavines. Here, the central structural moiety would be the polyamine, occurring in all three fabclavine types [122]. Furthermore, it was shown that the polyamine alone already exhibits a bioactivity (2.4). In a first step, its cationic amino groups could initiate a parallel association with the negatively charged membrane surface via electrostatic attraction. Subsequently, fabclavines accumulate and the polar head groups of the membrane could be forced apart via electrostatic repulsion by the hydroxy groups, present in the polyamine and the PKS-part of the fabclavines. This destabilizes and thins the membrane. Finally, reaching a locally high concentration, the fabclavines could switch their conformation to vary the polyamine from a parallel to an orthogonal orientation in relation to the surface and span through the membrane. For AMPs this is described as threshold concentration concept in dependence of the peptide-to-lipid ratio [137]. Concentrations above a certain value can lead to changes regarding the conformation, membrane localization and association of the AMPs [137]. The NRPS-PKS-part of the full-length and shortened fabclavines could act as an anchor to stabilize the insertion through interaction with the membrane surface. Here, the existence of many, variable NRPS-PKS-parts, differing in chemical moieties as well as in the number of incorporated amino acids and polyketide units, could represent an adaption to challenge different membrane compositions [122,124]. Furthermore, it can not be excluded that there is stabilization via interaction of the fabclavine derivatives among each other, presumable mediated by the NRPS-PKS-part. Following this theory, the polyamine resembles the bioactive component while the NRPS-PKS-part is responsible for a structured mode of action. This could explain the reduced bioactivity of the polyamine alone as its mode of action would be less structured and therefore requires higher concentrations (2.4).

Finally, the membrane disruption could lead to a loss of cytoplasmic macromolecules as it was observed for zeamine [129]. Otherwise the entrance for further fabclavines into the cytoplasma could be enabled, aiming on potential intracellular targets.

4.2 Natural function of fabclavines – more than a general defense mechanism?

The fabclavines were initially postulated as universal protection against a large number of food competitors [113]. A recently published study revealed that 11 out of 25 analyzed *Xenorhabdus* strains harbor the corresponding *fcl* BGC [138]. Thereby, the cluster structure as well as the identity of the single proteins are highly conserved (2.1 and 2.2) [122,124]. Subsequent analysis of eight *Xenorhabdus* strains led to the identification of 32 different full-length derivatives (2.2) [113,124]. Interestingly, the general fabclavine composition with its NRPS-, PKS- and polyamine-parts stays unaltered, indicating that the overall structure as well as single functional groups are essential for bioactivity [124]. Only certain chemical moieties are flexible, which could be assigned to promiscuous specificities of single domain and enzyme activities [124]. The highest diversity was observed for *X. indica* with twelve and the lowest for *X. hominickii* with four different full-length derivatives (2.2) [124].

Thereby, the generation of a large variety of compounds by the same pathway is common among secondary metabolism [139–141]. As SMs do not contribute directly to the survival of the organism, they can benefit significantly to reproductive fitness in complex ecosystems. This includes a huge number of tasks like communication and quorum sensing, supporting development, modulating signal cascades but also as response to competitors [13]. The γ-proteobacteria *Xenorhabdus* and *Photorhabdus* switch between a mutualistic and pathogenic lifestyle depending on the life cycle of their host nematode (Figure 10) [108]. Thus, they are exposed to different environmental conditions with non-predictable threats and demands. Especially the pathogenic lifestyle is challenging, as the bacteria are not able to influence the selection of the prey [111]. This process is mainly executed by the nematode and can be differentiated into an ambushing and cruising strategy according to their mobility [111]. Moreover, the nematode can also be attracted by external factors like caryophyllene, which is released by maize roots in response to an herbivore attack [142]. As the bacteria are required for the suppression of the immune system and killing of the insect, it is indispensable that the bacteria are able to react against a variety of different prey organisms. A recent study postulated that the natural compound library of cytotoxic rhabdopeptide/xenortide

peptides is produced in order to establish an efficient strategy to circumvent the unpredictability problem [143]. In general, multiple product libraries with slightly differing derivatives can be observed in the genera *Xenorhabdus* and *Photorhabdus* like the insectidal xenocyloins [144], xentrivalpeptides [145], photohexapeptides [140] or GameXPeptides [146].

In summary, we assume that the wide distribution of the *fcl* BGC in combination with the large chemical variety is the microbial response to the challenging lifestyle with unpredictable threats as it can be observed for further natural product libraries. Moreover, bioactivity analysis revealed that except for two strains, the main bioactivity against selected microorganism can be assigned to the fabclavines (2.2) [124]. Therefore, promoter exchange mutants were analyzed. Solely for *X. indica* and *X. cabanillasii* a residual bioactivity was observed, while the fabclavine production was inactivated, indicating one or more further bioactive compounds [124].

The hypothesis of an universal protection by fabclavines was based on the broad-spectrum bioactivity of single purified derivatives [113]. Additional indicators like the wide distribution among the genus *Xenorhabdus*, the high structural diversity and the contribution to the overall bioactivity of single strains, strengthened the initial hypothesis. Nevertheless, recently published studies indicate that this hypothesis needs to be extended with more aggressive aims, as the biological activity is not restricted to microbes. Analysis of culture supernatants enriched with fabclavines from *X. szentirmaii* revealed a bioactivity against higher eukaryotes like *Caenorhabditis elegans* [147]. Furthermore, the Xlt mode of action can be assumed also for fabclavines, as Xlt was regarded as fabclavine derivate (2.2) [124]. Briefly, Xlt from *X. innexi* is insecticidal via induction of cell death in the anterior midgut of insect larvae [131]. Further studies showed that fabclavine-producing strains like *X. szentirmaii*, *X. indica* or *X. stockiae* have also an insecticidal activity [148–150]. Although no responsible compound was determined in these studies, we speculate about a correlation with fabclavines.

Taken together, the spectrum of fabclavine-afflicted organism can be extended to higher eukaryotes. Especially the bioactivity against insect larvae, which are preys for the nematode-*Xenorhabdus* symbiosis, highly indicates that fabclavines are not only involved in protecting the carcass but also in killing the insect. Nevertheless, this speculation has to be verified in further experiments.

4.3 Possible applications of fabclavines

A biological activity of SMs in the interest of humans is a rare attribute [141]. Hence, bioactive SMs are initially often regarded as potential new drugs. Depending on the desired application, the compound needs to possess specific properties like activity, stability and safety [151]. Regarding the fabclavines, only two out of three conditions are met: First, this SM class exhibits a thermal stability, as it maintains activity after heating (2.4). Second, it posesses a potent bioactivity against a variety of organisms [113,124,147]. Nevertheless, the unspecific bioactivity did not pass the third safety critieria, as eukaryotic cell lines are also affected [113].

During this thesis, fabclavines were described as agent against endodontic infections caused by *Enterococcus faecalis* (2.3) [125]. Despite promising antibacterial effects of the analyzed supernatant of *X. cabanillasii*, a possible application seems to be uncertain, as this strain produces a comparable set of derivatives like *X. budapestensis*, which revealed cytotoxic activity [113,124,125].

Other potential applications are biological pest control agents (BCA). Generally, BCAs are organisms like viruses, bacteria, protozoa, fungi and nematodes, which were utilized to control pests [152]. Especially for insect control in agricultural applications the latter were analyzed intensely with a special focus on the genus *Steinernema* and *Heterorhabditis*, associated with *Xenorhabdus* and *Photorhabdus* bacteria [153]. Thereby, it was observed that the correct application is difficile, as efficiency depends strongly on biotic and abiotic factors like insect-nematode interaction, temperature or the relative ability of the nematodes to avoid desiccation [153]. However, nematode-based BCAs are commercially available in products like Nemaplus® (*Steinernema feltiae*) or Nematop® (*Heterorhabditis bacteriophora*) [154]. As *S. feltiae* is the nematode host of *X. bovienii* [155], a fabclavine-producing strain, other symbiotic pairs like *S. rarum* with *X. szentirmaii* or *S. bicornutum* with *X. budapestensis* could follow [156].

Another potential application correlates with global warming. Malaria, dengue or west nile fever are mosquito-transmitted diseases, which incidences are consequently coupled with their vectors [157]. As arthropods are cold-blooded, the climate change will afflict their habitats, resulting in a geographical shift of their occurence [157]. In order to minimize the spreading of such diseases and their influence on human health, suitable

applications are required against mosquitos. Here, fabclavines or corresponding producing strains with and without nematodes could act in a bifunctional way. Recently, a mosquito-deterrent activity was described for *X. budapestensis* [158,159]. Thereby, a partial purified fraction, containing fabclavine derivatives, was used as feeding-deterrence against *Aedes aegypti* with a similar or higher efficiency than the N,N-diethyl-3-methylbenzamide (DEET) [158]. DEET is a standard insect repellent and active ingredient in many products [158].

Additional to the deterrent activity of fabclavines, a mosquitocidal bioactivity was described for *X. innexi*, *X. indica*, *X. stockiae* and related isolates [127,131,149,150]. For all these strains, fabclavine production was confirmed (2.2) [124]. Nevertheless, only in *X. innexi* the mosquitocidal activity was directly linked to the fabclavine-like Xlt [127]. Although this bioactivity is interesting, the efficiency in field could be a limiting step as it often differs from results generated under laboratory conditions. Here, mosquito larvae are often directly exposed to bacterial cells or (diluted) supernatants [127,150]. In contrast, habitats of disease-transferring mosquito larvae of the genera *Aedes*, *Culex* or *Anopheles* are near to or directly in stagnant waters [157]. Consequently, utilization of bacterial suspensions or supernatants seems to be unrealistic, as the required concentration for a mosquitocidal activity can not be reached. Such problems could be circumvented using nematodes as vector systems for the bacteria in its natural symbiosis. Nevertheless, the environmental preferences of the nematodes have to be considered [153]. As we could identify a huge number of different strains, which produce fabclavines, their corresponding nematodes should be analyzed for their abilities to infect mosquito larvae under field conditions.

4.4 DH_{PKS} domain of *X. bovienii*

The analysis of *fcl* BGCs revealed an additional DH_{PKS} domain in *X. bovienii*, responsible for a novel deoxy-polyamine (2.4) [124]. Furthermore, this domain was successfully either covalently or as stand-alone enzyme integrated into further polyamine pathways, leading also to deoxy derivatives (2.4). Accordingly, the PKS-like and the FabA-like DH domains from the PUFA-biosynthesis of *Thraustochytrium* were also active as stand-alone enzymes [160]. Despite intensive efforts we were not able to

heterologously produce and purify the DH_{PKS} domain from *X. bovienii* (data not shown). As reductive loops are seen as integral units, the next step is to purify didomains, DH together with its adjacent KR domain in order to increase the solubility [72–75]. However, its activity as stand-alone enzyme could be utilized to convert fabclavine derivatives in the corresponding wild type strains in order to generate many novel deoxy-fabclavine derivatives (2.4) [124]. This could be performed in an easy and time-saving way via transformation of the DH_{PKS} domain on a separate plasmid.

Furthermore, *in silico* analysis revealed that a homologous DH domain can be found in the closely related zeamine BGC (2.4) [128]. However, the question remains to be answered, if this domain has a similar activity as in *X. bovienii*. As only hydroxy derivatives of the zeamine polyamine are described, it is possible that the zeamine DH domain is active as described for the PUFA-biosynthesis [105,116]. Here, the chain elongation depends on the activites of the PKS-like as well as FabA-like DH domain [105]. In contrast, the DH_{PKS} domain in *X. bovienii* is only required for the dehydration of the final β-ketogroup (2.4).

4.5 Further research opportunities

The fabclavine biosynthesis offers great oppurtunities for fundamental research, mainly based on three hallmarks. First, its highly specialized biosynthesis is derived from three different SM biosynthesis pathways. Hereby, it is important to consider that the PUFA-like and the NRPS-PKS-pathways work independently of each other. For the polyamine this was proven in multiple experiments like the heterologous production in *E. coli* or deletion of single genes (2.4). The NRPS-PKS-part is also independently generated, but it cannot be detected as it stays enzyme-bound on FclK [122]. Therefore, the condensation with the polyamine part is required. Nevertheless, this restriction can be circumvented by addition of the polyamine or co-cultivation experiments with polyamine-producing strains [122]. The junction between both pathways is the condensation domain-like protein FclL, which shows reduced substrate specificity regarding its amine substrate (2.4) [122].

Second, the *fcl* BGC is widely distributed, but still highly conserved regarding its synteny and protein identity (2.1 and 2.2) [122,124]. Consequently, there are many homologous

enzymes, which are slightly different, but still catalyze the same reaction. This facilitates the comparison as well as engineering approaches.
Finally, despite the high grade of homology of single proteins, there is still a large chemical diversity of produced derivatives (2.2) [124]. This suggests slight changes of the catalytic activity caused by slight differences between homologous enzymes or domains, which facilitates the identification of responsible domain structure or even single residues.
In conclusion, the independently working pathways of the biosynthesis in combination with the high conservation grade and large product diversity show great potential for further investigations.

4.5.1 Detailed elucidation of the polyamine biosynthesis

Biochemically, polyamines of the fabclavine biosynthesis are based on three to five amine units [124]. In detail, these long acyl chains (C_{28}-C_{44}) are substituted with multiple primary amines (N_4-N_6) and one hydroxy group [124]. The elucidation of the corresponding pathway is mainly based on single gene deletions, *in silico* analysis and comparison with the zeamine and PUFA biosynthesis (2.4) [122]. This revealed that the genes *fclCDEFG* are essential for polyamine formation, while *fclH* has an enhancing effect on the production titer (2.4) [122]. Furthermore, the role of an additional PKS-like DH domain, identified in *X. bovienii*, could be determined as essential factor for the formation of further deoxy derivatives (2.4).
Nevertheless, it remains unclear how the incorporation of different numbers of amine units is determined. The genes *fclC* and *fclD* as well as the *N*-terminal part of *fclE* are related to PUFA-biosynthesis, which can be described as mixed iterative type I system of PKS and FAS elements [97,122]. Thus, we expected that the chain length is regulated by a CLF domain, as it can be observed for PKS systems [126]. As such a domain can be found in FclD, gene exchange experiments were performed in a *X. szentirmaii* Δ*fclD* strain. This mutant was heterologously complemented with FclD from further fabclavine-producing strains, which naturally produce polyamines with different numbers of amine units. However, all heterologous complementation mutants produced polyamines with three incorporated amine units (Figure 14).

Although the determining factor is not FclD, all mutants produced polyamines, confirming a succesfull heterologous integration into the biosynthesis of *X. szentirmaii*. Strikingly, this suggests gene exchange experiments as suitable method in order to analyze further polyamine responsible genes. Moreover, the succesfull, covalent integration of the additional DH domain from *X. bovienii* into further fabclavine producing pathways indicates that also single domains could be exchanged among homologous enzymes (2.4). Combining both strategies could enable the identification of the chain length determining domain.

During PUFA-biosynthesis the specificity for different chain lengths of the two KS domains determines the final length of the polyenoic acyl chain [95]. Among the polyamine responsible enzymes also two KS domains occur, present in FclD as well as in FclC, which will be the aim in further experiments [122]. Another candidate is the thioester reductase FclG. As this enzyme is responsible for the reductive release of the polyamine intermediate as aldehyde, it could interrupt the chain elongation in a chain length or concentration dependent manner [122]. Furthermore, FclE as enoyl reductase/ aminotransferase and FclH as nitrilase can not be excluded at the current state of art. Finally, combinations of enzymes like FclC together with FclD are conceivable as well and have to be analyzed in future experiments.

4.5.2 Fabclavines in the genus *Photorhabdus*

While most of the presented work was focused on the genus *Xenorhabdus*, it is worth mentioning that homologous *fcl* genes were also identified in the genus *Photorhabdus* (2.1 and 2.2) [122,124]. Here as well, *fcl* BGCs are wide spread and can be found in three out of four species, respectively. These include *P. heterorhabditis* as well as multiple subspecies of *P. asymbiotica* and *P. temperata*, which are all closely related to each other (Figure 20) [161]. Depending on the synteny the BGCs can be classified into a *P. temperata*-, *P. asymbiotica*- and *P. heterorhabditis*-type (Figure 20). The first two harbor the PUFA-like genes *fclC*, *fclD* and *fclE* but not other adjacent *fcl* homologues (Figure 20). The massive BGC truncation in combination with a *X. bovienii*-similar domain organization imply the generation of a polyamine-like product (Figure 20) [124]. For instance, FclC harbors also an additional DH domain as it can be observed for

X. bovienii (2.4). Here, the DH domain is responsible for the formation of deoxy-polyamines (2.4). However, essential genes for the polyamine biosynthesis, like the ketoreductase FclF or the thioester reductase FclG, are missing in *Photorhabdus* (2.1) [122].

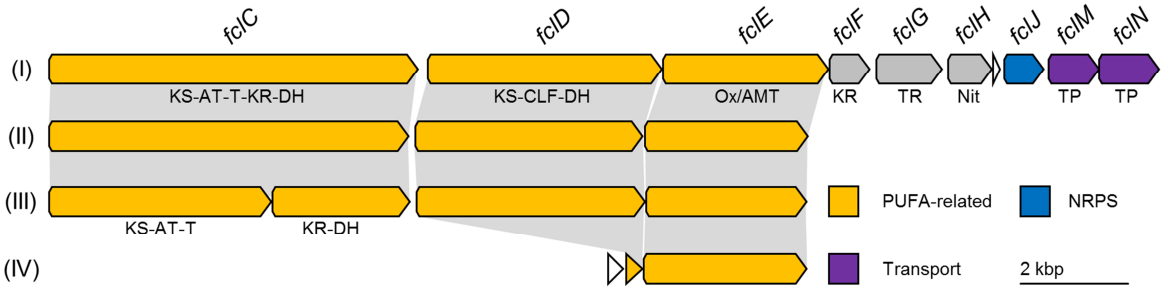

Figure 20. Types of *fcl* BGCs of the genus *Photorhabdus* in comparison with *X. bovienii* (2.4). (I) *X. bovienii* (II) *P. temperata*-type (including *P. temperata* subsp. *temperata*, subsp. *stackebrandtii*, subsp. *thracensis*, subsp. *khanii* and subsp. *tasmaniensis*) (III) *P. asymbiotica*-type (including *P. asymbiotica* subsp. *asymbiotica*, subsp. *australis* and *P. temperata* subsp. *cinerea*) (IV) *P. heterorhabditis*-type. Abbreviations: KS: ketosynthase, AT: acyltransferase, T: thiolation domain, KR: ketoreductase, DH: dehydratase, CLF: chain length factor domain, Ox: 2-nitropropane dioxygenase (enoyl reductase), AMT: aminotransferase, TR: thioester reductase, Nit: nitrilase, TP: transport

While all domains of FclC of the *P. temperata*-type BGC are encoded on one polypeptide, the *P. asymbiotica*-type FclC is subdivided into the tridomain KS-AT-T and the didomain KR-DH (Figure 20). Interestingly, the BGC of the strain *P. temperata* subsp. *cinerea* was also classified as *P. asymbiotica*-type (Figure 20). Finally, the *P. heterorhabditis*-type BGC harbors only a cryptic *fclD*-homologue beside *fclE*, indicating a non-functional biosynthesis (Figure 20). Despite extensive analysis of a *P. temperata* promoter-exchange mutant, no biosynthesis product could be detected, raising the question, if these BGCs are functional (2.2) [124]. However, a comparison of *P. temperata*, *P. asymbiotica* and *X. szentirmaii* revealed a high protein identity, which is only slightly lowered compared to alignments with other *Xenorhabdus* strains (2.1) [122]. Furthermore, the two FclC-parts of the *P. asymbiotica*-type are separated between the ACP domain and the didomain KR-DH (Figure 20). Such reductive loops appear as integral units, indicating that the subdivision of FclC can not be regarded as a non-specific gene disruption [72–75].

Assuming the *P. temperata*- and *P. asymbiotica*-type BGCs are functional, further analyses are required to identify biosynthesis products. Initially, *in silico* analysis could reveal whether these strains harbor further non-BGC encoded *fcl* homologues, especially *fclF* or *fclG*, which are essential for the biosynthesis in *Xenorhabdus* strains [122]. Due to the lack of release-responsible enzymes in these BGCs, other release mechanisms have to be considered. In reference to the expected PUFA-like biosynthesis the direct transfer on lipids or a release as fatty acid-like SM are conceivable [97,102,106]. As the initial analysis of the *P. temperata* promoter-exchange mutant was based on MALDI-MS analysis, the detection methods should be extended to high performance liquid chromatography- and gas chromatography-MS. Finally, co-expression experiments of *fclC*, *fclD* and *fclE* from the genus *Photorhabdus* with *fclF* and *fclG* from the genus *Xenorhabdus* could be conducted. As these genes are conserved and previous gene exchange experiments between *Xenorhabdus* strains already led to a functional biosynthesis, such chimeric pathways could be successful concerning product release and formation.

4.5.3 NRPS-NRPS-PKS interaction analyis

Type I NRPS or PKS are composed of single or multiple subunits or proteins [33,54]. In case of multiple subunits they have to interact with each other via *C*- and *N*-terminal communication-mediating (COM) or docking domains (DDs) to complete the SM assembly line [162–164]. Generally, DDs have a length of 15-60 amino acids and mediate specific non-covalent interactions to ensure the correct reaction order [162]. Hence, the exchange can alter the reaction order and thereby the resulting product as it was shown for the COM domains of the surfactin or tyrocidine biosynthesis [164,165]. Thereby, only certain key residues contribute to the selectivity between a DD pair, mainly by electrostatic or polar interactions [164]. While in NRPS systems the overall sequence homology between COM domains is relatively low, the *C*-terminal part appears to be more acidic while the *N*-terminal part contains more polar amino acids [164]. This pattern can also be observed in NRPS-PKS-hybrid systems [163]. During the fabclavine biosynthesis the NRPS FclI and FclJ as well as the PKS FclK are conserved between the different strains (2.1) [122]. Here, regarding the termini, the distribution of

negatively and positively charged residues indicates functionality as DDs or COM domains (Figure 21). Especially the terminal ends of FclJ are highly conserved with multiple identical residues between the compared homologues (Figure 21). Therefore, it is not surprising that gene exchanges of *fclJ* or *fclK* led to a heterologous functional biosynthesis (3.2 and 3.3).

(I)

```
       FclI C-terminus                  FclJ N-terminus
X.sz.  TAENPVRSGTIKRV----------VRGV-    -----MQQDTFKFKASLAQKRLWLHEQLEQQ
X.bud. TGGDSVRHNTISHNTSPQNTIKRVARERK    -----MQENTFQFKASLAQKRLWLHEQLEQQ
X.hom. TGEIPVRHSTIKRV----------VRRQE    -----MQENTYKFKASLAQKRLWLHEQLEQK
X.cab. TGEGSVRHNTISHNTGPKNTIKRVVRERK    -----MQENTFQFKASLAQKRLWLHEQLEQQ
X.ind. TGGDSVRHNTSSHNTGPQNTIKRVVRERK    -----MQENTFQFKASLAQKRLWLHEQLEQQ
X.sto. TGKVIDK-------NTQYNTIKRVVRGRK    -----MQENIFQFKASLAQKRLWLHEQLEQK
X.inn. TGKGAVH-----------NTIKRVVRGQK    MQEENMQENAFQFKASQAQKRVWLHEQLEQQ
       *.    :                .*           **:: ::**** ****:********:
```

(II)

```
       FclJ C-terminus                  FclK N-terminus
X.sz.  MNPNNLIDGRQRLAKRQKKMQHKG-----    MNNTDVNNTQKTQSMDLLPDYEMNAPEINDP
X.bud. VSQSNIADGRQRLAEMQKKMQQKQAKE--    MNNTEVNKVQVDHSQ---------MTQPMES
X.hom. INRDSIADGRQRLAQMQKKMQKKMQQQ--    MNNAELNKVQAMGSDE-----SMHGFEMNDF
X.cab. VSQSNIADGRQRLAEMQKKMQQK------    MNNTDVNKVQVDHSQ---------MAPSMES
X.ind. MSQSNIAGGRQRLAEMQKKMQQKQQQAKE    MNNTEVNKVQVDHSQ---------MTQSMEP
X.sto. TSLNNITDGRQRLAEMQKKMQQKR-----    MNNTDGNNVQREQA----------VESVSDL
X.inn. ASKNTIPEGRQRLAEMQKKMQQAKK----    -MNIDVNKNTDKNS-----DINEIQTKQIME
        . ..:  ******: *****:             * : *:     :
```

Figure 21. Postulated docking domains of FclI, FclJ and FclK. The alignment was performed with the online tool Clustal Omega (1.2.4). *X.sz.*: *Xenorhabdus szentirmaii*; *X.bud.*: *Xenorhabdus budapestensis*; *X.hom.*: *Xenorhabdus hominickii*; *X.cab.*: *X. cabanillasii*; *X.ind*: *X. indica*; *X.sto.*: *X. stockiae*; *X.inn.*: *X. innexi*.

While DDs are important to determine the correct reaction sequence in multi-enzymatic assembly lines, multiple studies claim the need for more structural elements involved to strengthen the protein-protein-interaction [163,165,166]. Potential candidates are the carrier-protein domains PCP and ACP [165]. During FAS in *E. coli* the corresponding ACP has to interact with at least 12 enzymes, which has to be precisely regulated via salt bridges and hydrophobic interactions [55].

Interestingly, in the fabclavine biosynthesis the subunits of the NRPS-PKS-hybrid-pathway are separated directly after the PCP domain of FclI and FclJ (Figure 11). Such

a separation can also be observed in the xenoamicin [167], cuidadopeptid or pseudotetratide biosynthesis [147]. Generally, the analysis of interactions between mega-enzymes *in vitro* is difficult due to the size of the involved proteins. Moreover, engineering approaches to manipulate the interaction surfaces often results in a disturbed three-dimensional structure. As *in vivo* experiments primarly analyze product formation, decreased production titers can result from a change in the subunit interaction or from an overall decreased enzyme activity, which are complicated to distinguish. Here, the fabclavine biosynthesis could serve as a suitable *in vivo* model system: The bifunctionality of FclJ as elongation as well as starting unit during peptide biosynthesis leads to the formation of full-length as well as shortened derivatives (2.1) [122]. This functionality serves as control mechanism to distinguish between manipulations afflicting the interaction with FclI and/or unintended disturbance of the enzyme activity of FclJ. Future works will include mutagenesis approaches to identify structural elements or amino acids, responsible for the interaction between both NRPS.

5 References

[1] N. Beales, Adaptation of Microorganisms to Cold Temperatures, Weak Acid Preservatives, Low pH, and Osmotic Stress: A Review, *Comprehensive Reviews in Food Science and Food Safety* 3 (2004) 1–20. https://doi.org/10.1111/j.1541-4337.2004.tb00057.x.

[2] C. Barria, M. Malecki, C.M. Arraiano, Bacterial adaptation to cold, *Microbiology* 159 (2013) 2437–2443. https://doi.org/10.1099/mic.0.052209-0.

[3] J.K. Kristjánsson, G.O. Hreggvidsson, Ecology and habitats of extremophiles, *World Journal of Microbiology & Biotechnology* 11 (1995) 17–25. https://doi.org/10.1007/BF00339134.

[4] C. Zhang, P.D. Straight, Antibiotic discovery through microbial interactions, *Current Opinion in Microbiology* 51 (2019) 64–71. https://doi.org/10.1016/j.mib.2019.06.006.

[5] S.W. Drew, A.L. Demain, Effect of primary metabolites on secondary metabolism, *Annual Review of Microbiology* 31 (1977) 343–356. https://doi.org/10.1146/annurev.mi.31.100177.002015.

[6] A.G. Fredrickson, G. Stephanopoulos, Microbial competition, *Sciences* 213 (1981) 972–979. https://doi.org/10.1126/science.7268409.

[7] L. Katz, R.H. Baltz, Natural product discovery: past, present, and future, *Journal of Industrial Microbiology & Biotechnology* 43 (2016) 155–176. https://doi.org/10.1007/s10295-015-1723-5.

[8] J. Davies, Specialized microbial metabolites: functions and origins, *The Journal of Antibiotics* 66 (2013) 361–364. https://doi.org/10.1038/ja.2013.61.

[9] J.S. Rokem, A.E. Lantz, J. Nielsen, Systems biology of antibiotic production by microorganisms, *Natural Product Reports* 24 (2007) 1262–1287. https://doi.org/10.1039/B617765B.

[10] S.A. Sieber, M.A. Marahiel, Molecular mechanisms underlying nonribosomal peptide synthesis: approaches to new antibiotics, *Chemical Reviews* 105 (2005) 715–738. https://doi.org/10.1021/cr0301191.

[11] A. Khan, P. Singh, A. Srivastava, Synthesis, nature and utility of universal iron chelator - Siderophore: A review, *Microbiological Research* 212-213 (2018) 103–111. https://doi.org/10.1016/j.micres.2017.10.012.

[12] N. Theis, M. Lerdau, The Evolution of Function in Plant Secondary Metabolites, *International Journal of Plant Sciences* 164 (2003) S93-S102. https://doi.org/10.1086/374190.

[13] Y.-M. Shi, H.B. Bode, Chemical language and warfare of bacterial natural products in bacteria-nematode-insect interactions, *Natural Product Reports* 35 (2018) 309–335. https://doi.org/10.1039/c7np00054e.

[14] K. Lewis, Antibiotics: Recover the lost art of drug discovery, *Nature* 485 (2012) 439–440. https://doi.org/10.1038/485439a.

[15] A. Fleming, On the Antibacterial Action of Cultures of a Penicillium, with Special Reference to their Use in the Isolation of *B. influenzæ*, *British Journal of Experimental Pathology* 10 (1929) 226–236.

[16] R.D. Cooper, P.V. DeMarco, J.C. Cheng, N.D. Jones, Structural studies on penicillin derivatives. I. The configuration of phenoxymethyl penicillin sulfoxide, *Journal of the American Chemical Society* 91 (1969) 1408–1415. https://doi.org/10.1021/ja01034a024.

[17] L. Valiquette, K.B. Laupland, Digging for new solutions*, The Canadian journal of infectious diseases & medical microbiology = Journal canadien des maladies infectieuses et de la microbiologie medicale* 26 (2015) 289–290. https://doi.org/10.1155/2015/971858.

[18] U. Galm, M.H. Hager, S.G. van Lanen, J. Ju, J.S. Thorson, B. Shen, Antitumor antibiotics: bleomycin, enediynes, and mitomycin, *Chemical Reviews* 105 (2005) 739–758. https://doi.org/10.1021/cr030117g.

[19] T. Schwecke, J.F. Aparicio, I. Molnár, A. König, L.E. Khaw, S.F. Haydock, M. Oliynyk, P. Caffrey, J. Cortés, J.B. Lester, The biosynthetic gene cluster for the polyketide immunosuppressant rapamycin, *Proceedings of the National Academy of Sciences of the United States of America* 92 (1995) 7839–7843. https://doi.org/10.1073/pnas.92.17.7839.

[20] F.E. Dayan, S.O. Duke, Natural compounds as next-generation herbicides, *Plant Physiology* 166 (2014) 1090–1105. https://doi.org/10.1104/pp.114.239061.

[21] R.H. Baltz, Natural product drug discovery in the genomic era: realities, conjectures, misconceptions, and opportunities, *Journal of Industrial Microbiology & Biotechnology* 46 (2019) 281–299. https://doi.org/10.1007/s10295-018-2115-4.

[22] B.O. Bachmann, S.G. van Lanen, R.H. Baltz, Microbial genome mining for accelerated natural products discovery: is a renaissance in the making?, *Journal of Industrial Microbiology & Biotechnology* 41 (2014) 175–184. https://doi.org/10.1007/s10295-013-1389-9.

[23] K. Blin, M.H. Medema, D. Kazempour, M.A. Fischbach, R. Breitling, E. Takano, T. Weber, antiSMASH 2.0--a versatile platform for genome mining of secondary metabolite producers, *Nucleic Acids Research* 41 (2013) W204-12. https://doi.org/10.1093/nar/gkt449.

[24] M.A. Marahiel, T. Stachelhaus, H.D. Mootz, Modular Peptide Synthetases Involved in Nonribosomal Peptide Synthesis, *Chemical Reviews* 97 (1997) 2651–2674. https://doi.org/10.1021/cr960029e.

[25] A.C. Mercer, M.D. Burkart, The ubiquitous carrier protein—a window to metabolite biosynthesis, *Natural Product Reports* 24 (2007) 750–773. https://doi.org/10.1039/b603921a.

[26] H. Jiang, R. Zirkle, J.G. Metz, L. Braun, L. Richter, S.G. van Lanen, B. Shen, The role of tandem acyl carrier protein domains in polyunsaturated fatty acid biosynthesis, *Journal of the American Chemical Society* 130 (2008) 6336–6337. https://doi.org/10.1021/ja801911t.

[27] J.N. Copp, B.A. Neilan, The phosphopantetheinyl transferase superfamily: phylogenetic analysis and functional implications in cyanobacteria, *Applied and Environmental Microbiology* 72 (2006) 2298–2305. https://doi.org/10.1128/AEM.72.4.2298–2305.2006.

[28] R.H. Lambalot, A.M. Gehring, R.S. Flugel, P. Zuber, M. LaCelle, M.A. Marahiel, R. Reid, C. Khosla, C.T. Walsh, A new enzyme superfamily — the phosphopantetheinyl transferases, *Chemistry & Biology* 3 (1996) 923–936. https://doi.org/10.1016/s1074-5521(96)90181-7.

[29] K.J. Weissman, H. Hong, M. Oliynyk, A.P. Siskos, P.F. Leadlay, Identification of a phosphopantetheinyl transferase for erythromycin biosynthesis in

Saccharopolyspora erythraea, *ChemBioChem* 5 (2004) 116–125. https://doi.org/10.1002/cbic.200300775.

[30] Y. Orikasa, T. Nishida, A. Hase, K. Watanabe, N. Morita, H. Okuyama, A phosphopantetheinyl transferase gene essential for biosynthesis of n-3 polyunsaturated fatty acids from *Moritella marina* strain MP-1, *FEBS letters* 580 (2006) 4423–4429. https://doi.org/10.1016/j.febslet.2006.07.008.

[31] H. Okuyama, Y. Orikasa, T. Nishida, K. Watanabe, N. Morita, Bacterial genes responsible for the biosynthesis of eicosapentaenoic and docosahexaenoic acids and their heterologous expression, *Applied and Environmental Microbiology* 73 (2007) 665–670. https://doi.org/10.1128/AEM.02270-06.

[32] M.A. Marahiel, Protein templates for the biosynthesis of peptide antibiotics, *Chemistry & Biology* 4 (1997) 561–567. https://doi.org/10.1016/S1074-5521(97)90242-8.

[33] H.D. Mootz, D. Schwarzer, M.A. Marahiel, Ways of Assembling Complex Natural Products on Modular Nonribosomal Peptide Synthetases, *ChemBioChem* 3 (2002) 490. https://doi.org/10.1002/1439-7633(20020603)3:6<490:AID-CBIC490>3.0.CO;2-N.

[34] T. Stachelhaus, H.D. Mootz, M.A. Marahiel, The specificity-conferring code of adenylation domains in nonribosomal peptide synthetases, *Chemistry & Biology* 6 (1999) 493–505. https://doi.org/10.1016/S1074-5521(99)80082-9.

[35] G.L. Challis, J. Ravel, C.A. Townsend, Predictive, structure-based model of amino acid recognition by nonribosomal peptide synthetase adenylation domains, *Chemistry & Biology* 7 (2000) 211–224. https://doi.org/10.1016/s1074-5521(00)00091-0.

[36] T. Stachelhaus, H.D. Mootz, V. Bergendahl, M.A. Marahiel, Peptide bond formation in nonribosomal peptide biosynthesis. Catalytic role of the condensation domain, *The Journal of Biological Chemistry* 273 (1998) 22773–22781. https://doi.org/10.1074/jbc.273.35.22773.

[37] T.A. Keating, D.E. Ehmann, R.M. Kohli, C.G. Marshall, J.W. Trauger, C.T. Walsh, Chain Termination Steps in Nonribosomal Peptide Synthetase Assembly Lines: Directed Acyl-S-Enzyme Breakdown in Antibiotic and Siderophore Biosynthesis,

ChemBioChem 2 (2001) 99–107. https://doi.org/10.1002/1439-7633(20010202)2:2<99:AID-CBIC99>3.0.CO;2-3.

[38] L. Du, L. Lou, PKS and NRPS release mechanisms, *Natural Product Reports* 27 (2010) 255–278. https://doi.org/10.1039/B912037H.

[39] F. Kopp, M.A. Marahiel, Macrocyclization strategies in polyketide and nonribosomal peptide biosynthesis, *Natural Product Reports* 24 (2007) 735–749. https://doi.org/10.1039/B613652B.

[40] M.A. Marahiel, Working outside the protein-synthesis rules: insights into non-ribosomal peptide synthesis, *Journal of Peptide Science* 15 (2009) 799–807. https://doi.org/10.1002/psc.1183.

[41] C.T. Walsh, R.V. O'Brien, C. Khosla, Nonproteinogenic amino acid building blocks for nonribosomal peptide and hybrid polyketide scaffolds, *Angewandte Chemie International Edition* 52 (2013) 7098–7124. https://doi.org/10.1002/anie.201208344.

[42] J. Li, S.E. Jensen, Nonribosomal biosynthesis of fusaricidins by *Paenibacillus polymyxa* PKB1 involves direct activation of a D-amino acid, *Chemistry & Biology* 15 (2008) 118–127. https://doi.org/10.1016/j.chembiol.2007.12.014.

[43] C. Rausch, I. Hoof, T. Weber, W. Wohlleben, D.H. Huson, Phylogenetic analysis of condensation domains in NRPS sheds light on their functional evolution, *BMC Evolutionary Biology* 7 (2007) 78. https://doi.org/10.1186/1471-2148-7-78.

[44] J.M. Reimer, M.N. Aloise, P.M. Harrison, T.M. Schmeing, Synthetic cycle of the initiation module of a formylating nonribosomal peptide synthetase, *Nature* 529 (2016) 239–242. https://doi.org/10.1038/nature16503.

[45] C.T. Walsh, H. Chen, T.A. Keating, B.K. Hubbard, H.C. Losey, L. Luo, C.G. Marshall, D.A. Miller, H.M. Patel, Tailoring enzymes that modify nonribosomal peptides during and after chain elongation on NRPS assembly lines, *Current Opinion in Chemical Biology* 5 (2001) 525–534. https://doi.org/10.1016/S1367-5931(00)00235-0.

[46] D.A. Miller, C.T. Walsh, L. Luo, C-methyltransferase and cyclization domain activity at the intraprotein PK/NRP switch point of yersiniabactin synthetase, *Journal of the American Chemical Society* 123 (2001) 8434–8435. https://doi.org/10.1021/ja016398w.

[47] J. Liu, B. Wang, H. Li, Y. Xie, Q. Li, X. Qin, X. Zhang, J. Ju, Biosynthesis of the anti-infective marformycins featuring pre-NRPS assembly line N-formylation and O-methylation and post-assembly line C-hydroxylation chemistries, *Organic Letters* 17 (2015) 1509–1512. https://doi.org/10.1021/acs.orglett.5b00389.

[48] T. Stachelhaus, M.A. Marahiel, Modular structure of peptide synthetases revealed by dissection of the multifunctional enzyme GrsA, *The Journal of Biological Chemistry* 270 (1995) 6163–6169. https://doi.org/10.1074/jbc.270.11.6163.

[49] K.A.J. Bozhüyük, F. Fleischhacker, A. Linck, F. Wesche, A. Tietze, C.-P. Niesert, H.B. Bode, *De novo* design and engineering of non-ribosomal peptide synthetases, *Nature Chemistry* 10 (2018) 275–281. https://doi.org/10.1038/nchem.2890.

[50] M. Winn, J.K. Fyans, Y. Zhuo, J. Micklefield, Recent advances in engineering nonribosomal peptide assembly lines, *Natural Product Reports* 33 (2016) 317–347. https://doi.org/10.1039/C5NP00099H.

[51] M.J. Calcott, D.F. Ackerley, Genetic manipulation of non-ribosomal peptide synthetases to generate novel bioactive peptide products, *Biotechnology Letters* 36 (2014) 2407–2416. https://doi.org/10.1007/s10529-014-1642-y.

[52] K.A.J. Bozhüyük, A. Linck, A. Tietze, J. Kranz, F. Wesche, S. Nowak, F. Fleischhacker, Y.-N. Shi, P. Grün, H.B. Bode, Modification and *de novo* design of non-ribosomal peptide synthetases using specific assembly points within condensation domains, *Nature Chemistry* 11 (2019) 653–661. https://doi.org/10.1038/s41557-019-0276-z.

[53] C. Hertweck, The biosynthetic logic of polyketide diversity, *Angewandte Chemie International Edition* 48 (2009) 4688–4716. https://doi.org/10.1002/anie.200806121.

[54] T. Robbins, Y.-C. Liu, D.E. Cane, C. Khosla, Structure and mechanism of assembly line polyketide synthases, *Current Opinion in Structural Biology* 41 (2016) 10–18. https://doi.org/10.1016/j.sbi.2016.05.009.

[55] A. Chen, R.N. Re, M.D. Burkart, Type II fatty acid and polyketide synthases: deciphering protein-protein and protein-substrate interactions, *Natural Product Reports* 35 (2018) 1029–1045. https://doi.org/10.1039/c8np00040a.

[56] M.A. Fischbach, C.T. Walsh, Assembly-line enzymology for polyketide and nonribosomal Peptide antibiotics: logic, machinery, and mechanisms, *Chemical Reviews* 106 (2006) 3468–3496. https://doi.org/10.1021/cr0503097.

[57] K. Wu, L. Chung, W.P. Revill, L. Katz, C.D. Reeves, The FK520 gene cluster of *Streptomyces hygroscopicus* var. ascomyceticus (ATCC 14891) contains genes for biosynthesis of unusual polyketide extender units, *Gene* 251 (2000) 81–90. https://doi.org/10.1016/S0378-1119(00)00171-2.

[58] E.A.B. Emmert, A.K. Klimowicz, M.G. Thomas, J. Handelsman, Genetics of zwittermicin a production by *Bacillus cereus*, *Applied and Environmental Microbiology* 70 (2004) 104–113. https://doi.org/10.1128/AEM.70.1.104–113.2004.

[59] S. Kosol, M. Jenner, J.R. Lewandowski, G.L. Challis, Protein-protein interactions in trans-AT polyketide synthases, *Natural Product Reports* 35 (2018) 1097–1109. https://doi.org/10.1039/c8np00066b.

[60] M.B. Austin, J.P. Noel, The chalcone synthase superfamily of type III polyketide synthases, *Natural Product Reports* 20 (2003) 79–110. https://doi.org/10.1039/b100917f.

[61] C.R. Valenzano, R.J. Lawson, A.Y. Chen, C. Khosla, D.E. Cane, The biochemical basis for stereochemical control in polyketide biosynthesis, *Journal of the American Chemical Society* 131 (2009) 18501–18511. https://doi.org/10.1021/ja908296m.

[62] X. Xie, A. Garg, A.T. Keatinge-Clay, C. Khosla, D.E. Cane, Epimerase and Reductase Activities of Polyketide Synthase Ketoreductase Domains Utilize the Same Conserved Tyrosine and Serine Residues, *Biochemistry* 55 (2016) 1179–1186. https://doi.org/10.1021/acs.biochem.6b00024.

[63] M.A. Skiba, A.P. Sikkema, W.D. Fiers, W.H. Gerwick, D.H. Sherman, C.C. Aldrich, J.L. Smith, Domain Organization and Active Site Architecture of a Polyketide Synthase C-methyltransferase, *ACS chemical biology* 11 (2016) 3319–3327. https://doi.org/10.1021/acschembio.6b00759.

[64] R.M. Kohli, C.T. Walsh, Enzymology of acyl chain macrocyclization in natural product biosynthesis, *Chemical Communications* (2003) 297–307. https://doi.org/10.1039/b208333g.

[65] R.H. Lambalot, D.E. Cane, J.J. Aparicio, L. Katz, Overproduction and characterization of the erythromycin C-12 hydroxylase, EryK, *Biochemistry* 34 (1995) 1858–1866. https://doi.org/10.1021/bi00006a006.

[66] S. Gaisser, J. Reather, G. Wirtz, L. Kellenberger, J. Staunton, P.F. Leadlay, A defined system for hybrid macrolide biosynthesis in *Saccharopolyspora erythraea*,

Molecular Microbiology 36 (2000) 391–401. https://doi.org/10.1046/j.1365-2958.2000.01856.x.

[67] M. Klaus, M. Grininger, Engineering strategies for rational polyketide synthase design, Natural Product Reports 35 (2018) 1070–1081. https://doi.org/10.1039/c8np00030a.

[68] H.G. Menzella, R. Reid, J.R. Carney, S.S. Chandran, S.J. Reisinger, K.G. Patel, D.A. Hopwood, D.V. Santi, Combinatorial polyketide biosynthesis by *de novo* design and rearrangement of modular polyketide synthase genes, *Nature Biotechnology* 23 (2005) 1171–1176. https://doi.org/10.1038/nbt1128.

[69] J.F. Barajas, J.M. Blake-Hedges, C.B. Bailey, S. Curran, J.D. Keasling, Engineered polyketides: Synergy between protein and host level engineering, *Synthetic and Systems Biotechnology* 2 (2017) 147–166. https://doi.org/10.1016/j.synbio.2017.08.005.

[70] A.F. Marsden, B. Wilkinson, J. Cortés, N.J. Dunster, J. Staunton, P.F. Leadlay, Engineering broader specificity into an antibiotic-producing polyketide synthase, *Science* 279 (1998) 199–202. https://doi.org/10.1126/science.279.5348.199.

[71] R. McDaniel, A. Thamchaipenet, C. Gustafsson, H. Fu, M. Betlach, G. Ashley, Multiple genetic modifications of the erythromycin polyketide synthase to produce a library of novel “unnatural” natural products, *Proceedings of the National Academy of Sciences of the United States of America* 96 (1999) 1846–1851. https://doi.org/10.1073/pnas.96.5.1846.

[72] L. Kellenberger, I.S. Galloway, G. Sauter, G. Böhm, U. Hanefeld, J. Cortés, J. Staunton, P.F. Leadlay, A polylinker approach to reductive loop swaps in modular polyketide synthases, *ChemBioChem* 9 (2008) 2740–2749. https://doi.org/10.1002/cbic.200800332.

[73] A. Hagen, S. Poust, T.d. Rond, J.L. Fortman, L. Katz, C.J. Petzold, J.D. Keasling, Engineering a Polyketide Synthase for *In Vitro* Production of Adipic Acid, *ACS synthetic biology* 5 (2016) 21–27. https://doi.org/10.1021/acssynbio.5b00153.

[74] S. Dutta, J.R. Whicher, D.A. Hansen, W.A. Hale, J.A. Chemler, G.R. Congdon, A.R.H. Narayan, K. Håkansson, D.H. Sherman, J.L. Smith, G. Skiniotis, Structure of a modular polyketide synthase, *Nature* 510 (2014) 512–517. https://doi.org/10.1038/nature13423.

[75] H. Hong, A.N. Appleyard, A.P. Siskos, J. Garcia-Bernardo, J. Staunton, P.F. Leadlay, Chain initiation on type I modular polyketide synthases revealed by limited proteolysis and ion-trap mass spectrometry, *The FEBS Journal* 272 (2005) 2373–2387. https://doi.org/10.1111/j.1742-4658.2005.04615.x.

[76] C.R. Raetz, Biochemistry of endotoxins, *Annual Review of Biochemistry* 59 (1990) 129–170. https://doi.org/10.1146/annurev.bi.59.070190.001021.

[77] J.B. Parsons, C.O. Rock, Bacterial lipids: metabolism and membrane homeostasis, *Progress in Lipid Research* 52 (2013) 249–276. https://doi.org/10.1016/j.plipres.2013.02.002.

[78] M. Grininger, Perspectives on the evolution, assembly and conformational dynamics of fatty acid synthase type I (FAS I) systems, *Current Opinion in Structural Biology* 25 (2014) 49–56. https://doi.org/10.1016/j.sbi.2013.12.004.

[79] M.S. Davis, J. Solbiati, J.E. Cronan, Overproduction of acetyl-CoA carboxylase activity increases the rate of fatty acid biosynthesis in *Escherichia coli*, *The Journal of Biological Chemistry* 275 (2000) 28593–28598. https://doi.org/10.1074/jbc.M004756200.

[80] D. Boehringer, N. Ban, M. Leibundgut, 7.5-Å cryo-em structure of the mycobacterial fatty acid synthase, *Journal of Molecular Biology* 425 (2013) 841–849. https://doi.org/10.1016/j.jmb.2012.12.021.

[81] S. Smith, S.-C. Tsai, The type I fatty acid and polyketide synthases: a tale of two megasynthases, *Natural Product Reports* 24 (2007) 1041–1072. https://doi.org/10.1039/b603600g.

[82] H. Lu, P.J. Tonge, Inhibitors of FabI, an enzyme drug target in the bacterial fatty acid biosynthesis pathway, *Accounts of Chemical Research* 41 (2008) 11–20. https://doi.org/10.1021/ar700156e.

[83] C.O. Rock, S. Jackowski, Forty years of bacterial fatty acid synthesis, *Biochemical and Biophysical Research Communications* 292 (2002) 1155–1166. https://doi.org/10.1006/bbrc.2001.2022.

[84] K.H. Choi, R.J. Heath, C.O. Rock, beta-ketoacyl-acyl carrier protein synthase III (FabH) is a determining factor in branched-chain fatty acid biosynthesis, *Journal of Bacteriology* 182 (2000) 365–370. https://doi.org/10.1128/jb.182.2.365-370.2000.

[85] P. Edwards, J. Sabo Nelsen, J.G. Metz, K. Dehesh, Cloning of the fabF gene in an expression vector and in vitro characterization of recombinant fabF and fabB encoded enzymes from *Escherichia coli*, *FEBS Letters* 402 (1997) 62–66. https://doi.org/10.1016/S0014-5793(96)01437-8.

[86] R.J. Heath, C.O. Rock, Roles of the FabA and FabZ beta-hydroxyacyl-acyl carrier protein dehydratases in *Escherichia coli* fatty acid biosynthesis, *The Journal of Biological Chemistry* 271 (1996) 27795–27801. https://doi.org/10.1074/jbc.271.44.27795.

[87] R. Ernst, C.S. Ejsing, B. Antonny, Homeoviscous Adaptation and the Regulation of Membrane Lipids, *Journal of Molecular Biology* 428 (2016) 4776–4791. https://doi.org/10.1016/j.jmb.2016.08.013.

[88] M. Sinensky, Homeoviscous adaptation—a homeostatic process that regulates the viscosity of membrane lipids in *Escherichia coli*, *Proceedings of the National Academy of Sciences of the United States of America* 71 (1974) 522–525. https://doi.org/10.1073/pnas.71.2.522.

[89] J. Yao, C.O. Rock, Phosphatidic acid synthesis in bacteria, *Biochimica et Biophysica Acta* 1831 (2013) 495–502. https://doi.org/10.1016/j.bbalip.2012.08.018.

[90] H. Lee, W.J. Park, Unsaturated fatty acids, desaturases, and human health, *Journal of Medicinal Food* 17 (2014) 189–197. https://doi.org/10.1089/jmf.2013.2917.

[91] J.M. Lee, H. Lee, S. Kang, W.J. Park, Fatty Acid Desaturases, Polyunsaturated Fatty Acid Regulation, and Biotechnological Advances, *Nutrients* 8 (2016) 23. https://doi.org/10.3390/nu8010023.

[92] T. Oura, S. Kajiwara, *Saccharomyces kluyveri* FAD3 encodes an omega3 fatty acid desaturase, *Microbiology* 150 (2004) 1983–1990. https://doi.org/10.1099/mic.0.27049-0.

[93] P. Vrinten, Z. Hu, M.-A. Munchinsky, G. Rowland, X. Qiu, Two FAD3 desaturase genes control the level of linolenic acid in flax seed, *Plant Physiology* 139 (2005) 79–87. https://doi.org/10.1104/pp.105.064451.

[94] J.P. Spychalla, A.J. Kinney, J. Browse, Identification of an animal omega-3 fatty acid desaturase by heterologous expression in *Arabidopsis*, *Proceedings of the National Academy of Sciences of the United States of America* 94 (1997) 1142–1147. https://doi.org/10.1073/pnas.94.4.1142.

[95] S. Hayashi, M. Naka, K. Ikeuchi, M. Ohtsuka, K. Kobayashi, Y. Satoh, Y. Ogasawara, C. Maruyama, Y. Hamano, T. Ujihara, T. Dairi, Control Mechanism for Carbon-Chain Length in Polyunsaturated Fatty-Acid Synthases, *Angewandte Chemie International Edition* 58 (2019) 6605–6610. https://doi.org/10.1002/anie.201900771.

[96] J.G. Metz, P. Roessler, D. Facciotti, C. Levering, F. Dittrich, M. Lassner, R. Valentine, K. Lardizabal, F. Domergue, A. Yamada, K. Yazawa, V. Knauf, J. Browse, Production of polyunsaturated fatty acids by polyketide synthases in both prokaryotes and eukaryotes, *Science* 293 (2001) 290–293. https://doi.org/10.1126/science.1059593.

[97] K. Gemperlein, S. Rachid, R.O. Garcia, S.C. Wenzel, R. Müller, Polyunsaturated fatty acid biosynthesis in myxobacteria: different PUFA synthases and their product diversity, *Chemical Science* 5 (2014) 1733. https://doi.org/10.1039/c3sc53163e.

[98] S. Sugihara, Y. Orikasa, H. Okuyama, An EntD-like phosphopantetheinyl transferase gene from *Photobacterium profundum* SS9 complements pfa genes of *Moritella marina* strain MP-1 involved in biosynthesis of docosahexaenoic acid, *Biotechnology Letters* 30 (2008) 411–414. https://doi.org/10.1007/s10529-007-9579-z.

[99] D.S. Nichols, T.A. McMeekin, Biomarker techniques to screen for bacteria that produce polyunsaturated fatty acids, *Journal of Microbiological Methods* 48 (2002) 161–170. https://doi.org/10.1016/S0167-7012(01)00320-7.

[100] E.E. Allen, D.H. Bartlett, Structure and regulation of the omega-3 polyunsaturated fatty acid synthase genes from the deep-sea bacterium *Photobacterium profundum* strain SS9, *Microbiology* 148 (2002) 1903–1913. https://doi.org/10.1099/00221287-148-6-1903.

[101] T. Ujihara, M. Nagano, H. Wada, S. Mitsuhashi, Identification of a novel type of polyunsaturated fatty acid synthase involved in arachidonic acid biosynthesis, *FEBS Letters* 588 (2014) 4032–4036. https://doi.org/10.1016/j.febslet.2014.09.023.

[102] J.G. Metz, J. Kuner, B. Rosenzweig, J.C. Lippmeier, P. Roessler, R. Zirkle, Biochemical characterization of polyunsaturated fatty acid synthesis in *Schizochytrium*: release of the products as free fatty acids, *Plant Physiology and Biochemistry* 47 (2009) 472–478. https://doi.org/10.1016/j.plaphy.2009.02.002.

[103] B. Leyland, S. Leu, S. Boussiba, Are *Thraustochytrids* algae?, *Fungal Biology* 121 (2017) 835–840. https://doi.org/10.1016/j.funbio.2017.07.006.

[104] S. Hayashi, Y. Satoh, T. Ujihara, Y. Takata, T. Dairi, Enhanced production of polyunsaturated fatty acids by enzyme engineering of tandem acyl carrier proteins, *Scientific Reports* 6 (2016) 35441. https://doi.org/10.1038/srep35441.

[105] S. Hayashi, Y. Satoh, Y. Ogasawara, C. Maruyama, Y. Hamano, T. Ujihara, T. Dairi, Control Mechanism for cis Double-Bond Formation by Polyunsaturated Fatty-Acid Synthases, *Angewandte Chemie International Edition* 58 (2019) 2326–2330. https://doi.org/10.1002/anie.201812623.

[106] M. Rodríguez-Guilbe, D. Oyola-Robles, E.R. Schreiter, A. Baerga-Ortiz, Structure, activity, and substrate selectivity of the Orf6 thioesterase from *Photobacterium profundum*, *The Journal of Biological Chemistry* 288 (2013) 10841–10848. https://doi.org/10.1074/jbc.M112.446765.

[107] H.B. Bode, Entomopathogenic bacteria as a source of secondary metabolites, *Current Opinion in Chemical Biology* 13 (2009) 224–230. https://doi.org/10.1016/j.cbpa.2009.02.037.

[108] H. Goodrich-Blair, D.J. Clarke, Mutualism and pathogenesis in *Xenorhabdus* and *Photorhabdus*: two roads to the same destination, *Molecular Microbiology* 64 (2007) 260–268. https://doi.org/10.1111/j.1365-2958.2007.05671.x.

[109] R. ffrench-Constant, N. Waterfield, P. Daborn, S. Joyce, H. Bennett, C. Au, A. Dowling, S. Boundy, S. Reynolds, D. Clarke, *Photorhabdus*: towards a functional genomic analysis of a symbiont and pathogen, *FEMS Microbiology Reviews* 26 (2003) 433–456. https://doi.org/10.1111/j.1574-6976.2003.tb00625.x.

[110] E.C. Martens, H. Goodrich-Blair, The *Steinernema carpocapsae* intestinal vesicle contains a subcellular structure with which *Xenorhabdus nematophila* associates during colonization initiation, *Cellular Microbiology* 7 (2005) 1723–1735. https://doi.org/10.1111/j.1462-5822.2005.00585.x.

[111] H.K. Kaya, R. Gaugler, Entomopathogenic Nematodes, *Annual Review of Entomology* 38 (1993) 181–206. https://doi.org/10.1146/annurev.en.38.010193.001145.

[112] E. Duchaud, C. Rusniok, L. Frangeul, C. Buchrieser, A. Givaudan, S. Taourit, S. Bocs, C. Boursaux-Eude, M. Chandler, J.-F. Charles, E. Dassa, R. Derose, S.

Derzelle, G. Freyssinet, S. Gaudriault, C. Médigue, A. Lanois, K. Powell, P. Siguier, R. Vincent, V. Wingate, M. Zouine, P. Glaser, N. Boemare, A. Danchin, F. Kunst, The genome sequence of the entomopathogenic bacterium *Photorhabdus luminescens*, *Nature Biotechnology* 21 (2003) 1307–1313. https://doi.org/10.1038/nbt886.

[113] S.W. Fuchs, F. Grundmann, M. Kurz, M. Kaiser, H.B. Bode, Fabclavines: bioactive peptide-polyketide-polyamino hybrids from *Xenorhabdus*, *ChemBioChem* 15 (2014) 512–516. https://doi.org/10.1002/cbic.201300802.

[114] J. Masschelein, W. Mattheus, L.-J. Gao, P. Moons, R. van Houdt, B. Uytterhoeven, C. Lamberigts, E. Lescrinier, J. Rozenski, P. Herdewijn, A. Aertsen, C. Michiels, R. Lavigne, A PKS/NRPS/FAS hybrid gene cluster from *Serratia plymuthica* RVH1 encoding the biosynthesis of three broad spectrum, zeamine-related antibiotics, *PloS ONE* 8 (2013) e54143. https://doi.org/10.1371/journal.pone.0054143.

[115] J. Zhou, H. Zhang, J. Wu, Q. Liu, P. Xi, J. Lee, J. Liao, Z. Jiang, L.-H. Zhang, A novel multidomain polyketide synthase is essential for zeamine production and the virulence of *Dickeya zeae*, *Molecular Plant-Microbe Interactions* 24 (2011) 1156–1164. https://doi.org/10.1094/MPMI-04-11-0087.

[116] J. Masschelein, C. Clauwers, U.R. Awodi, K. Stalmans, W. Vermaelen, E. Lescrinier, A. Aertsen, C. Michiels, G.L. Challis, R. Lavigne, A combination of polyunsaturated fatty acid, nonribosomal peptide and polyketide biosynthetic machinery is used to assemble the zeamine antibiotics, *Chemical Science* 6 (2015) 923–929. https://doi.org/10.1039/c4sc01927j.

[117] G. Berg, Diversity of antifungal and plant-associated *Serratia plymuthica* strains, *Journal of Applied Microbiology* 88 (2000) 952–960. https://doi.org/10.1046/j.1365-2672.2000.01064.x.

[118] L. Liao, Y. Cheng, S. Liu, J. Zhou, S. An, M. Lv, Y. Chen, Y. Gu, S. Chen, L.-H. Zhang, Production of novel antibiotics zeamines through optimizing *Dickeya zeae* fermentation conditions, *PloS ONE* 9 (2014) e116047. https://doi.org/10.1371/journal.pone.0116047.

[119] J. Houard, A. Aumelas, T. Noël, S. Pages, A. Givaudan, V. Fitton-Ouhabi, P. Villain-Guillot, M. Gualtieri, Cabanillasin, a new antifungal metabolite, produced by

entomopathogenic *Xenorhabdus cabanillasii* JM26, *The Journal of Antibiotics* 66 (2013) 617–620. https://doi.org/10.1038/ja.2013.58.

[120] N.A.R. Gow, B. Yadav, Microbe Profile: *Candida albicans*: a shape-changing, opportunistic pathogenic fungus of humans, *Microbiology* 163 (2017) 1145–1147. https://doi.org/10.1099/mic.0.000499.

[121] K. Ziegler, A. Diener, C. Herpin, R. Richter, R. Deutzmann, W. Lockau, Molecular characterization of cyanophycin synthetase, the enzyme catalyzing the biosynthesis of the cyanobacterial reserve material multi- L-arginyl-poly- L-aspartate (cyanophycin), *European Journal of Biochemistry* 254 (1998) 154–159. https://doi.org/10.1046/j.1432-1327.1998.2540154.x.

[122] S.L. Wenski, D. Kolbert, G.L.C. Grammbitter, H.B. Bode, Fabclavine biosynthesis in *X. szentirmaii*: shortened derivatives and characterization of the thioester reductase FclG and the condensation domain-like protein FclL, *Journal of Industrial Microbiology & Biotechnology* 46 (2019) 565–572. https://doi.org/10.1007/s10295-018-02124-8.

[123] E. Bode, A.O. Brachmann, C. Kegler, R. Simsek, C. Dauth, Q. Zhou, M. Kaiser, P. Klemmt, H.B. Bode, Simple “on-demand” production of bioactive natural products, *ChemBioChem* 16 (2015) 1115–1119. https://doi.org/10.1002/cbic.201500094.

[124] S.L. Wenski, H. Cimen, N. Berghaus, S.W. Fuchs, S. Hazir, H.B. Bode, Fabclavine diversity in *Xenorhabdus* bacteria, *Beilstein Journal of Organic Chemistry* 16 (2020) 956–965. https://doi.org/10.3762/bjoc.16.84.

[125] H. Donmez Ozkan, H. Cimen, D. Ulug, S. Wenski, S. Yigit Ozer, M. Telli, N. Aydin, H.B. Bode, S. Hazir, Nematode-Associated Bacteria: Production of Antimicrobial Agent as a Presumptive Nominee for Curing Endodontic Infections Caused by *Enterococcus faecalis*, *Frontiers in Microbiology* 10 (2019) 2672. https://doi.org/10.3389/fmicb.2019.02672.

[126] Y. Tang, S.-C. Tsai, C. Khosla, Polyketide chain length control by chain length factor, *Journal of the American Chemical Society* 125 (2003) 12708–12709. https://doi.org/10.1021/ja0378759.

[127] I.-H. Kim, S.K. Aryal, D.T. Aghai, Á.M. Casanova-Torres, K. Hillman, M.P. Kozuch, E.J. Mans, T.J. Mauer, J.-C. Ogier, J.C. Ensign, S. Gaudriault, W.G.

Goodman, H. Goodrich-Blair, A.R. Dillman, The insect pathogenic bacterium *Xenorhabdus innexi* has attenuated virulence in multiple insect model hosts yet encodes a potent mosquitocidal toxin, *BMC Genomics* 18 (2017) 927. https://doi.org/10.1186/s12864-017-4311-4.

[128] J.E.E.U. Hellberg, M.A. Matilla, G.P.C. Salmond, The broad-spectrum antibiotic, zeamine, kills the nematode worm *Caenorhabditis elegans*, *Frontiers in Microbiology* 6 (2015) 137. https://doi.org/10.3389/fmicb.2015.00137.

[129] J. Masschelein, C. Clauwers, K. Stalmans, K. Nuyts, W. de Borggraeve, Y. Briers, A. Aertsen, C.W. Michiels, R. Lavigne, The zeamine antibiotics affect the integrity of bacterial membranes, *Applied and Environmental Microbiology* 81 (2015) 1139–1146. https://doi.org/10.1128/AEM.03146-14.

[130] Z. Liang, L. Huang, F. He, X. Zhou, Z. Shi, J. Zhou, Y. Chen, M. Lv, Y. Chen, L.-H. Zhang, A Substrate-Activated Efflux Pump, DesABC, Confers Zeamine Resistance to *Dickeya zeae*, *mBio* 10 (2019) e00713-19. https://doi.org/10.1128/mBio.00713-19.

[131] I.-H. Kim, J. Ensign, D.-Y. Kim, H.-Y. Jung, N.-R. Kim, B.-H. Choi, S.-M. Park, Q. Lan, W.G. Goodman, Specificity and putative mode of action of a mosquito larvicidal toxin from the bacterium *Xenorhabdus innexi*, *Journal of Invertebrate Pathology* 149 (2017) 21–28. https://doi.org/10.1016/j.jip.2017.07.002.

[132] Y. Li, Q. Xiang, Q. Zhang, Y. Huang, Z. Su, Overview on the recent study of antimicrobial peptides: origins, functions, relative mechanisms and application, *Peptides* 37 (2012) 207–215. https://doi.org/10.1016/j.peptides.2012.07.001.

[133] R.E.W. Hancock, H.-G. Sahl, Antimicrobial and host-defense peptides as new anti-infective therapeutic strategies, *Nature Biotechnology* 24 (2006) 1551–1557. https://doi.org/10.1038/nbt1267.

[134] H. Jenssen, P. Hamill, R.E.W. Hancock, Peptide antimicrobial agents, *Clinical MIcrobiology Reviews* 19 (2006) 491–511. https://doi.org/10.1128/CMR.00056-05.

[135] K.A. Brogden, Antimicrobial peptides: pore formers or metabolic inhibitors in bacteria?, *Nature Reviews. Microbiology* 3 (2005) 238–250. https://doi.org/10.1038/nrmicro1098.

[136] R.E.W. Hancock, A. Rozek, Role of membranes in the activities of antimicrobial cationic peptides, *FEMS Microbiology Letters* 206 (2002) 143–149. https://doi.org/10.1111/j.1574-6968.2002.tb11000.x.

[137] V. Teixeira, M.J. Feio, M. Bastos, Role of lipids in the interaction of antimicrobial peptides with membranes, *Progress in Lipid Research* 51 (2012) 149–177. https://doi.org/10.1016/j.plipres.2011.12.005.

[138] N.J. Tobias, H. Wolff, B. Djahanschiri, F. Grundmann, M. Kronenwerth, Y.-M. Shi, S. Simonyi, P. Grün, D. Shapiro-Ilan, S.J. Pidot, T.P. Stinear, I. Ebersberger, H.B. Bode, Natural product diversity associated with the nematode symbionts *Photorhabdus* and *Xenorhabdus*, *Nature Microbiology* 2 (2017) 1676–1685. https://doi.org/10.1038/s41564-017-0039-9.

[139] S. Meyer, J.-C. Kehr, A. Mainz, D. Dehm, D. Petras, R.D. Süssmuth, E. Dittmann, Biochemical Dissection of the Natural Diversification of Microcystin Provides Lessons for Synthetic Biology of NRPS, *Cell Chemical Biology* 23 (2016) 462–471. https://doi.org/10.1016/j.chembiol.2016.03.011.

[140] L. Zhao, H.B. Bode, Production of a photohexapeptide library from entomopathogenic *Photorhabdus asymbiotica* PB68.1, *Organic & Biomolecular Chemistry* 17 (2019) 7858–7862. https://doi.org/10.1039/c9ob01489f.

[141] R.D. Firn, C.G. Jones, Natural products—a simple model to explain chemical diversity, *Natural Product Reports* 20 (2003) 382–391. https://doi.org/10.1039/b208815k.

[142] S. Rasmann, T.G. Köllner, J. Degenhardt, I. Hiltpold, S. Toepfer, U. Kuhlmann, J. Gershenzon, T.C.J. Turlings, Recruitment of entomopathogenic nematodes by insect-damaged maize roots, *Nature* 434 (2005) 732–737. https://doi.org/10.1038/nature03451.

[143] X. Cai, S. Nowak, F. Wesche, I. Bischoff, M. Kaiser, R. Fürst, H.B. Bode, Entomopathogenic bacteria use multiple mechanisms for bioactive peptide library design, *Nature Chemistry* 9 (2017) 379–386. https://doi.org/10.1038/nchem.2671.

[144] A. Proschak, Q. Zhou, T. Schöner, A. Thanwisai, D. Kresovic, A. Dowling, R. ffrench-Constant, E. Proschak, H.B. Bode, Biosynthesis of the insecticidal xenocyloins in *Xenorhabdus bovienii*, *ChemBioChem* 15 (2014) 369–372. https://doi.org/10.1002/cbic.201300694.

[145] Q. Zhou, A. Dowling, H. Heide, J. Wöhnert, U. Brandt, J. Baum, R. ffrench-Constant, H.B. Bode, Xentrivalpeptides A-Q: depsipeptide diversification in *Xenorhabdus*, *Journal of Natural Products* 75 (2012) 1717–1722. https://doi.org/10.1021/np300279g.

[146] F.I. Nollmann, C. Dauth, G. Mulley, C. Kegler, M. Kaiser, N.R. Waterfield, H.B. Bode, Insect-specific production of new GameXPeptides in *Photorhabdus luminescens* TTO1, widespread natural products in entomopathogenic bacteria, *ChemBioChem* 16 (2015) 205–208. https://doi.org/10.1002/cbic.201402603.

[147] E. Bode, A.K. Heinrich, M. Hirschmann, D. Abebew, Y.-N. Shi, T.D. Vo, F. Wesche, Y.-M. Shi, P. Grün, S. Simonyi, N. Keller, Y. Engel, S. Wenski, R. Bennet, S. Beyer, I. Bischoff, A. Buaya, S. Brandt, I. Cakmak, H. Çimen, S. Eckstein, D. Frank, R. Fürst, M. Gand, G. Geisslinger, S. Hazir, M. Henke, R. Heermann, V. Lecaudey, W. Schäfer, S. Schiffmann, A. Schüffler, R. Schwenk, M. Skaljac, E. Thines, M. Thines, T. Ulshöfer, A. Vilcinskas, T.A. Wichelhaus, H.B. Bode, Promoter Activation in Δ*hfq* Mutants as an Efficient Tool for Specialized Metabolite Production Enabling Direct Bioactivity Testing, *Angewandte Chemie International Edition* 58 (2019) 18957–18963. https://doi.org/10.1002/anie.201910563.

[148] C. Eroglu, H. Cimen, D. Ulug, M. Karagoz, S. Hazir, I. Cakmak, Acaricidal effect of cell-free supernatants from *Xenorhabdus* and *Photorhabdus* bacteria against *Tetranychus urticae* (Acari: Tetranychidae), *Journal of Invertebrate Pathology* 160 (2019) 61–66. https://doi.org/10.1016/j.jip.2018.12.004.

[149] M. Suwannaroj, T. Yimthin, C. Fukruksa, P. Muangpat, T. Yooyangket, S. Tandhavanant, A. Thanwisai, A. Vitta, Survey of entomopathogenic nematodes and associate bacteria in Thailand and their potential to control *Aedes aegypti*, *Journal of Applied Entomology* 1151 (2020) 747. https://doi.org/10.1111/jen.12726.

[150] A. Vitta, P. Thimpoo, W. Meesil, T. Yimthin, C. Fukruksa, R. Polseela, B. Mangkit, S. Tandhavanant, A. Thanwisai, Larvicidal activity of *Xenorhabdus* and *Photorhabdus* bacteria against *Aedes aegypti* and *Aedes albopictus*, *Asian Pacific Journal of Tropical Biomedicine* 8 (2018) 31-36. https://doi.org/10.4103/2221-1691.221134.

[151] M. Mahlapuu, J. Håkansson, L. Ringstad, C. Björn, Antimicrobial Peptides: An Emerging Category of Therapeutic Agents, *Frontiers in Cellular and Infection Microbiology* 6 (2016) 194. https://doi.org/10.3389/fcimb.2016.00194.

[152] G. Khachatourians, Production and use of biological pest control agents, *Trends in Biotechnology* 4 (1986) 120–124. https://doi.org/10.1016/0167-7799(86)90144-7.

[153] R. Georgis, A.M. Koppenhöfer, L.A. Lacey, G. Bélair, L.W. Duncan, P.S. Grewal, M. Samish, L. Tan, P. Torr, R.W.H.M. van Tol, Successes and failures in the use of parasitic nematodes for pest control, *Biological Control* 38 (2006) 103–123. https://doi.org/10.1016/j.biocontrol.2005.11.005.

[154] R.-U. Ehlers, D. Premachandra, O. Berndt, H.-M. Poehling, C. Borgemeister, Laboratory bioassays of virulence of entomopathogenic nematodes against soil-inhabiting stages of *Frankliniella occidentalis* Pergande (Thysanoptera: Thripidae), *Nematology* 5 (2003) 539–547. https://doi.org/10.1163/156854103322683256.

[155] E.E. Lewis, P.S. Grewal, S. Sardanelli, Interactions between the *Steinernema feltiae–Xenorhabdus bovienii* Insect Pathogen Complex and the Root-Knot Nematode *Meloidogyne incognita*, *Biological Control* 21 (2001) 55–62. https://doi.org/10.1006/bcon.2001.0918.

[156] K. Lengyel, E. Lang, A. Fodor, E. Szállás, P. Schumann, E. Stackebrandt, Description of four novel species of *Xenorhabdus*, family *Enterobacteriaceae*: *Xenorhabdus budapestensis* sp. nov., *Xenorhabdus ehlersii* sp. nov., *Xenorhabdus innexi* sp. nov., and *Xenorhabdus szentirmaii* sp. nov, *Systematic and Applied Microbiology* 28 (2005) 115–122. https://doi.org/10.1016/j.syapm.2004.10.004.

[157] A.A. Khasnis, M.D. Nettleman, Global warming and infectious disease, *Archives of Medical Research* 36 (2005) 689–696. https://doi.org/10.1016/j.arcmed.2005.03.041.

[158] M.K. Kajla, G.A. Barrett-Wilt, S.M. Paskewitz, Bacteria: A novel source for potent mosquito feeding-deterrents, *Science Advances* 5 (2019) eaau6141. https://doi.org/10.1126/sciadv.aau6141.

[159] M.K. Kajla, Symbiotic Bacteria as Potential Agents for Mosquito Control, *Trends in Parasitology* 36 (2020) 4–7. https://doi.org/10.1016/j.pt.2019.07.003.

[160] X. Xie, D. Meesapyodsuk, X. Qiu, Functional analysis of the dehydratase domains of a PUFA synthase from *Thraustochytrium* in *Escherichia coli*, *Applied*

Microbiology and Biotechnology 102 (2018) 847–856. https://doi.org/10.1007/s00253-017-8635-4.

[161] R.A.R. Machado, D. Wüthrich, P. Kuhnert, C.C.M. Arce, L. Thönen, C. Ruiz, X. Zhang, C.A.M. Robert, J. Karimi, S. Kamali, J. Ma, R. Bruggmann, M. Erb, Whole-genome-based revisit of *Photorhabdus* phylogeny: proposal for the elevation of most *Photorhabdus* subspecies to the species level and description of one novel species *Photorhabdus bodei* sp. nov., and one novel subspecies *Photorhabdus laumondii* subsp. clarkei subsp. nov, *International Journal of Systematic and Evolutionary Microbiology* 44 (2018) 92. https://doi.org/10.1099/ijsem.0.002820.

[162] J. Watzel, C. Hacker, E. Duchardt-Ferner, H.B. Bode, J. Wöhnert, A New Docking Domain Type in the Peptide-Antimicrobial-Xenorhabdus Peptide Producing Nonribosomal Peptide Synthetase from *Xenorhabdus bovienii*, *ACS Chemical Biology* 15 (2020) 982–989. https://doi.org/10.1021/acschembio.9b01022.

[163] A. Miyanaga, F. Kudo, T. Eguchi, Protein-protein interactions in polyketide synthase-nonribosomal peptide synthetase hybrid assembly lines, *Natural Product Reports* 35 (2018) 1185–1209. https://doi.org/10.1039/c8np00022k.

[164] M. Hahn, T. Stachelhaus, Harnessing the potential of communication-mediating domains for the biocombinatorial synthesis of nonribosomal peptides, *Proceedings of the National Academy of Sciences of the United States of America* 103 (2006) 275–280. https://doi.org/10.1073/pnas.0508409103.

[165] C. Chiocchini, U. Linne, T. Stachelhaus, In vivo biocombinatorial synthesis of lipopeptides by COM domain-mediated reprogramming of the surfactin biosynthetic complex, *Chemistry & Biology* 13 (2006) 899–908. https://doi.org/10.1016/j.chembiol.2006.06.015.

[166] S.E. O'Connor, C.T. Walsh, F. Liu, Biosynthesis of epothilone intermediates with alternate starter units: engineering polyketide-nonribosomal interfaces, *Angewandte Chemie International Edition* 42 (2003) 3917–3921. https://doi.org/10.1002/anie.200352077.

[167] Q. Zhou, F. Grundmann, M. Kaiser, M. Schiell, S. Gaudriault, A. Batzer, M. Kurz, H.B. Bode, Structure and biosynthesis of xenoamicins from entomopathogenic *Xenorhabdus*, *Chemistry* 19 (2013) 16772–16779. https://doi.org/10.1002/chem.201302481.

[168] A.O. Brachmann, S.A. Joyce, H. Jenke-Kodama, G. Schwär, D.J. Clarke, H.B. Bode, A type II polyketide synthase is responsible for anthraquinone biosynthesis in *Photorhabdus luminescens*, *ChemBioChem* 8 (2007) 1721–1728. https://doi.org/10.1002/cbic.200700300.

[169] C. Fu, W.P. Donovan, O. Shikapwashya-Hasser, X. Ye, R.H. Cole, Hot Fusion: an efficient method to clone multiple DNA fragments as well as inverted repeats without ligase, *PloS ONE* 9 (2014) e115318. https://doi.org/10.1371/journal.pone.0115318.

[170] R. Simon, U. Priefer, A. Pühler, A Broad Host Range Mobilization System for In Vivo Genetic Engineering: Transposon Mutagenesis in Gram Negative Bacteria, *Bio/Technology* 1 (1983) 784 EP -. https://doi.org/10.1038/nbt1183-784.

[171] S. Thoma, M. Schobert, An improved *Escherichia coli* donor strain for diparental mating, *FEMS Microbiology Letters* 294 (2009) 127–132. https://doi.org/10.1111/j.1574-6968.2009.01556.x.

[172] N. Philippe, J.-P. Alcaraz, E. Coursange, J. Geiselmann, D. Schneider, Improvement of pCVD442, a suicide plasmid for gene allele exchange in bacteria, *Plasmid* 51 (2004) 246–255. https://doi.org/10.1016/j.plasmid.2004.02.003.

[173] J. Xu, S. Lohrke, I.M. Hurlbert, R.E. Hurlbert, Transformation of *Xenorhabdus nematophilus*, *Applied and Environmental Microbiology* 55 (1989) 806–812.

6 Attachments

6.1 Fabclavine biosynthesis in *X. szentirmaii*: shortened derivatives and characterization of the thioester reductase FclG and the condensation domain-like protein FclL

Authors:

Sebastian L. Wenski[1] · Diana Kolbert[1] · Gina L. C. Grammbitter[1] · Helge B. Bode[1,2*]

[1] Molekulare Biotechnologie, Fachbereich Biowissenschaften, Goethe Universität Frankfurt, 60438 Frankfurt, Germany

[2] Buchmann Institute for Molecular Life Sciences (BMLS), Goethe Universität Frankfurt, 60438 Frankfurt, Germany

Published in:

Journal of Industrial Microbiology & Biotechnology 46 (2019) 565–572

doi: 10.1007/s10295-018-02124-8

Online access: https://link.springer.com/article/10.1007/s10295-018-02124-8

Reprinted with permission, licence number: 4865230936460

Attachment 1

Declaration of author contributions to the publication / manuscript (title):

Fabclavine biosynthesis in *X. szentirmaii*: shortened derivatives and characterization of the thioester reductase FclG and the condensation domain-like protein FclL

Status: published

Name of journal: Journal of Industrial Microbiology & Biotechnology, doi: 10.1007/s10295-018-02124-8

Contributing authors: Wenski SL (SLW), Kolbert D (DK), Grammbitter GLC (GLCG), Bode HB (HBB)

Additional explanation:
SLW: The work was performed as doctoral candidate.
SLW*: The work was performed as master student (MBT) and used for the master thesis "Untersuchungen zur Fabclavin-Biosynthese in *Xenorhabdus szentirmaii*", 2016 Goethe university Frankfurt am Main.

What are the contributions of the doctoral candidate and his co-authors?

(1) Concept and design

SLW (40%), HBB (35%), GLCG (25%)

(2) Conducting tests and experiments

Generation of mutants in *Xenorhabdus*: SLW (50%), DK (10%); Co-cultivation and cross-feeding experiments: SLW (15%), DK (5%); *in vitro* characterization of FclG: SLW (15%), SLW* (5%)

(3) Compilation of data sets and figures

MALDI-MS analysis of *Xenorhabdus* mutants: SLW (50%), DK (10%); Co-cultivation and cross-feeding experiments: SLW (15%), DK (5%); *in vitro* characterization of FclG: SLW (20%)

(4) Analysis and interpretation of data

MALDI-MS analysis: SLW (60%), GLCG (5%), DK (5%); GC-MS analysis: SLW (15%); NADPH-assay: SLW (10%), SLW* (5%)

(5) Drafting of manuscript

SLW (70%), HBB (30%)

I hereby certify that the information above is correct.

Date and place	Signature doctoral candidate
Date and place	Signature supervisor
Date and place	If required, signature of corresponding author

Journal of Industrial Microbiology & Biotechnology (2019) 46:565–572
https://doi.org/10.1007/s10295-018-02124-8

NATURAL PRODUCTS - ORIGINAL PAPER

Fabclavine biosynthesis in *X. szentirmaii*: shortened derivatives and characterization of the thioester reductase FclG and the condensation domain-like protein FclL

Sebastian L. Wenski[1] · Diana Kolbert[1] · Gina L. C. Grammbitter[1] · Helge B. Bode[1,2]

Received: 5 November 2018 / Accepted: 19 December 2018 / Published online: 4 January 2019
© Society for Industrial Microbiology and Biotechnology 2019

Abstract
Fabclavines, unusual peptide–polyketide–polyamine hybrids, show broad-spectrum bioactivity against a variety of different organism like Gram-positive and -negative bacteria, fungi and protozoa. We elucidated the biosynthesis of these NRPS–PKS hybrids in *Xenorhabdus szentirmaii* by deletion of most genes encoded in the fabclavine BGC and subsequent analysis of produced fabclavine or polyamine intermediates. Thereby, we identified shortened fabclavines similar to the bioactive zeamines. Furthermore, we analyzed the thioester reductase FclG and the free-standing condensation domain-like protein FclL in detail and observed low substrate specificity for both enzymes.

Keywords *Xenorhabdus* · Fabclavine · NRPS–PKS hybrid · Antibiotic · Natural product biosynthesis

Introduction

Entomopathogenic bacteria of the genera *Xenorhabdus* and *Photorhabdus* are a rich source for natural products with antibiotic, antifungal, anti-insecticidal or signaling bioactivity, which are often based on non-ribosomal peptide synthetases (NRPS) and polyketide synthases (PKS) [1]. These bacteria live in symbiosis with the soil-resident nematodes *Steinernema* or *Heterorhabditis*, respectively. Their symbiotic life cycle starts with the nematodes as infective juvenile containing their corresponding *Xenorhabdus* or *Photorhabdus* strain in the gut. The nematodes penetrate the insect larvae through anus, mouth or spiracles and once inside the insects, the nematodes release the bacteria into the hemocoel. There, the bacteria start producing natural products to suppress the insect immune response, kill the insect and protect the cadaver against food competitors. After several cycles of nematode development when all nutrients of the insect cadaver are consumed, the nematodes receive a so-called "food signal" from the bacteria to develop into infective juveniles that leave the empty insect carcass into the soil to find and infect novel insect prey [1, 15].

During our efforts to characterize the structures and functions of natural products from *Xenorhabdus* and *Photorhabdus,* we previously identified fabclavines that show broad-spectrum bioactivity against Gram-positive and -negative bacteria, fungi and protozoa and can be found in *Xenorhabdus szentirmaii* or *X. budapestensis* [6]. Structurally, fabclavines are peptide/polyketide hybrids that are connected to a polyamine moiety generated by a fatty acid/polyketide synthase with similarity to enzymes producing polyunsaturated fatty acids (PUFAs). Consequently, their biosynthesis gene cluster (BGC) encodes all required enzymes as described previously. The fabclavines are very similar to the (pre)zeamines, identified in *Serratia plymuthica*, which show a similar broad-spectrum bioactivity [10]. While the mode of action of fabclavines or zeamines is not known but for zeamines it was shown that they are able to permeabilize artificial bacterial and eukaryotic model membranes [11]. A structurally still unknown fabclavine derivative from *X.*

This article is part of the Special Issue "Natural Product Discovery and Development in the Genomic Era 2019".

Electronic supplementary material The online version of this article (https://doi.org/10.1007/s10295-018-02124-8) contains supplementary material, which is available to authorized users.

✉ Helge B. Bode
h.bode@bio.uni-frankfurt.de

[1] Molekulare Biotechnologie, Fachbereich Biowissenschaften, Goethe Universität Frankfurt, 60438 Frankfurt, Germany

[2] Buchmann Institute for Molecular Life Sciences (BMLS), Goethe Universität Frankfurt, 60438 Frankfurt, Germany

innexi was shown to induce membrane degradation at low concentrations in selected mosquito cell lines which led to apoptosis, while control cell lines stay morphologically unaffected [9]. These derivatives additionally induce a pH change in the mosquito larvae midgut [9].

Despite this interesting mode of action and broad spectrum biological activity, not many details are known about the fabclavine and zeamine biosynthesis. Here, we analyzed the biosynthesis of the fabclavines in *Xenorhabdus* via deletion of all individual genes being part of the fabclavine BGC. Furthermore, we analyzed the release of the unusual polyamine moiety by the thioester reductase FclG and the subsequent connection with the NRPS–PKS hybrid by the stand-alone condensation domain-like protein FclL. Additionally, we were able to generate novel fabclavine hybrids using the substrate flexibility of FclL.

Results and discussion

Fabclavine biosynthesis is widespread in *Xenorhabdus*

Fabclavines and their corresponding *fcl* BGCs were previously described in *X. budapestensis* and *X. szentirmaii* but highly similar BGCs have been found in several other *Xenorhabdus* strains (Table S1) [16]. Additionally, related BGCs showing only the genes encoding the polyamine biosynthesis were found in *X. bovienii* and two *Photorhabdus* strains. In *X. innexi* DSM 16336, a *fcl* BGC is proposed to be responsible for the biosynthesis of the xenorhabdus lipoprotein toxin (Xlt) that shows potent anti-mosquito activity [8]. This cluster differs to *X. szentirmaii fcl* BGC only in the flanking regions with a *tonB*-homologue upstream instead of the NUDIX-hydrolase FclA and a acyl-CoA-thioesterase gene downstream of the cluster instead of the transporter genes *fclM* and *fclN* [8]. The *fcl* BGCs show also high homology to the biosynthesis gene cluster of the (pre)zeamines from *Serratia plymuthica* and *Dickeya zeae* [6, 10]. There is also a structurally similarity between the prezeamines and the recently described fabclavines with the difference that the prezeamines are postulated to be prodrugs which are cleaved by the specific peptidase Zmn22 into the active zeamine and zeamine I [10]. Although a related prodrug activation mechanism has been described for the xenocoumacins in *Xenorhabdus*, no such peptidase is present as part of any *fcl* BGC [14].

Analysis of fabclavine biosynthesis via construction and analysis of deletion strains

To better understand the fabclavine biosynthesis, almost all genes encoded in the *fcl* BGC in *X. szentirmaii* DSM 16338 were deleted via biparental mating followed by double homologous recombination as described previously [3]. Subsequently, their phenotype was analyzed by MALDI-MS concerning the production of full-length fabclavines and the polyamine moiety, which both can be detected in the wild type (Table 1). The NRPS–PKS moiety cannot be detected as it is permanently enzyme bound. The first part of the *fcl* BGC in *X. szentirmaii* includes the genes *fclCDEFGH* and was postulated to be responsible for the biosynthesis of the unusual polyamine. The genes *fclC* and *fclD* encode an iterative type-I-PKS which share a high homology with enzymes involved in the biosynthesis of poly unsaturated fatty acids (PUFAs) [6]. The gene *fclE* is also similar to PUFA gene *pfaD* which acts as enoyl-reductase but consists additionally of an aminotransferase domain (AMT) [6]. Deletion mutants of the genes *fclC*, *fclD* and *fclE* alone or together in *X. szentirmaii* or *X. budapestensis* showed a complete loss of fabclavine and the polyamine moiety (Table 1). The 3-oxoacyl-ACP reductase FclF and the thioester reductase FclG were also both required for polyamine production (Table 1) [6]. The nitrilase homolog FclH was proposed to be responsible for the cyclization reaction between D-asparagine and threonine [6]. However, this could not be confirmed since a deletion mutant of *fclH* was still able to produce fabclavines (Table 1). Therefore, the cyclization might take place via nucleophilic attack of the asparagine side chain NH towards a threonine-derived dehydrobutyrine that is generated by the NRPS.

The second part of the fabclavine cluster encodes the NRPS subunits FclI, FclJ and the PKS FclK that generate the NRPS–PKS hybrid [6]. Considering the different fabclavine derivatives in *X. szentirmaii* or *X. budapestensis,* the only variations occur at the second and sixth adenylation domain that incorporate phenylalanine or histidine and valine, threonine, or proline, respectively. The type-I-PKS FclK is proposed to elongate the hexapeptide with one or two malonate units.

Single deletion mutants of *fclI*, *fclJ* or *fclK* in *X. szentirmaii* showed a lack of fabclavine but the presence of the polyamine (Table 1). Interestingly, in the *fclI* deletion mutant, four signals were increased (Fig. S3 and 4) which could be identified by high-resolution MALDI-MS and MS–MS experiments as shortened fabclavine derivatives (**8**–**11**). They consist of a dipeptide instead of the hexapeptide. Due to the fact that these compounds occur also in the wild type, we assume that FclJ can also be used as starting unit without FclI (Fig. S5**A**). The shortened fabclavine derivatives show a high structural similarity to the processed zeamines that have only one amino acid instead of a dipeptide and differ also in the polyamine chain (Fig. S5**B**). Therefore, the biosynthesis of the shortened fabclavines in *X. szentirmaii* can be regarded as an alternative pathway to zeamine-like products not requiring

Table 1 Deletion mutants in *X. szentirmaii* DSM 16338 and *X. budapestensis* DSM 16342 describing the production of full-length fabclavine and polyamine moiety

Strain	Proposed function	Fabclavines	Polyamine
X. szentirmaii DSM 16338			
WT	Wild type	+	+
Δ*fclA*	NUDIX hydrolase	+	+
Δ*fclCDE*	PKS/FAS	−	−
Δ*fclC*	PKS/FAS/PUFA	−	−
Δ*fclD*	PKS/FAS/PUFA	−	−
Δ*fclE*	FAS/enoylreductase/aminotransferase	−	−
Δ*fclF*	3-Oxoacyl-ACP reductase	−	−
Δ*fclG*	Thioester reductase	−	−
Δ*fclH*	Amidohydrolase	+	+
Δ*fclI*	NRPS	−	+
Δ*fclJ*	NRPS	−	+
Δ*fclK*	PKS	−	+
Δ*fclL*	Condensation protein	−	+
X. budapestensis DSM 16342			
WT	Wild type	+	+
Δ*fclE*	FAS/enoylreductase/aminotransferase	−	−
Δ*fclJ*	NRPS	−	+
Δ*fclK*	PKS	−	+

The results are based on high-resolution MALDI-MS spectra shown in Fig. S2

a final peptidase-processing step. Furthermore, the NRPS FclI and FclJ are promising starting points for biotechnological engineering to further increase the diversity of fabclavine derivatives using recently discovered NRPS-manipulation methods [2].

The central connection between the assembly lines for the polyamine and the NRPS/PKS part is proposed to be the stand-alone condensation domain-like protein FclL. This is supported by the loss of fabclavines but the presence of the polyamine in a Δ*fclL*-deletion mutant (Table 1). Similar release mechanisms can be found in other systems with stand-alone condensation domains like distamycin, paenilamicin or rhabdopeptide/xenortide-like peptide biosynthesis [4, 13, 17].

FclM is a homologue of an ABC transporter ATP-binding protein and FclN of an ABC transporter permease and both are, therefore, supposed to be responsible for the fabclavine secretion [6]. Since we were not able to delete *fclM,* we postulate that these genes are necessary to avoid a toxic concentration of fabclavines inside the producing cell. FclA is homologous to NUDIX hydrolases which are widespread in all classes of organism and are responsible for hydrolysis of pyrophosphates [6, 12]. A Δ*fclA* mutant was generated but no difference in comparison to the wild type could be observed (Table 1) suggesting that FclA is actually not part of the fabclavine BGC. In summary, we could confirm the previously postulated biosynthesis of the fabclavines and additionally identified an alternative biosynthesis leading to shortened fabclavines (Fig. 1 and Fig. S5) [6].

Characterization of the condensation domain-like protein FclL in vivo

Beside the observed phenotype for a Δ*fclL* mutant in *X. szentirmaii* which showed a lack in fabclavine derivatives but the presence of the polyamine, we further wanted to test whether FclL can also accept other (poly)amines to generate novel fabclavine derivatives (Table 1). Therefore, a polyamine-deficient and inducible NRPS–PKS hybrid-overproducing strain in *X. szentirmaii* was generated based on a single gene deletion of *fclE* with an inducible promoter in front of *fclI* (*X. szentirmaii* Δ*fclE* P_{BAD}*fclI*) which showed neither fabclavine nor polyamine production even with arabinose as inducer (Fig. 2). When different amines like pentylamine, phenylethylamine or agmatine (Fig. S10) were added to this polyamine-deficient mutant during induced conditions, no new derivatives were observed (data not shown).

Furthermore, a second strain was generated based on the Δ*fclL* single deletion mutant with an additional promoter exchange in front of *fclC* (*X. szentirmaii* Δ*fclL* P_{BAD}*fclC*). This strain was used as polyamine overproducer strain, showing only production of polyamine but not of fabclavine when induced with arabinose (Fig. 2). Both mutants were co-cultivated with and without arabinose. Analysis of the induced co-cultivation culture by MALDI-MS showed the typical *X. szentirmaii* fabclavines which did not occur in the non-induced culture (Fig. 2). The result suggests that the polyamine is secreted and can be taken up again by the cells. Whether this polyamine secretion or uptake is mediated by

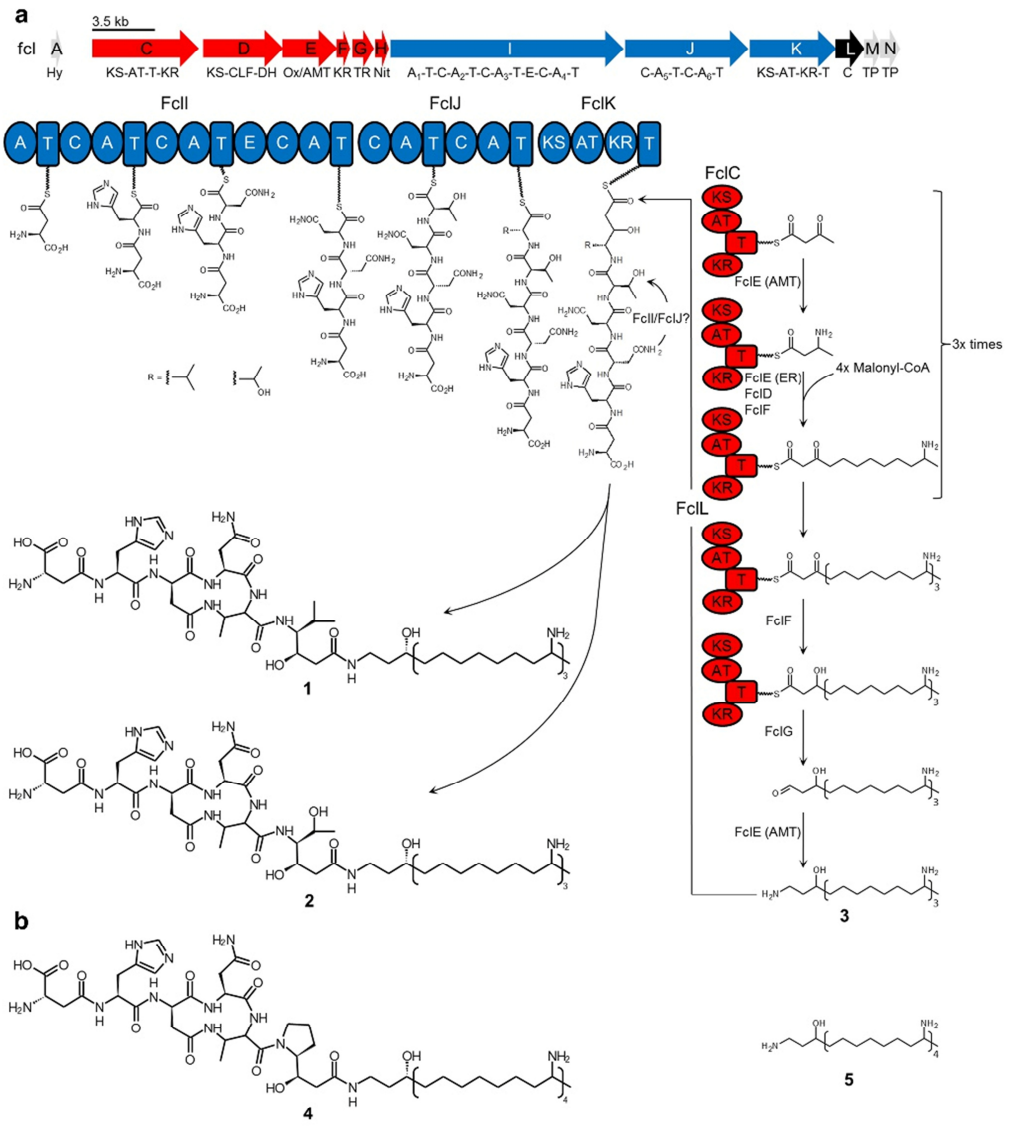

Fig. 1 Biosynthesis and structure of the fabclavine derivatives IVa (**1**), IVb (**2**) and the polyamine moiety (**3**) in *X. szentirmaii* (**a**) and structure of fabclavine IIb (**4**) and the polyamine moiety (**5**) of *X. budapestensis* (**b**). Domain and enzyme abbreviations: *Hy* hydrolase, *KS* ketosynthase, *AT* acyltransferase, *T* thiolation; corresponds to acyl carrier or peptidyl carrier protein, *KR* ketoreductase, *CLF* chain length factor domain, *DH* dehydratase, *Ox* 2-nitropropane dioxygenase, *AMT* aminotransferase, *TR* thioester reductase, *Nit* nitrilase, *A* adenylation, *C* condensation, *E* epimerization, *TP* transport

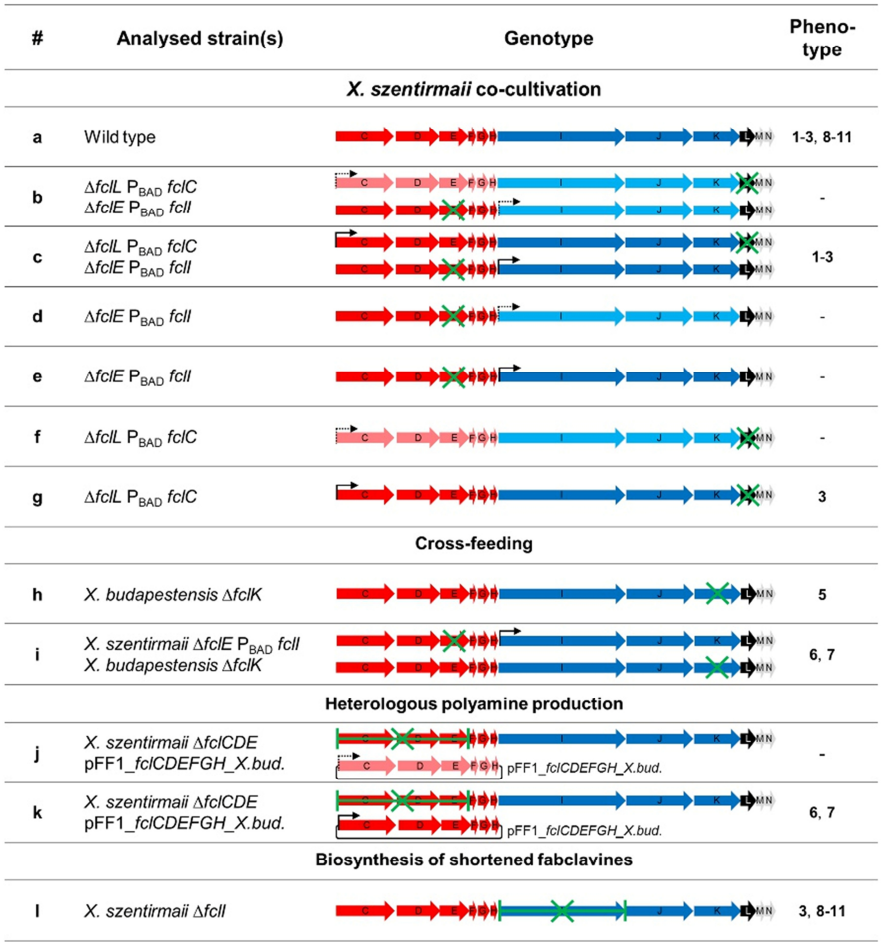

Fig. 2 Observed phenotypes concerning fabclavine derivatives of the co-cultivation, cross-feeding, heterologous polyamine production experiments and biosynthesis of shortened derivatives. Results are based on high-resolution measurements shown in Fig. S2–3 and S6-8 (red/blue genes: induced; light red/blue: non-induced; deleted genes are marked by green crosses; solid arrow: induced promoter; dashed arrow: non-induced promoter) (color figure online)

unspecific transporters or by the fabclavine transport system itself remains unclear.

Based on the successful incorporation of external polyamine complementation in a co-cultivation experiment, the NRPS–PKS-overproducing strain (*X. szentirmaii* Δ*fclE* P_{BAD}*fclI*) was cultivated in a supernatant from a *X. budapestensis* Δ*fclK* strain that only produced the longer *X. budapestensis* polyamine (**5**) (Fig. 1 and Table 1) [6].

High-resolution MALDI-MS of the cross-feeding culture revealed signals with a *m/z* of 1304.94 and 1306.92 which were not present in the LB control (Fig. 2 and Fig. S7). These signals correspond to the NRPS–PKS hybrids of the *X. szentirmaii* fabclavines IVa (**6**) and IVb (**7**) connected to the polyamine moiety of *X. budapestensis* (Figs. 2, 3 and Fig. S7). The structure of the new fabclavine derivative with *m/z* 1306.92 was confirmed by MALDI-MS^2 fragmentation which revealed characteristic fragment ions with *m/z* 598.67 for the y1 ion corresponding to the polyamine of *X. budapestensis* (**5**) or 709.33 for

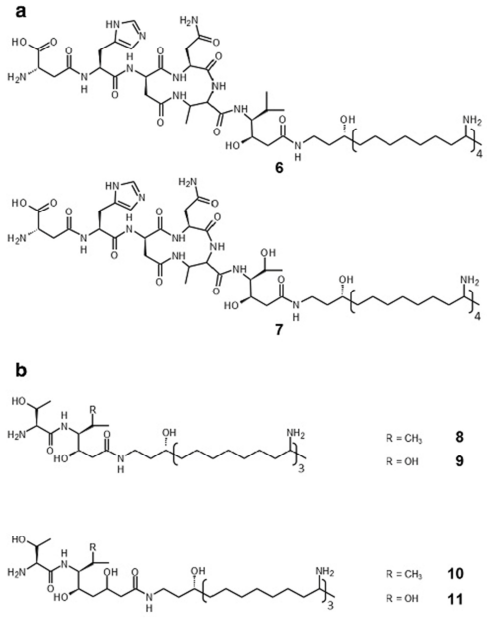

Fig. 3 Observed fabclavine derivatives of the cross-feeding and heterologous polyamine production experiment (**a**) and shortened fabclavines from *X. szentirmaii* Δ*fclI* (**b**)

the b6 ion which corresponds with the NRPS–PKS hybrid of fabclavine IVb (**2**) of *X. szentirmaii* (Fig. S9) [6].

Identical results could be observed by heterologous production of the *X. budapestensis* polyamine (**5**) in a polyamine-deficient *X. szentirmaii* mutant (Fig. 2). Briefly, the genes *fclCDE* were deleted in *X. szentirmaii* and complemented with the polyamine-responsible genes *fclCDEFGH* of *X. budapestensis* encoded on a plasmid under an arabinose-inducible promoter. As for the cross-feeding experiment, the induced mutant showed the production of the *X. budapestensis* polyamine **5** and of the new fabclavine derivatives **6** and **7,** whereas no signals in the non-induced variant could be observed (Fig. 2 and Fig. S8).

The generation and detection of these artificial fabclavine derivatives with longer polyamine moiety confirmed that FclL is able to accept a different amine as substrate for the condensation reaction with the FclK-bound NRPS–PKS hybrid. Similar results could be observed for the amide synthase VibH of the vibriobactin biosynthesis in *Vibrio cholera* or Kj12C from the rhabdopeptide biosynthesis in *Xenorhabdus* KJ12.1 [4, 7]. The successful incorporation of external polyamines highlights the FclL-mediated condensation reaction as a promising starting point for further approaches like mutasynthesis or heterologous amine production to generate further fabclavine derivatives.

Characterization of the thioester reductase FclG

FclG is proposed to be a thioester reductase which is responsible for the reductive release of the aldehyde precursor of the polyamine moiety from the thiolation (T) domain of FclC (Fig. 1). Therefore, FclG was heterologously produced in *E. coli* with an N-terminal Strep-Tag and purified by affinity chromatography (Fig. S11).

A spectrometric assay for FclG was used to determine the consumption of NADPH or NADH with different acyl-Coenzyme A (CoA) derivatives as described for Zmn14 from the zeamine biosynthesis [5, 10]. This assay was combined with an aldehyde derivatization and GC–MS detection of possible products. Purified FclG was incubated with NADH or NADPH as cofactor and palmitoyl-CoA as long-chain fatty acid CoA derivate to mimic the natural substrate. To observe the oxidation of NAD(P)H to $NAD(P)^+$, the decrease of extinction at 340 nm was measured (Fig. 4a) [18]. A significant decrease of extinction with a velocity of − 0.06 A_{340}/min was observed with NADPH which was not the case when boiled enzyme was used (Fig. 4a, sample I and IV) and almost no reduction was observed when NADH was used (Fig. 4a, sample II).

This shows that FclG can utilize palmitoyl-CoA as a substrate and has a preference for NADPH over NADH (Fig. 4, Table 2). The aldehyde derivatization was performed to detect expected products by adding *O*-(2,3,4,5,6-pentafluorobenzyl)hydroxylamine hydrochloride (PFBHA) to the samples used in the spectrometric assay and to measure the resulting oxime derivatives by GC–MS. This could only be detected when NADPH, palmitoyl-CoA and active enzyme were present (Fig. 4b, sample I). The resulting signal was confirmed as oxime derivative of hexadecanal by comparison with the derivatized hexadecanal standard (Fig. 4b, sample III). No signals could be detected in the samples with NADH or with boiled enzyme (Fig. 4b, sample II and IV).

In similar experiments with different CoA thioesters, it was shown that FclG is able to utilize CoA derivatives with acyl chain lengths between 8 and 16 carbons but chain length < 10 carbons is not well accepted (Table 2, Figure S1). Similar to the decreased enzyme activity, less aldehyde was detected by GC–MS (Table 2, Fig. S1). No aldehyde product could be detected in samples with the substrate hexanoyl-CoA (Fig. S1). Only with splitless sample injection of 1 µl sample, small amounts of the expected product hexanal could be detected (data not shown). Based on the in vitro study and the phenotype of *X. szentirmaii* Δ*fclG,* it could be confirmed that FclG acts as a NADPH-dependent thioester reductase which is responsible for the reductive release of the aldehyde precursor of the polyamine from the T-domain

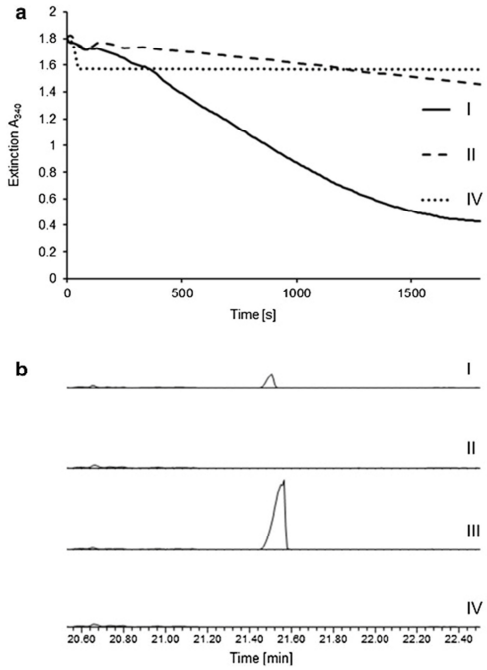

Fig. 4 NAD(P)H consumption of FclG by incubation with palmitoyl-CoA (**a**) and resulting products detected by GC–MS (**b**). Velocity of reaction IV (**a**) was −0.06 A_{340}/min (I: NADPH + Palmitoyl-CoA; II: NADH + Palmitoyl-CoA; III: Hexadecanal; IV: NADPH + palmitoyl-CoA (boiled FclG))

Table 2 NADPH consumption of FclG by incubation with different acyl-CoA derivatives

Substrate	Cofactor	FclG	Aldehyde
Palmitoyl-CoA	NADPH	+	+++
	NADPH	−	−
	NADH	+	−
Myristoyl-CoA	NADPH	+	+++
	NADPH	−	−
Lauroyl-CoA	NADPH	+	++
	NADPH	−	−
Decanoyl-CoA	NADPH	+	++
	NADPH	−	−
Octanoyl-CoA	NADPH	+	+
	NADPH	−	−
Hexanoyl-CoA	NADPH	+	−
	NADPH	−	−

Boiled FclG (negative control) is marked with a minus. Successful aldehyde detection is quantified with + based on GC–MS detection (Fig. 4 and Fig. S1)

of FclC (Fig. 1). In contrast to the analysis of the FclG-homologue Zmn14 of the zeamine biosynthesis, the NADPH consumption could be directly linked with the formation of an aldehyde and not the formation of an alcohol [10]. Due to the natural substrate chain length, we assume that FclG can use even longer substrates than palmitoyl-CoA.

Moreover, the observed acyl chain range of confirmed substrates and products implies that FclG can use more substrates than its native one and is, therefore, an additional promising starting point for biotechnological engineering.

Conclusion and outlook

In this study, we could confirm the previously postulated biosynthesis of the fabclavines by deletion of most genes encoded in the fabclavine BGC and subsequent analysis of produced fabclavine or polyamine intermediates. These deletion experiments also led to the identification of shortened fabclavine derivatives with high similarity to the zeamines. The thioester reductase FclG and the free-standing condensation domain-like protein FclL were characterized in detail leading to new fabclavines with a different polyamine moiety. Our detailed analysis sets the stage for a successful modification of these broad-spectrum natural products that might lead to derivatives with a selective bioactivity. Since several *fcl* BGCs have been identified in other Xenorhabdus strains, it would be interesting to identify their structures, possibly allowing the generation of further derivatives when genes involved in the production of different structural moieties are mixed as described in this work.

Acknowledgements This work was supported by the DFG and the LOEWE Schwerpunkt MegaSyn supported by the State of Hessen. H.B.B. acknowledges the Deutsche Forschungsgemeinschaft for funding of the Impact II qTof mass spectrometer (INST 161/810-1). Furthermore, we would like to thank Dr. Hendrik Wolff and Peter Grün for technical assistance with the GC–MS measurements and Prof. Dr. Michael Karas for support with the MALDI-MS measurements.

References

1. Bode HB (2009) Entomopathogenic bacteria as a source of secondary metabolites. Curr Opin Chem Biol 13:224–230. https://doi.org/10.1016/j.cbpa.2009.02.037
2. Bozhüyük KAJ, Fleischhacker F, Linck A, Wesche F, Tietze A, Niesert C-P, Bode HB (2018) De novo design and engineering of non-ribosomal peptide synthetases. Nat Chem 10:275–281. https://doi.org/10.1038/nchem.2890
3. Brachmann AO, Joyce SA, Jenke-Kodama H, Schwär G, Clarke DJ, Bode HB (2007) A type II polyketide synthase is responsible for anthraquinone biosynthesis in *Photorhabdus luminescens*. ChemBioChem 8:1721–1728. https://doi.org/10.1002/cbic.200700300
4. Cai X, Nowak S, Wesche F, Bischoff I, Kaiser M, Fürst R, Bode HB (2017) Entomopathogenic bacteria use multiple mechanisms

for bioactive peptide library design. Nat Chem 9:379–386. https://doi.org/10.1038/nchem.2671
5. Chhabra A, Haque AS, Pal RK, Goyal A, Rai R, Joshi S, Panjikar S, Pasha S, Sankaranarayanan R, Gokhale RS (2012) Nonprocessive 2 + 2 e-off-loading reductase domains from mycobacterial nonribosomal peptide synthetases. Proc Natl Acad Sci USA 109:5681–5686. https://doi.org/10.1073/pnas.1118680109
6. Fuchs SW, Grundmann F, Kurz M, Kaiser M, Bode HB (2014) Fabclavines: bioactive peptide-polyketide-polyamino hybrids from *Xenorhabdus*. ChemBioChem 15:512–516. https://doi.org/10.1002/cbic.201300802
7. Keating TA, Marshall CG, Walsh CT (2000) Vibriobactin biosynthesis in *Vibrio cholerae* VibH is an amide synthase homologous to nonribosomal peptide synthetase condensation domains. Biochemistry 39:15513–15521. https://doi.org/10.1021/bi001651a
8. Kim I-H, Aryal SK, Aghai DT, Casanova-Torres ÁM, Hillman K, Kozuch MP, Mans EJ, Mauer TJ, Ogier J-C, Ensign JC, Gaudriault S, Goodman WG, Goodrich-Blair H, Dillman AR (2017) The insect pathogenic bacterium *Xenorhabdus innexi* has attenuated virulence in multiple insect model hosts yet encodes a potent mosquitocidal toxin. BMC Genom 18:927. https://doi.org/10.1186/s12864-017-4311-4
9. Kim I-H, Ensign J, Kim D-Y, Jung H-Y, Kim N-R, Choi B-H, Park S-M, Lan Q, Goodman WG (2017) Specificity and putative mode of action of a mosquito larvicidal toxin from the bacterium *Xenorhabdus innexi*. J Invertebr Pathol 149:21–28. https://doi.org/10.1016/j.jip.2017.07.002
10. Masschelein J, Clauwers C, Awodi UR, Stalmans K, Vermaelen W, Lescrinier E, Aertsen A, Michiels C, Challis GL, Lavigne R (2015) A combination of polyunsaturated fatty acid, nonribosomal peptide and polyketide biosynthetic machinery is used to assemble the zeamine antibiotics. Chem Sci 6:923–929. https://doi.org/10.1039/c4sc01927j
11. Masschelein J, Clauwers C, Stalmans K, Nuyts K, de Borggraeve W, Briers Y, Aertsen A, Michiels CW, Lavigne R (2015) The zeamine antibiotics affect the integrity of bacterial membranes. Appl Environ Microbiol 81:1139–1146. https://doi.org/10.1128/AEM.03146-14
12. McLennan AG (2006) The nudix hydrolase superfamily. Cell Mol Life Sci 63:123–143. https://doi.org/10.1007/s00018-005-5386-7
13. Müller S, Garcia-Gonzalez E, Mainz A, Hertlein G, Heid NC, Mösker E, van den Elst H, Overkleeft HS, Genersch E, Süssmuth RD (2014) Paenilamicin: structure and biosynthesis of a hybrid nonribosomal peptide/polyketide antibiotic from the bee pathogen *Paenibacillus larvae*. Angew Chem Int Ed Engl 53:10821–10825. https://doi.org/10.1002/anie.201404572
14. Reimer D, Bode HB (2014) A natural prodrug activation mechanism in the biosynthesis of nonribosomal peptides. Nat Prod Rep 31:154–159. https://doi.org/10.1039/c3np70081j
15. Strauch O, Ehlers R-U (1998) Food signal production of *Photorhabdus luminescens* inducing the recovery of entomopathogenic nematodes *Heterorhabditis* spp. in liquid culture. Appl Microbiol Biotechnol 50:369–374. https://doi.org/10.1007/s002530051306
16. Tobias NJ, Wolff H, Djahanschiri B, Grundmann F, Kronenwerth M, Shi Y-M, Simonyi S, Grün P, Shapiro-Ilan D, Pidot SJ, Stinear TP, Ebersberger I, Bode HB (2017) Natural product diversity associated with the nematode symbionts *Photorhabdus* and *Xenorhabdus*. Nat Microbiol 2:1676–1685. https://doi.org/10.1038/s41564-017-0039-9
17. Vingadassalon A, Lorieux F, Juguet M, Le Goff G, Gerbaud C, Pernodet J-L, Lautru S (2015) Natural combinatorial biosynthesis involving two clusters for the synthesis of three pyrrolamides in *Streptomyces netropsis*. ACS Chem Biol 10:601–610. https://doi.org/10.1021/cb500652n
18. Ziegenhorn J, Senn M, Bücher T (1976) Molar absorptivities of beta-NADH and beta-NADPH. Clin Chem 22:151–160

Publisher's Note Springer Nature remains neutral with regard to jurisdictional claims in published maps and institutional affiliations.

Fabclavine biosynthesis in *X. szentirmaii*: Shortened derivatives and characterization of the thioester reductase FclG and the condensation domain-like protein FclL

Sebastian L. Wenski[1], Diana Kolbert[1], Gina L. C. Grammbitter[1], Helge B. Bode[1,2,]*

[1] Molekulare Biotechnologie, Fachbereich Biowissenschaften, Goethe Universität Frankfurt, 60438 Frankfurt, Germany. Telephone number: +49 69 798-29557 E-mail: h.bode@bio.uni-frankfurt.de

[2] Buchmann Institute for Molecular Life Sciences (BMLS), Goethe Universität Frankfurt, 60438 Frankfurt, Germany.

Material and methods

Strain cultivation

Xenorhabdus szentirmaii DSM 16338, *X. budapestensis* DSM 16342 and all mutant strains were cultivated on lysogeny broth (LB) agar plates and precultures were incubated overnight with shaking at 30°C. In general, cultures were inoculated 1:25 in fresh LB media and incubated shaking at 30°C for 3 days. *Escherichia coli* strains were incubated overnight on LB agar plates and in LB media at 37°C with shaking. If appropriate kanamycin [50 ng/ml] or ampicillin [100 ng/ml] were added.

Cocultivation- and cross-feeding-experiments

For the co-cultivation experiments LB media (supplemented with kanamycin and 0.2% L-arabinose if appropriate) were inoculated 1:25 with precultures of both strains and incubated for 3 days at 30°C. For the cross-feeding experiments 4 ml terrific broth (TB) supplemented with kanamycin and 0.2% L-arabinose were inoculated 1:25 with a preculture of *X. szentirmaii* Δ*fclL* P_{Bad} *fclI* and incubated for 3 days at 30°C. The supernatant of *X. budapestensis* Δ*fclK* was heated at 98°C for 15 min,

centrifuged and filtrated (0.2 µm pore size). At the first and the second day 2 ml of the processed supernatant were fed.

Generation of deletion and promoter exchange mutants

Promoter exchange and deletion mutants in *X. szentirmaii* DSM 16338 and *X. budapestensis* DSM 16342 were performed as described previously using the primers listed in Table S2 [2]. Briefly, for the generation of promoter exchange mutants, the first 300-1000 bp of the corresponding gene were cloned into the either digested or PCR-amplified plasmid backbone of pCEP_Kan and then transformed into *E. coli* S17-1 λpir or ST18 [11, 12, 1]. For gene deletions about 1000 bp of flanking down- und upstream regions of the gene were amplified by PCR and cloned into the either digested or PCR-amplified pDS132-backbone by Hot fusion assembly and then transformed into *E. coli* S17-1 λpir or ST18 strains prior to confugation into *Xenorhabdus* following established protocols [3, 9].

Heterologous polyamine production of *X. budapestensis*

For the heterologous polyamine production the responsible *fclCDEFGH* operon of *X. budapestensis* were amplified in 3 fragments of about 4.5-6.2 kb. The primers are listed in Table S2. All fragments contained homologous regions of 40-60 bp for overlap extension PCR and yeast homologous recombination (ExRec) [10]. 100-1000 ng of each fragment and the *Eco*RI/ *Sgs*I restricted pFF1 vector were used for the yeast transformation by the protocols of Gietz and Schiestl [5, 4]. The plasmid was isolated from yeast, re-transformed into *E. coli* DH10B::mtaA and confirmed by restriction. Confirmed plasmid was transformed into *X. szentirmaii* Δ*fclCDE* by heatshock transformation by an adapted protocol of Xu et al. [13].

MALDI-MS

Liquid cultures were spotted on a steel target with a volume of 0.3 µl mixed with 0.25 µl 1:10 diluted ProteoMass Normal Mass Calibration Mix [ProteoMass™ MALDI Calibration Kit, Sigma-Aldrich] for internal calibration and 0.9 µl α-cyano-4-hydroxycinnamic acid (CHCA) matrix [3 mg/ml in 75% acetonitrile, 0.1% trifluoroacetic acid]. After air-drying, the sample spot was washed with 5% formic acid and mixed again with 0.6 µl CHCA. Cell MALDI measurements were performed with a MALDI LTQ Orbitrap XL [Thermo Fisher Scientific, Inc., Waltham, MA] instrument with a nitrogen laser at 337 nm in FTMS scan mode with 100 shots per measurement in a mass range of 350 to 1500 *m/z* with high resolution. MALDI-MS^2 experiments were performed in CID-mode using ITMS scan mode with the same sample preparation with the following parameters: Normalized collision energy: 28 (32), Act. Q: 0.250, Act. Time (ms): 30.0. Data were analysed using Qual Browser version 2.0.7 [Thermo Fisher Scientific].

Cloning and purification of FclG

The gene *fclG* (1230 bp) was amplified from the gDNA of *X. szentirmaii* with the primers shown in Table S2 which contain additionally the sequence for a N-terminal streptavidin binding tag and a TEV protease restriction site. The fragment was cloned into the PCR-amplified (Table S2) pCOLA_DUET backbone by a Hot fusion assembly and transformed by electroporation into competent *E. coli* DH10B cells [3]. Transformants were selected on LB-agar supplemented with kanamycin and corresponding plasmids were analyzed by restriction. Afterwards the plasmid was transformed into electro-competent *E. coli* BL21 Star™ (DE3) containing a pTF16 plasmid with the chaperone trigger factor [8]. Production cultures were inoculated 1:100 with an overnight culture and supplemented with kanamycin, chloramphenicol,

1% glucose and 0.1% L-arabinose. After 2.5 h at 37°C and 0.5 h at 4°C the production was induced with 0.1 mM isopropyl β-D-1-thiogalactopyranoside (IPTG) and incubated for 5-6 h at 30°C. The culture was centrifuged (10 min, 10.000 rpm, 4°C) and the cell pellet was stored at -20°C. For the purification the cells were resuspended in strep tag binding buffer [100 mM Tris, 150 NaCl, pH 8] supplemented with EDTA-free Protease Inhibitor Cocktail [Roche Diagnostics]and lysozyme and lysed by ultrasound. The lysate was centrifuged (20 min, 20.000 rpm, 4°C), filtered and the supernatant was used for purification on the NGC™ Chromatography System [Bio-Rad] with a 5 ml StrepTrap^{TM} HP [GE Healthcare] (Fig. S11). Purified FclG was stored in strep elution buffer [100 mM Tris, 150 NaCl, 2,5 mM desthiobiotin, pH 8] overnight at 4°C.

NAD(P)H-assay of FclG and product detection by GC-MS

Purified FclG was concentrated in Amicon Ultra centrifugal filter units Ultra-4 [Merck] and the strep elution buffer was exchanged with PD-10 Desalting Columns [GE Healthcare] to phosphate buffer [250 mM NaCl, 10 mM NaH_2PO_4, pH 8]. One reaction in phosphate buffer consists of 55 µM FclG, 1 mM substrate and 0.5 mM NADH or NADPH in a total volume of 0.5 ml. The extinction at 340 nm of NAD(P)H was measured over a period of 30 min at room temperature in the GENESYS™ 10S UV-Vis spectrophotometer [Thermo Fisher Scientific]. Resulting spectra of corresponding samples were adjusted to an identical start extinction. The velocity was calculated by linear regression in a time intervall of >1 min and with a coefficient of determination $R^2 \geq 0.99$. After the measurement, 50 mM O-(2,3,4,5,6-pentafluorobenzyl)hydroxylamine hydrochloride was added and the sample was stored at -20°C. For the aldehyde detection, samples and corresponding aldehyde standards [1 mM in ethylacetate] were incubated shaking at 30°C for 2 h to

derivatize possible aldehydes with PFBHA, extracted by a hexane/MeOH mix (7:1). The upper phase was evaporated, dissolved in 80 µl hexane and samples were analysed by GC-MS using a 7890A model gas chromatograph [Agilent] with a CTC PAL CombiXTautosampler and a Series5975C mass selective detector [Agilent]. Samples were separated by a DB5ht column [Agilent] with a length of 30 m and an inner diameter of 0.25 mm using helium as the carrier gas. 1 µl sample was injected by an inlet temperature of 250°C in 1:20 split mode (1:10 for samples with palmitoyl- or hexanoyl-CoA and corresponding standards) with 7 min solvent delay. The oven temperature program had a starting temperature of 60°C, then 20°C/min to 85°C, followed by 8°C/min to 310°C, hold for 5 min and then decreased to the initial temperature within 1 min. The temperature of the transfer line was kept constant at 280°C. The temperature of the detector ion source was kept at 230°C, its quadrupole temperature at 150°C. Ionization of the analyte molecules was carried out by electron impact ionization at 70 keV.

Supplementary material:

Table S1 Identities of homologous proteins to the fabclavine related proteins in *X. szentirmaii* DSM16338. Protein alignments were performed by ClustalW alignment with the CostMatrix BLOSUM in Geneious 6.1.8. Identities in brackets belong to partial (*X. bovienii* FclJ) or subdivided (*P. asymbiotica* FclC) proteins. *X. bud.* = *X. budapestensis* DSM 16342; *X. cab.* = *X. cabanillasii* JM26-1; *X. ind.* = *X. indica* DSM 17382; *X. sto.* = *X. stockiae* DSM 17904; *X. hom.* = *X. hominickii* DSM 17903; *X. bov.* = *X. bovienii* SS-2004; *X. inn.* = *X. innexi* DSM 16336; *P. temp.* = *P. temperata* meg1; *P. asym.* = *P. asymbiotica* 68.1

		Identity [%]								
Protein	Proposed function	*X. bud.*	*X. cab.*	*X. ind.*	*X. sto.*	*X. hom.*	*X. bov.*	*X. inn.*	*P. temp.*	*P. asym.*
FclA	NUDIX hydrolase	82	82	82	82.5	87.2	86.2	/	/	/
FclC	PKS/FAS/PUFA	72.4	73	72.7	69.6	69.9	71.4	68.7	59.1	58.7 [11.2]
FclD	PKS/FAS/PUFA	76.6	76.9	76.4	74.7	72.7	74.4	74.4	61.9	61.3
FclE	FAS/enoylreductase /aminotransferase	82.2	81.9	81.1	79.7	81.1	82	77.5	71.1	71.5
FclF	3-oxoacyl-ACP reductase	82	82.7	83.1	81.6	76.1	78	81.6	/	/
FclG	Thioester reductase	76.1	76.1	76.3	75.9	64.6	67.3	76.8	/	/
FclH	Nitrilase	79.2	79.2	78.8	75.4	75.4	77.3	79.5	/	/
FclI	NRPS	70.8	71.3	70.8	67.8	70.3	/	65.7	/	/
FclJ	NRPS	76.6	76.5	76	73.4	74.1	[32.4]	70.8	/	/
FclK	PKS	69.6	70	69.3	68.8	71	/	66.5	/	/
FclL	Condensation protein	65.9	66.2	65.7	64.8	66.6	/	63.4	/	/
FclM	ATP-binding protein	81.9	82.8	81.6	78.2	79.4	78.5	/	/	/
FclN	ABC transporter	81.6	82.7	82.2	81.6	82.5	77.3	/	/	/

Table S2 Overview of the used primer and plasmids for the amplification of the homologous regions for the deletion and promoter exchange mutants in *X. szentirmaii* DSM 16338 and *X. budapestensis* DSM 16342 and the heterologous production plasmids encoding FclG and FclCDEFGH

Strain	Locus tag(s) of analyzed gene(s)	Primer	Sequence 5'-3'
ΔfclA X. sz.	Xsze_03746	SW120_A_LF_fw	CGATCCTCTAGAGTCGACCTGCAGAGTGAAAAATCTCACTATTAACTGAATTTACTG
		SW121_A_LF_rv	CATCCTTTCATTTTCAGGGACCTAAAAAACCTTCAGTAAATGTTCTG
		SW122_A_RF_fw	TTTACTGAAGGTTTTTTAGGTCCCTGAAAATGAAAGGATG
		SW123_A_RF_rv	GAGAGCTCAGATCTACGCGTTTCATATGTGCTAAAATTTGAAATCTCCG
ΔfclC X. sz.	Xsze_03745	SW371_XszC_LF_fw	CGATCCTCTAGAGTCGACCTGCAGCGTTAAGAGAAAGTGTTAAAGAATGCAGATGG
		SW372_XszC_LF_rv	AAAATGAATTACTGGACATTCCTCGTGCGTTGAATAAAACAAC
		SW373_XszC_RF_fw	ACGCACGAGGAATGTCCAGTAATTCATTTTACTAAATAATAAATAAATTAAACCG
		SW374_XszC_RF_rv	GAGAGCTCAGATCTACGCGTTTCATATGCTGATTTAATGGCATACAGTGCTG
ΔfclD X. sz.	Xsze_03744	SW379_XszD_LF_fw	CGATCCTCTAGAGTCGACCTGCAGGGTATTACTGCACACTGTGTCATTGC
		SW380_XszD_LF_rv	CACATCATCACCTTTAAAGGAGTGACTCCTTATTTTGATGGC
		SW381_XszD_RF_fw	AGGAGTCACTCCTTTAAAGGTGATGATGTGGCAGAGC
		SW382_XszD_RF_rv	GAGAGCTCAGATCTACGCGTTTCATATGCAAAAGCGGACAGAATTGCG
ΔfclE X. sz.	Xsze_03743	DA_13_E_del_fw	CTTCTAGAGGTACCGCATGCGCATACCTGCTGACGGAAAATC
		DA_14_E_del_fw	GAGCATTGTTTCACAAACACCGCAAGGCATCCAGACTGTCATG
		DA_15_E_del_fw	CATGACAGTCTGGATGCCTTGCGGTGTTTGTGAAACAATGCTC
		DA_16.1_E_del_rv	GGAATTCCCGGGAGAGCTCGCATTTTCCATGGCATCAAAG
ΔfclCDE X. sz.	Xsze_03743/	SW62_CDE_LF_fw	CGATCCTCTAGAGTCGACCTGCAGAACGGTGACAACATGCTGTTAAGG
	Xsze_03744/	SW63_CDE_LF_rv	ATCAATCACTTTGCGACATTCCTCGTGCGTTGAATAAAAC
	Xsze_03745	SW64_CDE_RF_fw	ACGCACGAGGAATGTCGCAAAGTGATTGATATCACCCTTAAAG
		SW65_CDE_RF_rv	GAGAGCTCAGATCTACGCGTTTCATATGTTGCCGGACAGTTCTGAGTATAGTTC
ΔfclF X. sz.	Xsze_03742	SW42_F_LF_fw	CGATCCTCTAGAGTCGACCTGCAGATCGATATCCTGACCTCCACG
		SW43_F_LF_rv	TATTCGGTGGTGTTTCCTGGTAATTGCAGTACCAAATCC
		SW44_F_RF_fw	ACTGCAATTACCAGGAAACACCACCGAATAAATGCG
		SW45_F_RF_rv	GAGAGCTCAGATCTACGCGTTTCATATGTCAACAAATGAAGGGTTTTGC
ΔfclG X. sz.	Xsze_03741	SW52_G_LF_fw	CGATCCTCTAGAGTCGACCTGCAGGCAAAGTGATTGATATCACCC
		SW53_G_LF_rv	GGCACATCAGGCCGAGCCTATCCCCTATGCTTAGG
		SW54_G_RF_fw	GCATAGGGGATAGGCTCGGCCTGATGTGCCGTC
		SW55_G_RF_rv	GAGAGCTCAGATCTACGCGTTTCATATGGAACGGGAAACGTGCTCTGG
ΔfclH X. sz.	Xsze_03740	SW104_H_LF_fw	CGATCCTCTAGAGTCGACCTGCAGGATATTACAGAGAAGAACTTTGG
		SW105_H_LF_rv	TATTACCAATACGCAATAAATGTAAACTCCGTTTCAATAC
		SW106_H_RF_fw	GTATTGAAACGGAGTTTACATTTATTGCGTATTGGTAATAAATTC
		SW107_H_RF_rv	GAGAGCTCAGATCTACGCGTTTCATATGTGATGGTATCGTCAATCG
ΔfclI X. sz.	Xsze_03739	SW112_I_LF_fw	CGATCCTCTAGAGTCGACCTGCAGCTATTTCAATTACTTGATTGAATGCGG
		SW113_I_LF_rv	CATTGTTCATTGATTGTTATTAGCCATCATTCCTTCAATAAGAATTTATTACC
		SW114_I_RF_fw	TATTGAAGGAATGATGGCTAATAACAATCAATGAACAATGGAATATAAAC
		SW115_I_RF_rv	GAGAGCTCAGATCTACGCGTTTCATATGCGGTGAATAACTCAGGTCACG

Strain	Locus tag(s) of analyzed gene(s)	Primer	Sequence 5'-3'
ΔfclJ X. sz.	Xsze_03738	SW387_XszJ_LF_fw	CGATCCTCTAGAGTCGACCTGCAGCGAAACCGTTGTGG
		SW388_XszJ_LF_rv	TGTTCCCTTTCCCAGTGACTCCCCTTCAATGTTGTTATATTCC
		SW389_XszJ_RF_fw	TTGAAGGGGAGTCACTGGGAAAAGGGAACACGAGC
		SW390_XszJ_RF_rv	GAGAGCTCAGATCTACGCGTTTCATATGGGTCGCTGTACCGTGTGC
ΔfclK X. sz.	Xsze_03737	SW337_Xsz_LF_fw	CGATCCTCTAGAGTCGACCTGCAGCATTCGACAAATCCCTTTCAACC
		SW338_Xsz_LF_rv	ACTATTGGCTTGTTGTAGCTCTGTTCCCTTTTCCCATTACC
		SW339_Xsz_RF_fw	AAGGGAACAGAGCTACAACAAGCCAATAGTGCGG
		SW340_Xsz_RF_rv	GAGAGCTCAGATCTACGCGTTTCATATGGGATCATCAGTGTCTCACTGCC
ΔfclL X. sz.	Xsze_03736	DA1_L_del_fw	TTCTTCTAGAGGTACCGCATGCGCAGATCCACGGTATTTTCC
		DA2_L_del_int_rv	CTTGGTGATAAGTTGGGAAAGGACAGGCAAGGGGTGTTGATTG
		DA3_L_del_int_fw	CCAATCAACACCCCTTGCCTGTCCTTTCCCAACTTATCACCAAG
		DA4_L_del_rv	TGTGGAATTCCCGGGAGAGCTCCCTGCCAATGTCATGAACAAG
ΔfclE X. bud.	Xbud_02636	SW239_XbudE_LF_fw	CGATCCTCTAGAGTCGACCTGCAGGTTCAAAGGAGAGCTTTGCTACCG
		SW240_XbudE_LF_rv	AATCACCTTCGCGGGCATGTGCTTTTGGCTGGTGACC
		SW241_XbudE_RF_fw	CAGCCAAAAGCACATGCCCGCAAGGTGATTGATATC
		SW242_XbudE_RF_rv	GAGAGCTCAGATCTACGCGTTTCATATGGCAGCTTTACTGGCTGCCC
ΔfclJ X. bud.	Xbud_02641	SW247_XbudJ_LF_fw	CGATCCTCTAGAGTCGACCTGCAGCATGGCAGGAGAGTTGTATATCGGG
		SW248_XbudJ_LF_rv	CTTCCCGTTTGCCCGAAAACCTCCGGCAAAATACCC
		SW249_XbudJ_RF_fw	TTTGCCGGAGGTTTTCGGGCAAACGGGAAGAGG
		SW250_XbudJ_RF_rv	GAGAGCTCAGATCTACGCGTTTCATATGCTCTGCCGGAACATCTGCC
ΔfclK X. bud.	Xbud_02642	SW192_XbudK_LF_fw	CGATCCTCTAGAGTCGACCTGCAGGTTACCGTGCCACAGAAGG
		SW193_XbudK_LF_rv	ATTTTCCGTTTTCTGAATCCGCTATTCCTCTCCC
		SW194_XbudK_RF_fw	GAGGAATAGCGGATTCAGAAACGGAAAATCTGACAG
		SW195_XbudK_RF_rv	GAGAGCTCAGATCTACGCGTTTCATATGGATACGCAACATGGGTGC
P-exc in front of *fclC* *X. sz.*	Xsze_03745	DA_p3f	GGCTAACAGGAGGCTAGCATATGTCTGAGACATATTTTTTACATGATAGAAAAATTC
		DA_p3r	GCAGAGCTCGAGCATGCACATCCCAAAAAGCCGGGAAAAC
P-exc in front of *fclI* *X. sz.*	Xsze_03739	EB_ ORF06379_fw	TTTGGGCTAACAGGAGGCTAGCATATGGTGATTTCAACTGAATTC
(Origin Edna Bode)		EB_ ORF06379_rv	TCTGCAGAGCTCGAGCATGCACATCGTAGTATCTTCTGCTGTCAG
Heterologous polyamine production	Xbud_02634 -02639	SW427_Xbud_F1_fw	TTATGCGAACTCTCTACTGTTTCTCCATACCCGTTTTTTTGGGCTAACAGGAGGAATTCCATGTCCAAGAGGTATTTTTTGCATGATAGG
		SW428_Xbud_F1_rv	ATAAAGGAGAGACTCCTTAATATGATAGCGTTCCCCTGAGCGAATATTTTCACTCAGGTATATTAGCAACCTG
		SW429_Xbud_F2_fw	TAAAAATTCAGGTTGCTAATATACCTGAGTGAAAATATTCGCTCAGGGGAACGCTATCATATTAAGG
		SW430_Xbud_F2_rv	TTTGGCTGGTGACCCGATAAATTGACAGATAAGTGCTGATTCATTTTGTGGCGTCCTGTTC
		SW431_Xbud_F3_fw	AGCAGGTGTAGCAGAATTGGAACAGGACGCCACAAAATGAATCAGCACTTATCTGTCAATTTATCGGG
		SW432_Xbud_F3_rv	CTTCACCTTTGCTCATGAACTCGCCAGAACCAGCAGCGGAGCCAGCGGATCCGGCGCGCCTCACTCCCTCAAAATGCTTTCTTTTAGAAC
Production FclG	Xsze_03741	SW1_DUET_fw	TTAACCTAGGGCTGCTG
		SW2_DUET_rev	GGTATATCTCCTTATTAAAGTTAAAC
		SW17_G_strp_fw	CTTTAATAAGGAGATATACCATGTGGAGCCACCCGCAGTTCGAAAAAGAGAACCTATACTTCCAGGGACTCAACCAGACTCAAAAAG
		SW16_G_rv	GTGGCAGCAGCCTACGGTTAATTACAGGTCTGCGTCAAATAAC

Table S3 Overview of used strains. Genome accession numbers for *X. szentirmaii* DSM 16338 (*X. sz.*) is NIBV00000000_NCBI and for *X. budapestensis* DSM 16342 (*X. bud.*) NIBS00000000_NCBI

Strain	Description	Mutation/ Locus tag	Origin
X. szentirmaii DSM 16338	Wild type		[6]
X. budapestensis DSM 16342	Wild type		[6]
E. coli S17 λ1-pir	used for conjugation		[11]
E. coli ST18	used for conjugation		[12]
E. coli BL21 Star™ (DE3)	used for protein production		Invitrogen
S. cerevisiae CEN.PK 2-1C	used for yeast cloning		Euroscarf
E. coli::mtaA	used for yeast cloning		[10]
X. sz. DSM 16338 Δ*fclA*	NUDIX hydrolase	Deletion of 546/546 Bp of Xsze_03746	This work
X. sz. DSM 16338 Δ*fclC*	PKS/FAS/PUFA	Deletion of 5988/5988 Bp of Xsze_03745	This work
X. sz. DSM 16338 Δ*fclD*	PKS/FAS/PUFA	Deletion of 4425/4470 Bp of Xsze_03744	This work
X. sz. DSM 16338 Δ*fclE*	FAS/ER/AMT	Deletion of 857/3081 Bp of Xsze_03743	This work
X. sz. DSM 16338 Δ*fclCDE*	PKS/FAS/PUFA/ER/AMT	Deletion of 13.712/13757 Bp of Xsze_03743-45	This work
X. sz. DSM 16338 Δ*fclF*	3-oxoacyl-ACP reductase	Deletion of 705/768 Bp of Xsze_03742	This work
X. sz. DSM 16338 Δ*fclG*	Thioester reductase	Deletion of 1230/1230 Bp of Xsze_03741	This work
X. sz. DSM 16338 Δ*fclH*	Amidohydrolase	Deletion of 783/783 Bp of Xsze_03740	This work
X. sz. DSM 16338 Δ*fclI*	NRPS	Deletion of 13.041/13.041 Bp of Xsze_03739	This work
X. sz. DSM 16338 Δ*fclJ*	NRPS	Deletion of 6927/6927 Bp of Xsze_03738	This work
X. sz. DSM 16338 Δ*fclK*	PKS	Deletion of 4845/4890 Bp of Xsze_03737	This work
X. sz. DSM 16338 Δ*fclL*	Condensation protein	Deletion of 1526/1596 Bp of Xsze_03736	This work
X. sz. DSM 16338 Δ*fclL* P_{BAD} *fclC*	Condensation protein	Deletion of 1526/1596 Bp of Xsze_03736 Promoter exchange in front of Xsze_03745	This work
X. sz. DSM 16338 Δ*fclE* P_{BAD} *fclI*	FAS/ER/AMT	Deletion of 857/3081 Bp of Xsze_03743 Promoter exchange in front of Xsze_03739	This work
X. bud. DSM 16342 Δ*fclE*	FAS/ER/AMT	Deletion of 2937/3037 Bp of Xbud_02636	This work
X. bud. DSM 16342 Δ*fclJ*	NRPS	Deletion of 6819/6819 Bp of Xbud_02641	This work
X. bud. DSM 16342 Δ*fclK*	PKS	Deletion of 4965/5010 Bp of Xbud_02642	This work

Table S4 Signal intensities of the compounds **2**, **9** and **3** in the deletion mutants compared to the wild type (**A**) and signal intensities of the compounds **6** and **7** of the novel hybrid producer *X. szentirmaii* Δ*fclCDE* pFF1_*fclCDEFGH_X.bud*. (induced) compared to the compounds **1** and **2** of the wild type (**B**). The comparisons are based on the absolute signal intensities of the compounds measured by high resolution MALDI-MS. – (compound not detetcted).

A

***X. szentirmaii* mutant**	Fabclavine IVb (**2**)	Shortened fabclavine (**9**)	Polyamine (**3**)
WT	100	100	100
Δ*fclA*	116	91	105
Δ*fclCDE*	-	-	-
Δ*fclC*	-	-	-
Δ*fclD*	-	-	-
Δ*fclE*	-	-	-
Δ*fclF*	-	-	-
Δ*fclG*	-	-	-
Δ*fclH*	32	155	17
Δ*fclI*	-	2390	194
Δ*fclJ*	-	-	375
Δ*fclK*	-	-	237
Δ*fclL*	-	-	43

B

***X. szentirmaii* mutant**	**Derivatives**	
WT	Fabclavine IVa (**1**)	Fabclavine IVb (**2**)
	100	100
Δ*fclCDE* pFF1_*fclCDEFGH_X.bud.*	Fabclavine hybrid (**6**)	Fabclavine hybrid (**7**)
	18	20

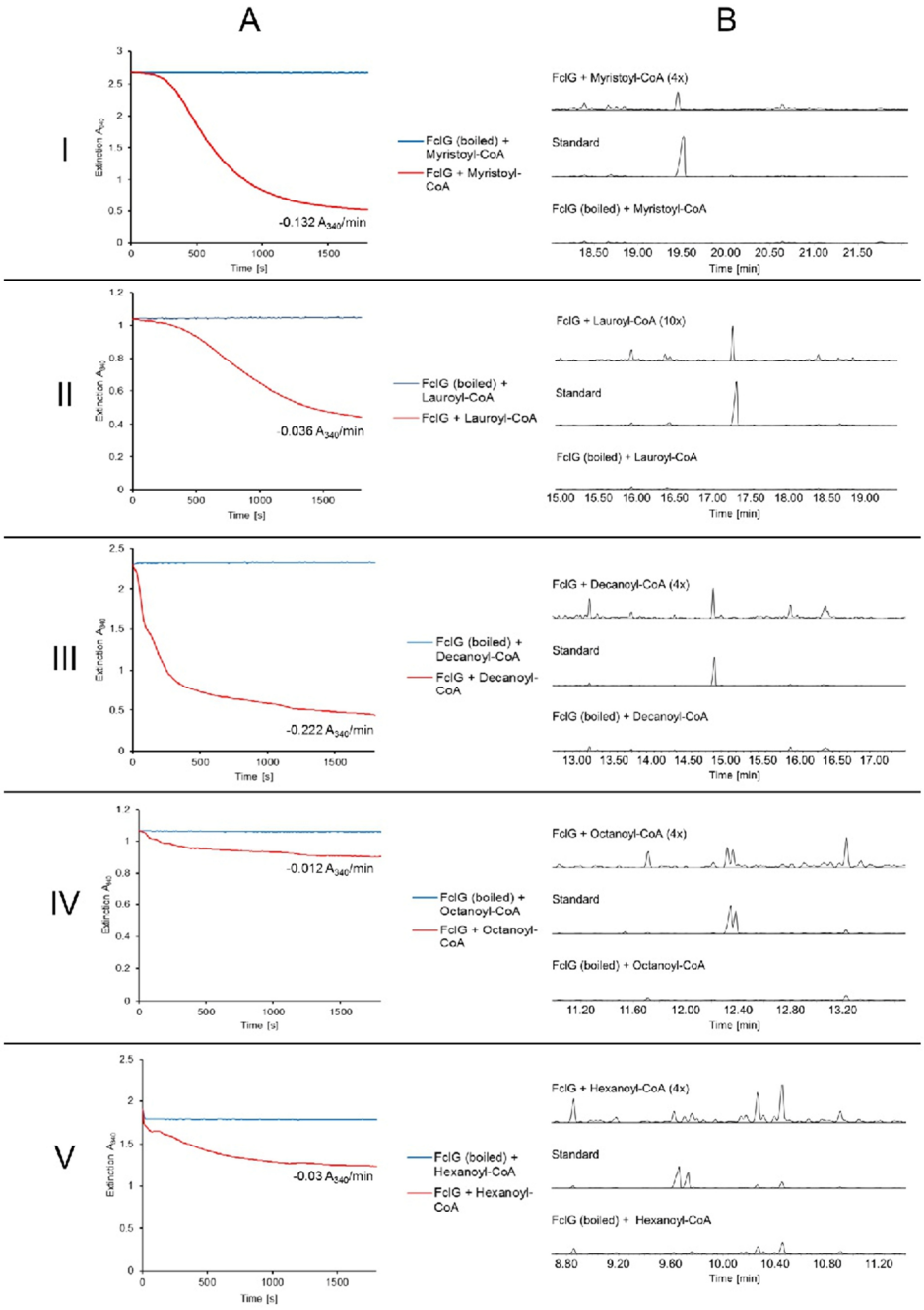
A
B
I
II
III
IV
V
Extinction A_{340}
Time [s]
-0.132 A_{340}/min
-0.036 A_{340}/min
-0.222 A_{340}/min
-0.012 A_{340}/min
-0.03 A_{340}/min
FclG (boiled) + Myristoyl-CoA
FclG + Myristoyl-CoA
FclG (boiled) + Lauroyl-CoA
FclG + Lauroyl-CoA
FclG (boiled) + Decanoyl-CoA
FclG + Decanoyl-CoA
FclG (boiled) + Octanoyl-CoA
FclG + Octanoyl-CoA
FclG (boiled) + Hexanoyl-CoA
FclG + Hexanoyl-CoA
FclG + Myristoyl-CoA (4x)
Standard
FclG (boiled) + Myristoyl-CoA
FclG + Lauroyl-CoA (10x)
FclG (boiled) + Lauroyl-CoA
FclG + Decanoyl-CoA (4x)
FclG (boiled) + Decanoyl-CoA
FclG + Octanoyl-CoA (4x)
FclG (boiled) + Octanoyl-CoA
FclG + Hexanoyl-CoA (4x)
FclG (boiled) + Hexanoyl-CoA
Time [min]

Fig. S1 NADPH-consumption of FclG by incubation with different acyl-CoA derivatives (**A**) and resulting products detected by GC-MS (**B**). I: Myristoyl-CoA; II: Lauroyl-CoA; III: Decanoyl-CoA; IV: Octanoyl-CoA; V: Hexanoyl-CoA.

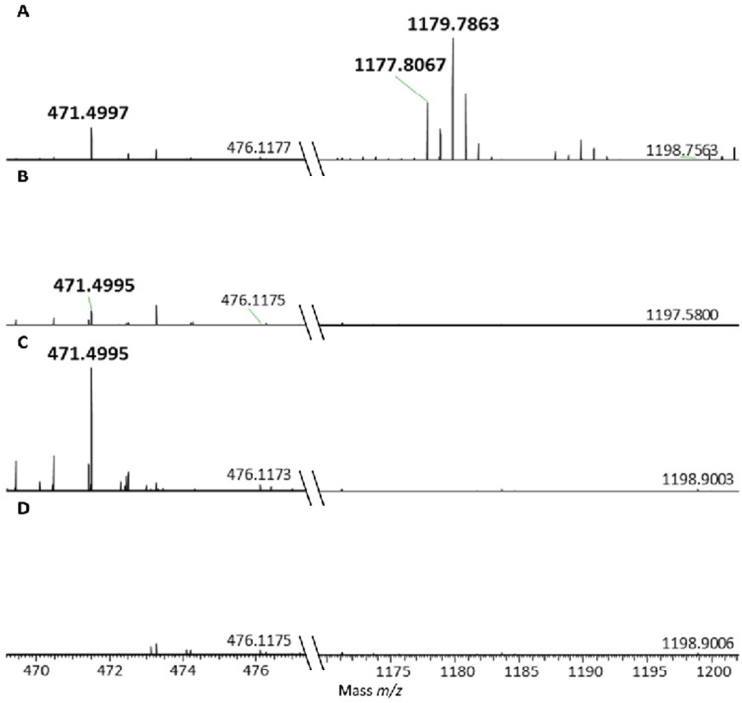

Fig. S2 High resolution MALDI-MS-spectra of *X. szentirmaii* WT (**A**), Δ*fclL* (**B**), Δ*fclJ* (**C**) and Δ*fclE* (**D**) as examples for evaluation of the phenotype of the single deletion mutants described in Table 1. **A** is representative for the presence of polyamine (**3**) and fabclavine (**1** and **2**), **B** and **C** for the presence of polyamine (**3**) but no fabclavine (**1** and **2**) and **D** for neither polyamine (**3**) nor fabclavine (**1** and **2**). The phenotype of entry **a** of Fig. 2 is based on spectrum **A**.

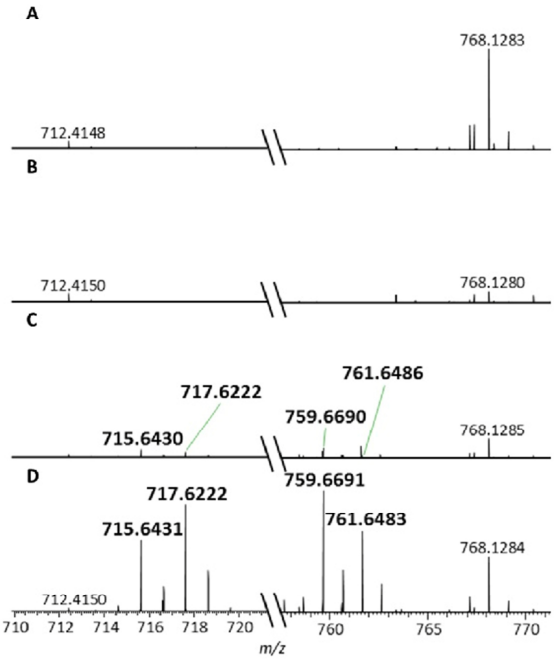

			X. szentirmaii WT		*ΔfclI*	
Compound	calc m/z	Sum formula	det m/z	error [Δppm]	det m/z	error [Δppm]
8	715.6419	$C_{39}H_{82}N_6O_5$	715.6430	+1.487	715.6431	+1.654
9	717.6212	$C_{38}H_{80}N_6O_6$	717.6222	+1.323	717.6222	+1.448
10	759.6682	$C_{41}H_{86}N_6O_5$	759.6690	+1.144	759.6691	+1.223
11	761.6474	$C_{40}H_{84}N_6O_7$	761.6486	+1.555	761.6483	+1.201

Fig. S3 High resolution MALDI-MS-spectra of *X. szentirmaii* Δ*fclC* (**A**), Δ*fclL* (**B**), wild type (**C**) and Δ*fclI* (**D**) including detected masses of the short fabclavine derivatives (**8**-**11**). The phenotype of entry **I** of Fig. 2 is based on spectrum **D**.

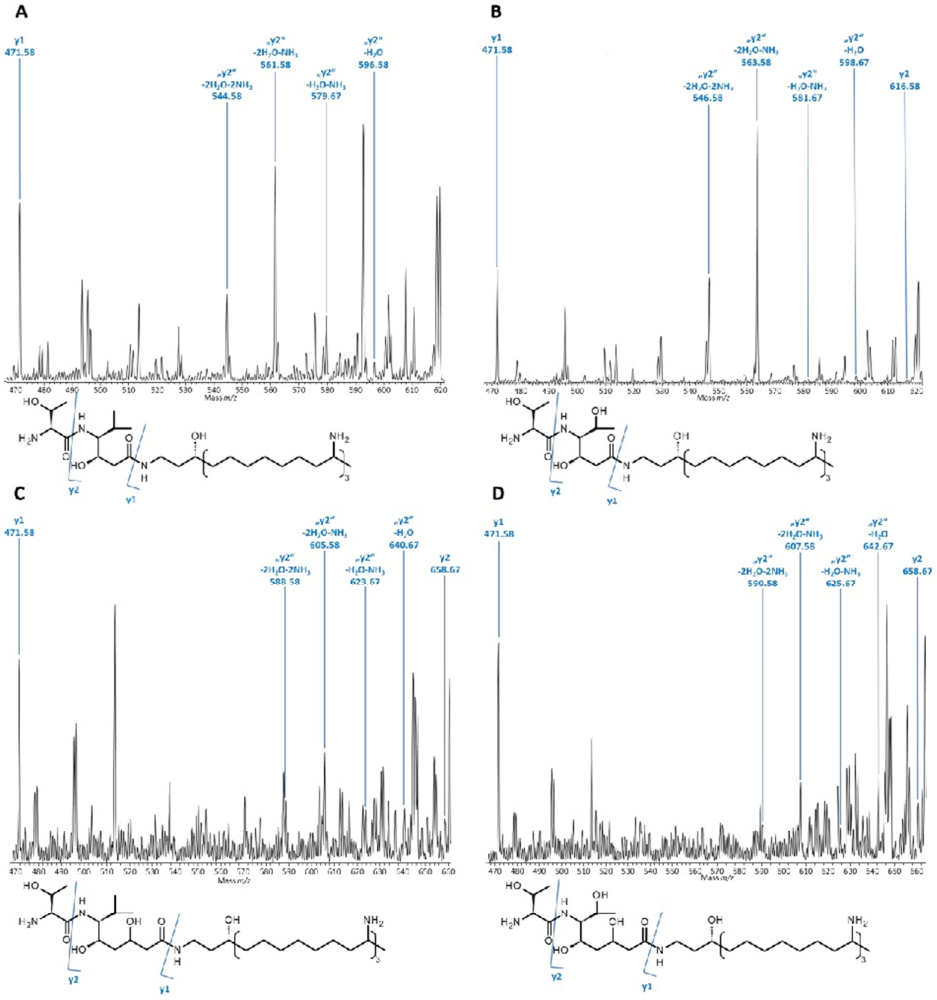
A
B
C
D

E	(A) sFcl compound 8			(B) sFcl compound 9			(C) sFcl compound 10			(D) sFcl compound 11		
Ion	Sum formula	Calc. m/z	Det. m/z	Sum formula	Calc. m/z	Det. m/z	Sum formula	Calc. m/z	Det. m/z	Sum formula	Calc. m/z	Det. m/z
y1	$C_{28}H_{63}N_4O$	471.50	471.58	$C_{28}H_{63}N_4O$	471.50	471.58	$C_{28}H_{63}N_4O$	471.50	471.58	$C_{28}H_{63}N_4O$	471.50	471.58
y2	$C_{35}H_{76}N_5O_3$	614.59	n.d.	$C_{34}H_{74}N_5O_4$	616.57	616.58	$C_{37}H_{80}N_5O_4$	658.62	658.67	$C_{36}H_{78}N_5O_5$	660.60	660.58
„y2“ $-H_2O$	$C_{35}H_{74}N_5O_2$	596.58	596.58	$C_{34}H_{72}N_5O_3$	598.56	598.67	$C_{37}H_{78}N_5O_3$	640.61	640.67	$C_{36}H_{76}N_5O_4$	642.59	642.67
„y2“ $-H_2O$ $-NH_3$	$C_{35}H_{71}N_4O_2$	579.56	579.67	$C_{34}H_{69}N_4O_3$	581.54	581.67	$C_{37}H_{75}N_4O_3$	623.58	623.67	$C_{36}H_{73}N_4O_4$	625.56	625.67
„y2“ $-2H_2O$ $-NH_3$	$C_{35}H_{69}N_4O$	561.55	561.58	$C_{34}H_{67}N_4O_2$	563.53	563.58	$C_{37}H_{73}N_4O_2$	605.57	605.58	$C_{36}H_{71}N_4O_3$	607.55	607.58
„y2“ $-2H_2O$ $-2NH_3$	$C_{35}H_{66}N_3O$	544.52	544.58	$C_{34}H_{64}N_3O_2$	546.50	546.58	$C_{37}H_{70}N_3O_2$	588.55	588.58	$C_{36}H_{68}N_3O_3$	590.53	590.58

Fig. S4 MALDI-MS^2-spectra of shortened fabclavines **8** (**A**), **9** (**B**), **10** (**C**) and **11** (**D**) of *X. szentirmaii* Δ*fclI* with proposed structure and expected fragment ions (**E**).

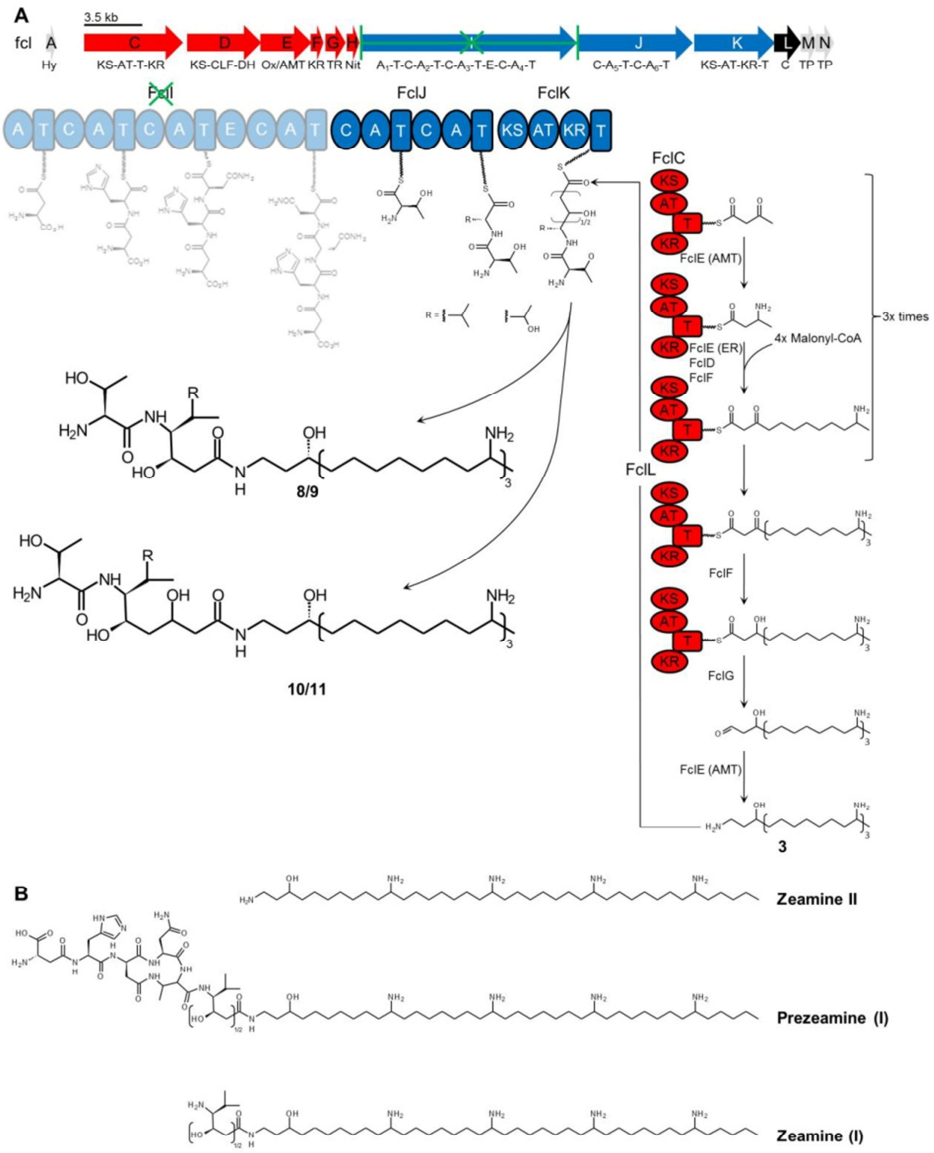

Fig. S5 Proposed biosynthesis of the shortened fabclavine derivatives (**8**-**11**) in *X. szentirmaii* Δ*fclI* (**A**) and the comparable structures of the (pre-)zeamines described for *S. plymuthica* (**B**) [7]. Domain and enzyme abbreviations: Hy (hydrolase), KS (ketosynthase), AT (acyltransferase), T (thiolation; corresponds to acyl carrier or peptidyl carrier protein), KR (ketoreductase), CLF (chain length factor

domain), DH (dehydratase), Ox (2-nitropropane dioxygenase), AMT (aminotransferase), TR (thioester reductase), Nit (nitrilase), A (adenylation), C (condensation), E (epimerization), TP (transport).

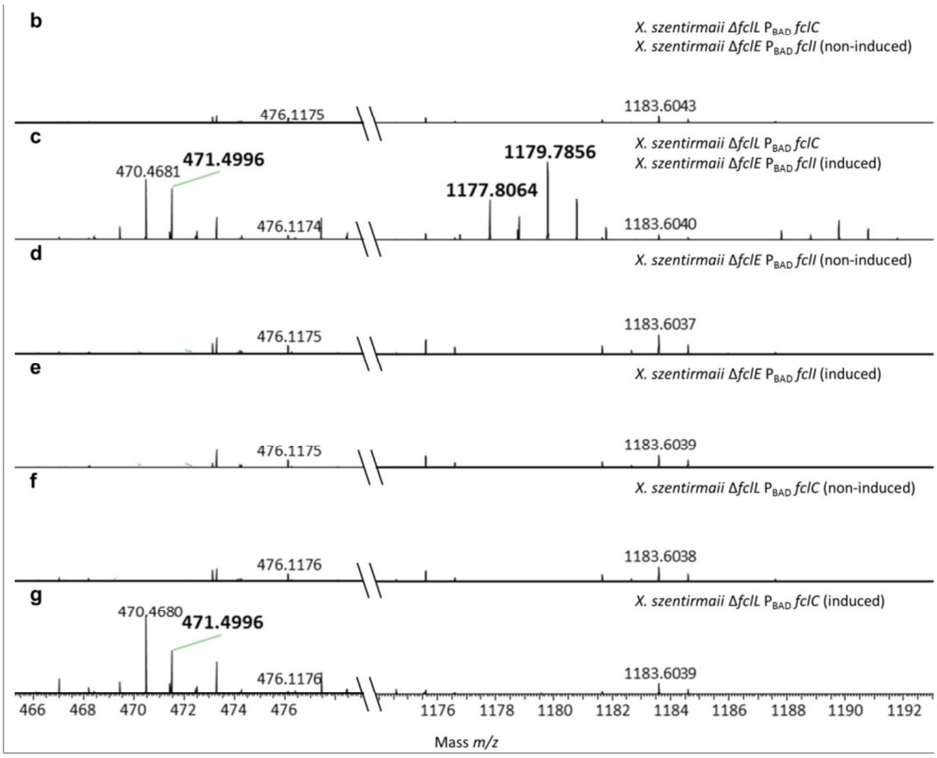

Fig. S6 High resolution MALDI-MS-spectra of the *X. szentirmaii* co-cultivation experiments summarized in Fig. 2. The phenotypes of entry **b**, **c**, **d**, **e**, **f**, and **g** of Fig. 2 are based on these spectra.

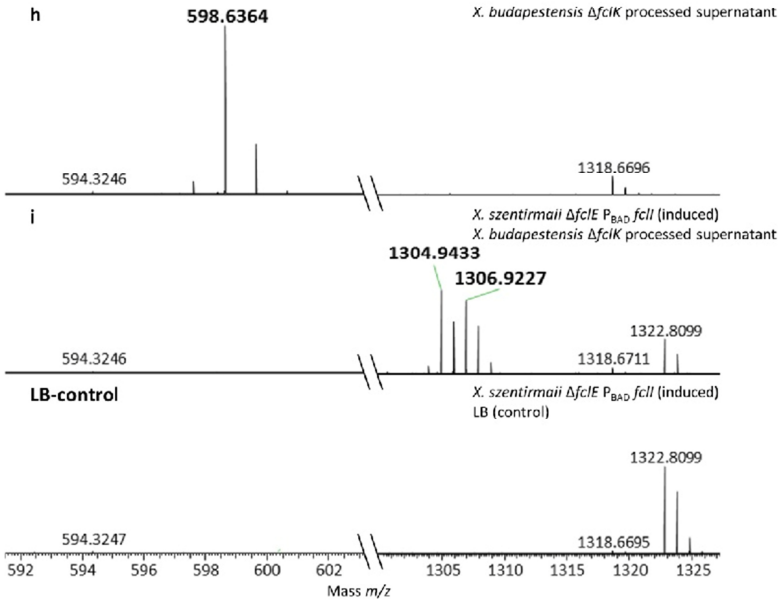

Fig. S7 High resolution MALDI-MS-spectra of the *X. szentirmaii* cross-feeding experiments summarized in Fig. 2. The phenotypes of entry **h** and **i** of Fig. 2 are based on these spectra.

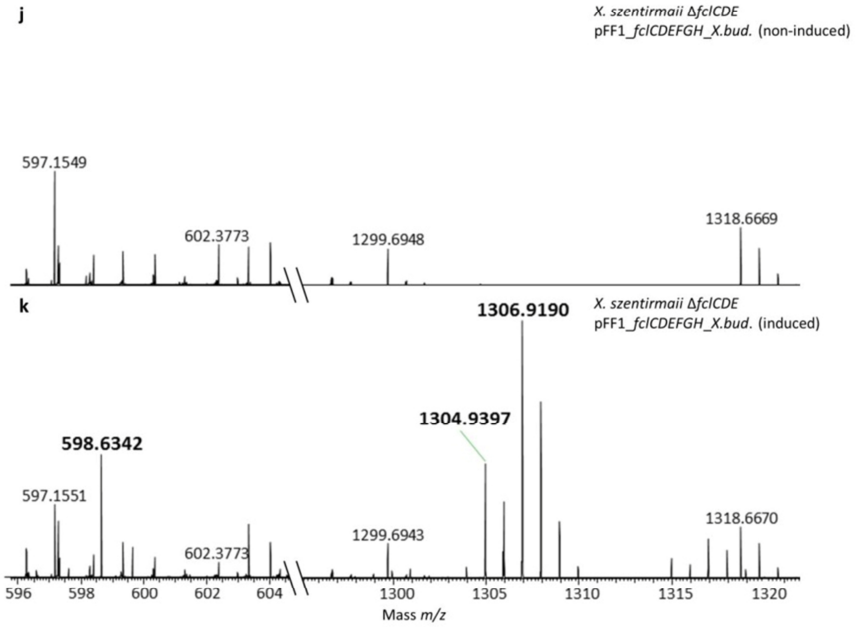

Fig. S8 High resolution MALDI-MS-spectra of the *X. szentirmaii* heterologous polyamine production experiments summarized in Fig. 2. The phenotypes of entry **j** and **k** of Fig. 2 are based on these spectra.

Expected fragmentions	Sum formula	m/z
y1 „Polyamine *X. bud.*“	$C_{36}H_{80}N_5O$	598.64
y2	$C_{42}H_{91}N_6O_4$	743.71
y5	$C_{54}H_{108}N_{11}O_9$	1054.83
y6	$C_{60}H_{115}N_{14}O_{10}$	1191.89
b1	$C_4H_6NO_3$	116.03
b2	$C_{10}H_{13}N_4O_4$	253.09
b5	$C_{22}H_{30}N_9O_9$	564.22
B6 „NRPS-PKS *X. sz.*“	$C_{20}H_{41}N_{10}O_{12}$	709.29

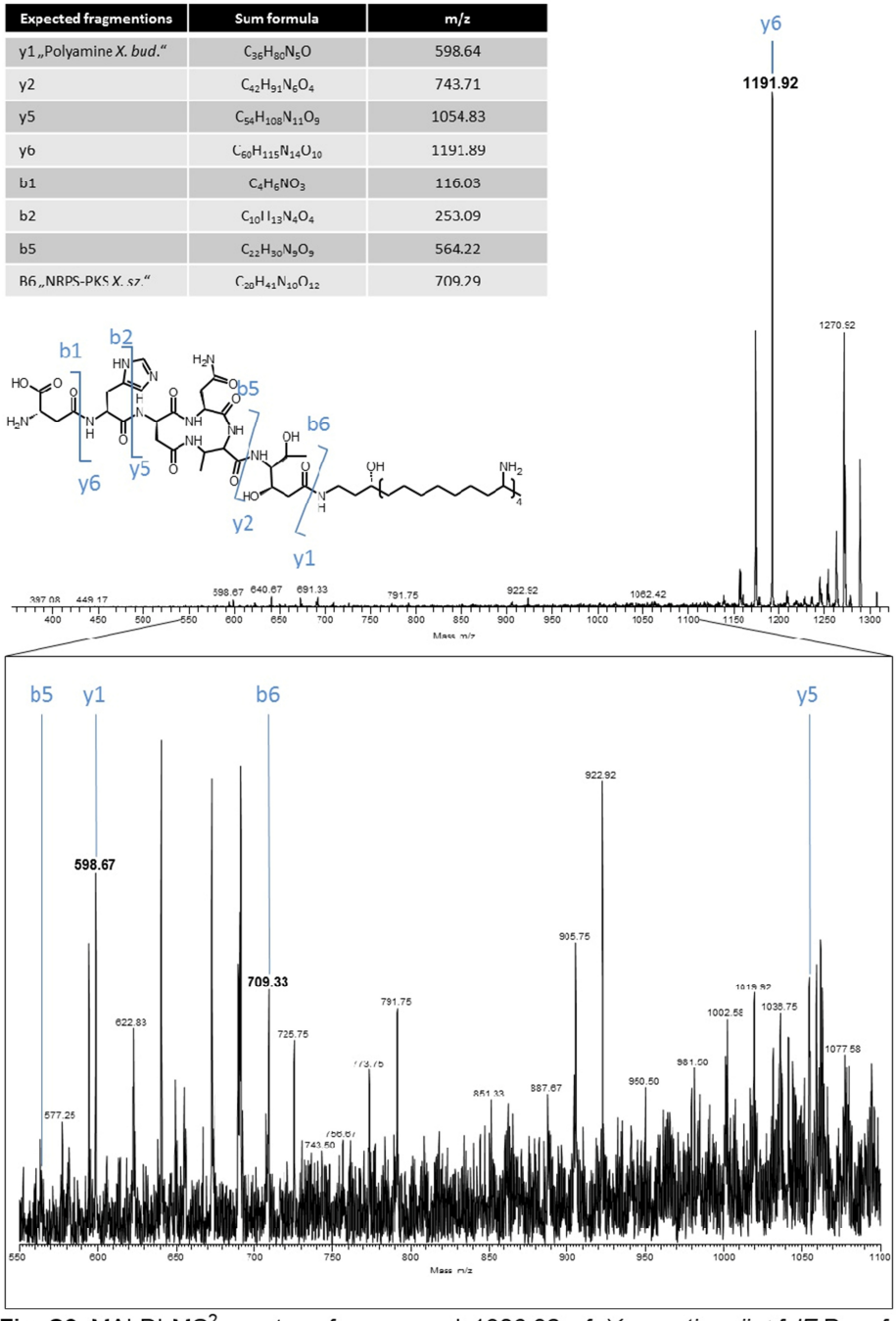

Fig. S9 MALDI-MS^2-spectra of compound 1306.92 of *X. szentirmaii* Δ*fclE* P_{BAD} *fclI* (induced) cross-fed with supernatant of *X. budapestensis* Δ*fclK* (processed supernatant) inclusive expected fragment ions and proposed structure.

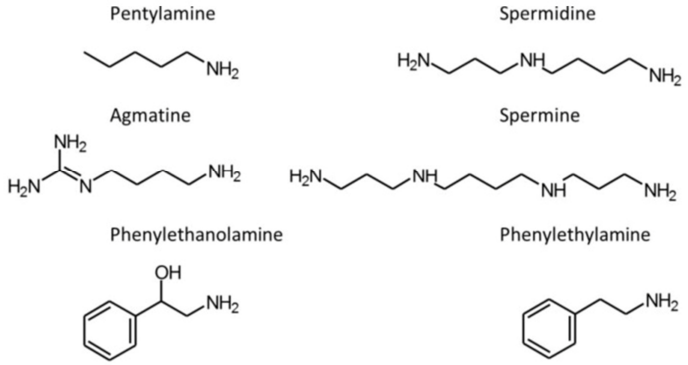

Fig. S10 Structures of amines fed to *X. szentirmaii* Δ*fclE* P_{BAD} *fclI*.

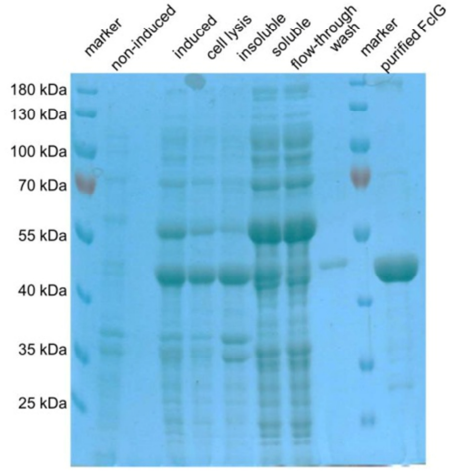

Fig. S11 Analysis of the Strep-Tag chromatography purification of FclG by sodium dodecyl sulfate polyacrylamide gel electrophoresis. Recombinant FclG has a size of 48 kDa. PageRuler™ prestained protein ladder [Thermo Fisher Scientific] was used as marker.

References

[1] Bode, E., Brachmann, A.O., Kegler, C., Simsek, R., Dauth, C., Zhou, Q., Kaiser, M., Klemmt, P., Bode, H.B. (2015) Simple "on-demand" production of bioactive

natural products. Chembiochem 16, 1115–1119. https://doi.org/10.1002/cbic.201500094

[2] Brachmann, A.O., Joyce, S.A., Jenke-Kodama, H., Schwär, G., Clarke, D.J., Bode, H.B. (2007) A type II polyketide synthase is responsible for anthraquinone biosynthesis in *Photorhabdus luminescens*. Chembiochem 8, 1721–1728. https://doi.org/10.1002/cbic.200700300

[3] Fu, C., Donovan, W.P., Shikapwashya-Hasser, O., Ye, X., Cole, R.H. (2014) Hot Fusion: an efficient method to clone multiple DNA fragments as well as inverted repeats without ligase. PLoS One 9, e115318. https://doi.org/10.1371/journal.pone.0115318

[4] Gietz, R.D., Schiestl, R.H. (2007) Frozen competent yeast cells that can be transformed with high efficiency using the LiAc/SS carrier DNA/PEG method. Nat Protoc 2, 1–4. https://doi.org/10.1038/nprot.2007.17

[5] Gietz, R.D., Schiestl, R.H. (2007) High-efficiency yeast transformation using the LiAc/SS carrier DNA/PEG method. Nat Protoc 2, 31–34. https://doi.org/10.1038/nprot.2007.13

[6] Lengyel, K., Lang, E., Fodor, A., Szállás, E., Schumann, P., Stackebrandt, E. (2005) Description of four novel species of *Xenorhabdus*, family Enterobacteriaceae: *Xenorhabdus budapestensis* sp. nov., *Xenorhabdus ehlersii* sp. nov., *Xenorhabdus innexi* sp. nov., and *Xenorhabdus szentirmaii* sp. nov. Syst Appl Microbiol 28, 115–122. https://doi.org/10.1016/j.syapm.2004.10.004

[7] Masschelein, J., Clauwers, C., Awodi, U.R., Stalmans, K., Vermaelen, W., Lescrinier, E., Aertsen, A., Michiels, C., Challis, G.L., Lavigne, R. (2015) A combination of polyunsaturated fatty acid, nonribosomal peptide and polyketide biosynthetic machinery is used to assemble the zeamine antibiotics. Chem Sci 6, 923–929. https://doi.org/10.1039/c4sc01927j

[8] Nishihara, K., Kanemori, M., Yanagi, H., Yura, T. (2000) Overexpression of Trigger Factor Prevents Aggregation of Recombinant Proteins in *Escherichia coli*. Appl Environ Microbiol 66, 884–889.

[9] Philippe, N., Alcaraz, J.-P., Coursange, E., Geiselmann, J., Schneider, D. (2004) Improvement of pCVD442, a suicide plasmid for gene allele exchange in bacteria. Plasmid 51, 246–255. https://doi.org/10.1016/j.plasmid.2004.02.003

[10] Schimming, O., Fleischhacker, F., Nollmann, F.I., Bode, H.B. (2014) Yeast Homologous Recombination Cloning Leading to the Novel Peptides Ambactin and Xenolindicin. Chembiochem 15, 1290–1294. https://doi.org/10.1002/cbic.201402065

[11] Simon, R., Priefer, U., Pühler, A. (1983) A Broad Host Range Mobilization System for *In Vivo* Genetic Engineering: Transposon Mutagenesis in Gram Negative Bacteria. Bio/Technology 1, 784 EP -. https://doi.org/10.1038/nbt1183-784

[12] Thoma, S., Schobert, M. (2009) An improved *Escherichia coli* donor strain for diparental mating. FEMS Microbiol. Lett. 294, 127–132. https://doi.org/10.1111/j.1574-6968.2009.01556.x

[13] Xu, J., Lohrke, S., Hurlbert, I.M., Hurlbert, R.E. (1989) Transformation of *Xenorhabdus nematophilus*. Appl Environ Microbiol. 55, 806–812.

6.2 Fabclavine diversity in *Xenorhabdus* bacteria

Authors:

Sebastian L. Wenski[1], Harun Cimen[2], Natalie Berghaus[1], Sebastian W. Fuchs[1], Selcuk Hazir[2] and Helge B. Bode[1,3,4*]

[1] Molekulare Biotechnologie, Fachbereich Biowissenschaften, Goethe Universität Frankfurt, Max-von-Laue-Str. 9, 60438 Frankfurt, Germany and

[2] Adnan Menderes University, Faculty of Arts and Sciences, Department of Biology, 09010 Aydin, TURKEY and

[3] Buchmann Institute for Molecular Life Sciences (BMLS), Goethe Universität Frankfurt, Max-von-Laue-Str. 15, 60438 Frankfurt, Germany and

[4] Senckenberg Gesellschaft für Naturforschung, Senckenberganlage 25, 60325 Frankfurt, Germany

Published in:

Beilstein Journal of Organic Chemistry 16 (2020) 956–965

doi: 10.3762/bjoc.16.84

Online access: https://www.beilstein-journals.org/bjoc/articles/16/84

© 2020 Wenski et al.; licensee Beilstein-Institut.

This is an Open Access article under the terms of the Creative Commons Attribution License (http://creativecommons.org/licenses/by/4.0). Please note that the reuse, redistribution and reproduction in particular requires that the authors and source are credited.

Attachment 1

Declaration of author contributions to the publication / manuscript (title):

Fabclavine diversity in *Xenorhabdus* bacteria

Status: published

Name of journal: Beilstein Journal of Organic Chemistry, doi: 10.3762/bjoc.16.84

Contributing authors:

Wenski, S. L. (SLW); Cimen, H. (HC); Berghaus, N. (NB); Fuchs, S. W. (SWF); Hazir, S. (SH); Bode, H. B. (HBB)

What are the contributions of the doctoral candidate and his co-authors?

(1) Concept and design

SLW (55%), HBB (35%), HC (5%), SH (5%)

(2) Conducting tests and experiments

Generation of promoter-exchange mutants: SLW (80%); Bioactivity assays: HC (20%)

(3) Compilation of data sets and figures

MALDI-MS-analysis of promoter-exchange mutants and wild type strains: SLW (70%), SWF (5%), NB (5%); Bioactivity assays: HC (20%)

(4) Analysis and interpretation of data

Identification and elucidation of novel derivatives: SLW (70%), NB (5%), SWF (5%); Bioactivity assays: HC (20%)

(5) Drafting of manuscript

SLW (75%), HBB (20%), HC (5%)

I hereby certify that the information above is correct.

Date and place	Signature doctoral candidate
Date and place	Signature supervisor
Date and place	If required, signature of corresponding author

BEILSTEIN JOURNAL OF ORGANIC CHEMISTRY

Fabclavine diversity in *Xenorhabdus* bacteria

Sebastian L. Wenski[1], Harun Cimen[2], Natalie Berghaus[1], Sebastian W. Fuchs[1], Selcuk Hazir[2] and Helge B. Bode[*1,3,4]

Full Research Paper

Open Access

Address:
[1]Molekulare Biotechnologie, Fachbereich Biowissenschaften, Goethe Universität Frankfurt, Max-von-Laue-Str. 9, 60438 Frankfurt, Germany, [2]Adnan Menderes University, Faculty of Arts and Sciences, Department of Biology, 09010 Aydin, Turkey, [3]Buchmann Institute for Molecular Life Sciences (BMLS), Goethe Universität Frankfurt, Max-von-Laue-Str. 15, 60438 Frankfurt, Germany and [4]Senckenberg Gesellschaft für Naturforschung, Senckenberganlage 25, 60325 Frankfurt am Main, Germany

Email:
Helge B. Bode[*] - h.bode@bio.uni-frankfurt.de

* Corresponding author

Keywords:
antibiotic; fabclavine; NRPS-PKS hybrid; secondary metabolite; *Xenorhabdus*

Beilstein J. Org. Chem. **2020,** *16,* 956–965.
doi:10.3762/bjoc.16.84

Received: 07 March 2020
Accepted: 23 April 2020
Published: 07 May 2020

Associate Editor: J. S. Dickschat

© 2020 Wenski et al.; licensee Beilstein-Institut.
License and terms: see end of document.

Abstract

The global threat of multiresistant pathogens has to be answered by the development of novel antibiotics. Established antibiotic applications are often based on so-called secondary or specialized metabolites (SMs), identified in large screening approaches. To continue this successful strategy, new sources for bioactive compounds are required, such as the bacterial genera *Xenorhabdus* or *Photorhabdus*. In these strains, fabclavines are widely distributed SMs with a broad-spectrum bioactivity. Fabclavines are hybrid SMs derived from nonribosomal peptide synthetases (NRPS), polyunsaturated fatty acid (PUFA), and polyketide synthases (PKS). Selected *Xenorhabdus* and *Photorhabdus* mutant strains were generated applying a chemically inducible promoter in front of the suggested fabclavine (*fcl*) biosynthesis gene cluster (BGC), followed by the analysis of the occurring fabclavines. Subsequently, known and unknown derivatives were identified and confirmed by MALDI–MS and MALDI–MS^2 experiments in combination with an optimized sample preparation. This led to a total number of 22 novel fabclavine derivatives in eight strains, increasing the overall number of fabclavines to 32. Together with the identification of fabclavines as major antibiotics in several entomopathogenic strains, our work lays the foundation for the rapid fabclavine identification and dereplication as the basis for future work of this widespread and bioactive SM class.

Introduction

The constantly increasing threat of multiresistant pathogens requires the development of new antibiotics, as they are indispensable to maintain the state of health of our society [1]. Bacterial natural products, also called secondary or specialized metabolites (SM), such as daptomycin, vancomycin, or erythromycin, have already been shown to be potent antibiotics [2-4].

Beilstein J. Org. Chem. 2020, 16, 956–965.

Consequently, research in the field of novel SMs with antimicrobial activity is vital to provide new avenues to new antiinfective drugs or lead compounds.

Beside traditional sources such as actinomycetes and myxobacteria, the genera *Photorhabdus* and *Xenorhabdus* are promising sources to discover new SMs since up to 6.5% of their overall genome sequence are associated with SM biosynthesis [5,6]. This includes antimicrobials like isopropylstilbene, xenocoumacins, amicoumacin, and several other SMs [7-11]. Naturally, *Photorhabdus* and *Xenorhabdus* are living in mutualistic symbiosis with nematodes of the genera *Steinernema* or *Heterorhabditis,* respectively [5,12]. Together, they infect and kill soil-living insects to use the cadaver as a food source and shelter [5]. After the infection of the insect by the nematode, the bacteria are released from the nematode gut into the insect hemocoel where they start producing a diversity of different natural products to suppress the immune response and to kill the insects, to defend the carcass against food competitors, and to trigger the development of the nematode [5,13].

The general interest on *Photorhabdus* and *Xenorhabdus* increased in recent years, not only because of their large number of SMs, but also due to their easy-to-handle cultivation under laboratory conditions in combination with the accessibility for genetic manipulations such as genomic integrations or deletions [14-17]. Furthermore, recently published studies focused on the possible application of *Photorhabdus* and *Xenorhabdus* as biological pest control agents with and without the corresponding nematodes [18,19].

In 2014, the fabclavines were identified in *X. budapestensis* and *X. szentirmaii*, and a 50 kb biosynthesis gene cluster (BGC) was identified to be responsible for their formation (Figure 1) [20]. These compounds were of special interest because of their broad-spectrum bioactivity against Gram-positive and -negative bacteria, fungi, and protozoa [20,21]. Fabclavines are hexapeptide/polyketide hybrids derived from nonribosomal peptide synthetases (NRPS) and a polyketide synthase (PKS), which are connected to an unusual polyamine derived from polyunsaturated fatty acid (PUFA) synthases [20]. Beside full-length fabclavines, also shortened derivatives were identified. These are generated when the peptide biosynthesis starts directly with the second NRPS enzyme FclJ, which results in the formation of a dipeptide instead of the usual hexapeptide (Figure 1) [22]. Structurally related compounds are the (pre)zeamines described for *Serratia plymuthica* and *Dickeya zeae* [23,24]. They also exhibit broad-spectrum bioactivity, but their biosynthesis includes an additional processing step, executed by an acylpeptide hydrolase, which could not be detected in the fabclavine BGC [20,25].

To date, 10 full-length fabclavines could be identified, and the structure of fabclavine Ia (**1**) could be determined by NMR spectroscopy [20]. Furthermore, bioinformatic analysis of *Xenorhabdus* and *Photorhabdus* genomes revealed that the ability to produce fabclavines or related compounds might be widespread in these strains [22,26]. In order to analyze the associated fabclavine diversity, selected strains were analyzed both chemically and genomically, and mutants in putative *fcl* BGCs were generated. Thereby, a list of derivatives was obtained, which was further correlated to the potential fabclavine-producing, but genetically not accessible *X. innexi* strain. Finally, the bioactivity of the culture supernatants was analyzed, revealing that the fabclavines contribute largely to the overall bioactivity of *Xenorhabdus* when grown under laboratory conditions.

Results

Biosynthetic gene clusters for the fabclavine production are highly conserved

During the screening for homologous *fcl* BGCs in *Xenorhabdus* and *Photorhabdus* strains, several candidate clusters were identified, which were conserved both in their BGC synteny as well as at the single protein level (Figure 2) [22].

The strain KK7.4 showed protein identities of ≥95% with *X. stockiae* and strain KJ12.1 (Figure S1, Supporting Information File 1). Similar identities could be observed for *X. budapestensis*, *X. cabanillasii*, and *X. indica* (≥91%, Table S3, Supporting Information File 1). Although both groups of strains also clustered together due to their close evolutionary relationship, the question was whether they would also produce the same fabclavine derivatives [26].

The BGC of *X. bovienii* encodes only the genes responsible for the polyamine biosynthesis as well as the transporter genes. A cryptic homologue of the NRPS *fclJ* in combination with the overall BGC structure suggested that the *fcl* BGC of *X. bovienii* originally also contained the NRPS-PKS-hybrid genes (Figure 2) [22]. In contrast, the BGC of *P. temperata* is reduced to only harbor the homologous genes of *fclC*, *fclD* and *fclE* (Figure 2) [22].

X. innexi also harbors a *fcl*-like BGC, with protein identities of 68–90% compared to *X. stockiae* (Figure S1, Supporting Information File 1). Nevertheless, *X. innexi* contains a *tonB*-homologue instead of the NUDIX-hydrolase *fclA* and an acyl-CoA-thioesterase instead of *fclM* and *fclN*, leading to the postulated compound Xenorhabdus lipoprotein toxin (Xlt, Figure S1, Supporting Information File 1) [27].

Beilstein J. Org. Chem. **2020,** *16,* 956–965.

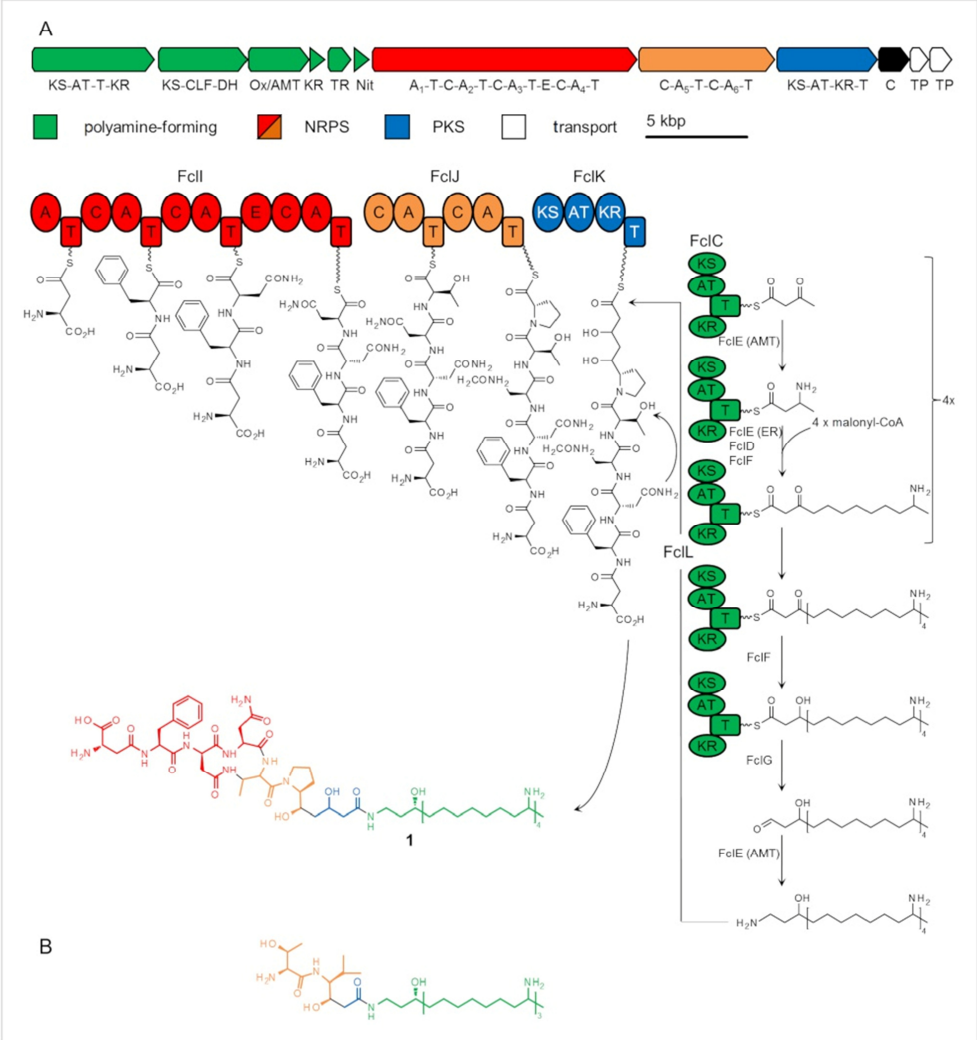

Figure 1: General biosynthesis of fabclavine Ia (**1**) in *X. budapestensis* (A) and representation of a shortened fabclavine derivative from *X. szentirmaii* (B), resulting from the alternative biosynthesis start at FclJ (the Figures were adapted and modified from [20] and [22]. KS: ketosynthase, AT: acyltransferase, T: thiolation domain, KR: ketoreductase, CLF: chain length factor domain, DH: dehydratase, Ox: 2-nitropropane dioxygenase (enoyl reductase), AMT: aminotransferase, TR: thioester reductase, Nit: nitrilase, A: adenylation, C: condensation, E: epimerization, TP: transport.

Furthermore, homologous BGCs can be found in *Serratia plymuthica* as well as in *Dickeya zeae* [20,25]. Like *Xenorhabdus* and *Photorhabdus*, these bacteria also belong to the order *Enterobacterales* and are producers of zeamines, which are structurally closely related to fabclavines and differ only in a postbiosynthetic modification step (Figure S1, Supporting Information File 1) [25].

Identification of new fabclavine derivatives

To analyze the identified *fcl* BGCs, mutant strains were generated with a chemically inducible promoter in front of *fclC* or corresponding homologues (Figure 2). The inducible promoter was integrated via conjugation, with *Escherichia coli* as a donor strain, followed by homologous recombination as described previously [14,22]. This led to a formal ‘knock out’ of the BGC

Beilstein J. Org. Chem. 2020, 16, 956–965.

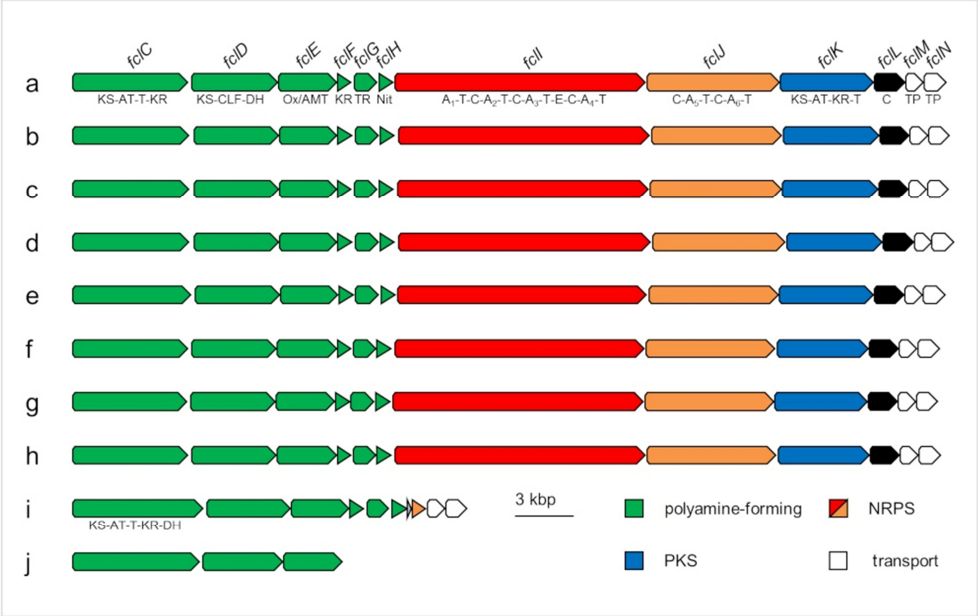

Figure 2: Comparison of the *fcl* BGCs in *Xenorhabdus* and *Photorhabdus* strains responsible for the fabclavine biosynthesis. a: *X. szentirmaii*, b: *X. budapestensis*, c: *X. cabanillasii*, d: *X. indica*, e: *X. hominickii*, f: *X. stockiae*, g: KK7.4, h: KJ12.1, i: *X. bovienii*, j: *P. temperata*. KS: ketosynthase, AT: acyltransferase, T: thiolation domain, KR: ketoreductase, CLF: chain length factor domain, DH: dehydratase, Ox: 2-nitropropane dioxygenase (enoyl reductase), AMT: aminotransferase, TR: thioester reductase, Nit: nitrilase, A: adenylation, C: condensation, E: epimerization, TP: transport.

and no production of the respective natural product without induction, whereas induced mutants showed mostly an overproduction of the respective natural product [14]. Initially, the non-induced promoter-exchange mutant was compared with the induced mutant and the wild type to identify signals, related to possible biosynthesis products of the *fcl* BGCs using the known structure of **1** as a reference [20]. To confirm these signals as fabclavine derivatives, high-resolution MALDI–MS measurements to determine the exact mass and MALDI–MS^2 fragmentation patterns of selected derivatives were acquired. If necessary, the measurements were repeated from mutants cultivated in ^{13}C media in order to determine the number of carbons in the sum formula [28].

The general structure of the fabclavines is highly conserved and differs only in the specified moieties as shown in Table 1. The NRPS part of the full-length fabclavines harbors six amino acids, whereby the second position (R^1) varies between phenylalanine (Phe), histidine (His), and alanine (Ala) and the sixth position (R^2/R^3) between proline (Pro), valine (Val) and threonine (Thr). The polyamine can differ in the length from three to five amine units (*m*) and is connected via one to three partially reduced polyketide C2 units (*n*) with the NRPS part.

In this work, 22 yet unknown derivatives could be identified, which led to a total of 32 full-length derivatives (Table 1). In the following, the fabclavine characteristics of the individual or multiple strains are highlighted.

Besides derivatives with a polyamine of four amine units (**1**–**4**), the already described fabclavine producer *X. budapestensis* showed also the incorporation of a three-amine unit polyamine (**5**–**8**, Table 1 and Figure S7, Supporting Information File 1). A similar set of derivatives could be observed for the closely related strains *X. indica* and *X. cabanillasii* (Table 1 and Figures S11, S12, S15, and S16, Supporting Information File 1). In these strains, additional derivatives with polyamines made of five amine units were identified (**9**–**12**, Table 1 and Figures S13 and S17, Supporting Information File 1).

In *X. hominickii*, only derivatives with polyamines made of five amine units were identified, but none with less (Table 1). Here, the polyamine was connected by one or two polyketide units to a NRPS part, with His in the second (Table 1, R^1) and Pro or Val in the sixth amino acid position (Table 1, R^2/R^3 and Figure S18, Supporting Information File 1), leading to the smallest set of identified derivatives (**11**–**14**).

Beilstein J. Org. Chem. **2020,** *16*, 956–965.

Table 1: Compound list of the fabclavine derivatives identified in this work. The structures are based on MALDI–HRMS and MALDI–MS^2 analyses using the known structure of **1** as a reference [20]. The derivatives **1**–**4** and **17**–**22** were described previously [20].

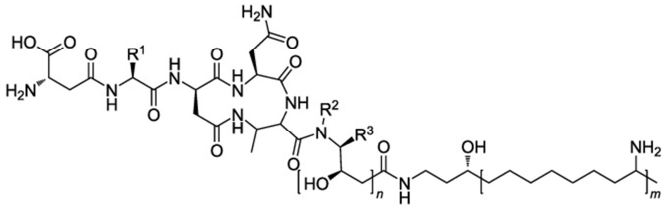

#	R^1	R^2	R^3	*n*	*m*	molecular formula	*m/z* $[M + H]^+$
1	Bn		–$(CH_2)_3$–	2	4	$C_{70}H_{125}N_{13}O_{13}$	1356.9593
2			–$(CH_2)_3$–	2	4	$C_{67}H_{123}N_{15}O_{13}$	1346.9498
3	Bn		–$(CH_2)_3$–	1	4	$C_{68}H_{121}N_{13}O_{12}$	1312.9330
4			–$(CH_2)_3$–	1	4	$C_{65}H_{119}N_{15}O_{12}$	1302.9235
5	Bn		–$(CH_2)_3$–	2	3	$C_{62}H_{108}N_{12}O_{13}$	1229.8232
6			–$(CH_2)_3$–	2	3	$C_{59}H_{106}N_{14}O_{13}$	1219.8137
7	Bn		–$(CH_2)_3$–	1	3	$C_{60}H_{104}N_{12}O_{12}$	1185.7969
8			–$(CH_2)_3$–	1	3	$C_{57}H_{102}N_{14}O_{12}$	1175.7874
9	Bn		–$(CH_2)_3$–	2	5	$C_{78}H_{142}N_{14}O_{13}$	1484.0954
10	Bn		–$(CH_2)_3$–	1	5	$C_{76}H_{138}N_{14}O_{12}$	1440.0691
11			–$(CH_2)_3$–	2	5	$C_{75}H_{140}N_{16}O_{13}$	1474.0859
12			–$(CH_2)_3$–	1	5	$C_{73}H_{136}N_{16}O_{12}$	1430.0596
13		H	iPr	1	5	$C_{73}H_{138}N_{16}O_{12}$	1432.0753
14		H	iPr	2	5	$C_{75}H_{142}N_{16}O_{13}$	1476.1015
15	CH_3	H	iPr	1	3	$C_{54}H_{102}N_{12}O_{12}$	1111.7813
16	CH_3	H		1	3	$C_{53}H_{100}N_{12}O_{13}$	1113.7606
17		H	iPr	1	3	$C_{57}H_{104}N_{14}O_{12}$	1177.8031

Beilstein J. Org. Chem. **2020,** *16*, 956–965.

Table 1: Compound list of the fabclavine derivatives identified in this work. The structures are based on MALDI–HRMS and MALDI–MS^2 analyses using the known structure of **1** as a reference [20]. The derivatives **1–4** and **17–22** were described previously [20]. (continued)

18		H		1	3	$C_{56}H_{102}N_{14}O_{13}$	1179.7824
19		H	iPr	2	3	$C_{59}H_{108}N_{14}O_{13}$	1221.8293
20	Bn	H	iPr	1	3	$C_{60}H_{106}N_{12}O_{12}$	1187.8126
21	Bn	H		1	3	$C_{59}H_{104}N_{12}O_{13}$	1189.7979
22	Bn	H	iPr	2	3	$C_{62}H_{110}N_{12}O_{13}$	1231.8388
23	Bn	H	iPr	1	4	$C_{68}H_{123}N_{13}O_{12}$	1314.9487
24	Bn	H		1	4	$C_{67}H_{121}N_{13}O_{13}$	1316.9280
25		H	iPr	1	4	$C_{65}H_{121}N_{15}O_{12}$	1304.9392
26		H		1	4	$C_{64}H_{119}N_{15}O_{13}$	1306.9185
27	Bn	H	iPr	2	4	$C_{70}H_{127}N_{13}O_{13}$	1358.9749
28	Bn	H		2	4	$C_{69}H_{125}N_{13}O_{14}$	1360.9542
29		H	iPr	2	4	$C_{67}H_{125}N_{15}O_{13}$	1348.9654
30		H		2	4	$C_{66}H_{123}N_{15}O_{14}$	1350.9447
31		H	iPr	3	4	$C_{69}H_{129}N_{15}O_{14}$	1392.9916
32	Bn	H	iPr	3	4	$C_{72}H_{131}N_{13}O_{14}$	1403.0011

In *X. szentirmaii*, derivatives with an Ala incorporated at the second amino acid position were identified (**15** and **16**, Table 1, R^1) in addition to the already described derivatives **17–22**. However, the derivatives featuring the described Ala incorporation were not detected in any other strain analyzed (Table 1 and Figure S2, Supporting Information File 1) [20]. Furthermore, besides the dominant derivatives with a Val or Thr residue in the sixth amino acid position (Table 1, R^2/R^3), derivatives containing Pro were also observed, but with a much lower signal intensity (Figure S3, Supporting Information File 1).

As expected, the close taxonomic relationship between *X. stockiae*, KJ12.1 and KK7.4 resulted also in a similar set of produced fabclavine derivatives: Here, a *X. szentirmaii*-similar NRPS-derived part was connected to a polyamine with four amine units (**23–30**, Table 1). A special feature of this group were derivatives with up to three incorporated polyketide units instead of the usual one or two (**31** and **32**, Table 1 and Figure S25, Supporting Information File 1). Further signals were detected with a low abundance, suggesting the incorporation of Pro as a sixth amino acid (Figures S21, S26, and S29, Supporting Information File 1).

For *P. temperata* and *X. bovienii*, no fabclavine derivatives could be detected (data not shown), probably resulting from the missing NRPS and PKS genes (Figure 2).

Beilstein J. Org. Chem. **2020,** *16,* 956–965.

After the identification of the full-length derivatives, all strains were analyzed for the presence of shortened fabclavines, previously identified in *X. szentirmaii* [22]. Therefore, their structure was predicted from the elucidated full-length derivatives (Table 2). Surprisingly, only in *X. szentirmaii*, the abundance of compounds with 715 and 717 Da could be clearly confirmed (Figure S4, Supporting Information File 1). In the other strains, the expected shortened derivatives were not detectable (data not shown).

Table 2: Occurrence of the different fabclavine derivatives in the analyzed *Xenorhabdus* strains. The results are based on the MALDI–HRMS and MALDI–MS^2 analyses shown in Figures S2–S29 (Supporting Information File 1).

strain	compound
X. budapestensis	**1–8**
X. indica	**1–12**
X. cabanillasii	**1–4**, **8**, **11**, **12**
X. hominickii	**11–14**
X. szentirmaii	**15–22**
KJ12.1	**23–32**
X. stockiae	**23–32**
KK7.4	**2**, **23–32**
X. innexi	**4**, **23–32**

Our observation indicates that all strains produce additional derivatives than described in Table 2. Due to the fact that some of these derivatives were hardly detectable, preventing a structure confirmation and elucidation by MALDI–MS^2, they are only shown as proposed minor derivatives in the supplementary results (Figure S33, Supporting Information File 1).

As we were not able to generate a promoter-exchange mutant in *X. innexi* DSM 16336, its fabclavine derivatives were identified in the wild type. MALDI–HRMS measurements revealed multiple signals corresponding to fabclavines (Figures S30 and S31, Supporting Information File 1). To confirm the signal at 1392.99 Da as corresponding to compound **31**, a MALDI–MS^2 analysis was performed, resulting in the characteristic fragment ions with 598 Da for the polyamine part, and 795 Da for the NRPS-PKS part (Figure S32, Supporting Information File 1). Considering the fragmentation pattern for compound **31** and standard deviations below 1.3 ppm for further fabclavine derivatives, *X. innexi* could indeed be confirmed as a producer of fabclavines similar to those from *X. stockiae* (Figures S30–S32, Supporting Information File 1).

Bioactivity of the different fabclavine producers

Previous studies revealed that the fabclavines show a broad-spectrum bioactivity against a variety of different organisms [20]. To verify the bioactivity of the derivatives described in this work, the inhibitory activity of the wild type and the promoter-exchange mutants (induced and non-induced) were analyzed against the human pathogens *Escherichia coli*, *Staphylococcus aureus*, *Enterococcus faecalis*, and *Klebsiella pneumoniae* by agar well-diffusion bioassays (Table 3). Briefly, cell-free supernatant was filled into wells of agar plates, which were inoculated with the pathogenic bacteria. Subsequently, the

Table 3: Inhibition zones of the wild type (WT) and promoter-exchange mutant strains (non-ind: non-induced, ind: induced) in mm against the human pathogens *Escherichia coli* (a, ATCC 25922), *Staphylococcus aureus* (b, ATCC 29213), *Enterococcus faecalis* (c, ATCC 29212), and *Klebsiella pneumoniae* (d, ATCC 700603). The corresponding agar well-diffusion bioassays were performed three times, with ten replicates for each sample. *X. sto.* = *X. stockiae*, *X. ind.* = *X. indica*, *X. hom.* = *X. hominickii*, *X. sze.* = *X. szentirmaii*, *X. cab.* = *X. cabanillasii*, *X. bud.* = *X. budapestensis*.

	sample	strain							
		KJ12.1	KK7.4	*X. sto.*	*X. ind.*	*X. hom.*	*X. sze.*	*X. cab.*	*X. bud.*
a	WT	12.4 ± 0.2	12.6 ± 0.1	11.4 ± 0.2	17.8 ± 0.2	10.2 ± 0.2	12.6 ± 0.2	18.4 ± 0.2	18.8 ± 0.2
	non-ind	0	0	0	9 ± 0.2	0	0	8.8 ± 0.2	0
	ind	12.4 ± 0.3	14.6 ± 0.3	16 ± 0.2	18.2 ± 0.2	11.8 ± 0.2	16.8 ± 0.3	18.8 ± 0.2	18.8 ± 0.2
b	WT	16.8 ± 0.2	17.2 ± 0.2	15.4 ± 0.2	23.4 ± 0.3	13.8 ± 0.2	14.8 ± 0.2	22.6 ± 0.2	21.8 ± 0.2
	non-ind	0	0	0	0	0	0	0	0
	ind	16.6 ± 0.2	19.6 ± 0.2	21 ± 0.3	25 ± 0.2	16 ± 0.2	20.8 ± 0.2	22.6 ± 0.2	22.4 ± 0.2
c	WT	11.2 ± 0.3	14.4 ± 0.2	12.6 ± 0.2	17 ± 0.2	13.2 ± 0.2	11.5 ± 0.3	19.4 ± 0.3	16.6 ± 0.3
	non-ind	0	0	0	0	0	0	0	0
	ind	14.6 ± 0.2	17.2 ± 0.3	18.6 ± 0.2	19.6 ± 0.3	15.6 ± 0.4	11.8 ± 0.2	20.4 ± 0.3	18.2 ± 0.2
d	WT	13.5 ± 0.2	13 ± 0.2	8.4 ± 0.3	18 ± 0.1	9.2 ± 0.2	10.7 ± 0.2	18.1 ± 0.2	13.3 ± 0.2
	non-ind	0	0	0	0	0	0	0	0
	ind	14.3 ± 0.2	15.2 ± 0.2	16.4 ± 0.1	20.3 ± 0.2	12.6 ± 0.2	12 ± 0.2	22.2 ± 0.3	18.4 ± 0.2

Beilstein J. Org. Chem. 2020, 16, 956–965.

diameters of the inhibition zones were measured after 48 h. As references, different kanamycin concentrations to generate comparable inhibition zones were used (Table S4, Supporting Information File 1).

All analyzed wild type strains showed inhibition zones against the selected pathogens. Additionally, a comparison of the induced and the non-induced promoter-exchange mutants confirmed that the main bioactivity of all strains strongly depends on the fabclavines (Table 3). Interestingly, the non-induced promoter-exchange mutants of *X. cabanillasii* and *X. indica* showed an additional bioactivity, which might be due to another bioactive compound class (Table 3).

Discussion

Together with the ten previously published fabclavine derivatives, in total 32 fabclavines were identified in this work, which can be extended to 37 if the minor derivatives are included as well (Table 1 and Figure S33, Supporting Information File 1). As variable positions in the general structure, the second (Phe, His, Ala) and sixth amino acid position (Pro, Val, Thr) were identified as well as one to three partially reduced polyketide units or three to five amine units in the polyamine part. Combining all four variable positions in the general structure, 81 different fabclavine derivatives are theoretically possible. Strikingly, except for some minor derivatives, each strain or group of strains has its own set of fabclavines with unique features, such as polyamines with different lengths or an additional polyketide unit.

Considering the fabclavine biosynthesis in *X. szentirmaii*, the responsible components for such a chemical variety seem to be the following: The first is a lowered substrate specificity of two A-domains A_2 and A_6 in the NRPSs FclI and FclJ (Figure 1) [22]. Surprisingly, the key residues of these domains are highly conserved or identical, even between strains that differ in the incorporated amino acids (Table S6, Supporting Information File 1). This indicates the involvement of further structural elements, such as C-domains for the amino acid specificity [29,30]. However, an A-domain promiscuity is common in NRPS, exemplified by the biosynthesis of microcystins from cyanobacteria, RXPs or xenematide from *Xenorhabdus* and *Photorhabdus* [31-33]. The second strategy includes the iterative use of the PKSs FclK, responsible for the elongation with polyketide units, and FclC, responsible for the generation of the polyamine (Figure 1) [22]. As described previously, the genes *fclC*, *fclD*, and *fclE* are related to the PUFA biosynthesis genes and are responsible for the polyamine formation [20]. As this biosynthesis is based on iterative cycles, the polyamine biosynthesis shows a similar pattern [22,34,35]. The elongation with one to three malonate units by the type I PKS FclK for product diversification is unusual. However, multiple examples for bacterial iterative type I PKS are known, such as enediynes, myxochromide, aureothin, micacocidin, and further SMs [36-42].

Multiple fabclavine derivatives were identified in *X. innexi* DSM 16336 by MALDI–MS experiments in combination with the generated compound list. According to the literature, the *X. innexi* strains HGB1681 and HGB1997 are responsible for the biosynthesis of Xlt with a major range of 1348 to 1402 Da, similar to that of the fabclavines identified in this work [27]. Furthermore, the strains KJ12.1, KK7.4, *X. stockiae*, and *X. innexi* can be phylogenetically grouped together, and our results show that taxonomically related strains also produce similar sets of fabclavines (Table 2) [26]. In addition to the high homology between the *xlt* and *fcl* BGCs, our results strongly suggest that Xlt and the fabclavines are identical. The bioactivity described for Xlt relies on the induction of epithelial cell apoptosis in the anterior midgut of larvae [43]. Consequently, this mode of action could also be possible for fabclavines.

Conclusion

This study revealed a large chemical diversity for fabclavine derivatives among different *Xenorhabdus* strains, which is achieved by the promiscuity of single enzymes or domains during the biosynthesis. The recently published "easy promoter-activated compound identification" approach utilizes mutants with a deletion of the chaperone Hfq, leading to a loss of SM production [15]. Subsequent reactivation of selected BGCs results in an almost exclusive production of one compound class, and the corresponding study revealed that fabclavines alone are the major bioactive compound class in *X. szentirmaii* [15]. In combination with our bioactivity data of fabclavine-producing mutants, it is obvious that this class of compounds is the major driver for the overall antibiotic activity against the tested Gram-positive and Gram-negative bacteria in the other strains analyzed (Table 3). Whether this bioactivity is due to individual members of the fabclavines or whether all of them have a comparable activity must be studied in the future after the isolation of the individual derivatives.

Nevertheless, synergistic effects with other compound classes, enhancing the overall inhibitory activity, cannot be excluded. As an example, *X. indica* and *X. cabanillasii* showed an additional bioactivity against Gram-negative bacteria even without fabclavine production (Table 3). This bioactivity might be caused by other compound(s) as both strains have the potential to produce further bioactive SMs, such as cabanillasin, PAX peptides, or rhabdopeptides [26,44-46], which will be studied in the future. Furthermore, the identification of fabclavine derivatives described here might support recent studies that revealed

Xenorhabdus and *Photorhabdus* strains having ascaricidal or larvicidal activity. Here, especially *X. szentirmaii*-, *X. indica*-, *X. stockiae*-, as well as *X. stockiae*-related isolates showed the best activity [18,19,47]. Although these strains were confirmed as fabclavine producers in our current study, future work is required to confirm fabclavines as the active compounds here as well (Table 3) [20].

Supporting Information

Supporting Information File 1

Material and methods, supplementary figures and tables, and MALDI–HRMS and MALDI–MS^2 spectra.
[https://www.beilstein-journals.org/bjoc/content/supplementary/1860-5397-16-84-S1.pdf]

Acknowledgements

The authors are grateful to Michael Karas for MALDI access.

Funding

This work was supported in part by the LOEWE Schwerpunkt MegaSyn funded by the State of Hesse and an ERC Advanced grant to H.B.B. (grant agreement number 835108).

ORCID® iDs

Harun Cimen - https://orcid.org/0000-0002-0106-4183
Selcuk Hazir - https://orcid.org/0000-0001-9298-1472
Helge B. Bode - https://orcid.org/0000-0001-6048-5909

References

1. Toner, E.; Adalja, A.; Gronvall, G. K.; Cicero, A.; Inglesby, T. V. *Health Secur.* **2015,** *13,* 153–155. doi:10.1089/hs.2014.0088
2. Felnagle, E. A.; Jackson, E. E.; Chan, Y. A.; Podevels, A. M.; Berti, A. D.; McMahon, M. D.; Thomas, M. G. *Mol. Pharmaceutics* **2008,** *5,* 191–211. doi:10.1021/mp700137g
3. Levine, D. P. *Clin. Infect. Dis.* **2006,** *42* (Suppl. 1), S5–S12. doi:10.1086/491709
4. Demain, A. L. *J. Ind. Microbiol. Biotechnol.* **2014,** *41,* 185–201. doi:10.1007/s10295-013-1325-z
5. Bode, H. B. *Curr. Opin. Chem. Biol.* **2009,** *13,* 224–230. doi:10.1016/j.cbpa.2009.02.037
6. Baltz, R. H. *J. Ind. Microbiol. Biotechnol.* **2019,** *46,* 281–299. doi:10.1007/s10295-018-2115-4
7. Williams, J. S.; Thomas, M.; Clarke, D. J. *Microbiology (London, U. K.)* **2005,** *151,* 2543–2550. doi:10.1099/mic.0.28136-0
8. McInerney, B. V.; Taylor, W. C.; Lacey, M. J.; Akhurst, R. J.; Gregson, R. P. *J. Nat. Prod.* **1991,** *54,* 785–795. doi:10.1021/np50075a006
9. Park, H. B.; Perez, C. E.; Perry, E. K.; Crawford, J. M. *Molecules* **2016,** *21,* No. 824. doi:10.3390/molecules21070824
10. Crawford, J. M.; Clardy, J. *Chem. Commun.* **2011,** *47,* 7559–7566. doi:10.1039/c1cc11574j
11. Shi, Y.-M.; Bode, H. B. *Nat. Prod. Rep.* **2018,** *35,* 309–335. doi:10.1039/c7np00054e
12. Goodrich-Blair, H.; Clarke, D. J. *Mol. Microbiol.* **2007,** *64,* 260–268. doi:10.1111/j.1365-2958.2007.05671.x
13. Strauch, O.; Ehlers, R.-U. *Appl. Microbiol. Biotechnol.* **1998,** *50,* 369–374. doi:10.1007/s002530051306
14. Bode, E.; Brachmann, A. O.; Kegler, C.; Simsek, R.; Dauth, C.; Zhou, Q.; Kaiser, M.; Klemmt, P.; Bode, H. B. *ChemBioChem* **2015,** *16,* 1115–1119. doi:10.1002/cbic.201500094
15. Bode, E.; Heinrich, A. K.; Hirschmann, M.; Abebew, D.; Shi, Y.-N.; Vo, T. D.; Wesche, F.; Shi, Y.-M.; Grün, P.; Simonyi, S.; Keller, N.; Engel, Y.; Wenski, S.; Bennet, R.; Beyer, S.; Bischoff, I.; Buaya, A.; Brandt, S.; Cakmak, I.; Çimen, H.; Eckstein, S.; Frank, D.; Fürst, R.; Gand, M.; Geisslinger, G.; Hazir, S.; Henke, M.; Heermann, R.; Lecaudey, V.; Schäfer, W.; Schiffmann, S.; Schüffler, A.; Schwenk, R.; Skaljac, M.; Thines, E.; Thines, M.; Ulshöfer, T.; Vilcinskas, A.; Wichelhaus, T. A.; Bode, H. B. *Angew. Chem.* **2019,** *131,* 19133–19139. doi:10.1002/ange.201910563
16. Muangpat, P.; Yooyangket, T.; Fukruksa, C.; Suwannaroj, M.; Yimthin, T.; Sitthisak, S.; Chantratita, N.; Vitta, A.; Tobias, N. J.; Bode, H. B.; Thanwisai, A. *Front. Microbiol.* **2017,** *8,* No. 1142. doi:10.3389/fmicb.2017.01142
17. Brachmann, A. O.; Joyce, S. A.; Jenke-Kodama, H.; Schwär, G.; Clarke, D. J.; Bode, H. B. *ChemBioChem* **2007,** *8,* 1721–1728. doi:10.1002/cbic.200700300
18. Vitta, A.; Thimpoo, P.; Meesil, W.; Yimthin, T.; Fukruksa, C.; Polseela, R.; Mangkit, B.; Tandhavanant, S.; Thanwisai, A. *Asian Pac. J. Trop. Biomed.* **2018,** *8,* 31–36. doi:10.4103/2221-1691.221134
19. Suwannaroj, M.; Yimthin, T.; Fukruksa, C.; Muangpat, P.; Yooyangket, T.; Tandhavanant, S.; Thanwisai, A.; Vitta, A. *J. Appl. Entomol.* **2020,** *144,* 212–223. doi:10.1111/jen.12726
20. Fuchs, S. W.; Grundmann, F.; Kurz, M.; Kaiser, M.; Bode, H. B. *ChemBioChem* **2014,** *15,* 512–516. doi:10.1002/cbic.201300802
21. Donmez Ozkan, H.; Cimen, H.; Ulug, D.; Wenski, S.; Yigit Ozer, S.; Telli, M.; Aydin, N.; Bode, H. B.; Hazir, S. *Front. Microbiol.* **2019,** *10,* No. 2672. doi:10.3389/fmicb.2019.02672
22. Wenski, S. L.; Kolbert, D.; Grammbitter, G. L. C.; Bode, H. B. *J. Ind. Microbiol. Biotechnol.* **2019,** *46,* 565–572. doi:10.1007/s10295-018-02124-8
23. Masschelein, J.; Mattheus, W.; Gao, L.-J.; Moons, P.; Van Houdt, R.; Uytterhoeven, B.; Lamberigts, C.; Lescrinier, E.; Rozenski, J.; Herdewijn, P.; Aertsen, A.; Michiels, C.; Lavigne, R. *PLoS One* **2013,** *8,* e54143. doi:10.1371/journal.pone.0054143
24. Zhou, J.; Zhang, H.; Wu, J.; Liu, Q.; Xi, P.; Lee, J.; Liao, J.; Jiang, Z.; Zhang, L.-H. *Mol. Plant-Microbe Interact.* **2011,** *24,* 1156–1164. doi:10.1094/mpmi-04-11-0087
25. Masschelein, J.; Clauwers, C.; Awodi, U. R.; Stalmans, K.; Vermaelen, W.; Lescrinier, E.; Aertsen, A.; Michiels, C.; Challis, G. L.; Lavigne, R. *Chem. Sci.* **2015,** *6,* 923–929. doi:10.1039/c4sc01927j
26. Tobias, N. J.; Wolff, H.; Djahanschiri, B.; Grundmann, F.; Kronenwerth, M.; Shi, Y.-M.; Simonyi, S.; Grün, P.; Shapiro-Ilan, D.; Pidot, S. J.; Stinear, T. P.; Ebersberger, I.; Bode, H. B. *Nat. Microbiol.* **2017,** *2,* 1676–1685. doi:10.1038/s41564-017-0039-9
27. Kim, I.-H.; Aryal, S. K.; Aghai, D. T.; Casanova-Torres, Á. M.; Hillman, K.; Kozuch, M. P.; Mans, E. J.; Mauer, T. J.; Ogier, J.-C.; Ensign, J. C.; Gaudriault, S.; Goodman, W. G.; Goodrich-Blair, H.; Dillman, A. R. *BMC Genomics* **2017,** *18,* No. 927. doi:10.1186/s12864-017-4311-4

28. Rinkel, J.; Dickschat, J. S. *Beilstein J. Org. Chem.* **2015,** *11,* 2493–2508. doi:10.3762/bjoc.11.271
29. Bloudoff, K.; Schmeing, T. M. *Biochim. Biophys. Acta, Proteins Proteomics* **2017,** *1865,* 1587–1604. doi:10.1016/j.bbapap.2017.05.010
30. Bozhüyük, K. A. J.; Fleischhacker, F.; Linck, A.; Wesche, F.; Tietze, A.; Niesert, C.-P.; Bode, H. B. *Nat. Chem.* **2018,** *10,* 275–281. doi:10.1038/nchem.2890
31. Meyer, S.; Kehr, J.-C.; Mainz, A.; Dehm, D.; Petras, D.; Süssmuth, R. D.; Dittmann, E. *Cell Chem. Biol.* **2016,** *23,* 462–471. doi:10.1016/j.chembiol.2016.03.011
32. Cai, X.; Nowak, S.; Wesche, F.; Bischoff, I.; Kaiser, M.; Fürst, R.; Bode, H. B. *Nat. Chem.* **2017,** *9,* 379–386. doi:10.1038/nchem.2671
33. Crawford, J. M.; Portmann, C.; Kontnik, R.; Walsh, C. T.; Clardy, J. *Org. Lett.* **2011,** *13,* 5144–5147. doi:10.1021/ol2020237
34. Metz, J. G.; Roessler, P.; Facciotti, D.; Levering, C.; Dittrich, F.; Lassner, M.; Valentine, R.; Lardizabal, K.; Domergue, F.; Yamada, A.; Yazawa, K.; Knauf, V.; Browse, J. *Science* **2001,** *293,* 290–293. doi:10.1126/science.1059593
35. Kaulmann, U.; Hertweck, C. *Angew. Chem., Int. Ed.* **2002,** *41,* 1866–1869. doi:10.1002/1521-3773(20020603)41:11<1866::aid-anie1866>3.0.co;2-3
36. Chen, X.; Ji, R.; Jiang, X.; Yang, R.; Liu, F.; Xin, Y. *IUBMB Life* **2014,** *66,* 587–595. doi:10.1002/iub.1316
37. Wenzel, S. C.; Kunze, B.; Höfle, G.; Silakowski, B.; Scharfe, M.; Blöcker, H.; Müller, R. *ChemBioChem* **2005,** *6,* 375–385. doi:10.1002/cbic.200400282
38. Hertweck, C. *Angew. Chem., Int. Ed.* **2009,** *48,* 4688–4716. doi:10.1002/anie.200806121
39. Busch, B.; Ueberschaar, N.; Sugimoto, Y.; Hertweck, C. *J. Am. Chem. Soc.* **2012,** *134,* 12382–12385. doi:10.1021/ja304454r
40. Kage, H.; Kreutzer, M. F.; Wackler, B.; Hoffmeister, D.; Nett, M. *Chem. Biol.* **2013,** *20,* 764–771. doi:10.1016/j.chembiol.2013.04.010
41. Antosch, J.; Schaefers, F.; Gulder, T. A. M. *Angew. Chem., Int. Ed.* **2014,** *53,* 3011–3014. doi:10.1002/anie.201310641
42. Parascandolo, J. S.; Havemann, J.; Potter, H. K.; Huang, F.; Riva, E.; Connolly, J.; Wilkening, I.; Song, L.; Leadlay, P. F.; Tosin, M. *Angew. Chem., Int. Ed.* **2016,** *55,* 3463–3467. doi:10.1002/anie.201509038
43. Kim, I.-H.; Ensign, J.; Kim, D.-Y.; Jung, H.-Y.; Kim, N.-R.; Choi, B.-H.; Park, S.-M.; Lan, Q.; Goodman, W. G. *J. Invertebr. Pathol.* **2017,** *149,* 21–28. doi:10.1016/j.jip.2017.07.002
44. Houard, J.; Aumelas, A.; Noël, T.; Pages, S.; Givaudan, A.; Fitton-Ouhabi, V.; Villain-Guillot, P.; Gualtieri, M. *J. Antibiot.* **2013,** *66,* 617–620. doi:10.1038/ja.2013.58
45. Fuchs, S. W.; Proschak, A.; Jaskolla, T. W.; Karas, M.; Bode, H. B. *Org. Biomol. Chem.* **2011,** *9,* 3130–3132. doi:10.1039/c1ob05097d
46. Zhao, L.; Kaiser, M.; Bode, H. B. *Org. Lett.* **2018,** *20,* 5116–5120. doi:10.1021/acs.orglett.8b01975
47. Eroglu, C.; Cimen, H.; Ulug, D.; Karagoz, M.; Hazir, S.; Cakmak, I. *J. Invertebr. Pathol.* **2019,** *160,* 61–66. doi:10.1016/j.jip.2018.12.004

License and Terms

This is an Open Access article under the terms of the Creative Commons Attribution License (http://creativecommons.org/licenses/by/4.0). Please note that the reuse, redistribution and reproduction in particular requires that the authors and source are credited.

The license is subject to the *Beilstein Journal of Organic Chemistry* terms and conditions: (https://www.beilstein-journals.org/bjoc)

The definitive version of this article is the electronic one which can be found at: doi:10.3762/bjoc.16.84

BEILSTEIN JOURNAL OF ORGANIC CHEMISTRY

Supporting Information

for

Fabclavine diversity in *Xenorhabdus* bacteria

Sebastian L. Wenski, Harun Cimen, Natalie Berghaus, Sebastian W. Fuchs, Selcuk Hazir and Helge B. Bode

Beilstein J. Org. Chem. **2020,** *16,* 956–965. doi:10.3762/bjoc.16.84

Material and methods, supplementary figures and tables, and MALDI–HRMS and MALDI–MS^2 spectra

License and Terms: This is a supporting information file under the terms of the Creative Commons Attribution License (http://creativecommons.org/licenses/by/4.0). Please note that the reuse, redistribution and reproduction in particular requires that the authors and source are credited.
The license is subject to the *Beilstein Journal of Organic Chemistry* terms and conditions: (https://www.beilstein-journals.org/bjoc)

Material and methods

1. Strain cultivation for MALDI–MS experiments

The strains were cultivated as described previously [1]: Briefly, all *Xenorhabdus* and *Photorhabdus* strains were grown on lysogeny broth (LB) agar plates at 30 °C. The production cultures were inoculated 1:25 with overnight cultures in fresh LB medium and incubated shaking at 30 °C for three days. *Escherichia coli* strains were grown on LB agar plates and in LB medium at 37 °C with shaking. If appropriate, kanamycin (50 µg/mL) or L-(+)-arabinose (0.2%) were added. The cultures were harvested as whole cell cultures and stored at −20 °C.

2. Isotope labeling and reverse feeding experiments

For the isotope-labeling experiments, overnight cultures were washed three times with H_2O and inoculated 1:100 in ISOGRO®-13C (Sigma-Aldrich). If appropriate, kanamycin and L-(+)-arabinose (0.2%) were added, and the cultures were incubated shaking at 30 °C for 2 d. For reverse feeding experiments, 2 mM of the substrate was added each day.

3. Generation of promoter-exchange mutants

The promoter-exchange mutants were generated as described previously [1]: Briefly, about 600–1200 bp of the starting *fclC* (homologues) were amplified (the corresponding oligonucleotides are listed in Table S1), cloned into the pCEP_Kan backbone (pCEP: cluster expression plasmid) by hot fusion assembly, and transformed into *E. coli* S17-1 λpir or ST18 as described previously [2-5]. After the conjugation with the corresponding *E. coli* ST18/S17 strains, the kanamycin-resistant conjugants were confirmed by colony PCR or by MALDI–MS for a successful promoter exchange.

4. MALDI–MS

MALDI–MS experiments were performed as described previously [1]: Briefly, 0.3 µL of a liquid culture were mixed on a MALDI target with 0.25 µL 1:10 diluted ProteoMass Normal Mass Calibration Mix (ProteoMass™ MALDI Calibration Kit, Sigma-Aldrich) for internal calibration and 0.9 µL α-cyano-4-hydroxycinnamic acid (CHCA) matrix (3 mg/mL in 75% acetonitrile, 0.1% trifluoroacetic acid). After drying, the resulting spot was coated with 5% formic acid, and after removal of the 5% formic acid solution mixed again with 0.6 µL

CHCA. Cell MALDI measurements were performed with a MALDI LTQ Orbitrap XL (Thermo Fisher Scientific, Inc., Waltham, MA) instrument (nitrogen laser at 337 nm in FTMS scan mode) with 100 shots per measurement with high resolution. Alternatively, 4-chloro-α-cyanocinnamic acid can be used as the matrix, but we observed a decreased quality of the resulting spectra. The CID mode using the ITMS scan mode was used for MALDI–MS^2 experiments, with the same sample preparation having the following parameters: Normalized collision energy: 28–32, Act. Q: 0.250, Act. Time (ms): 30.0. The data were analyzed using Qual Browser version 2.0.7 (Thermo Fisher Scientific). As the signal intensities of the stacked spectra were normalized and the intensity is displayed by the relative abundance in a range from 0 to 100%, the y axis is not shown. Since not all detected signals could be detected with a sufficient signal intensity to confirm them by MS^2 experiments, we decided to show them in the supplementary figures of the corresponding strain, but without a compound number.

5. Bioactivity analysis

5.1 Generating cell-free supernatant

The promoter-exchange mutant strains were cultivated on LB agar, supplemented with a 50 µg/mL final concentration of kanamycin, and incubated at 30 °C for 48 h. A single colony was transferred into 10 mL LB medium, supplemented with a 50 µg/mL final concentration of kanamycin to obtain a culture overnight at 200 rpm and 30 °C. The optical densities of the overnight cultures (20 mL LB) were measured at 600 nm. The final OD of the cultures was adjusted to 0.1 after inoculation. For each strain, two flasks were prepared, and the cultures were incubated at 30 °C for 1 h. One of the flasks was induced with 0.2% L-arabinose, and the other flask was not treated with arabinose (non-induced). All induced and non-induced cultures were incubated for 24 h at 200 rpm and 30 °C. Wild type strains were grown on LB agar at 30 °C for 48 h. A single colony was transferred in 10 mL LB medium and incubated overnight at 30 °C in a rotary shaker at 200 rpm to generate precultures. The LB medium was inoculated 1:100 with the preculture and cultivated at 200 rpm and 30 °C for 72 h. The bacterial broth was harvested by centrifugation at 10,000 rpm for 10 min, and the supernatant was filtered through a 0.22 µm millipore filter (Thermo scientific).

65 **5.2 Agar well-diffusion bioassay**

66 The antibacterial activity of the wild type, induced, and noninduced promoter-exchange
67 mutant supernatants was determined by the agar well-diffusion method [6]. *Escherichia*
68 *coli* (ATCC 25922), *Enterococcus faecalis* (ATCC 29212), *Staphyllococcus aureus* (ATCC
69 29213), and *Klebsiella pneumoniae* (ATCC 700603) were used in the experiments. For
70 the preparation of overnight cultures of the test organisms, 20 mL LB medium was
71 inoculated with a loopful of the bacterium and incubated at 37 °C in a rotary shaker at 200
72 rpm. Briefly, 200 µL of the pathogen bacteria from an overnight culture was spread on a
73 Mueller–Hinton agar (blood agar was used for *E. faecalis*) with a glass rod. Subsequently,
74 three wells were made in each of these plates using a 5 mm diameter sterile transfer tube.
75 Each well was filled with 60 µL of induced, non-induced mutant, or wild type of the bacterial
76 supernatants. Kanamycin was used as a positive control at different concentrations (25,
77 50, 100, 200, 400, and 800 µL/mg). Petri dishes (10 mm) were incubated at 37 °C for 48
78 h. After the incubation period, the diameter of the inhibition zones (mm) was assessed by
79 measuring the diameter in two perpendicular directions and taking the average [7]. Ten
80 petri dishes were used for each replicate, and the experiments were conducted three
81 times on different dates.
82
83

Supplementary material:

Table S1: Overview of oligonucleotides used in this work for the amplification of the homologous regions of the promoter-exchange mutants.

strain	locus tag(s) of analyzed gene(s)	oligonucleotide	sequence 5'–3'
X. szentirmaii **pCEP_fcl**	Xsze_03745	SW159_XszC_fw SW160_XszC_rv	TTTGGGCTAACAGGAGGCTAGCATATGTCTGAGACATATTTTTTACATGATAGAAAAATTCGTGG TCTGCAGAGCTCGAGCATGCACATGCAATATTCCCGCACGGGTATATGC
X. budapestensis **pCEP_fcl**	Xbud_02634	SW271_Xbud_fw SW272_Xbud_rv	TTTGGGCTAACAGGAGGCTAGCATATGTCCAAGACGTATTTTTTGCATG TCTGCAGAGCTCGAGCATGCACATCTTCATTCCACTCAAGATACATTCCG
X. indica **pCEP_fcl**	Xind_02757	SW132_Xind_fw SW133_Xind_rv	TTTGGGCTAACAGGAGGCTAGCATATGTCCAAGACGTATTTTTTGCATG TCTGCAGAGCTCGAGCATGCACATCGCTTTTACCTGCCCTTCC
X. hominickii **pCEP_fcl**	Xhom_02793	SW130_Xhom_fw SW131_XHom_rv	TTTGGGCTAACAGGAGGCTAGCATATGTCTGAGTCATATCTTTTACATGATGG TCTGCAGAGCTCGAGCATGCACATCTTCAACTAATTGAATATCGCTCGG
X. stockiae **pCEP_fcl**	Xsto_00102	SW273_uni_fw SW276_Xsto_rv	TTTGGGCTAACAGGAGGCTAGCATATGTCCAGGACATATTTTTTGCATG TCTGCAGAGCTCGAGCATGCACATGCCAAGATCAAAATAACTGGCG
X. **KJ12.1** **pCEP_fcl**	Xekj_00388	SW153_KJ12.1_fw SW154_KJ12.1_rv	TTTGGGCTAACAGGAGGCTAGCATATGTCCAGGACATATTTTTTGCATG TCTGCAGAGCTCGAGCATGCACATCCATCACTGGAAGCTTCAACG
X. **KK7.4** **pCEP_fcl**	ctg22_41	SW155_KK7.4_fw SW156_KK7.4_rv	TTTGGGCTAACAGGAGGCTAGCATTTGCATGACAGAAAAATTAATGGAG TCTGCAGAGCTCGAGCATGCACATGTGCAAAAATACTCTTTGCACGG
P. temperata **pCEP_fcl**	MEG1DRAFT_01183	SW267_Ptemp_fw SW268_Ptemp_rv	TTTGGGCTAACAGGAGGCTAGCATATGTCTGAGACATATTTAATGCGTGG TCTGCAGAGCTCGAGCATGCACATAAGTTGCTTTTCGACAGTGCC

Table S2: Strains used in this work.

strain	#	description	origin
X. szentirmaii	DSM 16338	Wild type	[8]
X. budapestensis	DSM 16342	Wild type	[8]
X. cabanillasii	JM26	Wild type	[9]
X. indica	DSM 17382	Wild type	[10]
X. hominickii	DSM 17903	Wild type	[9]
X. stockiae	DSM 17904	Wild type	[9]
X. KJ12.1	KJ12.1	Wild type	[11]
X. KK7.4	KK7.4	Wild type	[12]
X. innexi	DSM 16336	Wild type	[8]
P. temperata	meg1	Wild type	[13]
X. szentirmaii pCEP_fcl	DSM 16338	Promoter exchange in front of Xsze_03745	This work
X. budapestensis pCEP_fcl	DSM 16342	Promoter exchange in front of Xbud_02634	This work
X. cabanillasii pCEP_fcl	JM26	Promoter exchange in front of Xcab_02060	[14]
X. indica pCEP_fcl	DSM 17382	Promoter exchange in front of Xind_02757	This work
X. hominickii pCEP_fcl	DSM 17903	Promoter exchange in front of Xhom_02793	This work
X. stockiae pCEP_fcl	DSM 17904	Promoter exchange in front of Xsto_00102	This work
X. KJ12.1 pCEP_fcl	KJ12.1	Promoter exchange in front of Xekj_00388	This work
X. KK7.4 pCEP_fcl	KK7.4	Promoter exchange in front of ctg22_41	This work
P. temperata pCEP_fcl	meg1	Promoter exchange in front of MEG1DRAFT_01183	This work
E. coli	S17 λ1-pir	used for conjugation	[3]
E. coli	ST18	used for conjugation	[4]
E. coli	ATCC25922	Bioactivity analysis	ATCC
Enterococcus faecalis	ATCC29212	Bioactivity analysis	ATCC
Staphyllococcus aureus	ATCC29213	Bioactivity analysis	ATCC
Klebsiella pneumoniae	ATCC700603	Bioactivity analysis	ATCC

Table S3: Comparison of protein identities [%] from FclA to FclN in *X. budapestensis* DSM 16342 with *X. cabanillasii* JM26 (A) and *X. indica* DSM 17382 (B). Protein alignments were performed by ClustalW alignment with the CostMatrix BLOSUM in Geneious 6.1.8.

Identity	FclA	FclB	FclC	FclD	FclE	FclF	FclG	FclH	FclI	FclJ	FclK	FclL	FclM	FclN
A	96.5	92.2	95.6	94.8	97.2	96.1	96.1	97.4	93.6	96.4	93.6	92.8	98.7	97.8
B	97.1	91.6	95.4	95.6	96.3	97.3	94.9	97.4	93.5	94.7	93.8	94.1	97.8	97

Table S4: Diameters of inhibition zones of different kanamycin concentrations against *Escherichia coli* (ATCC 25922), *Enterococcus faecalis* (ATCC 29212), *Staphyllococcus aureus* (ATCC 29213) and *Klebsiella pneumoniae* (ATCC 700603).

	kanamycin concentration [µg/ml]					
	25	**50**	**100**	**200**	**400**	**800**
E. coli	13.5	16.9	20.1	23.0	25.3	28.2
S. aureus	0.0	0.0	13.3	18.5	21.6	24.7
E. faecalis	0.0	0.0	11.9	16.5	19.3	24.1
K. pneumoniae	0.0	0.0	0.0	0.0	11.7	15.3

Table S5: Overview of the NCBI accession numbers of the strains used in this study.

strain	accession number
***Xenorhabdus szentirmaii* DSM 16338**	NIBV00000000
***Xenorhabdus budapestensis* DSM 16342**	NIBS00000000
***Xenorhabdus cabanillasii* JM26**	NJGH00000000
***Xenorhabdus indica* DSM 17382**	NKHP00000000
***Xenorhabdus hominickii* DSM 17903**	NJAI00000000
***Xenorhabdus stockiae* DSM17904**	NJAJ00000000
***Xenorhabdus* KJ12.1**	NJCW00000000
***Xenorhabdus* KK7.4**	NJAH00000000
***Xenorhabdus bovienii* SS-2004**	FN667741
***Xenorhabdus innexi* DSM 16336**	NIBU00000000
***Photorhabdus temperata* subsp. *temperata* Meg1**	NZ_JGVH00000000

Table S6: Stachelhaus-codes and corresponding amino acid prediction of the promiscous A-domains A_2 and A_6 in the analyzed strains [15,16].

	A-domain A_2		A-domain A_6	
strain	**Stachelhaus**	**prediction**	**Stachelhaus**	**prediction**
X. budapestensis	DTWTLASVGK	phe	DAWFIGGTFK	val
X. indica	DTWTLASVGK	phe	DAWFIGGTFK	val
X. cabanillasii	DTWTLASVGK	phe	DAWFIGGTFK	val
X. hominickii	DTWTIASVGK	phe	DALFIGGTFK	val
X. szentirmaii	DVWTMSAVGK	ser	DALFIGGTFK	val
KJ12.1	DTWTIASVGK	phe	DAWFIGGTFK	val
X. stockiae	DTWTIASVGK	phe	DAWFIGGTFK	val
KK7.4	DTWTIASVGK	phe	DAWFVGGTFK	val
X. innexi	DTWTMASVGK	phe	DAWFVGGTFK	val

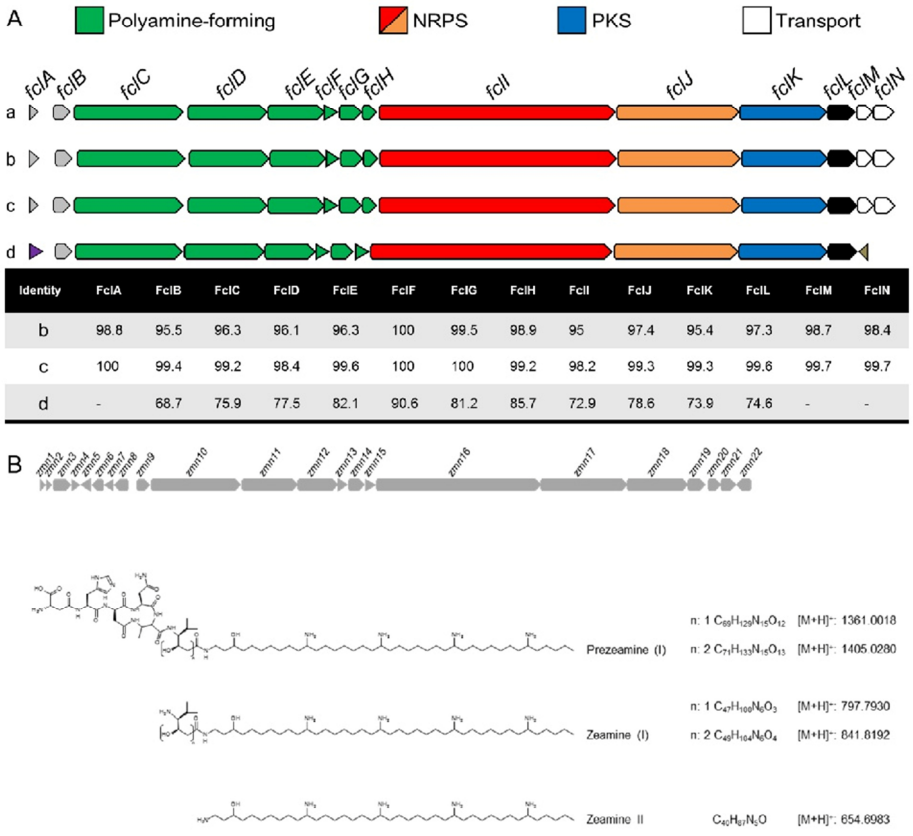

Identity	FclA	FclB	FclC	FclD	FclE	FclF	FclG	FclH	FclI	FclJ	FclK	FclL	FclM	FclN
b	98.8	95.5	96.3	96.1	96.3	100	99.5	98.9	95	97.4	95.4	97.3	98.7	98.4
c	100	99.4	99.2	98.4	99.6	100	100	99.2	98.2	99.3	99.3	99.6	99.7	99.7
d	-	68.7	75.9	77.5	82.1	90.6	81.2	85.7	72.9	78.6	73.9	74.6	-	-

Figure S1: (A) Comparison of the *fcl* BGCs in *X. stockiae* DSM 17904 (a), KK7.4 (b), KJ12.1 (c) and the homologous gene cluster in *X. innexi* DSM 16336 (d). Shown are protein identities in comparison with X. stockiae [%]. Protein alignments were performed by ClustalW alignments with the CostMatrix BLOSUM in Geneious 6.1.8. The two aberrant genes of the *X. innxei* BGC are shown in purple (encoding a TonB homologue) and in brown (encoding an Acyl-CoA-thioesterase) [17]. (B) Zeamine biosynthesis gene cluster and corresponding compounds from *Serratia plymuthica* RVH1 [18,19].

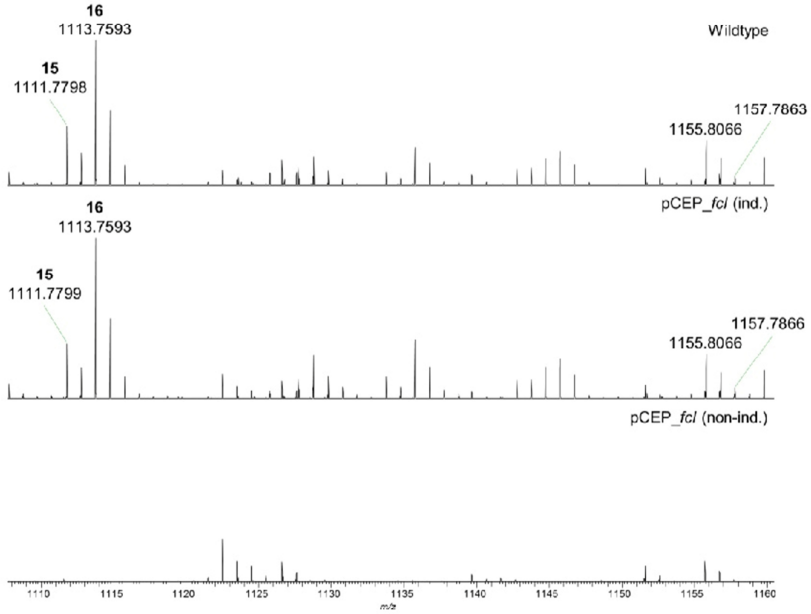

#	Sum formula	Calc. m/z	Det. m/z		Δppm	
			WT	pCEP_*fcl*	WT	pCEP_*fcl*
15	$C_{54}H_{102}N_{12}O_{12}$	1111.7813	1111.7798	**1111.7799**	-1.370	-1.244
16	$C_{53}H_{100}N_{12}O_{13}$	1113.7606	1113.7593	**1113.7593**	-1.120	-1.129
-	$C_{56}H_{106}N_{12}O_{13}$	1155.8075	1155.8066	**1155.8066**	-0.820	-0.759
-	$C_{55}H_{104}N_{12}O_{14}$	1157.7868	1157.7863	**1157.7866**	-0.408	-0.175

Figure S2: MALDI–HRMS spectra of *X. szentirmaii* wild type (WT) and pCEP_*fcl* promoter-exchange mutant (induced and noninduced) with compounds **15** and **16** showing sum formulas, calculated and detected masses and corresponding Δppm.

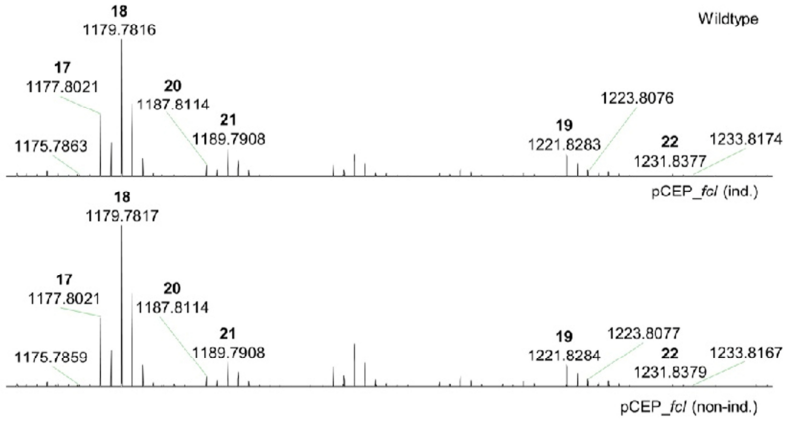

#	Sum formula	Calc. m/z	Det. m/z		Δppm	
			WT	pCEP_*fcl*	WT	pCEP_*fcl*
-	$C_{57}H_{102}N_{14}O_{12}$	1175.7874	1175.7863	1175.7859	-0.945	-1.294
17	$C_{57}H_{104}N_{14}O_{12}$	1177.8031	1177.8021	1177.8021	-0.850	-0.816
18	$C_{58}H_{102}N_{14}O_{13}$	1179.7824	1179.7816	1179.7817	-0.657	-0.539
20	$C_{60}H_{106}N_{12}O_{12}$	1187.8126	1187.8114	1187.8114	-1.013	-1.004
21	$C_{59}H_{104}N_{12}O_{13}$	1189.7979	1189.7908	1189.7908	-0.872	-0.914
19	$C_{59}H_{108}N_{14}O_{13}$	1221.8293	1221.8283	1221.8284	-0.839	-0.782
-	$C_{58}H_{106}N_{14}O_{14}$	1223.8086	1223.8076	1223.8077	-0.760	-0.736
22	$C_{62}H_{110}N_{12}O_{13}$	1231.8388	1231.8377	1231.8379	-0.875	-0.713
-	$C_{61}H_{108}N_{12}O_{14}$	1233.8181	1233.8174	1233.8167	-0.569	-1.104

Figure S3: MALDI–HRMS spectra of *X. szentirmaii* wild type (WT) and pCEP_*fcl* promoter-exchange mutant (induced and noninduced) with compounds **17–22** showing sum formulas, calculated and detected masses and corresponding Δppm. Compounds **17–22** were described previously [20].

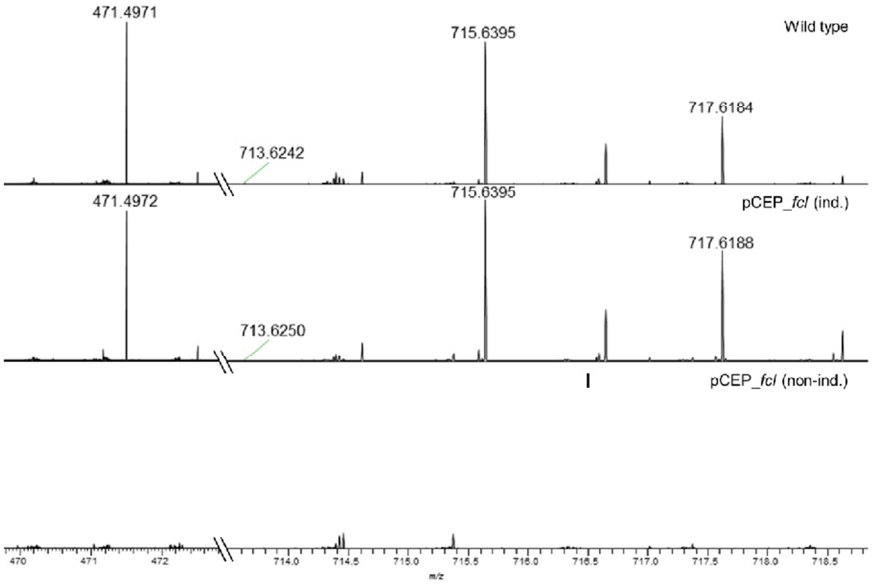

Description	Sum formula	Calc. m/z	Det. m/z		Δppm	
			WT	pCEP_*fcl*	WT	pCEP_*fcl*
Polyamine	$C_{28}H_{52}N_4O$	471.4996	471.4971	471.4972	-5.470	-5.237
Shortened Fabclavine	$C_{36}H_{60}N_6O_5$	713.6263	713.6243	713.6250	-2.867	-1.858
Shortened Fabclavine	$C_{39}H_{82}N_6O_5$	715.6419	715.6395	715.6395	-3.362	-3.474
Shortened Fabclavine	$C_{38}H_{80}N_6O_5$	717.6212	717.6184	717.6188	-3.861	-3.345

Figure S4: MALDI–HRMS spectra of *X. szentirmaii* wild type (WT) and pCEP_*fcl* promoter-exchange mutant (induced and noninduced) with polyamine and shortened fabclavines showing sum formulas, calculated and detected masses and corresponding Δppm.

Expected Fragmentions	Sum formula	m/z
y1	$C_{28}H_{63}N_4O$	471.4996
y2	$C_{35}H_{76}N_5O_3$	614.5943
y5	$C_{47}H_{93}N_{10}O_8$	925.7172
y6	$C_{50}H_{98}N_{11}O_9$	996.7544
b1	$C_4H_6NO_3$	116.0342
b2	$C_7H_{11}N_2O_4$	187.0713
b5	$C_{19}H_{28}N_7O_9$	498.1943
b6	$C_{26}H_{41}N_8O_{11}$	641.2889

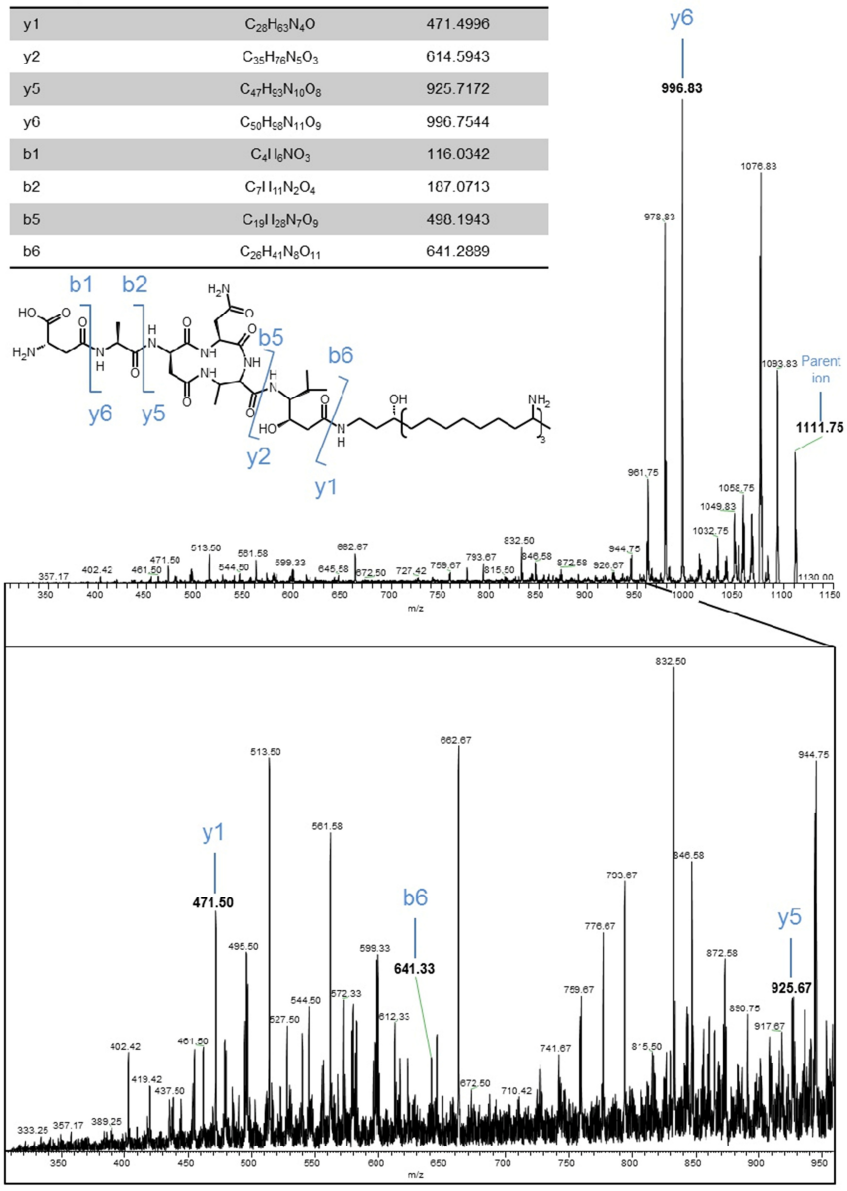

Figure S5: MALDI–MS^2 spectra of compound 1111.78 (**15**) of *X. szentirmaii* pCEP_*fcl* (induced) showing expected fragment ions and proposed structure.

Expected Fragmentions	Sum formula	m/z
y1	$C_{28}H_{63}N_4O$	471.4996
y2	$C_{34}H_{74}N_5O_4$	616.5735
y5	$C_{46}H_{91}N_{10}O_9$	927.6965
y6	$C_{49}H_{96}N_{11}O_{10}$	998.7336
b1	$C_4H_6NO_3$	116.0342
b2	$C_7H_{11}N_2O_4$	187.0713
b5	$C_{19}H_{28}N_7O_9$	498.1943
b6	$C_{25}H_{39}N_8O_{12}$	643.2682

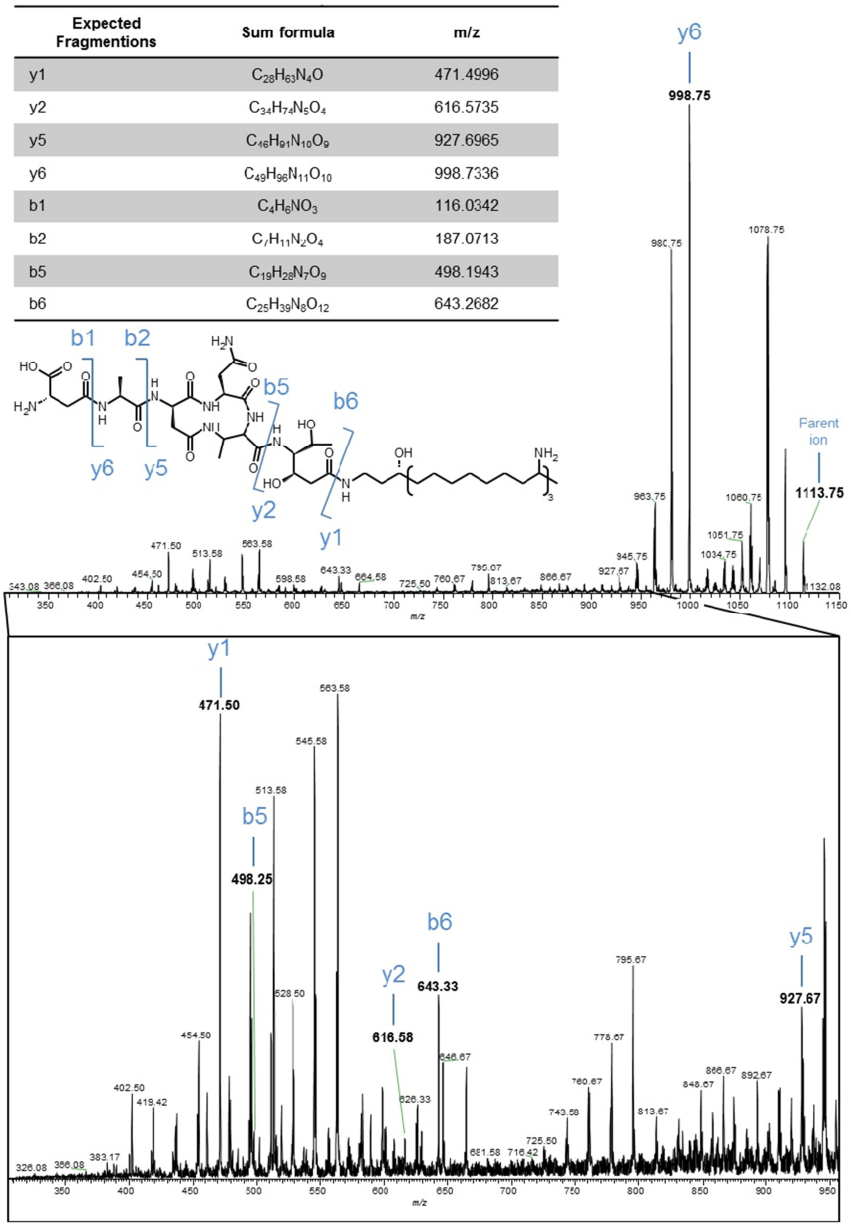

Figure S6: MALDI–MS^2 spectra of compound 1113.76 (**16**) of *X. szentirmaii* pCEP_*fcl* (induced) showing expected fragment ions and proposed structure.

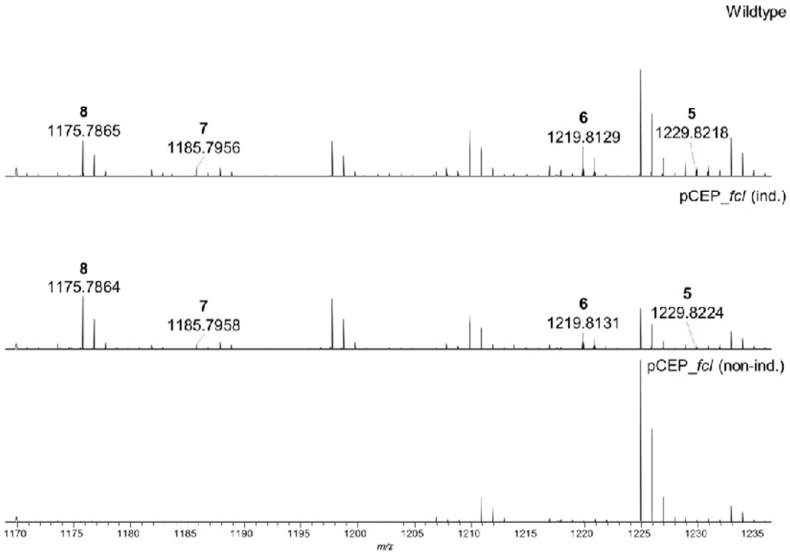

#	Sum formula	Calc. m/z	Det. m/z		Δppm	
			WT	pCEP_*fcl*	WT	pCEP_*fcl*
8	$C_{57}H_{102}N_{14}O_{12}$	1175.7874	1175.7865	1175.7865	-0.800	-0.843
7	$C_{60}H_{104}N_{12}O_{12}$	1185.7969	1185.7956	1185.7958	-1.107	-0.981
6	$C_{59}H_{106}N_{14}O_{13}$	1219.8137	1219.8129	1219.8131	-0.619	-0.480
5	$C_{62}H_{108}N_{12}O_{13}$	1229.8232	1229.8218	1229.8224	-1.088	-0.608

Figure S7: MALDI–HRMS spectra of *X. budapestensis* wild type (WT) and pCEP_*fcl* promoter-exchange mutant (induced and noninduced) with compounds **5**–**8** showing sum formulas, calculated and detected masses and corresponding Δppm.

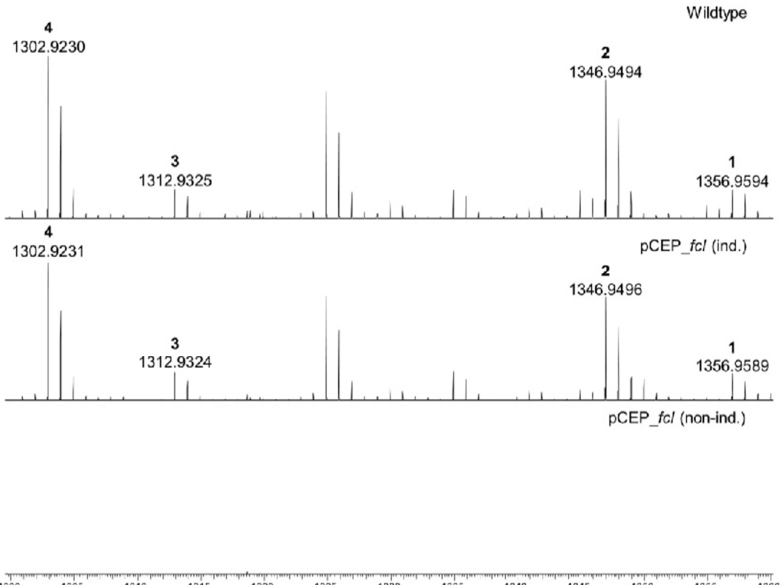

#	Sum formula	Calc. m/z	Det. m/z		Δppm	
			WT	pCEP_*fcl*	WT	pCEP_*fcl*
4	$C_{65}H_{119}N_{15}O_{12}$	1302.9235	1302.9230	1302.9231	-0.399	-0.338
3	$C_{68}H_{121}N_{13}O_{12}$	1312.9330	1312.9325	1312.9324	-0.451	-0.459
2	$C_{67}H_{123}N_{15}O_{13}$	1346.9498	1346.9494	1346.9496	-0.256	-0.100
1	$C_{70}H_{125}N_{13}O_{13}$	1356.9593	1356.9594	1356.9589	0.098	-0.248

Figure S8: MALDI–HRMS spectra of *X. budapestensis* wild type (WT) and pCEP_*fcl* promoter-exchange mutant (induced and noninduced) with compounds **1–4** showing sum formulas, calculated and detected masses and corresponding Δppm. Compounds **1–4** were described previously [20].

Expected Fragmentions	Sum formula	m/z
y1	$C_{28}H_{63}N_4O$	471.4996
y2	$C_{35}H_{74}N_5O_3$	612.5786
y5	$C_{47}H_{91}N_{10}O_8$	923.7016
y6	$C_{53}H_{98}N_{13}O_9$	1060.7605
b1	C_4H_5NO3	116.0342
b2	$C_{10}H_{13}N_4O_4$	253.0931
b5	$C_{21}H_{30}N_9O_9$	564.2161
b6	$C_{29}H_{41}N_{10}O_{11}$	705.2951

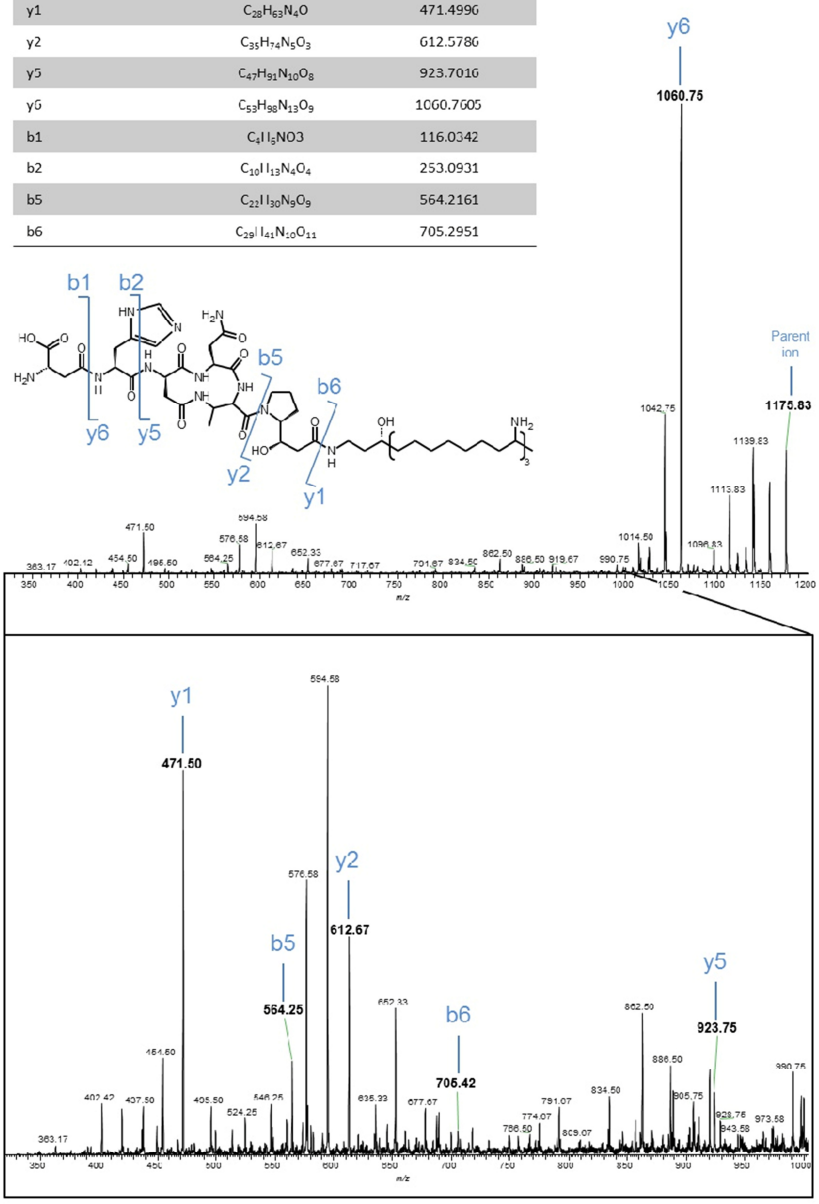

Figure S9: MALDI–MS^2 spectra of compound 1175.78 (**8**) of *X. budapestensis* pCEP_*fcl* (induced) showing expected fragment ions and proposed structure.

Expected Fragmentions	Sum formula	m/z
y1	$C_{28}H_{63}N_4O$	471.4996
y2	$C_{37}H_{78}N_5O_4$	656.6048
y5	$C_{49}H_{95}N_{10}O_8$	967.7278
y6	$C_{55}H_{102}N_{13}O_{10}$	1104.7867
b1	$C_4H_6NO_3$	116.0342
b2	$C_{16}H_{13}N_4O_4$	253.0931
b5	$C_{22}H_{36}N_9O_9$	564.2161
b6	$C_{31}H_{45}N_{10}O_{12}$	749.3213

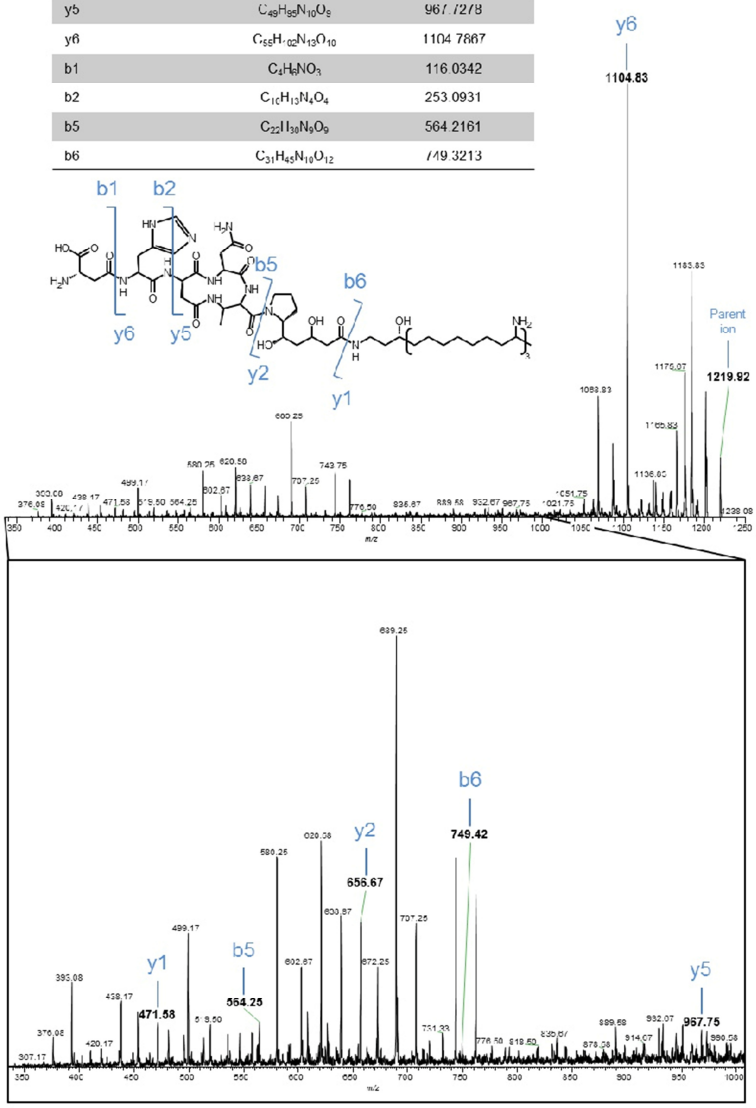

Figure S10: MALDI–MS^2 spectra of compound 1219.81 (**6**) of *X. budapestensis* pCEP_*fcl* (induced) showing expected fragment ions and proposed structure.

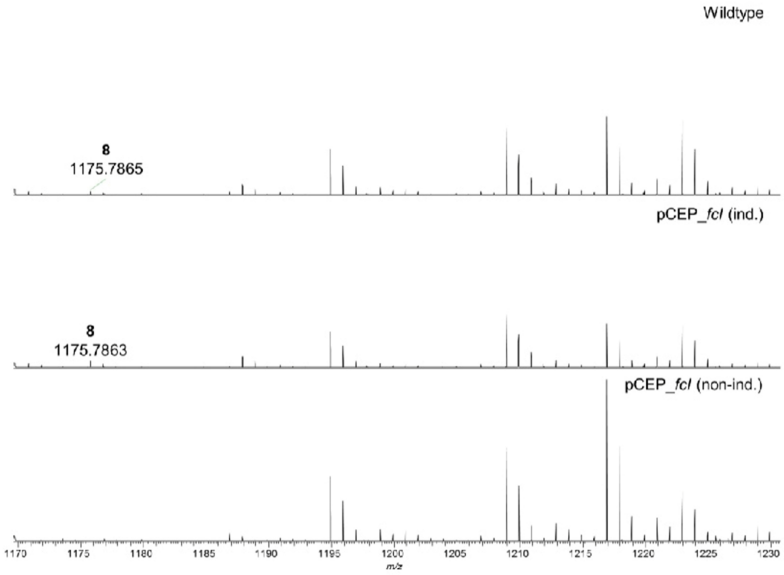

#	Sum formula	Calc. m/z	Det. m/z		Δppm	
			WT	pCEP_*fcl*	WT	pCEP_*fcl*
8	$C_{57}H_{102}N_{14}O_{12}$	1175.7874	1175.7865	1175.7863	-0.834	-1.004
7	$C_{60}H_{104}N_{12}O_{12}$	1185.7969	1185.7952	1185.7947	-1.495	-1.892
6	$C_{59}H_{106}N_{14}O_{13}$	1219.8137	1219.8132	1219.8129	-0.398	-0.652
5	$C_{62}H_{108}N_{12}O_{13}$	1229.8232	1229.8221	1229.8229	-0.860	-0.234

Figure S11: MALDI–HRMS spectra of *X. indica* wild type (WT) and pCEP_*fcl* promoter-exchange mutant (induced and noninduced) with compounds **5–8** showing sum formulas, calculated and detected masses and corresponding Δppm. Due to unspecific signals in all three spectra with high intensities the compounds **5–7** are not visible, but could be confirmed by HRMS.

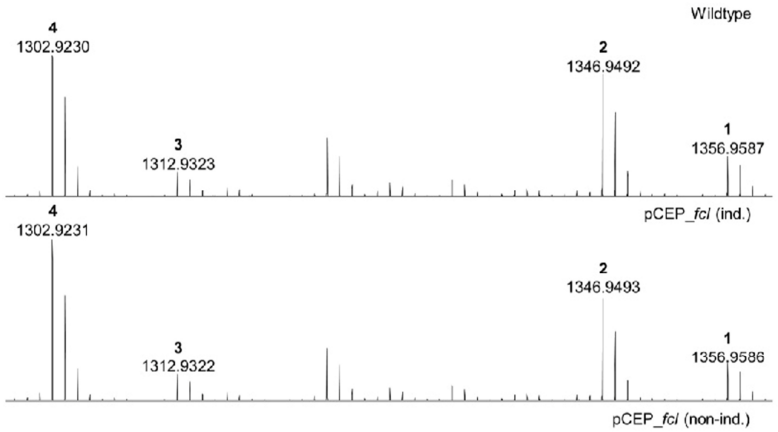

#	Sum formula	Calc. m/z	Det. m/z		Δppm	
			WT	pCEP_*fcl*	WT	pCEP_*fcl*
4	$C_{85}H_{119}N_{15}O_{12}$	1302.9235	1302.9230	1302.9231	-0.453	-0.361
3	$C_{69}H_{121}N_{13}O_{12}$	1312.9330	1312.9323	1312.9322	-0.558	-0.626
2	$C_{67}H_{123}N_{15}O_{13}$	1346.9498	1346.9492	1346.9493	-0.397	-0.323
1	$C_{70}H_{125}N_{13}O_{13}$	1356.9593	1356.9587	1356.9586	-0.447	-0.492

Figure S12: MALDI–HRMS spectra of *X. indica* wild type (WT) and pCEP_*fcl* promoter-exchange mutant (induced and noninduced) with compounds **1–4** showing sum formulas, calculated and detected masses and corresponding Δppm.

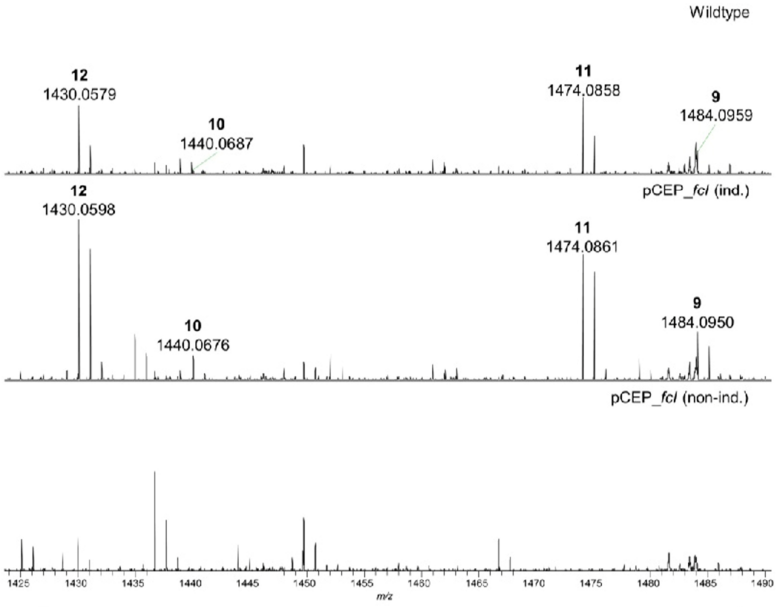

#	Sum formula	Calc. m/z	Det. m/z		Δppm	
			WT	pCEP_*fcl*	WT	pCEP_*fcl*
12	$C_{73}H_{136}N_{16}O_{12}$	1430.0596	1430.0579	1430.0598	-1.238	0.084
10	$C_{76}H_{138}N_{14}O_{12}$	1440.0691	1440.0687	1440.0676	-0.286	-1.043
11	$C_{75}H_{140}N_{16}O_{13}$	1474.0859	1474.0858	1474.0861	-0.030	0.180
9	$C_{78}H_{142}N_{14}O_{13}$	1484.0954	1484.0959	1484.0951	0.359	-0.207

Figure S13: MALDI–HRMS spectra of *X. indica* wild type (WT) and pCEP_*fcl* promoter-exchange mutant (induced and noninduced) with compounds **9–12** showing sum formulas, calculated and detected masses and corresponding Δppm.

Expected Fragmentions	Sum formula	m/z
y1	$C_{44}H_{97}N_6O$	725.7718
y2	$C_{51}H_{108}N_7O_3$	866.8508
y5	$C_{60}H_{125}N_{12}O_6$	1177.9738
y6	$C_{69}H_{132}N_{15}O_9$	1315.0327
b1	$C_4H_6NO_3$	116.0342
b2	$C_{10}H_{13}N_4O_4$	253.0931
b5	$C_{22}H_{30}N_9O_9$	564.2161
b6	$C_{29}H_{41}N_{10}O_{11}$	705.2951

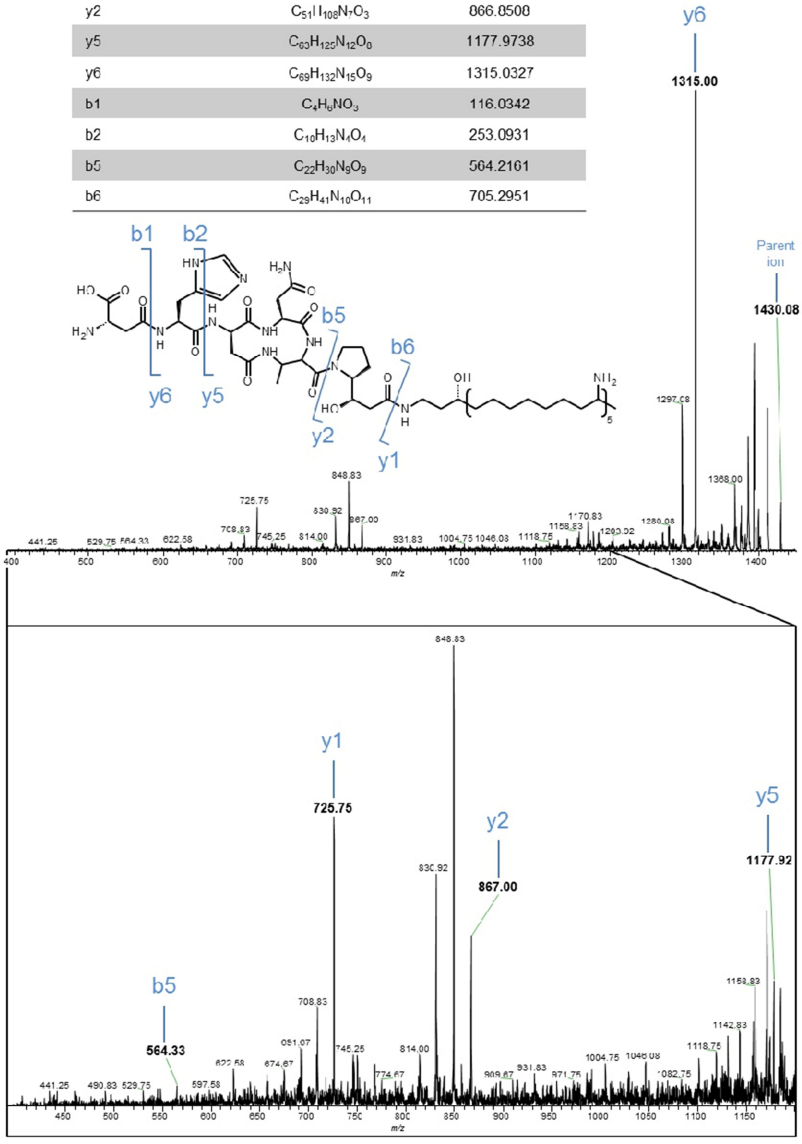

Figure S14: MALDI–MS^2 spectra of compound 1430.05 (**12**) of *X. indica* pCEP_*fcl* (induced) showing expected fragment ions and proposed structure.

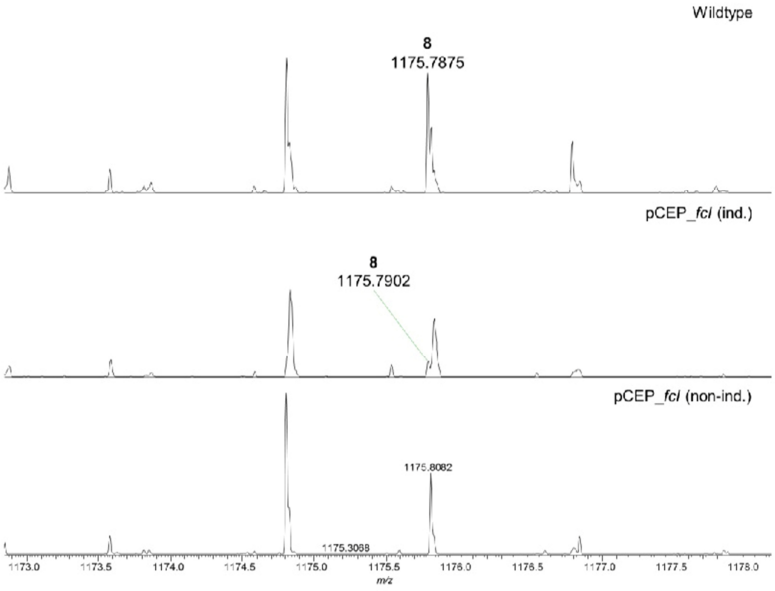

#	Sum formula	Calc. m/z	Det. m/z		Δppm	
			WT	pCEP_*fcl*	WT	pCEP_*fcl*
8	$C_{57}H_{102}N_{14}O_{12}$	1175.7874	1175.7875	1175.7902	0.050	2.355

Figure S15: MALDI–HRMS spectra of *X. cabanillasii* wild type (WT) and pCEP_*fcl* promoter-exchange mutant (induced and noninduced) with compound **8** showing sum formula, calculated and detected masses and corresponding Δppm.

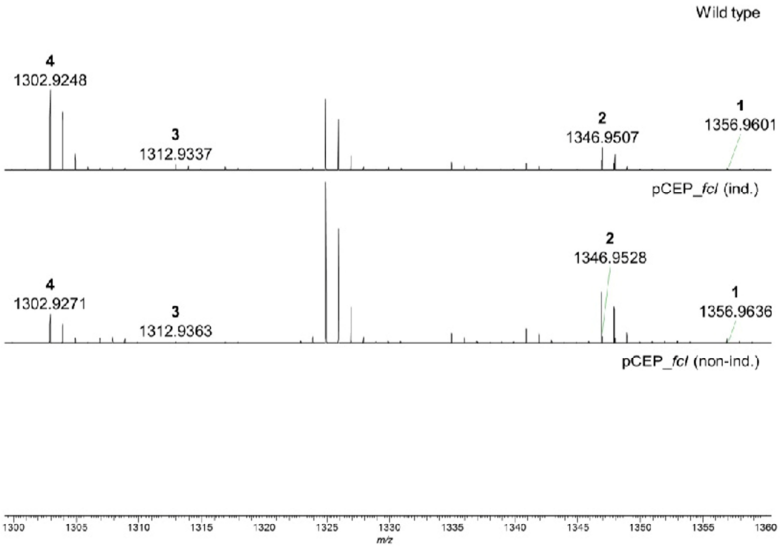

#	Sum formula	Calc. m/z	Det. m/z		Δppm	
			WT	pCEP_*fcl*	WT	pCEP_*fcl*
4	$C_{65}H_{119}N_{15}O_{12}$	1302.9235	1302.9248	1302.9271	0.990	2.747
3	$C_{66}H_{121}N_{13}O_{12}$	1312.9330	1312.9337	1312.9363	0.516	2.481
2	$C_{67}H_{123}N_{15}O_{13}$	1346.9498	1346.9507	1346.9528	0.679	2.275
1	$C_{76}H_{125}N_{13}O_{13}$	1356.9593	1356.9601	1356.9636	0.636	3.193

Figure S16: MALDI–HRMS spectra of *X. cabanillasii* wild type (WT) and pCEP_*fcl* promoter-exchange mutant (induced and noninduced) with compounds **1–4** showing sum formulas, calculated and detected masses and corresponding Δppm. Compounds **1–4** were described previously [14].

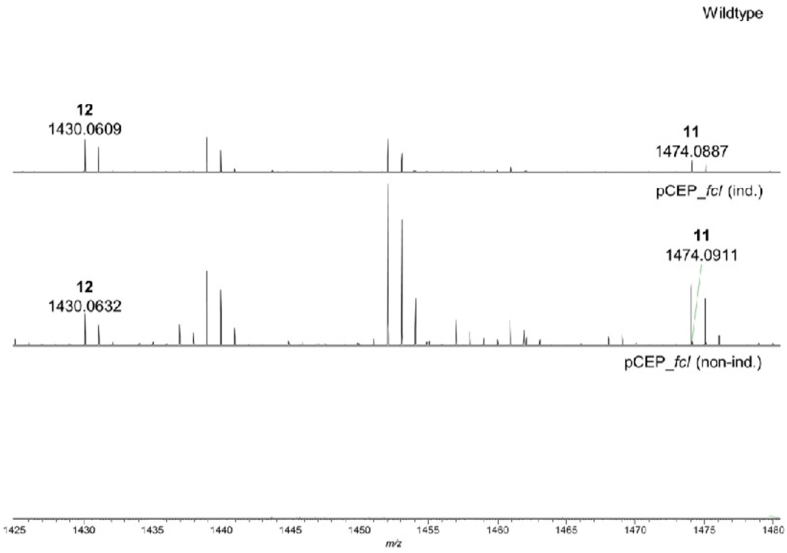

#	Sum formula	Calc. m/z	Det. m/z		Δppm	
			WT	pCEP_*fcl*	WT	pCEP_*fcl*
12	$C_{73}H_{136}N_{16}O_{12}$	1430.0596	1430.0609	1430.0633	0.860	2.524
11	$C_{75}H_{140}N_{16}O_{13}$	1474.0859	1474.0887	1474.0911	1.930	3.586

Figure S17: MALDI–HRMS spectra of *X. cabanillasii* wild type (WT) and pCEP_*fcl* promoter-exchange mutant (induced and noninduced) with compounds **11** and **12** showing sum formulas, calculated and detected masses and corresponding Δppm.

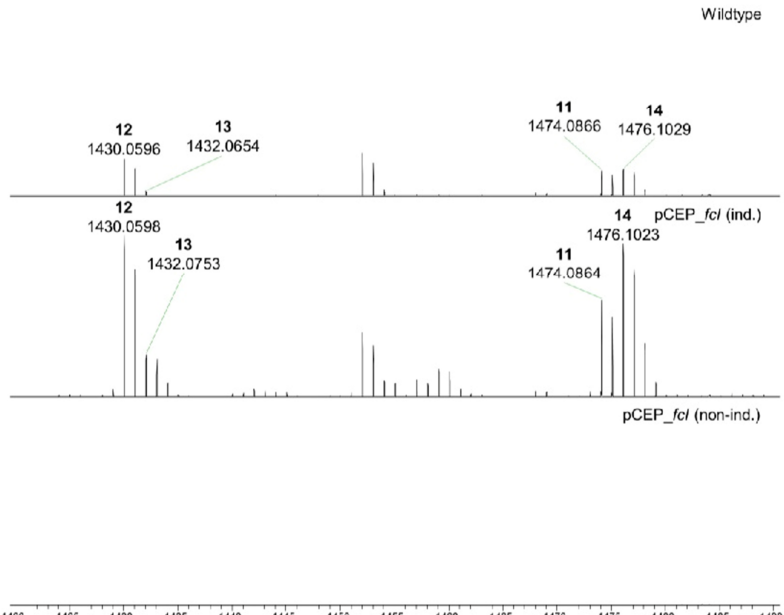

#	Sum formula	Calc. m/z	Det. m/z		Δppm	
			WT	pCEP_*fcl*	WT	pCEP_*fcl*
12	$C_{73}H_{136}N_{16}O_{12}$	1430.0596	1430.0596	1430.0599	0.000	0.147
13	$C_{73}H_{138}N_{16}O_{12}$	1432.0753	1432.0654	1432.0753	-6.913	0.021
11	$C_{75}H_{140}N_{16}O_{13}$	1474.0859	1474.0866	1474.0864	0.485	0.370
14	$C_{75}H_{142}N_{16}O_{13}$	1476.1015	1476.1029	1476.1023	0.972	0.532

Figure S18: MALDI–HRMS spectra of *X. hominickii* wild type (WT) and pCEP_*fcl* promoter-exchange mutant (induced and noninduced) with compounds **11–14** showing sum formulas, calculated and detected masses and corresponding Δppm.

Expected Fragmentions	Sum formula	m/z
y1	$C_{44}H_{97}N_6O$	725.7718
y2	$C_{51}H_{108}N_7O_3$	866.8508
y5	$C_{63}H_{125}N_{17}O_8$	1177.9736
y6	$C_{63}H_{132}N_{15}O_9$	1315.0327
b1	$C_4H_6NO_3$	116.0342
b2	$C_{11}H_{13}N_4O_4$	253.0931
b5	$C_{22}H_{30}N_9O_9$	564.2161
b6	$C_{29}H_{41}N_{10}O_{11}$	705.2951

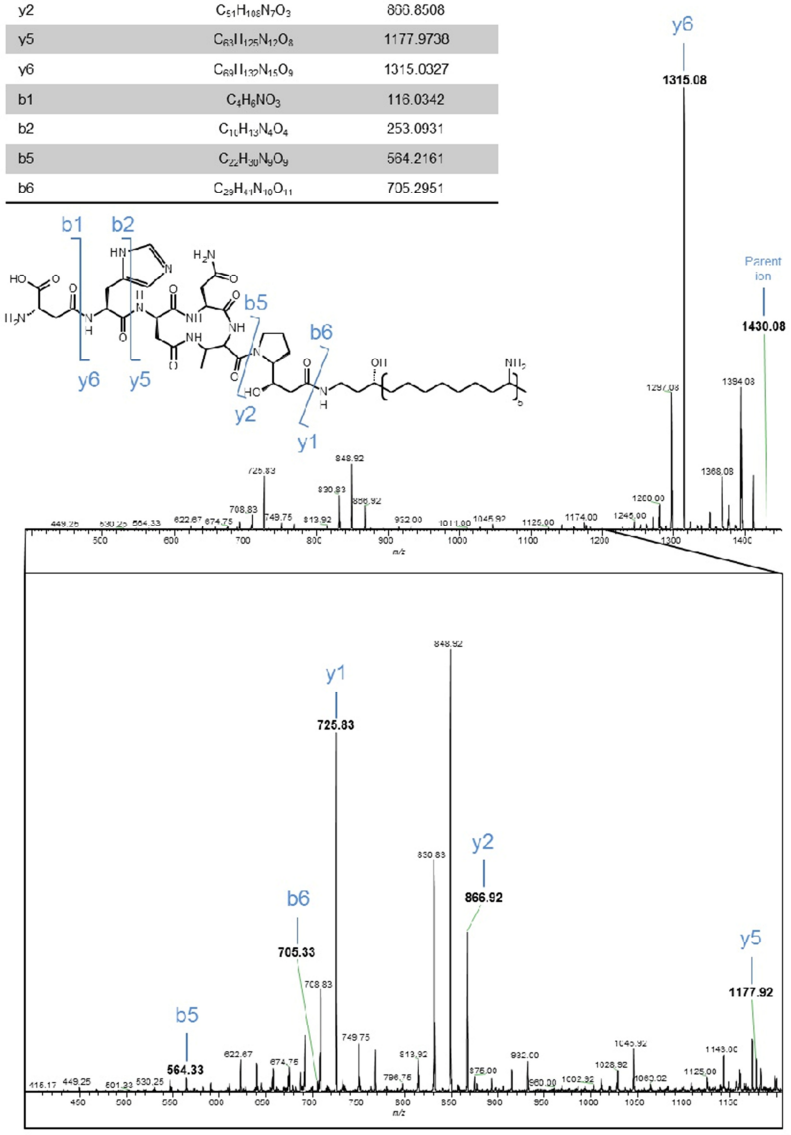

Figure S19: MALDI–MS^2 spectra of compound 1430.05 (**12**) of *X. hominickii* pCEP_*fcl* (induced) showing expected fragment ions and proposed structure.

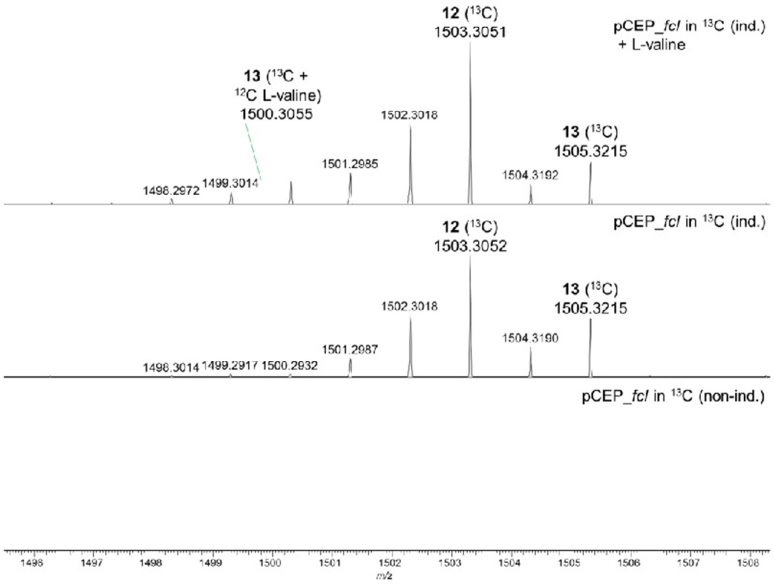

#	Sum formula	Calc. m/z	Det. m/z		Δppm	
			pCEP_*fcl*	pCEP_*fcl* + L-valine	pCEP_*fcl*	pCEP_*fcl* + L-valine
12 (^{13}C)	$^{13}C_{73}H_{136}N_{16}O_{12}$	1503.3048	1503.3052	1503.3051	0.2727	0.2262
13 (^{13}C)	$^{13}C_{73}H_{138}N_{16}O_{12}$	1505.3204	1505.3215	1505.3215	0.6842	0.7241
13 (^{13}C + ^{12}C L-valine)	$^{13}C_{68}C_5H_{138}N_{16}O_{12}$	1500.3037	-	1500.3055	-	1.2131

Figure S20: MALDI–HRMS spectra of the reverse feeding experiment in ^{13}C medium of *X. hominickii* pCEP_*fcl* mutant (induced and noninduced) with compounds **12** and **13** (with and without feeding of ^{12}C L-valine) showing sum formulas, calculated and detected masses and corresponding Δppm.

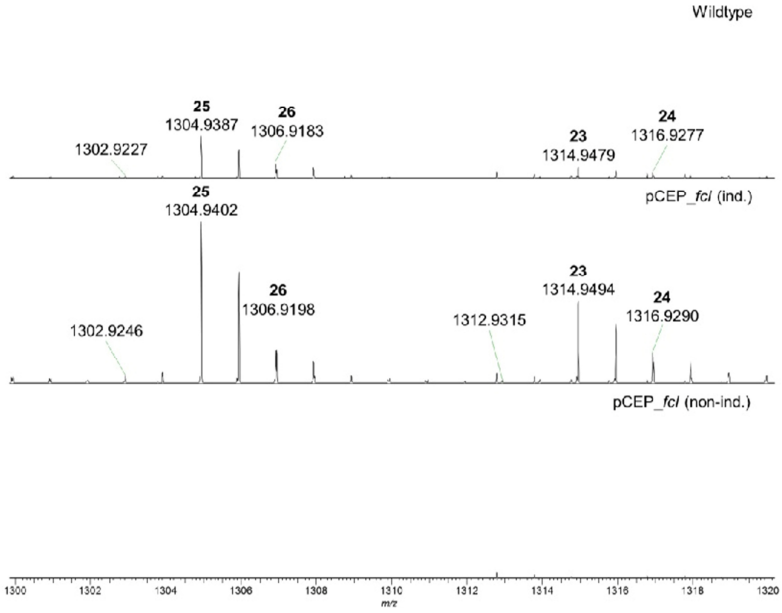

#	Sum formula	Calc. m/z	Det. m/z		Δppm	
			WT	pCEP_*fcl*	WT	pCEP_*fcl*
-	$C_{65}H_{119}N_{15}O_{12}$	1302.9235	1302.9227	1302.9246	-0.630	0.813
25	$C_{65}H_{121}N_{15}O_{12}$	1304.9392	1304.9387	1304.9402	-0.384	0.774
26	$C_{64}H_{118}N_{15}O_{13}$	1306.9185	1306.9183	1306.9198	-0.149	1.029
-	$C_{66}H_{121}N_{13}O_{12}$	1312.9330	1312.9290	1312.9315	-3.064	-1.167
23	$C_{68}H_{123}N_{13}O_{12}$	1314.9487	1314.9479	1314.9494	-0.595	0.568
24	$C_{67}H_{121}N_{13}O_{13}$	1316.9280	1316.9277	1316.9290	-0.218	0.769

Figure S21: MALDI–HRMS spectra of KJ12.1 wild type (WT) and pCEP_*fcl* promoter-exchange mutant (induced and noninduced) with compounds **23**–**26** showing sum formulas, calculated and detected masses and corresponding Δppm.

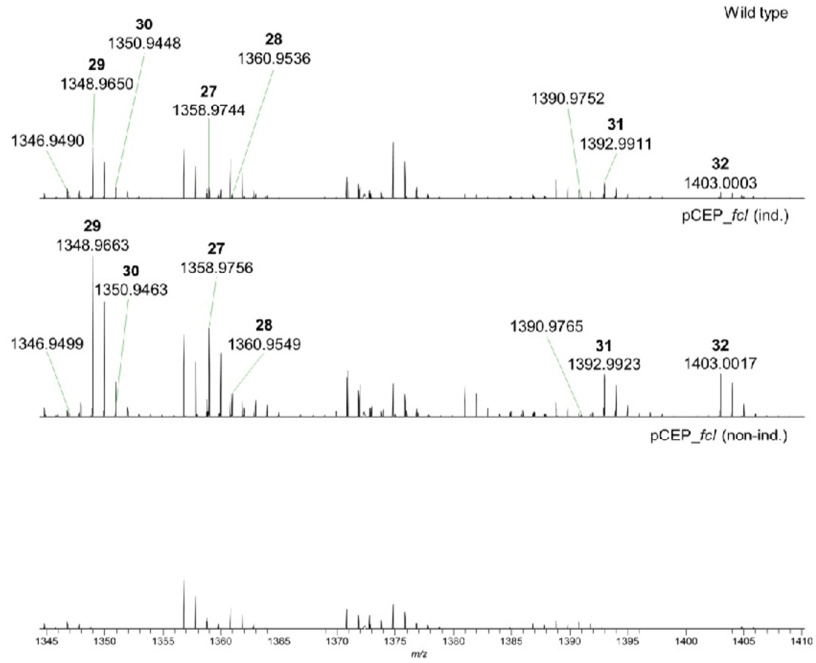

#	Sum formula	Calc. m/z	Det. m/z		Δppm	
			WT	pCEP_*fcl*	WT	pCEP_*fcl*
-	$C_{67}H_{123}N_{15}O_{13}$	1346.9498	1346.9490	1346.9499	-0.575	0.115
29	$C_{67}H_{125}N_{15}O_{13}$	1348.9654	1348.9650	1348.9663	-0.323	0.626
30	$C_{66}H_{123}N_{15}O_{14}$	1350.9447	1350.9448	1350.9463	0.096	1.222
27	$C_{70}H_{127}N_{13}O_{13}$	1358.9749	1358.9744	1358.9756	-0.403	0.480
28	$C_{69}H_{125}N_{13}O_{14}$	1360.9542	1360.9536	1360.9549	-0.442	0.542
-	$C_{69}H_{127}N_{15}O_{14}$	1390.9760	1390.9752	1390.9765	-0.546	0.403
31	$C_{69}H_{129}N_{15}O_{14}$	1392.9916	1392.9911	1392.9923	-0.366	0.467
32	$C_{72}H_{131}N_{13}O_{14}$	1403.0011	1403.0003	1403.0017	-0.593	0.398

Figure S22: MALDI–HRMS spectra of KJ12.1 wild type (WT) and pCEP_*fcl* promoter-exchange mutant (induced and noninduced) with compounds **27–32** showing sum formulas, calculated and detected masses and corresponding Δppm.

Expected Fragmentions	Sum formula	m/z
y1	$C_{36}H_{68}N_5O$	598.6357
y2	$C_{43}H_{93}N_8O_3$	741.7304
y5	$C_{55}H_{110}N_{11}O_8$	1052.8533
y6	$C_{61}H_{117}N_{14}O_9$	1189.9122
b1	$C_4H_6NO_3$	116.0342
b2	$C_{10}H_{13}N_4O_4$	253.0931
b5	$C_{22}H_{30}N_9O_9$	564.2161
b6	$C_{26}H_{43}N_{10}O_{11}$	707.3107

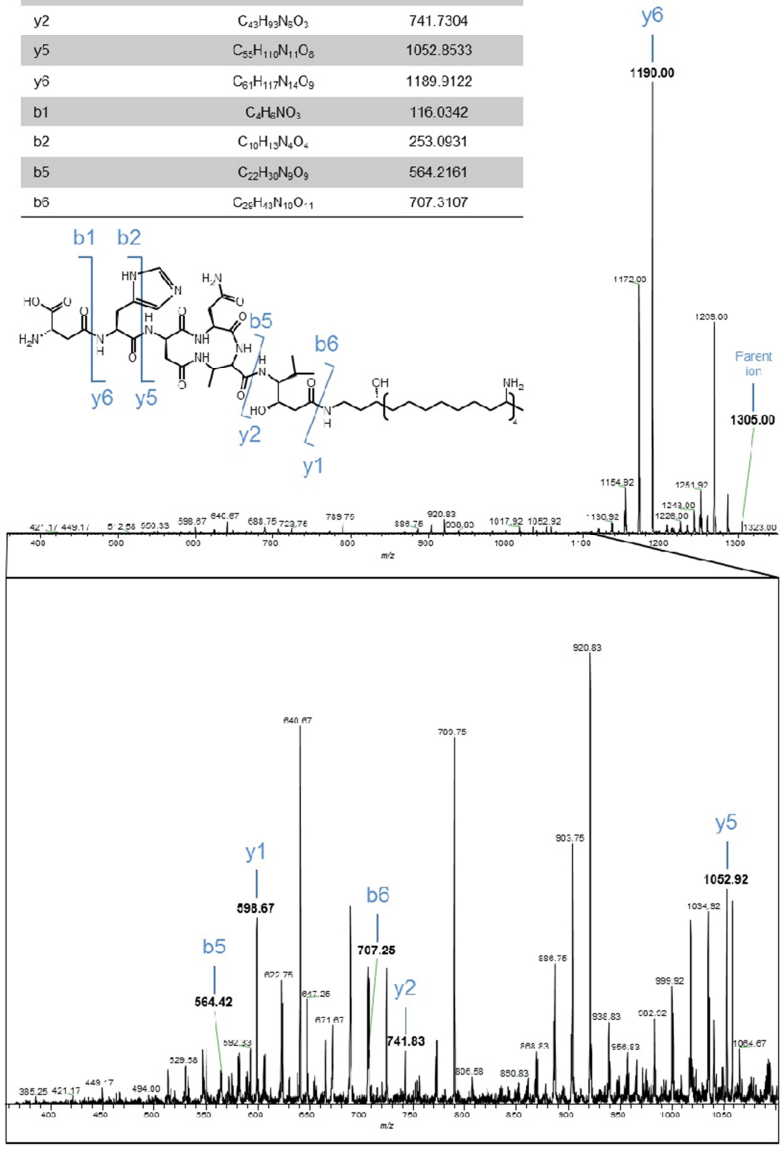

Figure S23: MALDI–MS^2 spectra of compound 1304.94 (**25**) of KJ12.1 pCEP_*fcl* (induced) showing expected fragment ions and proposed structure.

Expected Fragmentions	Sum formula	m/z
y1	$C_{36}H_{80}N_5O$	598.6357
y2	$C_{42}H_{91}N_6O_4$	743.7096
y5	$C_{54}H_{108}N_{11}O_9$	1054.8326
y6	$C_{60}H_{112}N_{14}O_{10}$	1191.8915
b1	$C_4H_5NO_3$	116.0342
b2	$C_{10}H_{13}N_4O_4$	253.0931
b5	$C_{22}H_{30}N_9O_9$	564.2161
b6	$C_{28}H_4{}_4N_{10}O_{12}$	709.29

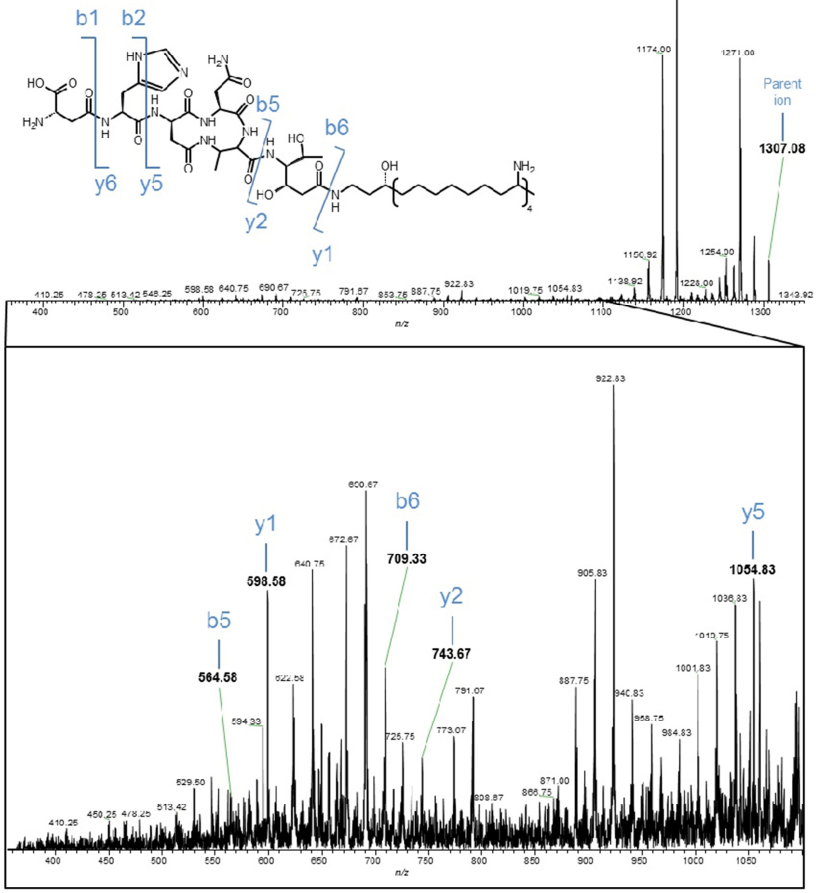

Figure S24: MALDI–MS^2 spectra of compound 1306.91 (**26**) of KJ12.1 pCEP_*fcl* (induced) showing expected fragment ions and proposed structure.

Expected Fragmentions	Sum formula	m/z
y1	$C_{36}H_{80}N_5O$	598.6357
y2	$C_{47}H_{111}N_6O_5$	829.7828
y5	$C_{59}H_{118}N_{11}O_{10}$	1140.9058
y6	$C_{65}H_{125}N_{14}O_{11}$	1277.9647
b1	$C_7H_6NO_3$	116.0342
b2	$C_{10}H_{13}N_4O_4$	253.0931
b5	$C_{22}H_{30}N_9O_9$	564.2161
b6	$C_{33}H_{51}N_{10}O_{13}$	795.3632

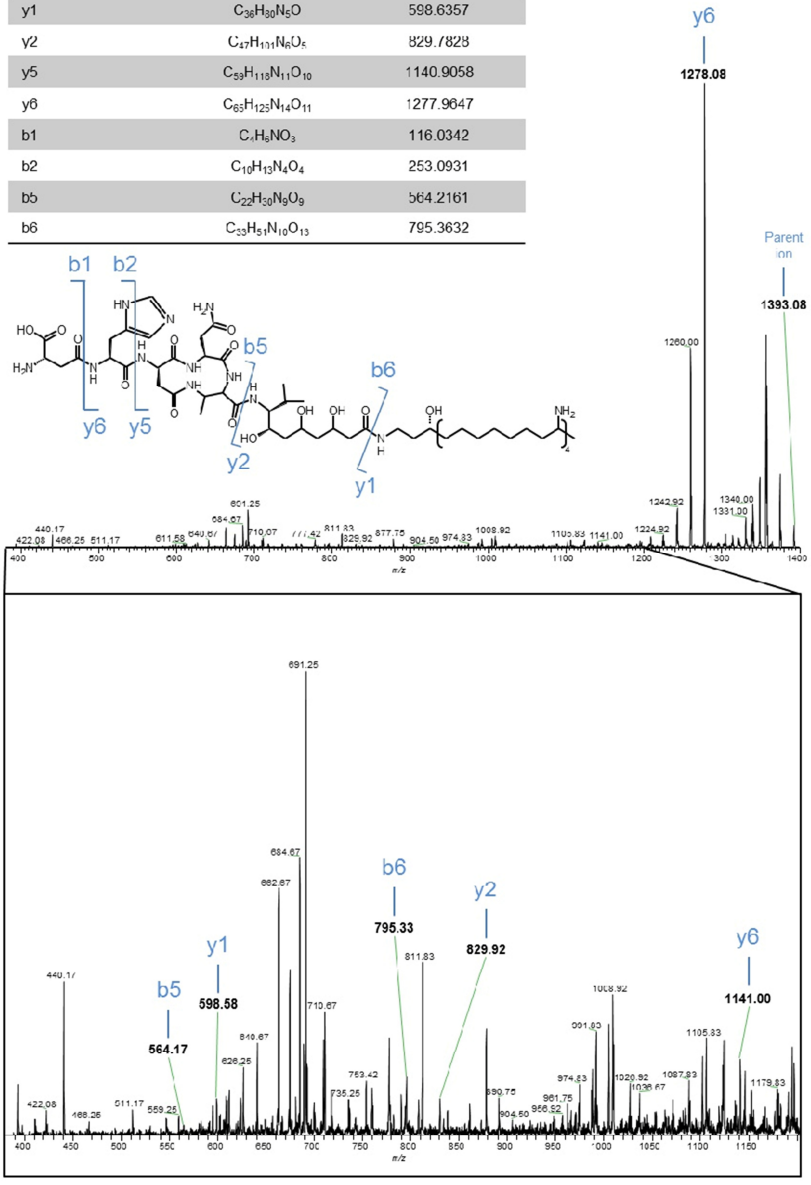

Figure S25: MALDI–MS^2 spectra of compound 1392.99 (**31**) of KJ12.1 pCEP_*fcl* (induced) showing expected fragment ions and proposed structure.

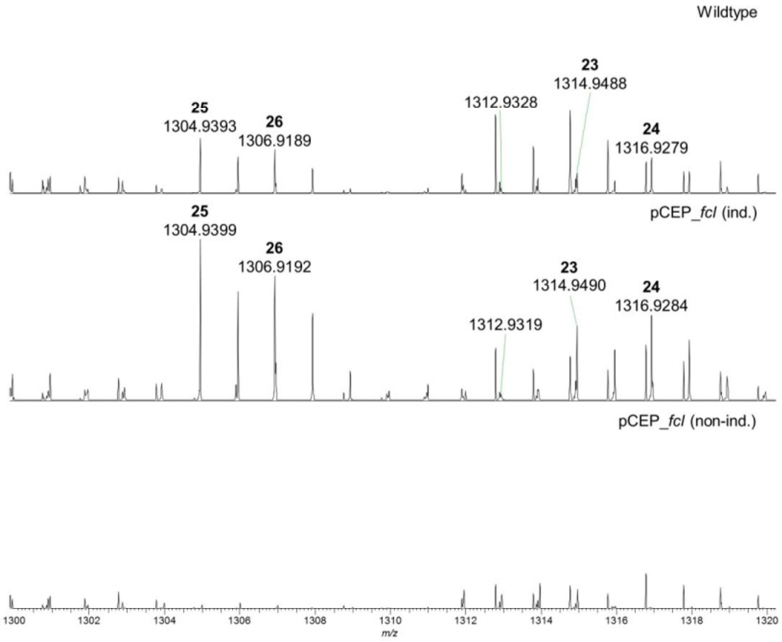

#	Sum formula	Calc. m/z	Det. m/z		Δppm	
			WT	pCEP_*fcl*	WT	pCEP_*fcl*
25	$C_{65}H_{121}N_{15}O_{12}$	1304.9392	1304.9393	1304.9399	0.046	0.521
26	$C_{64}H_{119}N_{15}O_{13}$	1306.9185	1306.9189	1306.9192	0.371	0.570
-	$C_{68}H_{121}N_{13}O_{12}$	1312.9330	1312.9328	1312.9319	-0.192	-0.870
23	$C_{68}H_{123}N_{13}O_{12}$	1314.9487	1314.9488	1314.9490	0.112	0.241
24	$C_{67}H_{121}N_{13}O_{13}$	1316.9280	1316.9279	1316.9284	-0.066	0.359

Figure S26: MALDI–HRMS spectra of *X. stockiae* wild type (WT) and pCEP_*fcl* promoter-exchange mutant (induced and noninduced) with compounds **23**–**26** showing sum formulas, calculated and detected masses and corresponding Δppm.

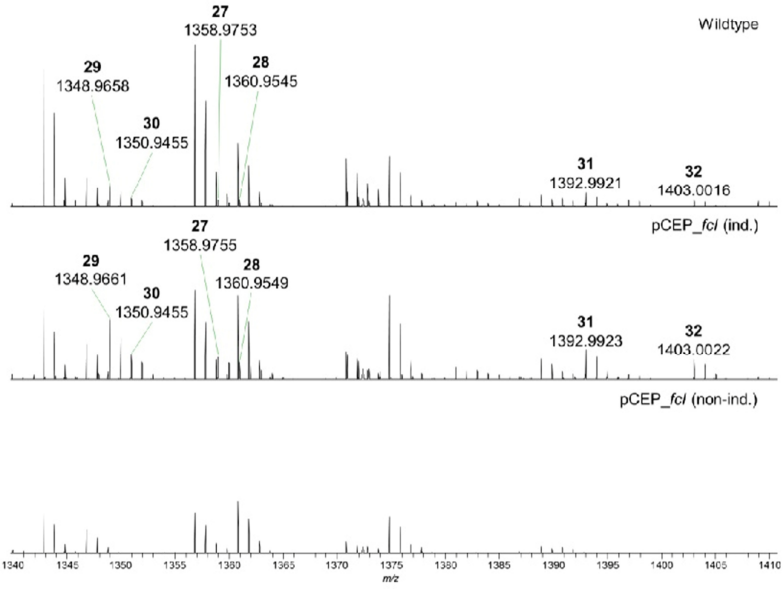

#	Sum formula	Calc. m/z	Det. m/z		Δppm	
			WT	pCEP_*fcl*	WT	pCEP_*fcl*
29	$C_{67}H_{125}N_{15}O_{13}$	1348.9654	1348.9658	1348.9661	0.285	0.545
30	$C_{68}H_{123}N_{15}O_{14}$	1350.9447	1350.9455	1350.9455	0.615	0.629
27	$C_{70}H_{127}N_{13}O_{13}$	1358.9749	1358.9753	1358.9755	0.318	0.429
28	$C_{69}H_{125}N_{13}O_{14}$	1360.9542	1360.9545	1360.9549	0.226	0.520
31	$C_{69}H_{129}N_{15}O_{14}$	1392.9916	1392.9922	1392.9923	0.381	0.467
32	$C_{72}H_{131}N_{13}O_{14}$	1403.0011	1403.0016	1403.0022	0.334	0.747

Figure S27: MALDI–HRMS spectra of *X. stockiae* wild type (WT) and pCEP_*fcl* promoter-exchange mutant (induced and-noninduced) with compounds **27–32** showing sum formulas, calculated and detected masses and corresponding Δppm.

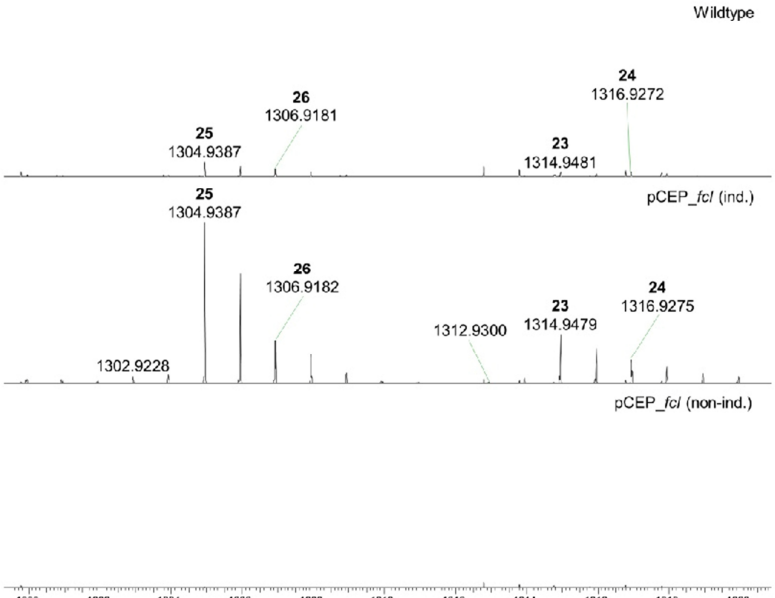

#	Sum formula	Calc. m/z	Det. m/z		Δppm	
			WT	pCEP_*fcl*	WT	pCEP_*fcl*
-	$C_{65}H_{119}N_{15}O_{12}$	1302.9235	1302.9242	1302.9228	0.499	-0.561
25	$C_{65}H_{121}N_{15}O_{12}$	1304.9392	1304.9387	1304.9387	-0.407	-0.361
26	$C_{64}H_{119}N_{15}O_{13}$	1306.9185	1306.9181	1306.9182	-0.279	-0.172
-	$C_{69}H_{121}N_{13}O_{12}$	1312.9330	1312.9287	1312.9300	-3.285	-2.317
23	$C_{68}H_{123}N_{13}O_{12}$	1314.9487	1314.9481	1314.9479	-0.489	-0.587
24	$C_{67}H_{121}N_{13}O_{13}$	1316.928	1316.9272	1316.9275	-0.544	-0.324

Figure S28: MALDI–HRMS spectra of KK7.4 wild type (WT) and pCEP_*fcl* promoter-exchange mutant (induced and noninduced) with compounds **23–26** showing sum formulas, calculated and detected masses and corresponding Δppm.

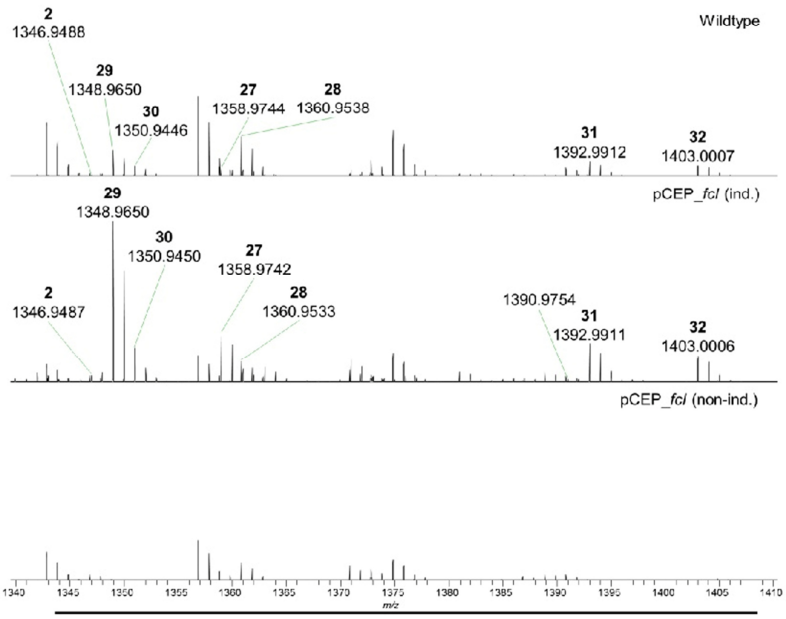

#	Sum formula	Calc. m/z	Det. m/z		Δppm	
			WT	pCEP_*fcl*	WT	pCEP_*fcl*
2	$C_{67}H_{123}N_{15}O_{13}$	1346.9498	1346.9488	1346.9487	-0.731	-0.791
29	$C_{67}H_{125}N_{15}O_{13}$	1348.9654	1348.9650	1348.9650	-0.323	-0.315
30	$C_{66}H_{123}N_{15}O_{14}$	1350.9447	1350.9446	1350.9450	-0.037	0.244
27	$C_{70}H_{127}N_{13}O_{13}$	1358.9749	1358.9744	1358.9742	-0.359	-0.506
28	$C_{69}H_{125}N_{13}O_{14}$	1360.9542	1360.9538	1360.9533	-0.273	-0.670
31	$C_{69}H_{129}N_{15}O_{14}$	1392.9916	1392.9912	1392.9911	-0.323	-0.388
-	$C_{69}H_{127}N_{15}O_{14}$	1390.976	1390.9767	1390.9754	0.539	-0.410
32	$C_{72}H_{131}N_{13}O_{14}$	1403.0011	1403.0007	1403.0006	-0.322	-0.401

Figure S29: MALDI–HRMS spectra of KK7.4 wild type (WT) and pCEP_*fcl* promoter-exchange mutant (induced and noninduced) with compounds **2** and **27–32** showing sum formulas, calculated and detected masses and corresponding Δppm.

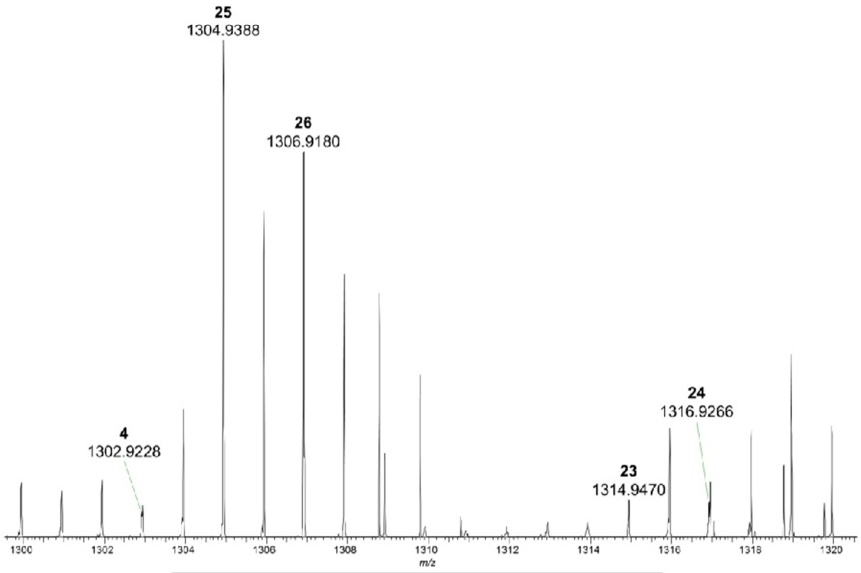

#	Sum formula	Calc. m/z	Det. m/z	Δppm
4	$C_{85}H_{119}N_{15}O_{12}$	1302.9235	1302.9228	-0.607
25	$C_{85}H_{121}N_{15}O_{12}$	1304.9392	1304.9388	-0.299
26	$C_{84}H_{119}N_{15}O_{13}$	1306.9185	1306.9180	-0.356
23	$C_{88}H_{123}N_{13}O_{12}$	1314.9487	1314.9470	-1.280
24	$C_{87}H_{121}N_{13}O_{13}$	1316.928	1316.9266	-1.015

Figure S30: MALDI–HRMS spectra of *X. innexi* wild type with compounds **4** and **23–26** showing sum formulas, calculated and detected masses and corresponding Δppm.

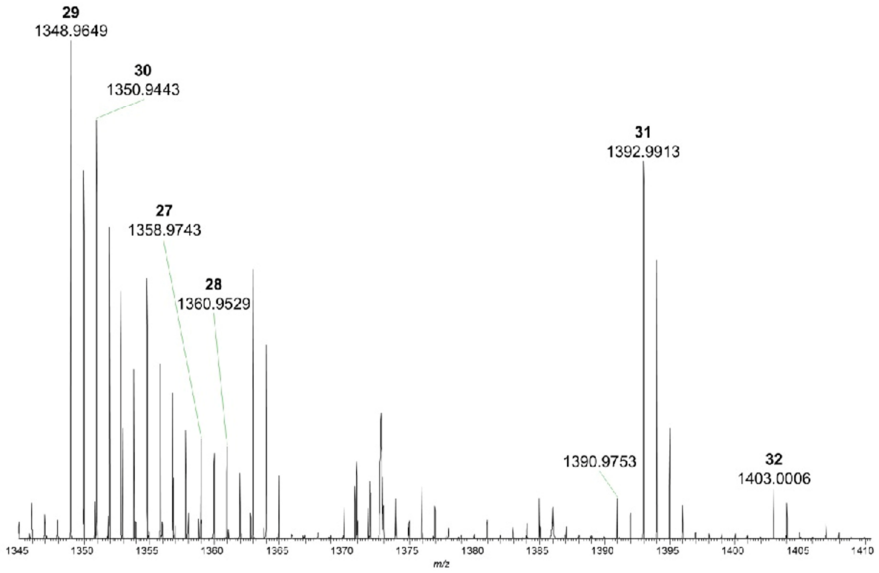

#	Sum formula	Calc. m/z	Det. m/z	Δppm
29	$C_{67}H_{125}N_{15}O_{13}$	1348.9654	1348.9649	-0.374
30	$C_{66}H_{123}N_{15}O_{14}$	1350.9447	1350.9443	-0.281
27	$C_{70}H_{127}N_{13}O_{13}$	1358.9749	1358.9743	-0.462
28	$C_{69}H_{125}N_{13}O_{14}$	1360.9542	1360.9529	-0.912
-	$C_{65}H_{127}N_{15}O_{14}$	1390.976	1390.9753	-0.460
31	$C_{69}H_{129}N_{15}O_{14}$	1392.9916	1392.9913	-0.244
32	$C_{72}H_{131}N_{13}O_{14}$	1403.0011	1403.0006	-0.351

Figure S31: MALDI–HRMS spectra of *X. innexi* wild type with compounds **27**–**32** showing sum formulas, calculated and detected masses and corresponding Δppm.

Expected Fragmentions	Sum formula	m/z
y1	$C_{36}H_{66}N_6O$	598.6357
y2	$C_{47}H_{101}N_6O_5$	829.7828
y5	$C_{59}H_{118}N_{11}O_{10}$	1140.9058
y6	$C_{65}H_{125}N_{14}O_{11}$	1277.9647
b1	$C_4H_6NO_3$	116.0342
b2	$C_{10}H_{13}N_4O_4$	253.0931
b5	$C_{22}H_{30}N_9O_9$	564.2161
b6	$C_{33}H_{51}N_{13}O_{13}$	795.3632

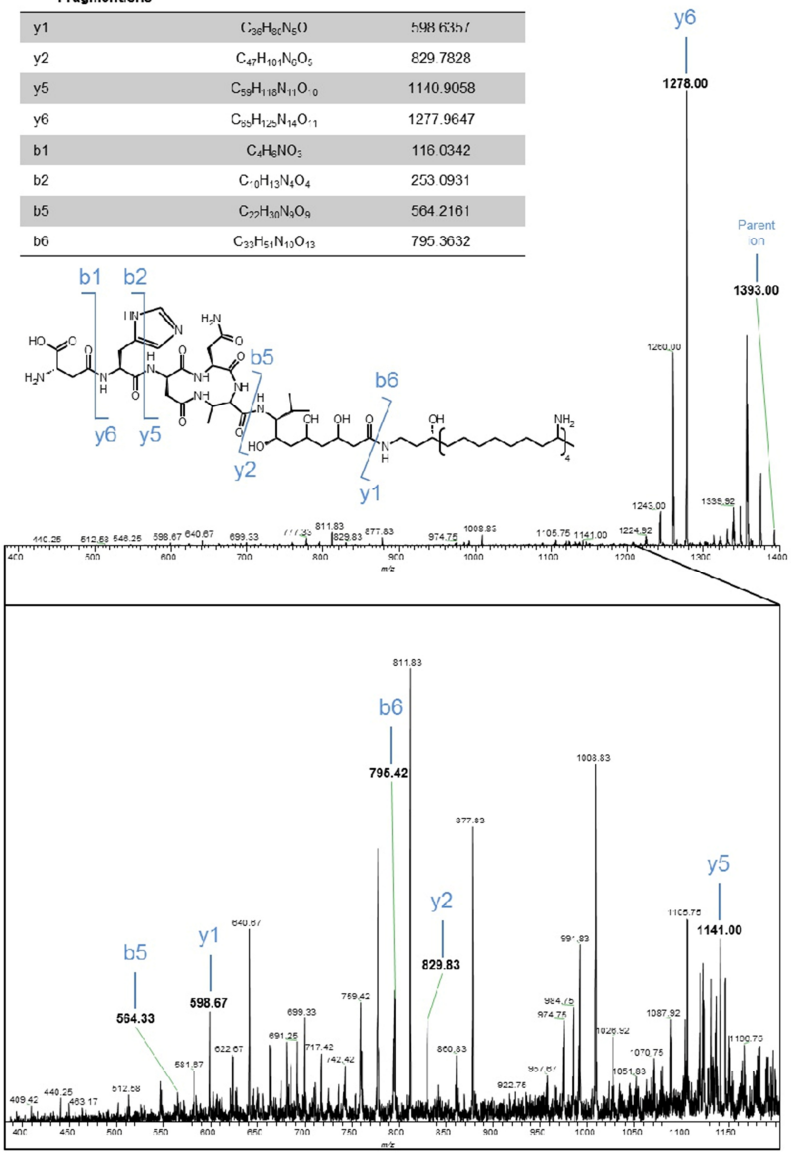

Figure S32: MALDI–MS^2 spectra of compound 1392.99 (**31**) of *X. innexi* showing expected fragment ions and proposed structure.

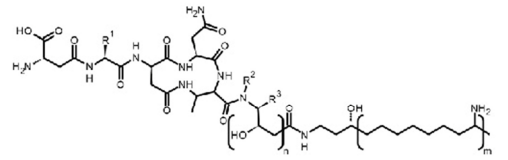

Occurence	R^1	R^2	R^3	n	m	Sum formula	[M+H]⁺
a	CH_3	H		2	3	$C_{56}H_{106}N_{12}O_{13}$	1155.8075
a	CH_3	H		2	3	$C_{55}H_{104}N_{12}O_{14}$	1157.7868
a		H		2	3	$C_{58}H_{106}N_{14}O_{14}$	1223.8086
b				3	4	$C_{66}H_{127}N_{15}O_{14}$	1390.9760
a		H		2	3	$C_{61}H_{108}N_{12}O_{14}$	1233.8181

Figure S33: Proposed minor derivatives found in *Xenorhabdus* strains (a: *X. szentirmaii*; b: KJ12.1, KK7.4). Identification is based on MALDI–HRMS spectra (Figure S2, S3, S22, and S29).

References

1. Wenski, S. L.; Kolbert, D.; Grammbitter, G. L. C.; Bode, H. B. *J. Ind. Microbiol. Biotechnol.* **2019**, 46 (3-4), 565-572. doi:10.1007/s10295-018-02124-8
2. Bode, E.; Brachmann, A. O.; Kegler, C.; Simsek, R.; Dauth, C.; Zhou, Q.; Kaiser, M.; Klemmt, P.; Bode, H. B. *Chembiochem* **2015,** *16* (7), 1115–1119. doi:10.1002/cbic.201500094
3. Simon, R.; Priefer, U.; Pühler, A. *Nat Biotechnol* **1983,** *1*, 784 EP -. doi:10.1038/nbt1183-784
4. Thoma, S.; Schobert, M. *FEMS Microbiol. Lett.* **2009,** *294* (2), 127–132. doi:10.1111/j.1574-6968.2009.01556.x
5. Fu, C.; Donovan, W. P.; Shikapwashya-Hasser, O.; Ye, X.; Cole, R. H. *PLoS ONE* **2014,** *9* (12), e115318. doi:10.1371/journal.pone.0115318
6. Agarwal, P.; Agarwal, N.; Gupta, R.; Gupta, M.; Sharma, B. *J Microb Biochem Technol* **2016,** *08* (05). doi:10.4172/1948-5948.1000316
7. Fang, X. L.; Li, Z. Z.; Wang, Y. H.; Zhang, X. *J. Appl. Microbiol.* **2011,** *111* (1), 145–154. doi:10.1111/j.1365-2672.2011.05033.x
8. Lengyel, K.; Lang, E.; Fodor, A.; Szállás, E.; Schumann, P.; Stackebrandt, E. *Syst. Appl. Microbiol.* **2005,** *28* (2), 115–122. doi:10.1016/j.syapm.2004.10.004
9. Tailliez, P.; Pagès, S.; Ginibre, N.; Boemare, N. *Int. J. Syst. Evol. Microbiol.* **2006,** *56* (Pt 12), 2805–2818. doi:10.1099/ijs.0.64287-0
10. Somvanshi, V. S.; Lang, E.; Ganguly, S.; Swiderski, J.; Saxena, A. K.; Stackebrandt, E. *Syst. Appl. Microbiol.* **2006,** *29* (7), 519–525. doi:10.1016/j.syapm.2006.01.004
11. Thanwisai, A.; Tandhavanant, S.; Saiprom, N.; Waterfield, N. R.; Ke Long, P.; Bode, H. B.; Peacock, S. J.; Chantratita, N. *PLoS ONE* **2012,** *7* (9), e43835. doi:10.1371/journal.pone.0043835
12. Tobias, N. J.; Wolff, H.; Djahanschiri, B.; Grundmann, F.; Kronenwerth, M.; Shi, Y.-M.; Simonyi, S.; Grün, P.; Shapiro-Ilan, D.; Pidot, S. J.; Stinear, T. P.; Ebersberger, I.; Bode, H. B. *Nat. Microbiol.* **2017,** *2* (12), 1676–1685. doi:10.1038/s41564-017-0039-9
13. Hurst, S. G.; Ghazal, S.; Morris, K.; Abebe-Akele, F.; Thomas, W. K.; Badr, U. M.; Hussein, M. A.; AbouZaied, M. A.; Khalil, K. M.; Tisa, L. S. *Genome Announc* **2014,** *2* (6). doi:10.1128/genomeA.01273-14
14. Donmez Ozkan, H.; Cimen, H.; Ulug, D.; Wenski, S.; Yigit Ozer, S.; Telli, M.; Aydin, N.; Bode, H. B.; Hazir, S. *Front Microbiol* **2019,** *10*, 2672. doi:10.3389/fmicb.2019.02672
15. Stachelhaus, T.; Mootz, H. D.; Marahiel, M. A. *Chem. Biol.* **1999,** 6 (8), 493-505. doi: 10.1016/S1074-5521(99)80082-9
16. Challis, G. L.; Ravel, J.; Townsend, C. A. *Chem. Biol.* **2000,** 7 (3), 211-224. doi: 10.1016/s1074-5521(00)00091-017.Kim, I.-H.; Aryal, S. K.; Aghai, D. T.; Casanova-Torres, Á. M.; Hillman, K.; Kozuch, M. P.; Mans, E. J.; Mauer, T. J.; Ogier, J.-C.; Ensign, J. C.; Gaudriault, S.; Goodman, W. G.; Goodrich-Blair, H.; Dillman, A. R. *BMC Genomics* **2017,** *18* (1), 927. doi:10.1186/s12864-017-4311-4
17. Kim, I.-H.; Aryal, S. K.; Aghai, D. T.; Casanova-Torres, Á. M.; Hillman, K.; Kozuch, M. P.; Mans, E. J.; Mauer, T. J.; Ogier, J.-C.; Ensign, J. C.; Gaudriault, S.; Goodman, W. G.; Goodrich-Blair, H.; Dillman, A. R. *BMC Genomics* **2017,** *18* (1), 927. doi:10.1186/s12864-017-4311-4
18. Masschelein, J.; Mattheus, W.; Gao, L.-J.; Moons, P.; van Houdt, R.; Uytterhoeven, B.; Lamberigts, C.; Lescrinier, E.; Rozenski, J.; Herdewijn, P.; Aertsen, A.; Michiels, C.; Lavigne, R. *PLoS ONE* **2013,** *8* (1), e54143. doi:10.1371/journal.pone.0054143

19. Masschelein, J.; Clauwers, C.; Awodi, U. R.; Stalmans, K.; Vermaelen, W.; Lescrinier, E.; Aertsen, A.; Michiels, C.; Challis, G. L.; Lavigne, R. *Chem. Sci.* **2015,** *6* (2), 923–929. doi:10.1039/c4sc01927j
20. Fuchs, S. W.; Grundmann, F.; Kurz, M.; Kaiser, M.; Bode, H. B. *Chembiochem* **2014,** *15* (4), 512–516. doi:10.1002/cbic.201300802

6.3 Nematode-Associated Bacteria: Production of Antimicrobial Agent as a Presumptive Nominee for Curing Endodontic Infections Caused by *Enterococcus faecalis*

Authors:

Hicran Donmez Ozkan[1]*, Harun Cimen[2], Derya Ulug[2], Sebastian Wenski[3], Senem Yigit Ozer[1], Murat Telli[4], Neriman Aydin[4], Helge B. Bode[3] and Selcuk Hazir[2]*

[1] Department of Endodontics, Faculty of Dentistry, Adnan Menderes University, Aydin, Turkey

[2] Department of Biology, Faculty of Arts and Sciences, Adnan Menderes University, Aydin, Turkey

[3] Molekulare Biotechnologie, Fachbereich Biowissenschaften, Buchmann Institute for Molecular Life Sciences (BMLS), Goethe Universität Frankfurt Biozentrum, Frankfurt am Main, Germany

[4] Department of Microbiology, Faculty of Medicine, Adnan Menderes University, Aydin, Turkey

Published in:

Frontiers in Microbiology 10 (2019) 2672

doi: 10.3389/fmicb.2019.02672

Online access: https://www.frontiersin.org/articles/10.3389/fmicb.2019.02672/full

Copyright © 2019 Donmez Ozkan, Cimen, Ulug, Wenski, Yigit Ozer, Telli, Aydin, Bode and Hazir. This is an open-access article distributed under the terms of the Creative Commons Attribution License (CC BY). The use, distribution or reproduction in other forums is permitted, provided the original author(s) and the copyright owner(s) are credited and that the original publication in this journal is cited, in accordance with accepted academic practice. No use, distribution or reproduction is permitted which does not comply with these terms.

Attachment 1

Declaration of author contributions to the publication / manuscript (title):

Nematode-Associated Bacteria: Production of Antimicrobial Agent as a Presumptive Nominee for Curing Endodontic Infections Caused by *Enterococcus faecalis*

Status: published

Name of journal: Frontiers in Microbiology, doi: 10.3389/fmicb.2019.02672

Contributing authors:

Donmez Ozkan H (HDO), Cimen H (HC), Ulug D (DU), Wenski S (SW), Yigit Ozer S (SYO), Telli M (MT), Aydin N (NA), Bode HB (HBB), Hazir S (SH)

What are the contributions of the doctoral candidate and his co-authors?

(1) Concept and design

HDO (45%), SH (45%), HC (10%)

(2) Conducting tests and experiments

Generation of *X. cabanillasii* mutants: SW (20%); Bioactivity assays: HC (30%), HDO (20%), DU (15%), MT (5%), NA (5%), SYO (5%)

(3) Compilation of data sets and figures

MALDI-MS analysis: SW (30%); Bioactivity assays: HC (30%), HDO (20%), DU (20%)

(4) Analysis and interpretation of data

Confirmation of fabclavine derivatives: SW (30%); Bioactivity assays: HC (30%), HDO (20%), DU (20%)

(5) Drafting of manuscript

SH (70%), HBB (30%)

I hereby certify that the information above is correct.

Date and place	Signature doctoral candidate
Date and place	Signature supervisor
Date and place	If required, signature of corresponding author

frontiers in Microbiology

ORIGINAL RESEARCH
published: 22 November 2019
doi: 10.3389/fmicb.2019.02672

Nematode-Associated Bacteria: Production of Antimicrobial Agent as a Presumptive Nominee for Curing Endodontic Infections Caused by *Enterococcus faecalis*

Hicran Donmez Ozkan[1], Harun Cimen[2], Derya Ulug[2], Sebastian Wenski[3], Senem Yigit Ozer[1], Murat Telli[4], Neriman Aydin[4], Helge B. Bode[3] and Selcuk Hazir[2]**

[1] Department of Endodontics, Faculty of Dentistry, Adnan Menderes University, Aydin, Turkey, [2] Department of Biology, Faculty of Arts and Sciences, Adnan Menderes University, Aydin, Turkey, [3] Molekulare Biotechnologie, Fachbereich Biowissenschaften, Buchmann Institute for Molecular Life Sciences (BMLS), Goethe Universität Frankfurt Biozentrum, Frankfurt am Main, Germany, [4] Department of Microbiology, Faculty of Medicine, Adnan Menderes University, Aydin, Turkey

OPEN ACCESS

Edited by:
Fabian Cieplik,
University Medical Center
Regensburg, Germany

Reviewed by:
Daniel Manoil,
Karolinska University Hospital,
Sweden
Prasanna Neelakantan,
The University of Hong Kong,
Hong Kong

***Correspondence:**
Hicran Donmez Ozkan
hicran.donmez@adu.edu.tr
Selcuk Hazir
selcuk.hazir@gmail.com

Specialty section:
This article was submitted to Antimicrobials, Resistance and Chemotherapy, a section of the journal Frontiers in Microbiology

Received: 28 June 2019
Accepted: 04 November 2019
Published: 22 November 2019

Citation:
Donmez Ozkan H, Cimen H, Ulug D, Wenski S, Yigit Ozer S, Telli M, Aydin N, Bode HB and Hazir S (2019) Nematode-Associated Bacteria: Production of Antimicrobial Agent as a Presumptive Nominee for Curing Endodontic Infections Caused by Enterococcus faecalis. Front. Microbiol. 10:2672. doi: 10.3389/fmicb.2019.02672

Xenorhabdus and/or *Photorhabdus* bacteria produce antibacterial metabolites to protect insect cadavers against food competitors allowing them to survive in nature with their nematode host. The effects of culture supernatant produced by *Xenorhabdus* and *Photorhabdus* spp. were investigated against the multidrug-resistant dental root canal pathogen *Enterococcus faecalis*. The efficacy of seven different cell-free supernatants of *Xenorhabdus* and *Photorhabdus* species against *E. faecalis* was assessed with overlay bioassay and serial dilution techniques. Additionally, time-dependent inactivation of supernatant was evaluated. Among the seven different bacterial species, *X. cabanillasii* produced the strongest antibacterial effects. Loss of bioactivity in a phosphopantetheinyl transferase-deficient mutant of *X. cabanillasii* indicated that this activity is likely based on non-ribosomal peptide synthetases (NRPSs) or polyketide synthases (PKSs). Subsequent *in silico* analysis revealed multiple possible biosynthetic gene clusters (BGCs) in the genome of *X. cabanillasii* including a BGC homologous to that of zeamine/fabclavine biosynthesis. Fabclavines are NRPS-derived hexapeptides, which are connected by PKS-derived malonate units to an unusual polyamine, also PKS-derived. Due to the known broad-spectrum bioactivity of the fabclavines, we generated a promoter exchange mutant in front of the fabclavine-like BGC. This leads to over-expression by induction or a knock-out by non-induction which resulted in a bioactive and non-bioactive mutant. Furthermore, MS and MS^2 experiments confirmed that *X. cabanillasii* produces the same derivatives as *X. budapestensis*. The medicament potential of 10-fold concentrated supernatant of induced fcl promoter exchanged *X. cabanillasii* was also assessed in dental root canals. Calcium hydroxide paste, or chlorhexidine gel, or fabclavine-rich supernatant was applied to root canals. Fabclavine-rich supernatant exhibited the highest inactivation efficacy of $\geq$3 $\log_{10}$ steps CFU reduction, followed by calcium hydroxide paste ($\leq$2 $\log_{10}$ step). The mean percentage of *E. faecalis*-free dental root canals after treatment was

63.6, 45.5, and 18.2% for fabclavine, calcium hydroxide, and chlorhexidine, respectively. Fabclavine in liquid form or preferably as a paste or gel formulation is a promising alternative intracanal medicament.

Keywords: endodontic infections, *Enterococcus faecalis*, fabclavine, *Photorhabdus*, *Xenorhabdus*

INTRODUCTION

Enterococcus faecalis is a species of the Enterococci that is associated with humans as part of the microbiota of the gastrointestinal system. However, the bacterium sometimes is an opportunistic human pathogen (Karchmer, 2000). *E. faecalis* is the most common etiological agent of human enterococcal infections (Kayaoglu and Orstavik, 2004). Moreover, this bacterium can exist as a nosocomial infection and result in mortalities surpassing 50% in some immunocompromised and cancer patients (Schmidt-Hieber et al., 2007; Arias and Murray, 2012).

In dentistry, *E. faecalis* is linked to persistent periradicular lesions with major endodontic infections and persistent infections of the root canal (Sanchez-Sanhueza et al., 2015). Eradication of *E. faecalis* is challenging because it creates a biofilm, utilizes diverse compounds as energy sources, and survives extreme environmental conditions (Gilmore et al., 2002; Tendolkar et al., 2003). These characteristics contribute to bacterial tenacity and virulence in tooth infections (Stojicic et al., 2010).

The number of bacterial cells can be reduced by shaping of the root canal with mechanical instrumentation and irrigation with antimicrobial agents. However, these techniques are inept in adequately eliminating *E. faecalis* due to the complex anatomy of the root canal system (Stuart et al., 2006; Vianna and Gomes, 2009; Asnaashari et al., 2017). Accordingly, intracanal treatment is recommended for lowering the number of bacteria before filling the root canal (Bystrom et al., 1985). Calcium hydroxide ($Ca(OH)_2$) pastes and chlorhexidine (CHX) gels are commonly used as intracanal medicaments (Siqueira and de Uzeda, 1997; Tervit et al., 2009).

Even though CHX and $Ca(OH)_2$ are regular intracanal medicaments in endodontic therapy, previous studies have revealed that *E. faecalis* can still persist (Orstavik and Haapasalo, 1990; Heling et al., 1992; Evans et al., 2002; Delgado et al., 2010). Moreover, an effective antibiotic to decolonize patients with antibiotic-resistant *E. faecalis* is unknown or unavailable. The health care concern posed by *E. faecalis* stresses the pressing urgency for new approaches for decolonization and therapeutic treatment. The discovery of novel antibiotics or antibacterial agents can serve as alternatives for *E. faecalis* suppression. The most important antibacterial sources in nature are viruses (Suttle, 1994; Fuhrman, 1999), fungi (Brian and Hemming, 1947; Zhang et al., 2012), bacteria (Kirkup, 2006; Gillor and Ghazaryan, 2007; Newman and Cragg, 2016), and plants (Cowan, 1999). Various fungi and bacteria produce antimicrobial compounds as secondary metabolites to compete with other organisms. Among bacteria, research over the past three decades has shown that the genera *Photorhabdus* and *Xenorhabdus* produce antimicrobial compounds that may have potential use against an array of bacterial pathogens (Boemare and Akhurst, 2006; Shi and Bode, 2018).

Xenorhabdus and *Photorhabdus* species are insect pathogenic bacteria that are symbiotically associated with nematodes in the families Steinernematidae and Heterorhabditidae, respectively (Hazir et al., 2003). These entomopathogenic nematodes (EPNs) with their bacteria are obligate, lethal parasites of soil insects. The symbiotic organisms have many positive attributes such as safety to humans and nontarget organisms and ease of mass production (Fodor et al., 2017).

The nematode-killed insect is protected from secondary invasion by contaminating organisms that allow the nematodes to develop in the cadaver. The protection is provided by *Photorhabdus* and *Xenorhabdus* by the production of a variety of small antibiotic molecules. For example, *Xenorhabdus* spp. synthesize a variety of secondary metabolites including antimicrobials made of linear and cyclic peptides (Bode, 2009; Shi and Bode, 2018). To date, the compounds examined from *X. bovienii*, *X. nematophila*, and *X. cabanillasii*, are indole, xenorhabdin, xenocoumacin, PAX peptides, and cabanillasin with antibacterial, antifungal, or both activities (Gu et al., 2009; Hazir et al., 2016). It was stated that *Photorhabdus* species also generate antimicrobial compounds including isopropylstilbenes and the β-lactam carbapenem (Webster et al., 2002). Some of these compounds especially from *P. temperata* and *P. luminescens* subsp. *luminescens* are known to have antibiotic properties. The trans-stilbenes and anthraquinone pigments were detected as antibacterial (Boemare and Akhurst, 2006). These findings of antimicrobial compounds have attracted considerable interest for pharmaceutical and agronomic purposes (Webster et al., 2002; Hazir et al., 2016). It is known that different species/strains of *Xenorhabdus* and *Photorhabdus* produce various antimicrobial compounds. Hence, we hypothesized that some species of *Xenorhabdus* and/or *Photorhabdus* spp. produce active compound(s) in their secondary metabolites that will inhibit the growth of antibiotic-resistant *E. faecalis*. Accordingly, we tested this hypothesis with seven different supernatants of *Xenorhabdus* and *Photorhabdus* species against antibiotic-resistant *E. faecalis* with *in vitro* antibacterial tests. Subsequently, the medicament potential of the antibacterial compound obtained from the most effective species was compared with CHX and $Ca(OH)_2$ against *E. faecalis* in root canals.

MATERIALS AND METHODS

Source of Bacteria and Supernatant Preparation

Antibiotic activity of seven bacterial isolates of *Xenorhabdus* and *Photorhabdus* was tested against *E. faecalis*. The nematode species and strains from which each tested bacterial species

or subspecies was isolated is presented in **Supplementary Table S1**. Henceforth, we will refer to all isolates as bacterial species even though we recognize that *P. luminescens* includes two subspecies (*luminescens* and *laumondii*).

Bacterial isolates were recovered from nematode-infected *Galleria mellonella* (Lepidoptera: Pyralidae) larva (Kaya and Stock, 1997). *Xenorhabdus* and *Photorhabdus* bacteria have phase-changing capabilities when cultured *in vitro*. Phase-I is associated with nematodes and produces toxins, enzymes, antibiotics, etc. that provide better support for nematode growth in insect cadavers, whereas phase-II occurs spontaneously under unfavorable conditions or long incubation periods (Leclerc and Boemare, 1991; Boemare, 2002). Thus, we used only phase-I of each of the bacterial isolates as observed by their distinctive colony and cell morphology on NBTA (nutrient agar 31 g/L, bromothymol blue 25 mg/L, and 2,3,5-triphenyl tetrazolium chloride 40 mg/L) plates and by a catalase test. After isolating the phase-I bacterium, each isolate was stored at −80°C until further use (Boemare and Akhurst, 2006).

To conduct the experiments, each bacterial isolate was streaked onto a NBTA plate and after 24 h, a loopful of bacterial cells was transferred to 100 ml of Tryptic Soy Broth (TSB) (Difco, Detroit, MI) in an Erlenmeyer flask. Because the optimum time for antibiotic production is 120–144 h (Furgani et al., 2008), cultures were incubated at 28°C and 150 rpm for 144 h (Hazir et al., 2016). Later on, supernatants were obtained from the centrifuged bacterial culture at 4°C and 20,000 *g* for 15 min. To eliminate all bacterial cells, the supernatants were filtered through a 0.22 µm Millipore filter (Thermo scientific, NY). Each cell-free supernatant was stored at 4°C in sterile falcon tubes (Corning, NY) and used within 2 weeks.

Pathogen Cultures

Multidrug-resistant *Enterococcus faecalis* V583 (ATCC 700802) was used for the experiments. The strain was grown overnight in Trypticase Soy broth (TSB) (Merck) (Awori et al., 2016) and the bacterial stock suspension was kept at −80°C (Boemare and Akhurst, 2006).

Antibacterial Activity of Different *Photorhabdus* and *Xenorhabdus* Spp. Against *Enterococcus faecalis*

Overlay Bioassay

Cell-to-cell competition of test bacteria with the antibiotic producer colony on a solid media (slightly modified method of Furgani et al., 2008) was used for the antibacterial test. The overlay bioassay permitted us to assess the efficacy of different species of antibiotic producing *Xenorhabdus* and *Photorhabdus* spp. against *E. faecalis* by measuring the inactivation zones. *Xenorhabdus* and *Photorhabdus* cultures were prepared by inoculating a loopful of bacteria from NBTA plate into 50 ml of TSB and incubating them at 150 rpm and 28°C in an incubator overnight. A 5-µl bacterial sample from the overnight culture was transferred onto the center of Mueller Hinton Agar (MHA) (Merck) plates. The bacteria were incubated for 5 days at 28°C (Furgani et al., 2008). For preparation of overnight *E. faecalis* culture, *E. faecalis* was inoculated in 50 ml of TSB medium and incubated at 37°C and 150 rpm. A volume of 100 µl of the pathogen culture (44×10^8 CFU/ml) was added to 3.5 ml of soft agar (0.6% w/v) at 45–50°C, which was then poured into the test plates where the *Xenorhabdus* or *Photorhabdus* colony had been growing. To prevent bacterial expansion on agar media, the propagated *Xenorhabdus* or *Photorhabdus* colony was left under UV light for 5 min before layering the mixture of *E. faecalis* and soft agar over the plate. After the solidification of soft agar, the petri dishes were incubated for 48 h at 37°C. The zone diameter around the colony of antibiotic-producing cells was measured in two directions perpendicular to each other and the average was taken (Mattigatti et al., 2012). Each bacterial species had 10 replicates and the experiment was conducted three times.

Antibacterial Activity of Cell-Free *Xenorhabdus* or *Photorhabdus* Supernatants

The cell-free supernatants of all species of *Xenorhabdus* and *Photorhabdus* listed in **Supplementary Table S1** were tested against *E. faecalis*. Different proportions (1, 5, 10, 20, 30, 40, 50, and 100%) of supernatants containing bacterial metabolites were tested for inactivation of growth of *E. faecalis*. For each proportion (1, 5, 10, 20, 30, 40, 50, and 100%), filtrated supernatants were incorporated on a *v/v* basis into test tubes with 2 ml of sterile Mueller Hinton Broth (MHB) (Merck) (Gualtieri et al., 2012). According to supernatant proportions, the same amount of MHB was discarded before adding bacterial supernatant (for example, for 5%, 0.1 ml supernatant was incorporated into 1.9 ml of MHB). A volume of 10 µl of a culture of *E. faecalis* (44×10^8 CFU/ml) incubated overnight was pipetted into the test tubes containing MHB and cell-free supernatants. There were positive and negative control groups. Positive control included MHB and *E. faecalis*, whereas the negative control was only cell-free supernatant. The tubes were incubated in the shaker incubator at 150 rpm and 37°C for 48 h. Following the incubation period, bacterial growth was evaluated visually to determine maximum inhibiting dilutions (MIDs; according to Furgani et al., 2008, we used the term "dilution" not concentration]. The MID is the maximum supernatant dilution that yields no visible growth. In each series of tubes, the last tube with clear supernatant was considered to be without any growth and was assumed to give the MID value. Turbidity in the tubes indicated growth of *E. faecalis*. Visual evaluations were made independently by three examiners and a consensus opinion was agreed upon (Furgani et al., 2008; Aarati et al., 2011). An aliquot of 100 µl was taken from each tube where no bacterial growth had been observed visually and was transferred to the blood-agar medium (5% sheep blood) to determine maximum bactericidal dilution (MBD). After streaking the subsamples on the blood-agar medium, the petri dishes were incubated at 37°C for 48 h to verify total inactivation. The smaller the MID or MBD values, the stronger the antibiotic production obtained (Furgani et al., 2008). National Committee

for Clinical Laboratory Standart Institute (CLSI) recommended procedures were used for MID and MBD determination.

Three replicates were used for each supernatant proportion and the experiment was conducted three times.

Time-Dependent Inactivation of Cell-Free Supernatant

Depending on the results of the experiment on overlay bioassay and the MID and MBD values, bacterial supernatant that produced the maximum antibacterial activity (*X. cabanillasii* supernatant) was used to determine the time to inactivation of *E. faecalis*. This was done by using 25 ml of sterile TSB mixed with 25 ml of cell-free supernatant of *X. cabanillasii* in a 100-ml flask. A 0.5-ml aliquot of *E. faecalis* from an overnight culture (44×10^8 CFU/ml) was transferred to the 50% supernatant, and afterward the flask was incubated at 37°C at 150 rpm. On a 2-h basis from 0 to 16 h, a 10-µl subsample was pipetted from the flask and spread on a blood agar. Plates were incubated for 48 h at 37°C. Three replicates were used and the experiment was conducted three times.

Identification of Bioactive Antibacterial Compound

To determine the bioactive compound, promoter exchanged mutants of *X. cabanillasii* were generated and matrix assisted laser desorption/ionization-mass spectrometry (MALDI-MS) and MALDI-MS^2 experiments were performed.

Generation of Deletion and Promoter Exchange Mutants in *Xenorhabdus cabanillasii*

Due to the phosphopantetheinyl transferase (PPTase)-dependence of NRPS- and PKS-derived secondary metabolites, we deleted the responsible gene in *X. cabanillasii*. This should lead to a loss of production and bioactivity in the mutant if the compound is NRPS- or PKS-derived.

Deletion of the phosphopantetheinyl transferase (Xcab_04003) in *X. cabanillasii* was performed by double homologous recombination. About 1,000 bps were amplified by PCR with the primers SW305_Xcab_LF_fw (5′-CGATCCTCTAGAGTCGACCTGCAGTGTATAGGTCATAGCGCATTTTCC-3′) and SW306_Xcab_LF_rv (5′-TTTCATCTCTTATTTTGTTGTTCTTGGGTATTGTTCG-3′) for the upstream and SW307_Xcab_RF_fw (5′-TACCCAAGAACAACAAAATAAGAGATGAAAACCCCGG-3′) and SW308_Xcab_RF_rv (5′-GAGAGCTCAGATCTACGCGTTTCATATGGGTTTTAGCCCAATCTTATGCC-3′) for the downstream regions. Both were integrated by Hot Fusion assembly into the *Pst*I/*Nde*I digested deletion vector pDS132 and transformed into *E. coli* ST18 (Fu et al., 2014). The plasmid pDS132 containing the *sacB* gene and a kanamycin resistance cassette. *X. cabanillasii* was conjugated with *E. coli* ST18 and insertion mutants were selected on kanamycin-supplemented LB agar plates. The second homologous recombination was then enforced by cultivation on sucrose-supplemented LB agar plates, which is toxic due to the SacB conversion.

Promoter exchange in front of the fcl-homologous gene cluster was performed upstream of the *fclC*-like gene (Xcab_02060) in *X. cabanillasii*. The first 1,000 bps of Xcab_02060 were amplified by the primers SW128_Xcab_fw (5′-TTTGGGCTAACAGGAGGCTAGCATATGACCAAGACGTATTTTTTGCATG-3′) and SW129_Xcab_rv (5′-TCTGCAGAGCTCGAGCATGCACATTTTACCTGCCCTTCCAGACG-3′) and cloned into the PCR-amplified vector pCEP_kan by Hot Fusion assembly (Fu et al., 2014; Bode et al., 2015). After transformation, positive *E. coli* S17 clones were confirmed by restriction, conjugated with *X. cabanillasii*, and insertion mutants selected on kanamycin-supplemented LB agar plates (**Supplementary Table S2**). Successfully generated deletion and promoter exchange mutants were verified by colony PCR and analyzed by MALDI-MS.

Identification of Antibacterial Compound by MALDI-MS and MALDI-MS^2

Cultures for MALDI-MS measurements were prepared with 10 ml of lysogeny broth media supplemented with kanamycin (50 µg/ml) if appropriate, inoculated with 400 µl of a preculture, and incubated at 30°C for 72 h with shaking. Induced promoter exchange mutants were additionally supplemented with 0.2% L-arabinose (Bode et al., 2015). Liquid cultures were spotted on a steel target with a volume of 0.3 µl mixed with 0.25 µl of 1:10 diluted ProteoMass Normal Mass Calibration Mix (Sequazyme™ Peptide Mass Standards Kit) for internal calibration and 0.9 µl of alpha-Cyano-4-hydroxycinnamic acid (CHCA) matrix (3 mg/ml in 75% acetonitrile, 0.1% trifluoroacetic acid). After air-drying, the sample spot was washed with 5% formic acid and mixed again with 0.6 µl of CHCA. Cell MALDI measurements were performed with a MALDI LTQ Orbitrap XL (Thermo Fisher Scientific, Inc., Waltham, MA) instrument with a nitrogen laser at 337 nm in FTMS scan mode with 100 shots per measurement in a mass range of 350–1,500 m/z with high resolution. MALDI-MS^2 experiments were performed in CID-mode using ITMS scan mode with the following parameters: Normalized collision energy, 28; Act. Q, 0.250; and Act. Time (ms), 30.0. Data were analyzed using Qual Browser version 2.0.7 (Thermo Fisher Scientific, Inc., Waltham, MA).

Testing the Antibacterial Activity of *Xenorhabdus cabanillasii* Mutant Strains

Antibacterial activity of 5-day-old cell-free supernatants of wild-type, pptase deletion mutant, induced (with arabinose) and non-induced (without arabinose) *fclC* promoter exchange mutant of *X. cabanillasii* was tested with agar-well diffusion bioassay as described before. Each petri dish included four wells and each well was filled with 70 µl of one of the cell-free *X. cabanillasii* supernatants. After the incubation period for 48 h at 37°C, the inactivation zones (mm) on plates were measured (Mattigatti et al., 2012). Five replicates were used and the experiment was conducted three times.

Medicament Potential of the Antibacterial Compound in Dental Root Canals

One-day-old cell-free supernatant of induced *fclC* mutant strain of *X. cabanillasii* was concentrated 10-fold using an evaporator and tested in dental root canals. Recently extracted human mandibular premolars were collected from patients who signed a patients' consent protocol (2016/1052) approved by Adnan Menderes University, Local Ethical Committee. Soft tissue remnants and calculus were removed from the external root surfaces by using a periodontal scaler. Periapical radiographs were taken from both buccolingual and mesiodistal directions to determine the teeth that have a straight single root canal. Next, a dental operating microscope (Leica M320) was used to select the teeth with no resorption, defect, or cracks. According to these criteria, 44 mandibular premolar teeth with curvature less than 5° and 15–18 mm long were selected (Schneider, 1971; Pladisai et al., 2016). The roots were sectioned using a diamond disk, perpendicular to the long axis into samples 13 mm long from the cementoenamel junction to the apical root end (Pladisai et al., 2016). A single endodontist removed the pulp tissue and checked the canal patency with a #10 stainless steel K-File (Mani Inc. Tochigi, Japan) until it was visible at the apical foramen. Working length was set at 1 mm short of this length. Then root canals were instrumented with Protaper Next rotary system (Dentsply, Ballaigues, Switzerland) up to X3 (0.30 mm tip with 7% taper) by the same endodontist in a crown-down manner, at a rotational speed of 300 rpm and 200 g/cm torque. Root canals were washed with 2 ml of 5% NaOCl using a 27-gauge notched-tip irrigation needle (Ultradent, UT, USA) between each instrument. At the end of the instrumentation, a final flush was applied using a sequence of 5 ml of 17% EDTA and 5 ml of 5% NaOCl to remove the smear layer, followed by 5 ml of 10% sodium thiosulfate and 5 ml of sterile distilled water (Sasanakul et al., 2019). Finally, specimens were dried with paper points. All teeth were sterilized in an autoclave (121°C for 15 min) before using in the experiments (Alves et al., 2013; Zan et al., 2013).

A 10-µl aliquot of *E. faecalis* from an overnight culture adjusted to 5×10^5 CFU/ml (Ardizzoni et al., 2009) was placed in the root canals of 44 teeth using a sterile micropipette. The teeth were placed individually in 2-ml capacity sterile centrifuge tubes containing 1 ml of BHI broth and incubated for 21 days at 37°C. This is to allow bacteria to penetrate the dentinal tubules and biofilm formation (Pladisai et al., 2016). The media were replaced with sterile BHI every other day (Sasanakul et al., 2019).

After the incubation period, the teeth were embedded in the silicone impression material to create a closed-end channel (Tay et al., 2010). Then, to imitate the final irrigation process before medicament applications in clinical conditions, the specimens were irrigated with 3 ml of 17% EDTA, 3 ml of 5% NaOCl, 3 ml of 10% sodium thiosulfate, and 3 ml of sterile distilled water, respectively. The root canals were subsequently dried with paper points and they were randomly divided into four groups (n = 11 specimens per group).

The root canals of the first and second groups were filled with $Ca(OH)_2$ paste (Ultracal XS, Ultradent Products Inc., USA) and 2% CHX gluconate gel (Gluco-Chex, Cerkamed, Poland) by using a Lentulo spiral (Dentsply-Maillefer), respectively. The root canals in the third group were filled with 10-fold concentrated supernatant of *fclC*-induced *X. cabanillasii* with the help of a sterile syringe. The remaining 11 teeth were filled with sterile BHI medium and this served as the control group. Coronal access of the teeth was closed with parafilm. After the treatments, silicon impression material around the specimens was removed and it was placed in 2-ml sterile centrifuge tubes containing BHI medium individually. The tubes were incubated aerobically at 37°C for 7 days. The media were replaced with sterile BHI every other day.

At the end of experimental period, a ProTaper X3 rotary instrument was used for 20 s to remove CHX gel and Ca(OH)2 paste. For the neutralization of Ca(OH)2, 3 ml of 5% citric acid, and for CHX gel, the mixture of 0.3% L-α-Lecithin and 3% Tween 80 were used. Then both medicament groups were irrigated with 3 ml of physiological saline (Pektas et al., 2013). The specimens in supernatant applied and control group were treated with 6 ml of sterile physiological saline.

The remaining bacteria in the root canals and inner dentins were collected by shaving the root canal walls with a No. 4 Peeso reamer (Dentsply-Maillefer). The collected dentin chips were transferred to 0.5 ml of BHI medium in Eppendorf tube and vortexed vigorously. Then, 50-µl sample was streaked on blood-agar plates. The plates were incubated at 37°C for 48 h and the colonies on blood agar were counted and inferred as colony forming units (CFUs).

Statistical Analysis

SPSS 25.0 (IBM Corp., Chicago, IL, USA) package program with a level of significance set at 0.05 was used. Differences in antibacterial effects of the supernatants were compared with one-way ANOVA and the means separated using Tukey's test. The data of time-dependent CFU reduction and medicament potential of the antibacterial compound in dental root canals were shown as medians, including 25 and 75% quartiles. In these results, horizontal dotted, solid, and dashed lines represent reductions of 2, 3, and 5 $\log_{10}$ steps CFU, respectively. Medians on or below these lines exhibit bacterial killing efficacy of 99% (2 $\log_{10}$), 99.9% (3 $\log_{10}$), and 99.999 (5 $\log_{10}$) (Boyce and Pittet, 2002).

RESULTS

Antibacterial Activity of Different *Xenorhabdus* and *Photorhabdus* Spp. Against *Enterococcus faecalis*

Overlay Bioassay

The antibiotic production of *Xenorhabdus* and *Photorhabdus* against *E. faecalis* differed significantly among species (F = 527.73; df = 6, 202; $p < 0.001$) (**Figure 1**). *Xenorhabdus cabanillasii* had the most pronounced inactivation (50.4 mm) and *X. bovienii* and *P. luminescens laumondii* the lowest (**Figure 1**).

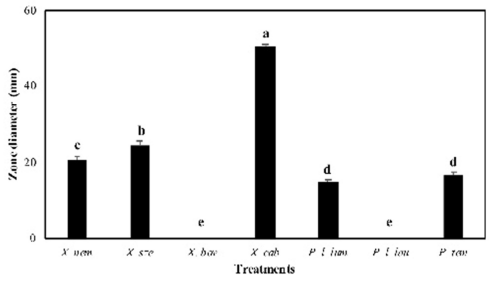

FIGURE 1 | Inactivation zones (mm) resulting from overlay experiments using species of *Xenorhabdus* and *Photorhabdus* against *Enterococcus faecalis*. X. nem, *Xenorhabdus nematophilus*; X. sze, *X. szentirmaii*; X. bov, *X. bovienii*; X. cab, *X. cabanillasii*; P. l. lum, *Photorhabdus luminescens luminescens*; P. l. lau, *P. luminescens laumondii*; P. tem, *P. temperata*. Means indicated by the different lower-case letters on the bars are significantly different ($p < 0.05$).

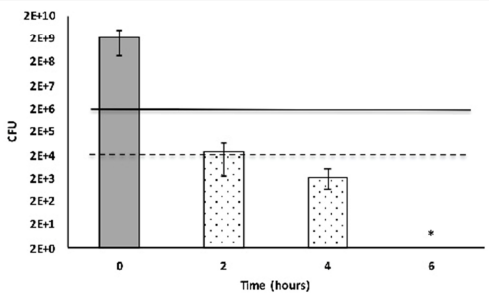

FIGURE 2 | Time-dependent inactivation of *Enterococcus faecalis* cells incubated in 50% *Xenorhabdus cabanillasii* supernatant. Data in this figure are shown as CFU medians with 25 and 75% quartiles. Solid and dashed lines represent reductions of ≥3 and ≥ 5 $\log_{10}$ steps CFU, respectively. * indicates reduction below detection limit.

Antibacterial Activity of Cell-Free *Xenorhabdus* or *Photorhabdus* Supernatants

All *Photorhabdus* and *X. bovienii* supernatants caused inactivation (based on lack of visible growth; MID) when undiluted supernatants were used (**Supplementary Table S3**). *Xenorhabdus nematophila* and *X. szentirmaii* caused inactivation at 20 and 40% proportions of supernatant including cultures, respectively. The greatest inactivation was achieved by *X. cabanillasii,* which showed inactivation even at a 1% concentration of supernatant. After the transfer of samples where no visually bacterial growth was observed on the blood-agar media, *E. faecalis* colonies were observed even at undiluted supernatants (100%) of *X. nematophila*, *X. bovienii,* and all *Photorhabdus* species (**Supplementary Table S3**). *Xenorhabdus szentirmaii* exhibited complete inactivation (MBD) only at 100% supernatant concentration. Similar to the visual inactivation results, we observed that the 5% supernatant of *X. cabanillasii* eliminated all cells of *E. faecalis* (**Supplementary Table S3**). *Enterococcus faecalis* proliferated in all positive controls, whereas no bacterial growth was observed in the negative control groups.

Time-Dependent Inactivation of Cell-Free Supernatant

Bacterial culture media that included 50% *X. cabanillasii* supernatant showed inactivation starting from the time of the first subsample (2 h after inoculation) and the number of colonies of *E. faecalis* gradually decreased over time. The supernatant killed 99.999% of the bacteria after 2 h. Complete inactivation of *E. faecalis* occurred 6 h after the inoculation (**Figure 2**).

Testing the Antibacterial Activity of *Xenorhabdus cabanillasii* Mutant Strains

Wild-type and induced *fclC* promoter exchange mutant of *X. cabanillasii* supernatants exhibited average of 18 (±1.4) and 17.5 (±0.8) mm zone diameters, respectively. But, there was no inactivation circle around the wells of Δ*pptase* and non-induced *fclC* mutants (**Figure 3**).

Identification of Bioactive Antibacterial Compound Produced by *Xenorhabdus cabanillasii*

Since the Δ*pptase* mutant showed no more bioactivity (**Figure 3**), it can be postulated that the responsible compound is generated by a non-ribosomal peptide synthetase (NRPS) or a polyketide synthase (PKS). *In silico* analysis of the *X. cabanillasii* genome revealed multiple potential NRPS- and PKS-BGCs. Due to the known broad-spectrum bioactivity of zeamine/fabclavine, we focused on the fcl-homologous BGC (Fuchs et al., 2014; Masschelein et al., 2015a,b). We performed a promoter exchange in front of the first essential biosynthesis gene *fclC* and observed that the bioactive antibacterial compound is produced by this BGC (**Figure 3**) (Wenski et al., 2019). High-resolution MALDI-MS comparison revealed that the active compounds are the fabclavines Ia, Ib, IIa, and IIb, which were previously described for *X. budapestensis* DSM 16342 (**Figure 4**) as confirmed by the fragmentation pattern of signal 1302.92 (IIb) (**Supplementary Table S4** and **Supplementary Figure S1**).

Medicament Potential of the Antibacterial Compound in Dental Root Canals

Fabclavine-rich supernatant exhibited the highest inactivation efficacy of ≥3 $\log_{10}$ steps CFU reduction, followed by calcium hydroxide paste (≤2 $\log_{10}$ step) (**Figure 5**).

If we considered no tolerance to any bacterial growth in root canals (even one cell), the fabclavine-rich supernatant completely eradicated *E. faecalis* in 63.6% of the treated teeth. The mean percentage of *E. faecalis*-free dental root canals after treatment was 45.5% for $Ca(OH)_2$ and 18.2% for CHX. The median number of colonies were 0, 10, and 20 for fabclavine-rich supernatant, $Ca(OH)_2$, and CHX, respectively. However, number of colonies in the control group was 1,120 CFU (**Figure 5**).

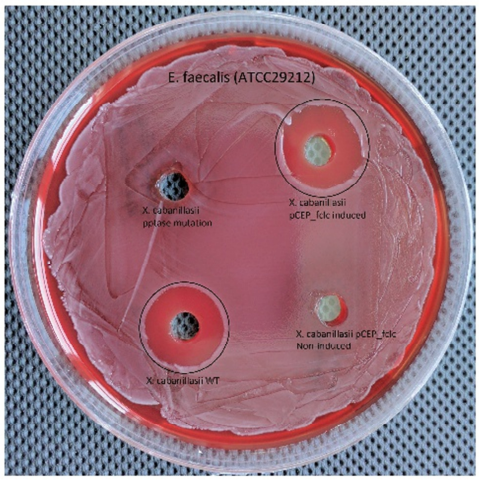

FIGURE 3 | Comparison of wild-type, Δ*pptase*, pCEP-*fclC* induced, and pCEP-*fclC* non-induced mutant of *X. cabanillasii* against *Enterococcus faecalis*.

DISCUSSION

Our data showed that there were significant variations among the seven bacterial species in the production of effective antibacterial compounds against multidrug-resistant *E. faecalis*. Overall, the supernatant of *X. cabanillasii* exhibited the greatest inhibitory and bactericidal effect followed by supernatants of *X. nematophila* and *X. szentirmaii*. On the other hand, supernatants of *X. bovienii* and *P. luminescens laumondii* did not display any antibacterial efficacy against *E. faecalis*. Prior studies have reported variations among *Xenorhabdus* or *Photorhabdus* species (or strains) in the production of antimicrobial metabolites, and the efficacy of metabolites differed depending on the target organisms (Furgani et al., 2008; Fodor et al., 2010; Hazir et al., 2016). Furgani et al. (2008) reported that *X. cabanillasii* and *X. szentirmaii* produced larger diameter inhibitory zones than *X. nematophila* and *X. bovienii* against the primary mastitis pathogens *Staphylococcus aureus*, *Klebsiella pneumoniae*, and *Escherichia coli* when a cell-to-cell competition bioassay was conducted. In another study, *X. szentirmaii* produced a larger inhibitory zone (73.7 mm) than *X. cabanillasii* (60.7 mm) against Gram positive *S. aureus* (Fodor et al., 2010). However, in our overlay bioassay, cell-free supernatant of *X. cabanillasii* resulted in an inactivation zone of 50.4 mm, whereas

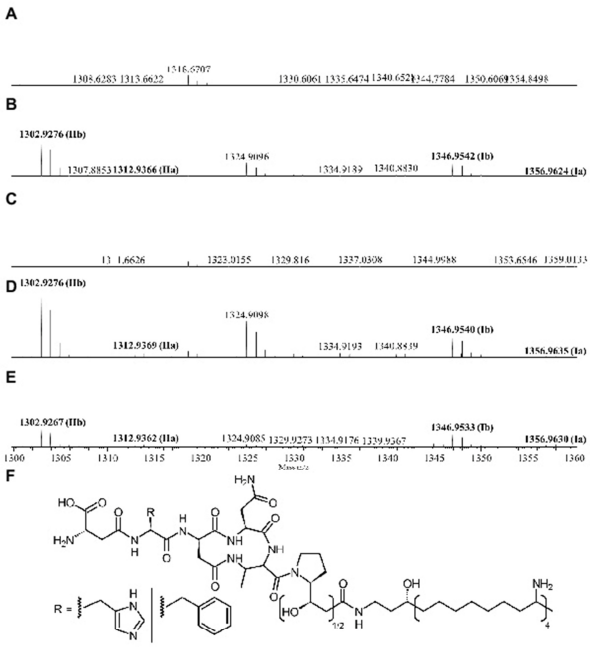

FIGURE 4 | High-resolution MALDI-MS data of liquid cultures of *X. cabanillasii* Δ*ppt* **(A)**, *X. cabanillasii* JM26 WT **(B)**, *X. cabanillasii* P_{BAD}-*fclC* (non-induced) **(C)**, *X. cabanillasii* P_{BAD}-*fclC* (induced) **(D)**, *X. budapestensis* DSM 16342 **(E)**, and the corresponding fabclavine derivatives **(F)**. Highlighted in bold are signals that correspond with identified fabclavines in *X. budapestensis* (Fuchs et al., 2014). Cultures were grown for 72 at 30°C. MALDI-MS measurement was internally calibrated.

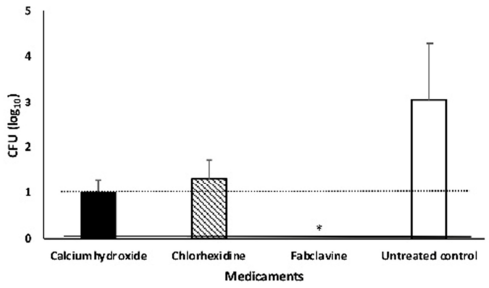

FIGURE 5 | Median number of *Enterococcus faecalis* colony after treating dental root canals with different medicaments. Data were shown as CFU medians. Dotted and solid lines represent reductions of ≥2 and ≥ 3 log_{10} steps CFU, respectively. * indicates reduction below detection limit.

X. szentirmaii exhibited an inactivation zone of 24.4 mm with *E. faecalis*. This discrepancy probably can be attributed to differences in the target organisms, or possibly strain differences in *X. szentirmaii* and *X. cabanillasii* used in the two different studies.

Previous studies demonstrated that *Xenorhabdus* and *Photorhabdus* secrete antimicrobial compounds (Furgani et al., 2008; Fodor et al., 2010; Hazir et al., 2016). Furgani et al. (2008) and Gualtieri et al. (2012) observed antibiotic activity when used not only as the purified antimicrobial compound, but also the cell-free supernatants of *Xenorhabdus* spp. Similarly, we observed antibacterial activity and determined MID and MBD values of *Xenorhabdus* and *Photorhabdus* in cell-free supernatants. The best MID and MBD values against *E. faecalis* were obtained from *X. cabanillasii* supernatant. Concentrations of 1 and 5% of *X. cabanillasii* supernatant were sufficient to inhibit bacterial growth (MID) and completely eliminate *E. faecalis* (MBD), respectively. Gualtieri et al. (2012) determined MBC values as the lowest concentration of antibiotic that resulted in 0.1% survival in the subculture. But we aimed for the complete inactivation of *E. faecalis* to prevent its re-colonization in the dental root canal. Therefore, our MBD values were designated according to full eradication. Our data clearly demonstrated that *X. cabanillasii* produce bactericidal molecule(s) rather than one with bacteriostatic effects, whereas other *Xenorhabdus* and *Photorhabdus* spp. tested in our study showed only a bacteriostatic effect.

To restrict the quantity of potential biosynthesis gene clusters responsible for the bactericidal compound, we compared the WT and Δ*pptase* mutant of *X. cabanillasii*. The loss of bioactivity of the Δ*pptase* mutant suggested the antibacterial compound against *E. faecalis* to be a natural product dependent on a PPTase as it is the case for typical NRPS- or PKS-derived natural products. Different biosynthetic gene clusters are known for *X. cabanillasii*, which could produce potential bioactive compounds like PAX-peptides, rhabdopeptides, or fabclavines (Tobias et al., 2017). The bioactivity of the mutant strain with a promoter exchange in front of the fabclavine-homologous gene cluster indeed confirmed that the bioactive compounds are fabclavines (Fuchs et al., 2014; Fodor et al., 2017). Biochemically, they are derived from a NRPS that produces a hexapeptide, which is elongated with one or two malonate units by a PKS and connected with an unusual polyamine (Fuchs et al., 2014; Wenski et al., 2019). Furthermore, our MALDI-MS and MS^2 experiments confirmed that the fabclavines produced by *X. cabanillasii* are identical to the already described derivatives of *X. budapestensis* (Fuchs et al., 2014). It was reported that fabclavines Ia and Ib had a broad-spectrum bioactivity against different organisms such as *Micrococcus luteus, Escherichia coli, Bacillus subtilis, Saccharomyces cerevisiae, Trypanosoma cruzi, T. brucei,* and *Plasmodium falciparum* (Fuchs et al., 2014). Tobias et al. (2017) stated that except for *Photorhabdus asymbiotica* that might produce a shortened fabclavine derivative, other *Photorhabdus* species do not produce fabclavines, which were more widespread in *Xenorhabdus* strains. These data can explain why none of our tested *Photorhabdus* showed antibacterial efficacy against *E. faecalis*.

The success of endodontic treatment depends mainly on the complete inactivation of the infecting microorganisms from the root canal and prevention of reinfection. However, it is known that conventional root canal irrigants have limited action inside dentinal tubules beyond which viable bacteria are present (Gu et al., 2009). Our control data also showed that the irrigation of root canal with conventional irrigants (EDTA and NaOCl) was not enough to eradicate *E. faecalis* from dentinal tubules. Therefore, the use of intracanal medicaments between appointments is suggested for complete inactivation of bacteria before filling root canals (Bystrom et al., 1985; Pektas et al., 2013). Over the years, a number of synthetic antimicrobial agents have been employed as endodontic irrigants and medicaments against *E. faecalis*. Because of toxic and harmful side effects of common antibacterial agents and the increased antibiotic resistance to antimicrobial agents, a search for alternative agents that are non-toxic, affordable, and effective is needed.

Calcium hydroxide and CHX gel are known as the most effective intracanal medicaments and commonly used in dental practices (Haapasalo and Orstavik, 1987; Evans et al., 2003; Lakhani et al., 2017). However, they are not sufficient for the complete inactivation of *E. faecalis* from root canals in all cases (Siqueira, 2001; Evans et al., 2003; Mozayeni et al., 2014). The results of our study showed that 9 and 5 of 11 teeth treated with CHX and $Ca(OH)_2$ were still contaminated with *E. faecalis*, respectively. Fabclavine-rich supernatant of *X. cabanillasii* exhibited more antimicrobial efficacy than CHX and $Ca(OH)_2$ in root canals with complete inactivation from 7 of 11 teeth. Furthermore, $Ca(OH)_2$ and CHX are formulated as paste and gluconate gel, respectively, to provide longer and better contact with microorganisms in root canals, whereas bacterial supernatant was in liquid form. This could be a possible reason why we did not obtain complete eradication in the root canals of all teeth (even though *X. cabanillasii* supernatant exhibited very strong bactericidal activity). We observed that some of the supernatant filled in root canal run off from the apex. Thus, it might be that the antibacterial compound does not reach *E. faecalis* hidden deep in the dentinal tubules. Accordingly, it will be useful to test the efficacy of formulated fabclavine-rich supernatant in future studies.

Fabclavines show very strong antimicrobial effects against both prokaryotic and eukaryotic pathogens and therefore they might

also display adverse effects to host cells (Fuchs et al., 2014; Fodor et al., 2017; Tobias et al., 2017).

Our data clearly revealed that the fabclavine in the supernatant of *X. cabanillasii* has strong antibacterial activity against *E. faecalis*. Here we used fabclavine-rich supernatant as intracanal medicament for simplicity and it was highly effective against multidrug-resistant *E. faecalis*. Fabclavines might not display equivalent efficiencies against all bacterial species especially in primary endodontic infections which are polymicrobial. In this type of situation, they can be combined with other antibiotics which would lead to synergistic effects on pathogens while simultaneously reducing the potential adverse side effects (Fuchs et al., 2014).

We also compared the efficacy of cell-free supernatant of *X. cabanillasii* against multidrug-resistant V583 (ATCC 700802), antibiotic susceptible (ATCC 29212) and a clinic isolate (obtained from root canal of a patient) of *E. faecalis* using overlay bioassay method and there was no difference among the zone diameters (data were not shown in the manuscript). This indicates that the antibacterial mechanism of fabclavine derivatives has a different mode of action than commonly used traditional antibiotics. Based on the structural similarities to the (pre-)zeamines, we assume a similar mode of action (Masschelein et al., 2015a). Zeamines also show a broad-spectrum bioactivity against a wide variety of organisms, which is probably caused by a membrane disruptive mode of action (Masschelein et al., 2015b).

In conclusion, the data of the induced and non-induced fabclavine promoter exchange mutants clearly show that fabclavine derivatives are bioactive compounds responsible for the bactericidal effect. Although commonly used synthetic intracanal medicaments CHX gel and $Ca(OH)_2$ paste do not eradicate infected root canals in all cases, they are commonly used as medicaments in root canals. Instead, purified and formulated fabclavine derivatives have a great potential to be used as intracanal medicament against dental root canal infections. Further studies with fabclavine-rich derivatives at different concentrations, different formulations and combine applications with other medicaments are needed to test against potential root canal pathogens in *in vitro* and *in vivo* bioassays. Of course one must determine the toxicity of fabclavines against eukaryotic cells at the applied concentration, since they also show some bioactivity against cell lines (Fuchs et al., 2014). However, the large number of fabclavine derivatives found in other *Xenorhabdus* strains might enable the identification of more specific derivatives with less toxicity.

Though *Enterococcus faecalis* is a commensal organism of humans, it is the third most common pathogen isolated from human bloodstream infections (Karchmer, 2000). It can also cause endocarditis; meningitis; and nosocomial, urinary tract, and wound infections (Kau et al., 2005). The efficacy of fabclavine derivatives obtained from *X. cabanillasii* can also be evaluated against these infections in the future.

DATA AVAILABILITY STATEMENT

All datasets generated for this study are included in the article/**Supplementary Material**.

ETHICS STATEMENT

The studies involving human participants were reviewed and approved by Adnan Menderes University, Local Ethical Committee. The patients/participants provided their written informed consent to participate in this study.

AUTHOR CONTRIBUTIONS

SH and HD designed the research. HD, HC, DU, and MT carried out the research, collected the data, and contributed to data analyses. HB and SW generated promoter exchanged mutant strains. NA and SY assisted with the experiments. SH and HB wrote the paper. All authors discussed the results and commented on the manuscript.

FUNDING

This work was financially supported by Aydin Adnan Menderes University (project number DHF-19009) and work in the Bode lab was supported by an ERC advanced grant under grant agreement no. 835108.

ACKNOWLEDGMENTS

We appreciate Dr. Harry K. Kaya from the University of California, Davis-USA, and Dr. David Shapiro-Ilan from USDA-ARS, SEA SE Fruit and Tree Nut Research Unit, Byron-USA, for editing the manuscript.

SUPPLEMENTARY MATERIAL

The Supplementary Material for this article can be found online at: https://www.frontiersin.org/articles/10.3389/fmicb.2019.02672/full#supplementary-material

REFERENCES

Aarati, N., Ranganath, N. N., Soumya, G. B., Kishore, B., and Mithun, K. (2011). Evaluation of antibacterial and anticandidal efficacy of aqueous and alcoholic extract of neem (*Azadirachta indica*) an in vitro study. *Int. J. Res. Ayurveda Pharm.* 2, 230–235.

Alves, F. R., Neves, M. A., Silva, M. G., Roças, I. N., and Siqueira, J. F. Jr. (2013). Antibiofilm and antibacterial activities of farnesol and xylitol as potential endodontic irrigants. *Braz. Dent. J.* 24, 224–229. doi: 10.1590/0103-644020130218 7

Ardizzoni, A., Blasi, E., Rimoldi, C., Giardino, L., Ambu, E., Righi, E., et al. (2009). An *in vitro* and *ex vivo* study on two antibiotic-based endodontic irrigants: a challenge to sodium hypochlorite. *New Microbiol.* 32, 57–66.

Arias, C. A., and Murray, B. E. (2012). The rise of the enterococcus: beyond vancomycin resistance. *Nat. Rev. Microbiol.* 10, 266–278. doi: 10.1038/nrmicro2761

Asnaashari, M., Ashraf, H., Rahmati, A., and Amini, N. (2017). A comparison between effect of photo-dynamic therapy by LED and calcium hydroxide therapy for root canal disinfection against *Enterococcus faecalis*: a randomized controlled trial. *Photodiagn. Photodyn. Ther.* 17, 226–232. doi: 10.1016/j.pdpdt.2016.12.009

Awori, R. M., Nganga, P. N., Nyongesa, L. N., Amugune, N. O., and Masiga, D. (2016). Mursamacin: a novel class of antibiotics from soil-dwelling roundworms of Central Kenya that inhibits methicillin-resistant *Staphylococcus aureus*. *F1000Res* 5, 2431–2439. doi: 10.12688/f1000research.9652.1

Bode, H. B. (2009). Entomopathogenic bacteria as a source of secondary metabolites. *Curr. Opin. Chem. Biol.* 13, 224–230. doi: 10.1016/j.cbpa.2009.02.037

Bode, E., Brachmann, A. O., Kegler, C., Simsek, R., Dauth, C., Zhou, Q., et al. (2015). Simple "on-demand" production of bioactive natural products. *ChemBioChem* 16, 1115–1119. doi: 10.1002/cbic.201500094

Boemare, N. (2002). "Biology, taxonomy and systematics of *Photorhabdus* and *Xenorhabdus*" in *Entomopathogenic nematology*. ed. R. Gaugler (UK: CABI Publishing), 35–56.

Boemare, N. E., and Akhurst, R. J. (2006). "The genera *Photorhabdus* and *Xenorhabdus*" in *The prokaryotes*. eds. M. Dworkin, S. Falkow, E. Rosenberg, K. H. Schleifer, and E. Stackebrandt (New York: Springer Science + Business Media Inc.), 451–494.

Boyce, J. M., and Pittet, D. (2002). Guideline for hand hygiene in health-care settings: recommendations of the healthcare infection control practices advisory committee and the HICPAC/SHEA/APIC/IDSA hand hygiene task force. *Infect. Control Hosp. Epidemiol.* 23, 3–40.

Brian, P. W., and Hemming, H. G. (1947). Production of antifungal and antibacterial substances by fungi; preliminary examination of 166 strains of fungi imperfecti. *J. Gen. Microbiol.* 1, 158–167. doi: 10.1099/00221287-1-2-158

Bystrom, A., Claesson, R., and Sundqvist, G. (1985). The antibacterial effect of camphorated paramonochlcorophenol, camphorated phenol and calcium hydroxide in the treatment of infected root canals. *Endod. Dent. Traumatol.* 1, 170–175. doi: 10.1111/j.1600-9657.1985.tb00652.x

Cowan, M. M. (1999). Plant products as antimicrobial agents. *Clin. Microbiol. Rev.* 12, 564–582. doi: 10.1128/CMR.12.4.564

Delgado, R. J., Gasparoto, T. H., Sipert, C. R., Pinheiro, C. R., Moraes, I. G., Garcia, R. B., et al. (2010). Antimicrobial effects of calcium hydroxide and chlorhexidine on *Enterococcus faecalis*. *J. Endod.* 36, 1389–1393. doi: 10.1016/j.joen.2010.04.013

Evans, M. D., Baumgartner, J. C., Khemaleelakul, S. U., and Xia, T. (2003). Efficacy of calcium hydroxide: chlorhexidine paste as an intracanal medication in bovine dentin. *J. Endod.* 29, 338–339. doi: 10.1097/00004770-200305000-00005

Evans, M., Davies, J. K., Sundqvist, G., and Figdor, D. (2002). Mechanisms involved in the resistance of *Enterococcus faecalis* to calcium hydroxide. *Int. Endod. J.* 35, 221–228. doi: 10.1046/j.1365-2591.2002.00504.x

Fodor, A., Fodor, A. M., Forst, S., Hogan, J. S., Klein, M. G., Lengley, K., et al. (2010). Comparative analysis of antibacterial activities of *Xenorhabdus* species on related and non-related bacteria *in vivo*. *J. Microbiol. Antimicrob.* 2, 36–46.

Fodor, A., Makrai, L., Fodor, L., Venekei, I., Husveth, F., Pal, L., et al. (2017). Anti-coccidiosis potential of autoclaveable antimicrobial peptides from *Xenorhabdus budapestensis* resistant to proteolytic (pepsin, trypsin) digestion based on *in vitro* studies. *Microbiol. Res. J. Int.* 22, 1–17. doi: 10.9734/MRJI/2017/38516

Fu, C., Donovan, W. P., Shikapwashya-Hasser, O., Ye, X., and Cole, R. H. (2014). Hot fusion: an efficient method to clone multiple DNA fragments as well as inverted repeats without ligase. *PLoS One* 9:e115318. doi: 10.1371/journal.pone.0115318

Fuchs, S. W., Grundmann, F., Kurz, M., Kaiser, M., and Bode, H. B. (2014). Fabclavines: bioactive peptide-polyketide-polyamino hybrids from *Xenorhabdus*. *ChemBioChem* 15, 512–516. doi: 10.1002/cbic.201300802

Fuhrman, J. A. (1999). Marine viruses and their biogeochemical and ecological effects. *Nature* 399, 541–548. doi: 10.1038/21119

Furgani, G., Böszörmenyi, E., Fodor, A., Mathe-Fodor, A., Forst, S., Hogan, J. s., et al. (2008). *Xenorhabdus* antibiotics: a comparative analysis and potential utility for controlling mastitis caused by bacteria. *J. Appl. Microbiol.* 104, 745–758. doi: 10.1111/j.1365-2672.2007.03613.x

Gillor, O., and Ghazaryan, L. (2007). Recent advances in bacteriocin application as antimicrobials. *Recent Pat. Antiinfect. Drug Discov.* 2, 115–122. doi: 10.2174/157489107780832613

Gilmore, M. S., Clewell, D. B., Courvalin, P., Dunny, G. M., Murray, B. E., and Rice, L. B. (2002). *The enterococci: Pathogenesis, molecular biology, and antibiotic resistance*. Washington DC: ASM Press, 439.

Gu, L. S., Kim, J. R., Ling, J., Choi, K. K., Pashley, D. H., and Tay, F. R. (2009). Review of contemporary irrigant agitation techniques and devices. *J. Endod.* 35, 791–804. doi: 10.1016/j.joen.2009.03.010

Gualtieri, M., Villain-Guillot, P., Givaudan, A., and Pages, S. (2012). Nemaucin, an antibiotic produced by entomopathogenic *Xenorhabdus cabanillasii*. Google Patents.

Haapasalo, M., and Orstavik, D. (1987). *In vitro* infection and disinfection of dentinal tubules. *J. Dent. Res.* 66, 1375–1379.

Hazir, S., Kaya, H. K., Stock, S. P., and Keskin, N. (2003). Entomopathogenic nematodes (Steinernematidae and Heterorhabditidae) for biocontrol of soil pests. *Turk. J. Biol.* 27, 181–202.

Hazir, S., Shapiro-Ilan, D. I., Bock, C. H., Hazir, C., Leite, L. G., and Hotchkiss, M. W. (2016). Relative potency of culture supernatants of *Xenorhabdus* and *Photorhabdus* spp. on growth of some fungal phytopathogens. *Eur. J. Plant Pathol.* 146, 369–381. doi: 10.1007/s10658-016-0923-9

Heling, M., Steinberg, D., Kenig, S., Gavrilovich, I., Sela, M. N., and Friedman, M. (1992). Efficacy of a sustained-release device containing chlorhexidine and $Ca(OH)_2$ in preventing secondary infection of dentinal tubules. *Int. Endod. J.* 25, 20–24. doi: 10.1111/j.1365-2591.1992.tb00944.x

Karchmer, A. W. (2000). Nosocomial bloodstream infections: organisms, risk factors, and implications. *Clin. Infect. Dis.* 31, 139–143. doi: 10.1086/314078

Kau, A. L., Martin, S. M., Lyon, W., Hayes, E., Caparon, M. G., and Hultgren, S. J. (2005). *Enterococcus faecalis* tropism for the kidneys in the urinary tract of C57BL/6J mice. *Infect. Immun.* 73, 2461–2468. doi: 10.1128/IAI.73.4.2461-2468.2005

Kaya, H. K., and Stock, S. P. (1997). "Techniques in nematology" in *Manual of techniques in insect pathology*. ed. L. A. Lacey (San Diego: Academic Press), 281–324.

Kayaoglu, G., and Orstavik, D. (2004). Virulence factors of *Enterococcus faecalis*: relationship to endodontic disease. *Crit. Rev. Oral Biol. Med.* 15, 308–320. doi: 10.1177/154411130401500506

Kirkup, B. C. Jr. (2006). Bacteriocins as oral and gastrointestinal antibiotics: theoretical considerations, applied research, and practical applications. *Curr. Med. Chem.* 13, 3335–3350. doi: 10.2174/092986706778773068

Lakhani, A. A., Sekhar, K. S., Gupta, P., Tejolatha, B., Gupta, A., Kashyap, S., et al. (2017). Efficacy of triple antibiotic paste, moxifloxacin, calcium hydroxide and 2% chlorhexidine gel in elimination of *E. faecalis*: an in vitro study. *J. Clin. Diagn. Res.* 11, 6–9. doi: 10.7860/JCDR/2017/22394.9132

Leclerc, M. C., and Boemare, N. (1991). Plasmids and phase variations in *Xenorhabdus* spp. *Appl. Environ. Microbiol.* 57, 2597–2601.

Masschelein, J., Clauwers, C., Awodi, U. R., Stalmans, K., Vermaelen, W., Lescrinier, E., et al. (2015a). A combination of polyunsaturated fatty acid, nonribosomal peptide and polyketide biosynthetic machinery is used to assemble the zeamine antibiotics. *Chem. Sci.* 6, 923–929. doi: 10.1039/c4sc01927j

Masschelein, J., Clauwers, C., Stalmans, K., Nuyts, K., De Borggraeve, W., Briers, Y., et al. (2015b). The zeamine antibiotics affect the integrity of bacterial membranes. *Appl. Environ. Microbiol.* 81, 1139–1146. doi: 10.1128/AEM.03146-14

Mattigatti, S., Ratnakar, P., Moturi, S., varma, S., and Rairam, S. (2012). Antimicrobial effect of conventional root canal medicaments vs. propolis against *Enterococcus faecalis*, *Staphylococcus aureus* and *Candida albicans*. *J. Contemp. Dent. Pract.* 13, 305–309. doi: 10.5005/jp-journals-10024-1142

Mozayeni, M. A., Haeri, A., Dianat, O., and Jafari, A. R. (2014). Antimicrobial effects of four intracanal medicaments on *Enterococcus faecalis*: an in vitro study. *Iran. Endod. J.* 9, 195–198.

Newman, D. J., and Cragg, G. M. (2016). Natural products as sources of new drugs from 1981 to 2014. *J. Nat. Prod.* 79, 629–661. doi: 10.1021/acs.jnatprod.5b01055

Orstavik, D., and Haapasalo, M. (1990). Disinfection by endodontic irrigants and dressings of experimentally infected dentinal tubules. *Endod. Dent. Traumatol.* 6, 142–149. doi: 10.1111/j.1600-9657.1990.tb00409.x

Pektas, B. A., Yurdakul, P., Gülmez, D., and Görduysus, Ö. (2013). Antimicrobial effects of root canal medicaments against *Enterococcus faecalis* and *Streptococcus mutans*. *Int. Endod. J.* 46, 413–418. doi: 10.1111/iej.12004

Pladisai, P., Ampornaramveth, R. S., and Chivatxaranukul, P. (2016). Effectiveness of different disinfection protocols on the reduction of bacteria in *Enterococcus faecalis* biofilm in teeth with large root canals. *J. Endod.* 42, 460–464. doi: 10.1016/j.joen.2015.12.016

Sanchez-Sanhueza, G., González-Rocha, G., Dominguez, M., and Bello-Toledo, H. (2015). *Enterococcus* spp. isolated from root canals with persistent chronic apical periodontitis in a Chilean population. *Braz. J. Oral. Sci.* 14, 240–245. doi: 10.1590/1677-3225v14n3a13

Sasanakul, P., Ampornaramveth, R. S., and Chivatxaranukul, P. (2019). Influence of adjuncts to irrigation in the disinfection of large root canals. *J. Endod.* 45, 332–337. doi: 10.1016/j.joen.2018.11.015

Schmidt-Hieber, M., Blau, I. W., Schwartz, S., Uharek, L., Weist, K., Eckmanns, T., et al. (2007). Intensified strategies to control vancomycin-resistant enterococci in immunocompromised patients. *Int. J. Hematol.* 86, 158–162. doi: 10.1532/IJH97.E0632

Schneider, S. W. (1971). A comparison of canal preparations in straight and curved root canals. *Oral Surg. Oral Med. Oral Pathol.* 32, 271–275. doi: 10.1016/0030-4220(71)90230-1

Shi, Y. M., and Bode, H. B. (2018). Chemical language and warfare of bacterial natural products in bacteria–nematode–insect interactions. *Nat. Prod. Rep.* 35, 309–335. doi: 10.1039/C7NP00054E

Siqueira, J. F. Jr. (2001). Aetiology of root canal treatment failure: why well-treated teeth can fail. *Int. Endod. J.* 34, 1–10. doi: 10.1046/j.1365-2591.2001.00396.x

Siqueira, J. F. Jr., and de Uzeda, M. (1997). Intracanal medicaments: evaluation of the antibacterial effects of chlorhexidine, metronidazole, and calcium hydroxide associated with three vehicles. *J. Endod.* 23, 167–169. doi: 10.1016/S0099-2399(97)80268-3

Stojicic, S., Zivkovic, S., Qian, W., Zhang, H., and Haapasalo, M. (2010). Tissuse dissolution by sodium hypochlorite: effect of concentration, temperature, agitation and surfactant. *J. Endod.* 36, 1558–1562. doi: 10.1016/j.joen.2010.06.021

Stuart, C. H., Schwartz, S. A., Beeson, T. J., and Owatz, C. B. (2006). *Enterococcus faecalis*: its role in root canal treatment failure and current concepts in retreatment. *J. Endod.* 32, 93–98. doi: 10.1016/j.joen.2005.10.049

Suttle, C. A. (1994). The significance of viruses to mortality in aquatic microbial communities. *Microb. Ecol.* 28, 237–243. doi: 10.1007/BF00166813

Tay, F. R., Gu, L. S., Schoeffel, G. J., Wimmer, C., Susin, L., Zhang, K., et al. (2010). Effect of vapor lock on root canal debridement by using a side-vented needle for positive-pressure irrigant delivery. *J. Endod.* 36, 745–750. doi: 10.1016/j.joen.2009.11.022

Tendolkar, P. M., Baghdayan, A. S., and Shankar, N. (2003). Pathogenic *Enterococci*: new developments in the 21st century. *Cell. Mol. Life Sci.* 60, 2622–2636. doi: 10.1007/s00018-003-3138-0

Tervit, C., Paquette, L., Torneck, C. D., Basrani, B., and Friedman, S. (2009). Proportion of healed teeth with apical periodontitis medicated with two percent chlorhexidine gluconate liquid: a case-series study. *J. Endod.* 35, 1182–1185. doi: 10.1016/j.joen.2009.05.010

Tobias, N. J., Heinrich, A. K., Eresmann, H., Wright, P. R., Neubacher, N., and Backofen, R. (2017). *Photorhabdus*-nematode symbiosis is dependent on *hfq*-mediated regulation of secondary metabolites. *Environ. Microbiol.* 19, 119–129. doi: 10.1111/1462-2920.13502

Vianna, M. E., and Gomes, B. P. (2009). Efficacy of sodium hypochlorite combined with chlorhexidine against *Enterococcus faecalis* in vitro. *Oral Surg. Oral Med. Oral Pathol. Oral Radiol Endod.* 107, 585–589. doi: 10.1016/j.tripleo.2008.10.023

Webster, J. M., Chen, G., Hu, K., and Li, J. (2002). "Bacterial metabolites" in *Entomopathogenic nematology*. ed. R. Gaugler (London: CABI International), 9–114.

Wenski, S. L., Kolbert, D., Grammbitter, G. L. C., and Bode, H. B. (2019). Fabclavine biosynthesis in *X. szentirmaii*: shortened derivatives and characterization of the thioester reductase FclG and the condensation domain-like protein FclL. *J. Ind. Microbiol. Biotechnol.* 46, 565–572. doi: 10.1007/s10295-018-02124-8

Zan, R., Hubbezoglu, I., Ozdemir, A. K., Tunc, T., Sumer, Z., and Alici, O. (2013). Antibacterial effect of different concentration of boric acid against *Enterococcus faecalis* biofilms in root canal. *Marmara Dent. J.* 2, 76–80.

Zhang, X. Y., Bao, J., Wang, G. H., He, F., Xu, X. Y., and Qi, S. H. (2012). Diversity and antimicrobial activity of culturable fungi isolated from six species of the South China Sea gorgonians. *Microb. Ecol.* 64, 617–627. doi: 10.1007/s00248-012-0050-x

Conflict of Interest: The authors declare that the research was conducted in the absence of any commercial or financial relationships that could be construed as a potential conflict of interest.

Copyright © 2019 Donmez Ozkan, Cimen, Ulug, Wenski, Yigit Ozer, Telli, Aydin, Bode and Hazir. This is an open-access article distributed under the terms of the Creative Commons Attribution License (CC BY). The use, distribution or reproduction in other forums is permitted, provided the original author(s) and the copyright owner(s) are credited and that the original publication in this journal is cited, in accordance with accepted academic practice. No use, distribution or reproduction is permitted which does not comply with these terms.

Supplementary Material

Supplementary Table S1. The bacterial species and subspecies and their nematode host species (and strain where known) used in the assay against *Enterococcus faecalis*.

Mutualistic bacteria	**Entomopathogenic nematode**	**Nematode strain**
Xenorhabdus nematophila	*Steinernema carpocapsae*	Rize
Xenorhabdus szentirmaii	*Steinernema rarum*	17C&E
Xenorhabdus bovienii	*Steinernema feltiae*	09-38
Xenorhabdus cabanillasii	*Steinernema riobrave*	355
Photorhabdus luminescens luminescens	*Heterorhabditis bacteriophora*	09-20
Photorhabdus luminescens laumondii	*Heterorhabditis bacteriophora*	48-02
Photorhabdus temperata	*Heterorhabditis megidis*	UCDavis

Supplementary Table S2. Used strains and plasmids.

Strain/ plasmid	**Description**	**Origin**
***X. cabanillasii* JM26**	Wild type strain	[3]
***X. budapestensis* DSM 16342**	Wild type strain	[4]
X. cabanillasii* Δ*ppt	Deletion of phosphopantetheinyl transferase (Xcab_04003)	This work
X. cabanillasii* PBad-*fclC	Promotorexchange in front of fabclavine-homologeous cluster	This work
***E. coli* S17-1λpir**	Conjugation strain	[5]
***E. coli* ST18**	Conjugation strain	[6]
pDS132	Deletion vector	[7]
pCEP_km	Promotorexchange vector	[2]
pSW_Δ*ppt*	pDS132 with up- and downstream regions of Xcab_04003	This work
pSW_P_{Bad}-*fclC*	pCEP_km with about first 1000 bp of Xcab_02060	This work

Supplementary Table S3. Antibiotic activity (maximum inhibiting dilution; MID and maximum bactericidal dilution; MBD) of 6-day-old cell-free cultures of *Xenorhabdus* and *Photorhabdus* spp. against *Enterococcus faecalis*.

Bacterial Supernatant	Maximum inhibiting dilution (MID) of bacterial supernatant (%)	Maximum bactericidal dilution (MBD) of bacterial supernatant (%)
Xenorhabdus nematophila	20	-
Xenorhabdus szentirmaii	40	100
Xenorhabdus bovienii	100	-
Xenorhabdus cabanillasii	1	5
Photorhabdus luminescens luminescens	100	-
Photorhabdus luminescens laumondii	100	-
Photorhabdus temperata	100	-

(-) indicating no complete inhibition of *E. faecalis* at any supernatant doses.

Supplementary Table S4. High resolution MALDI-MS masses for the fabclavine derivatives detected in liquid cell cultures of *X. budapestensis* DSM 16342 (Figure 4, **E**) and *X. cabanillasii* P_{Bad}-*fclC* (ind.) (Figure 4, **D**). Cultures were grown for 72 h at 30°C. MALDI-MS measurement was internally calibrated.

		X. budapestensis		*X. cabanillasii* P_{Bad}-*fclC* (ind.)	
Fabclavine	calc m/z	det m/z	error [Δppm]	det m/z	error [Δppm]
Ia	1356.9588	1356.9630	+2.773	1356.9635	+3.141
Ib	1346.9493	1346.9533	+2.610	1346.9540	+3.166
IIa	1312.9324	1312.9362	+2.435	1312.9369	+2.923
IIb	1302.9230	1302.9267	+2.425	1302.9276	+3.116

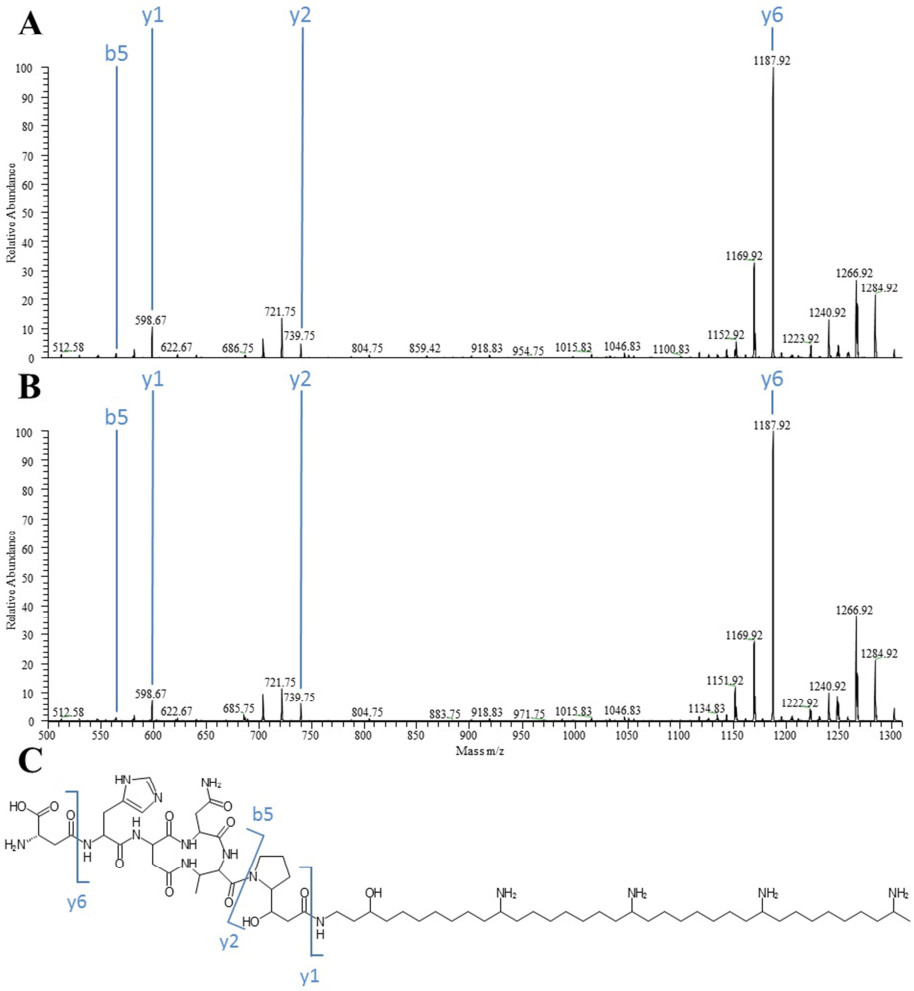

Supplementary Figure S1. MALDI-MS^2-spectras of signal 1302,92 (IIb) in liquid cell cultures of *X. cabanillasii* P_{Bad}-*fclC* (ind.) (**A**), *X. budapestensis* DSM 16342 (**B**) and structure of fabclavine IIb with marked fragment-ions (**C**) [1]. Marked in blue are signals which corresponds with identified fabclavine fragment-ions in *X. budapestensis* [1]. Cultures were grown for 72 h at 30°C.

References of supporting information:

[1] Fuchs, S. W., Grundmann, F., Kurz, M., Kaiser, M., Bode, H. B. (2014). Fabclavines: bioactive peptide-polyketide-polyamino hybrids from *Xenorhabdus*. *Chembiochem*. 15(4), 512-516.

[2] Bode, E., Brachmann, A. O., Kegler, C., Simsek, R., Dauth, C., Zhou, Q., et al. (2015) Simple "on-demand" production of bioactive natural products. *Chembiochem*. 16(7), 1115-1119.

[3] Tailliez, P., Pagès, S., Ginibre, N., Boemare, N. (2006). New insight into diversity in the genus *Xenorhabdus*, including the description of ten novel species. *Int. J. Syst. Evol. Microbiol*. 56, 2805-2818.

[4] Lengyel, K., Lang, E., Fodor, A., Szállás, E., Schumann, P., Stackebrandt, E. (2005). Description of four novel species of *Xenorhabdus*, family Enterobacteriaceae: *Xenorhabdus budapestensis* sp. nov., *Xenorhabdus ehlersii* sp. nov., *Xenorhabdus innexi* sp. nov., and *Xenorhabdus szentirmaii* sp. nov. *Syst. Appl. Microbiol*. 28(2), 115-122.

[5] Simon, R., Priefer, U., Pühler, A. (1983). A Broad Host Range Mobilization System for *In Vivo* Genetic Engineering: Transposon Mutagenesis in Gram Negative Bacteria. Bio/Technology volume 1, pages 784–791.

[6] Thoma, S., and Schobert, M. (2009). An improved Escherichia coli donor strain for diparental mating. *FEMS Microbiol. Lett*. 294(2), 127-132.

[7] Philippe, N., Alcaraz, J. P., Coursange, E., Geiselmann, J., Schneider, D. (2004). Improvement of pCVD442, a suicide plasmid for gene allele exchange in bacteria. *Plasmid*. 51(3), 246-255.

6.4 Structure and biosynthesis of deoxy-polyamine in *X. bovienii*

Authors:

Sebastian L. Wenski[1], Natalie Berghaus[1], Nadine Keller[1], Helge B. Bode[1,2,3,*]

[1] Molekulare Biotechnologie, Fachbereich Biowissenschaften, Goethe Universität Frankfurt, 60438 Frankfurt, Germany. Telephone number: +49 69 798-29557
E-mail: h.bode@bio.uni-frankfurt.de

[2] Buchmann Institute for Molecular Life Sciences (BMLS), Goethe Universität Frankfurt, 60438 Frankfurt, Germany.

[3] Senckenberg Gesellschaft für Naturforschung, 60325 Frankfurt, Germany

Status:

Submitted manuscript.

Attachment 1

Declaration of author contributions to the publication / manuscript (title):

Structure and biosynthesis of deoxy-polyamine in *X. bovienii*

Status: submitted

Contributing authors:

Sebastian L. Wenski (SLW), Natalie Berghaus (NB), Nadine Keller (NK), Helge B. Bode (HBB)

What are the contributions of the doctoral candidate and his co-authors?

(1) Concept and design

SLW (80%), HBB (20%)

(2) Conducting tests and experiments

Generation of polyamine production plasmids: SLW (50%), NK (15%); Generation of *Xenorhabdus* mutants: NB (30 %), SLW (5%)

(3) Compilation of data sets and figures

Sequence alignments: SLW (10%); Polyamine production experiments: SLW (70%), NK (5%); Bioactivity assays: NB (15%)

(4) Analysis and interpretation of data

Polyamine production experiments: SLW (85%); Bioactivity assays: NB (15%)

(5) Drafting of manuscript

SLW (80%), HBB (20%)

I hereby certify that the information above is correct.

Date and place	Signature doctoral candidate
Date and place	Signature supervisor
Date and place	If required, signature of corresponding author

Structure and biosynthesis of deoxy-polyamine in *X. bovienii*

Sebastian L. Wenski[1], Natalie Berghaus[1], Nadine Keller[1], Helge B. Bode[1,2,3,*]

[1] Molekulare Biotechnologie, Fachbereich Biowissenschaften, Goethe Universität Frankfurt, 60438 Frankfurt, Germany. Telephone number: +49 69 798-29557

E-mail: h.bode@bio.uni-frankfurt.de

[2] Buchmann Institute for Molecular Life Sciences (BMLS), Goethe Universität Frankfurt, 60438 Frankfurt, Germany.

[3] Senckenberg Gesellschaft für Naturforschung, 60325 Frankfurt, Germany

Acknowledgements

This work was funded in part by an ERC Advanced Grant (grant agreement number 835108) and the LOEWE Schwerpunkt MegaSyn funded by the State of Hesse. The authors would like to thank Prof. Dr. Michael Karas for MALDI access.

Keywords

Biological activity; Fabclavine; Natural products; Polyunsaturated fatty acid biosynthesis; PKS engineering.

Abstract

Polyamine moieties have been described as part of the fabclavine and zeamine family of natural products. While the corresponding biosynthetic gene clusters have been found in many different proteobacteria, a unique BGC was identified in the entomopathogenic bacterium *Xenorhabdus bovienii*. Mass spectrometric analysis of a *X. bovienii* mutant strain revealed a new deoxy-polyamine. The corresponding biosynthesis includes two additional reductive steps, initiated by an additional dehydratase (DH) domain, which were not found in any other *Xenorhabdus* strain. Moreover, this DH domain could be successfully integrated into homologous biosynthesis pathways, leading to the formation of other deoxy-polyamines. Additional heterologous production experiments revealed that the DH domain could act *in cis* as well as *in trans*.

Introduction

There has been a constant interest in polyketide synthases (PKS) and natural products derived thereof since the identification of erythromycin, an antibiotic identified in the early 1950's [4, 17]. In general, a minimal set of domains in these multidomain multifunctional giant enzymes includes a β-ketoacylsynthase (KS), an acyl transferase domain (AT) and an acyl carrier protein (ACP) [9]. Following the Claisen ester condensation of the acyl units, the reduction of the β-keto group is optional and requires additional domains like a ketoreductase (KR), a dehydratase (DH) and/or an enoyl reductase (ER) domain [9, 16, 17]. In the biochemically closely related fatty acid biosynthesis (FAS) the β-keto group is completely reduced after each elongation of the acyl chain [9]. A combination of both pathways can be observed for the polyunsaturated fatty acid biosynthesis

(PUFA), which is described for marine proteobacteria as well as terrestrial myxobacteria and thraustochytrids [6, 14, 15, 18]. Natural products resulting from the (*pfa*) biosynthesis gene cluster (BGC) are the long chain PUFAs eicosapentaenoic acid (EPA, 20:5, n-3) or docosahexaenoic acid (DHA, 22:6, n-3). Both show anti-inflammatory properties which might help in human chronic diseases like diabetes or obesity [12]. Furthermore, the colonization of the gastric mucosa in mice with *Helicobacter pylori*, whose infection in humans is associated with several gastric diseases, can be reduced by supplementation of EPA [24].

Homologous *pfa* genes can be found in several microorganisms for which the production of PUFAs or derivatives thereof is mostly unknown [18]. Furthermore, a PUFA-related biosynthesis was observed in *Serratia plymutica* and *Xenorhabdus budapestensis*, both producing the closely related zeamine and fabclavine natural products [5, 13]. Biochemically, both compound classes show a highly complex biosynthesis including non-ribosomal peptide synthases (NRPS) and a type I PKS beside the PUFA-like biosynthesis (Fig. S1) [5, 13, 20]. Resulting products in *Xenorhabdus* strains are full-length as well as shortened fabclavines and polyamines (Fig. 1) [20]. While full-length derivatives show a broad-spectrum bioactivity, the roles of the shortened fabclavines and the polyamine part are not fully understood yet [5, 20].

Fabclavine-producing BGCs (*fcl*) are widespread in *Xenorhabdus* strains and detailed analysis revealed a large chemical diversity of derivatives in each strain [21]. This diversity results from flexible adenylation domains, an iterative type I PKS as well as the PUFA-related biosynthesis part [21]. The type I PKS FclC and FclD as well as the ER domain from the bi-functional enzyme FclE are related to PUFA-biosynthesis, which are

extended by the aminotransferase domain of FclE, the 3-oxoacyl-ACP reductase FclF and the thioester reductase FclG [5, 20]. Strikingly, the resulting product is a long acyl chain, substituted with amine moieties instead of unsaturated double bonds, as they would be expected for a PUFA-like biosynthesis product (Fig. 1). The polyamine is generated in multiple cycles by elongation with malonate units, with the intermediary β-keto moiety being either transaminated to an amine or reduced (Fig. S1) [20]. Depending on the number of cycles the resulting polyamine chain length differs from three to five eight-carbon amine units in different *Xenorhabdus* strains (Fig. 1) [21].

In this work the (fabclavine-like) polyamine biosynthesis in *X. bovienii* was elucidated, leading to the identification of a yet unknown deoxy-polyamine derived from an additional PKS-like DH domain as part of FclC.

Results and Discussion

X. bovienii produces a deoxy-polyamine

Previous analysis of multiple *Xenorhabdus* strains revealed a wide distribution of the *fcl* BGC, resulting in a large structural diversity [21]. However, in *X. bovienii* only genes are encoded responsible for polyamine formation and two transporter genes, while the NRPS and PKS genes usually present in *fcl* BGCs are not found or are truncated (Fig. 2) [21]. Since this suggests that *X. bovienii* is neither able to produce full-length nor shortened fabclavines but a polyamine-like compound, a promoter-exchange mutant was generated to identify corresponding products of this unusual *fcl* BGC [21]. In general, chemical induction leads mostly to an overproduction of the analyzed BGC while without induction a “knock-out” phenotype is observed [1, 2]. Matrix-assisted laser de-

sorption/ionization high resolution mass spectrometry (MALDI-HRMS) revealed two signals in the induced mutant with a m/z of 582.64 (**1**) and 598.63 (**2**) (Fig. S2). Compound **2** was identified as the already described four amine unit polyamine ($C_{36}H_{79}N_5O$, Δppm -3.990) from *X. budapestensis* [5]. Isotope-labelling experiments and MALDI-HRMS confirmed the sum formula $C_{36}H_{79}N_5$ (Δppm -4.332) for compound **1** (Fig. S2-S3), which concludes that **1** is the deoxy-derivate of **2** (Fig. 2).

An additional dehydratase domain in FclC is responsible for the production of deoxy-polyamine

In general, fabclavine-producing strains like *X. szentirmaii* usually harbor only one FabA-like DH domain in FclD (Fig. S4-S5) [21]. However, detailed *in silico* analysis revealed a second one in the C-terminus of FclC from *X. bovienii*, which is PKS-related (Fig. S5) [21]. Two different types of DH domains can also be observed in the PUFA biosynthesis of *Shewanella pneumatophori* (Fig. S5) [6]. Further homologues of the PKS-like DH domain from *X. bovienii* could be identified in multiple strains like the zeamine producing bacteria *Serratia plymuthica* and *Dickeya zeae*, *Photorhabdus temperata*, *Fischerella thermalis* or *Agrobacterium tumefaciens* (Table S3) [8, 13, 22]. However, the occurrence in the genus *Xenorhabdus* seems to be restricted to *X. bovienii* and its subspecies (Table S3 and Fig. S4).

During the fabclavine biosynthesis in *X. szentirmaii* the genes *fclCDEFG* are essential for polyamine formation [20]. Furthermore, deletion of *fclH* leads to over 70% decrease in the polyamine production titer (Fig. S6). Thus, *fclCDEFGH* from *X. bovienii* were cloned in an inducible plasmid for the heterologous production in *Escherichia coli*. Consequently, induced and non-induced production cultures were analyzed by high-

performance liquid chromatography high resolution mass spectrometry (HPLC-HRMS). The production of the compounds **1** and **2** were confirmed in the promoter exchange mutant of *X. bovienii* as well as in *E. coli* (Fig. 3a and b). To analyze the function of the additional PKS-like DH domain, its encoding region was removed from the *E. coli* plasmid (Fig. S7). Subsequent analysis revealed an increased production of **2** while the formation of **1** was abolished (Fig. 3c and Fig. S8). This confirmed that the additional DH domain is involved in the formation of the deoxy-polyamine. Based on these results the postulated biosynthesis is shown in Figure 2: The recently described pathway leading to the formation of **2** is extended by two additional reduction steps [20]. The dehydration of the hydroxy-group is optional and introduced by the PKS-like DH domain of FclC. The resulting enoyl-derivate is suggested to be further reduced by FclE, harboring the only ER domain encoded in the *fcl* BGC (Fig. 2). Referring to the recently published biosynthesis, the resulting intermediate is reductively released and transaminated to form the final deoxy-polyamine (**1**) (Fig. 2) [20].

Recently published studies showed that during the PUFA-biosynthesis in *Aureispira marina* the PKS-like DH domain is required for the dehydration in the early stages of arachidonic acid formation and an inactivation leads to dramatic decrease in the production titer [7]. However, during polyamine biosynthesis the loss of the PKS-like DH domain led to the exclusive production of a hydroxylated polyamine as it can be observed for the deletion mutant or in further fabclavine producing strains (Fig. 1 and 3) [21]. This indicates that this domain is only required in the late stages of the biosynthesis, while all other dehydration steps during chain elongation and saturation can be performed by the FabA-like DH domain of FclD.

Addition of DH domain changes products to deoxy-polyamines

The manipulation of reductive loops (KR, DH and ER domain) is an effective tool to change the product spectra used for PKS engineering [3, 10, 11, 19]. Due to its non-essential role during the chain elongation, the PKS-like DH domain of *X. bovienii* might be used in engineering approaches. Previously published studies showed that FclC is highly conserved among the different fabclavine producing strains except for the occurrence of the DH domain in *X. bovienii* [20, 21]. Detailed alignments revealed that multiple strains including *X. bovienii*, *X. budapestensis* and *X. hominickii* share a common motif C-terminal of the ketoreductase domain (Fig. S4). This so-called “YxAxK”-motif was identified as last conserved motif before the protein identity in FclC drastically decreases. In an engineering approach this motif was used as junction to fuse the PKS-like DH domain from *X. bovienii* covalently to FclC from *X. budapestensis* (Fig. S7), which originally produces polyamine **2** (Fig. 3e and Fig. S9). Subsequent HPLC-analysis showed that the engineered FclC is functional, resulting in the product formation of **1** as well as **2** (Fig. 3f and Fig. S9). Comparable results were observed during the manipulation of polyamine biosynthesis of *X. hominickii*, which naturally produces a five-amine unit polyamine (Fig. 1 and S10-11) [21]. In summary, these results highlight that the DH domain initiates the formation of the deoxy-polyamine, and further showed its compatibility with homologous FclC enzymes from other fabclavine producing strains.

The DH domain can also act in trans

After the successful covalent fusion of the DH domain to homologous FclC enzymes, further experiments analyzed the ability of this domain to act *in trans* as stand-alone domain. Therefore, *E. coli* strains were used encoding *fclCDEFGH* from

X. budapestensis or *fclC*(∆*DH*)*DEFGH* from *X. bovienii*. Both *E. coli* strains produce compound **2** (Fig. 3c and e). Furthermore, the additional DH domain from *X. bovienii* (exact amino acid sequence is shown in Fig. S7) was cloned into a plasmid and co-expressed in both *E. coli* strains. Subsequent HPLC analysis of the mutants revealed that the plasmid-based co-expression of the stand-alone DH domain changed the product formation to **1**, while **2** was not produced anymore or at much lower levels (Fig. 3d and g). For the polyamine biosynthesis of *X. hominickii* a similar shift from the hydroxylated to the deoxy derivate was observed (Fig. S10-11). This confirmed the ability of the DH domain to act *in trans*. A recently published study showed comparable results: PKS- and FabA-like DH domains from the PUFA-biosynthesis of *Thraustochytrium* were expressed as stand-alone enzymes in an *E. coli* mutant and were able to restore the defective phenotype [23].

Deoxy-polyamine can be incorporated into full-length fabclavine

In the fabclavine biosynthesis the polyamine is conjugated with the enzyme-bound NRPS-PKS-intermediate by the condensation-domain like protein FclL, which showed relaxed substrate specificity with respect to polyamine chain length (Fig. S1) [20]. Consequently, the four-amine unit polyamine from *X. budapestensis* as well as the five-amine unit polyamine from *X. hominickii* can be integrated into the biosynthesis of *X. szentirmaii* (Fig. 1 and S12) [20, 21]. Nevertheless, small amines like pentylamine or spermine were not accepted [20]. Hence, we were interested in the role of the hydroxy-group for polyamine recognition by FclL. As the deoxy-polyamine from *X. bovienii* lacks this chemical moiety, the conjugation with the NRPS-PKS-intermediate from *X. szentirmaii* was analyzed. Therefore, the polyamine-deficient mutant *X. szentirmaii*

Δ*fclCDE* was complemented with the polyamine-forming genes *fclCDEFGH* from *X. bovienii*. MALDI-MS analysis of the induced production culture revealed a signal with a m/z of 1290.93 ($C_{64}H_{119}N_{15}O_{12}$), corresponding to a fabclavine hybrid, which consists of a NRPS-PKS-part from *X. szentirmaii* and the deoxy-polyamine from *X. bovienii* (Fig. S12). These results confirmed that the hydroxy-group of the polyamine is not essential for the FclL-catalyzed condensation with the NRPS-PKS-part.

Polyamines are the smallest bioactive fabclavine parts

The elucidation of the fabclavine biosynthesis revealed that *X. szentirmaii* produces full-length and shortened fabclavines as well as the polyamine (Fig. 1) [20]. However, only for the first class or mixtures a bioactivity was confirmed [5, 21]. Therefore, mutants with deletions of *fclK* or *fclI* were generated, leading to a restricted fabclavine biosynthesis with an exclusive production of the polyamine alone or in combination with the shortened derivatives [1, 2, 20]. Subsequent analyses revealed bioactivity of the shortened fabclavines and the polyamine from *X. szentirmaii* against selected microbial strains (Table S4). Finally, we were interested in the polyamines of the strains *X. hominickii*, KJ12.1 or *X. bovienii*, which differ in the number of incorporated amine units or the hydroxy-group (Fig. 1-2) [21]. Here, analyses of corresponding mutants confirmed their bioactivity as well, highlighting the important role of the polyamines in the fabclavine biosynthesis (Table S4).

Conclusion

In this work, the (fabclavine) polyamine biosynthesis in *X. bovienii* was elucidated, revealing a novel deoxy-polyamine (**1**) beside an already described polyamine **2** (Fig. 2). The corresponding *fcl* BGC encodes an additional PKS-like DH domain in FclC, which occurs exclusively in *X. bovienii* within the genus *Xenorhabdus* (Table S3 and Fig. S4). This additional domain initiates a dehydration step at the β-hydroxy group of the full length intermediate, followed by an enoyl reduction, leading to the formation of **1**. Furthermore, this PKS-like DH domain was successfully introduced into the homologous (fabclavine) polyamine biosynthesis of *X. budapestensis* and *X. hominickii*, both possessing naturally only the FabA-like DH domain in FclD. Thereby, deoxy-polyamines were produced independently of the PKS-like DH domain being covalently fused to FclC or co-expressed as stand-alone DH domain.

Following the previously identified large diversity of fabclavine derivatives among the genus *Xenorhabdus*, this additional DH domain seems to be another diversification mechanism during fabclavine biosynthesis [21]. Future work will show, if this DH domain can also be used to manipulate non-fabclavine like PKS biosynthesis pathways.

Tables and Figures:

a

Incorporated amine units [n]	
X. szentirmaii	3
KJ12.1	4
X. hominickii	5
X. budapestensis	3 - 4
X. indica	3 - 5

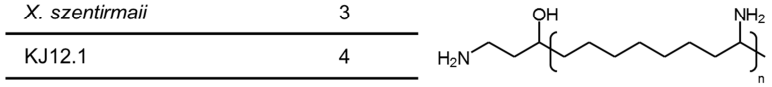

b

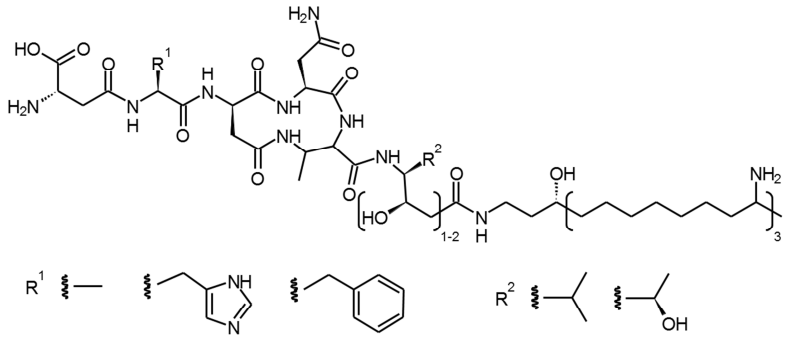

c

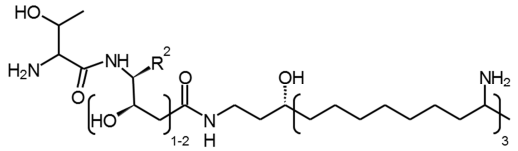

Figure 1. Types of fabclavines. Shown are polyamines from different *Xenorhabdus* strains (a) as well as the full-length (b) and shortened derivatives (c) from *X. szentirmaii* [20, 21].

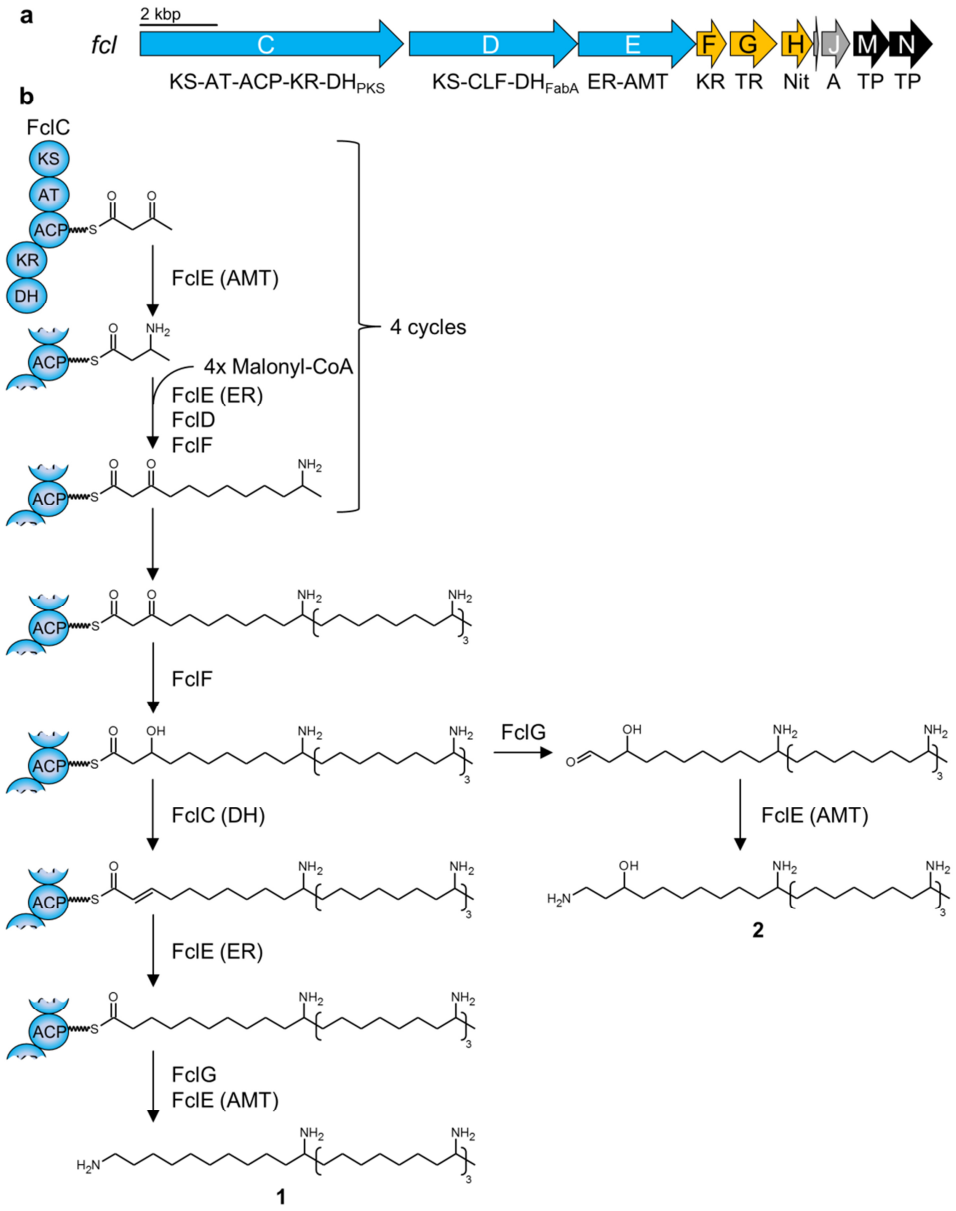

Figure 2. Fabclavine BGC (**a**) and postulated biosynthesis of the polyamines in *X. bovienii* (**b**) [20, 21]. The general pathway is based on the previously described biosynthesis for *X. szentirmaii* for the formation of **2** and is extended by two reductive steps for the formation of **1** [20]. Abbreviations: *KS* ketosynthase, *AT* acyltransferase, *ACP* acyl carrier protein, *KR* ketoreductase, *DH* dehydratase (PKS- or FabA-like), *CLF* chain length factor, *ER* enoyl reductase, *AMT* aminotransferase, *TR* thioester reductase, *Nit* nitrilase, *A* adenylation, *TP* transport.

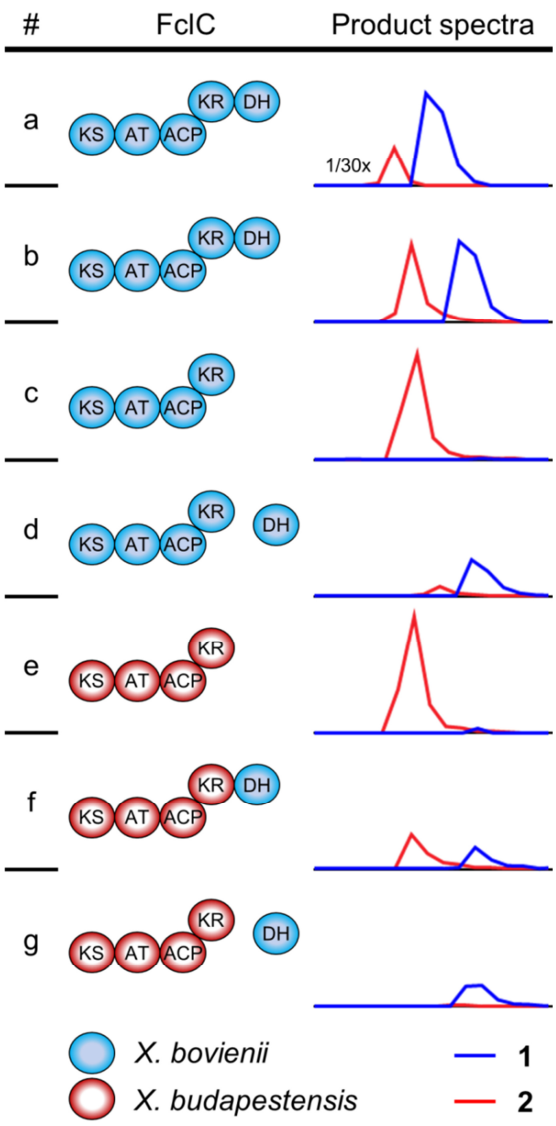

Figure 3. Product spectra of native and engineered FclC in the polyamine biosynthesis of *X. bovienii* and *X. budapestensis*. FclC was expressed together with FclDEFGH either in the native producer *X. bovienii* (a) or heterologously in *E. coli* (b-g) (Fig. 2). Domain organization and origin of FclC is shown as well as the extracted ion chromatograms of the double charged masses for **1** ($[M+2H]^{2+}$ 291.8241) and **2** ($[M+2H]^{2+}$ 299.8215) (Fig. S8-9). Production titer in *X. bovienii* were 30x higher compared to that in *E. coli*. Abbreviations: *KS* ketosynthase, *AT* acyltransferase, *ACP* acyl carrier protein, *KR* ketoreductase, *DH* dehydratase

References

1. Bode E, Brachmann AO, Kegler C et al. (2015) Simple “on-demand” production of bioactive natural products. ChemBioChem 16:1115–1119. doi: 10.1002/cbic.201500094
2. Bode E, Heinrich AK, Hirschmann M et al. (2019) Promoter Activation in Δ *hfq* Mutants as an Efficient Tool for Specialized Metabolite Production Enabling Direct Bioactivity Testing. Angew Chem Int Ed 131:19133–19139. doi: 10.1002/anie.201910563
3. Bozhüyük KA, Micklefield J, Wilkinson B (2019) Engineering enzymatic assembly lines to produce new antibiotics. Curr Opin Microbiol 51:88–96. doi: 10.1016/j.mib.2019.10.007
4. Demain AL (2014) Importance of microbial natural products and the need to revitalize their discovery. J Ind Microbiol Biotechnol 41:185–201. doi: 10.1007/s10295-013-1325-z
5. Fuchs SW, Grundmann F, Kurz M et al. (2014) Fabclavines: bioactive peptide-polyketide-polyamino hybrids from *Xenorhabdus*. ChemBioChem 15:512–516. doi: 10.1002/cbic.201300802
6. Gemperlein K, Rachid S, Garcia RO et al. (2014) Polyunsaturated fatty acid biosynthesis in myxobacteria: different PUFA synthases and their product diversity. Chem Sci 5:1733. doi: 10.1039/c3sc53163e
7. Hayashi S, Satoh Y, Ogasawara Y et al. (2019) Control Mechanism for cis Double-Bond Formation by Polyunsaturated Fatty-Acid Synthases. Angew Chem Int Ed Engl 58:2326–2330. doi: 10.1002/anie.201812623
8. Hellberg JEEU, Matilla MA, Salmond GPC (2015) The broad-spectrum antibiotic, zeamine, kills the nematode worm *Caenorhabditis elegans*. Front Microbiol 6:137. doi: 10.3389/fmicb.2015.00137
9. Hertweck C (2009) The biosynthetic logic of polyketide diversity. Angew Chem Int Ed Engl 48:4688–4716. doi: 10.1002/anie.200806121
10. Keatinge-Clay AT (2012) The structures of type I polyketide synthases. Nat Prod Rep 29:1050–1073. doi: 10.1039/C2NP20019H
11. Klaus M, Grininger M (2018) Engineering strategies for rational polyketide synthase design. Nat Prod Rep 35:1070–1081. doi: 10.1039/c8np00030a
12. Lorente-Cebrián S, Costa AGV, Navas-Carretero S et al. (2013) Role of omega-3 fatty acids in obesity, metabolic syndrome, and cardiovascular diseases: a review of the evidence. J Physiol Biochem 69:633–651. doi: 10.1007/s13105-013-0265-4
13. Masschelein J, Clauwers C, Awodi UR et al. (2015) A combination of polyunsaturated fatty acid, nonribosomal peptide and polyketide biosynthetic machinery is used to assemble the zeamine antibiotics. Chem Sci 6:923–929. doi: 10.1039/c4sc01927j
14. Metz JG, Roessler P, Facciotti D et al. (2001) Production of polyunsaturated fatty acids by polyketide synthases in both prokaryotes and eukaryotes. Science 293:290–293. doi: 10.1126/science.1059593
15. Metz JG, Kuner J, Rosenzweig B et al. (2009) Biochemical characterization of polyunsaturated fatty acid synthesis in *Schizochytrium*: release of the products as free fatty acids. Plant Physiol Biochem 47:472–478. doi: 10.1016/j.plaphy.2009.02.002
16. Nivina A, Yuet KP, Hsu J et al. (2019) Evolution and Diversity of Assembly-Line Polyketide Synthases. Chem Rev 119:12524–12547. doi: 10.1021/acs.chemrev.9b00525
17. Robbins T, Liu Y-C, Cane DE et al. (2016) Structure and mechanism of assembly line polyketide synthases. Curr Opin Struct Biol 41:10–18. doi: 10.1016/j.sbi.2016.05.009

18. Shulse CN, Allen EE (2011) Widespread occurrence of secondary lipid biosynthesis potential in microbial lineages. PLoS ONE 6:e20146. doi: 10.1371/journal.pone.0020146
19. Weissman KJ (2016) Genetic engineering of modular PKSs: from combinatorial biosynthesis to synthetic biology. Nat Prod Rep 33:203–230. doi: 10.1039/c5np00109a
20. Wenski SL, Kolbert D, Grammbitter GLC et al. (2019) Fabclavine biosynthesis in *X. szentirmaii*: shortened derivatives and characterization of the thioester reductase FclG and the condensation domain-like protein FclL. J Ind Microbiol Biotechnol 46:565–572. doi: 10.1007/s10295-018-02124-8
21. Wenski SL, Cimen H, Berghaus N et al. (2020) Fabclavine diversity in *Xenorhabdus* bacteria. Beilstein J Org Chem 16:956–965. doi: 10.3762/bjoc.16.84
22. Wu J, Zhang H-B, Xu J-L et al. (2010) 13C labeling reveals multiple amination reactions in the biosynthesis of a novel polyketide polyamine antibiotic zeamine from *Dickeya zeae*. Chem Commun (Camb) 46:333–335. doi: 10.1039/b916307g
23. Xie X, Meesapyodsuk D, Qiu X (2018) Functional analysis of the dehydratase domains of a PUFA synthase from *Thraustochytrium* in *Escherichia coli*. Appl Microbiol Biotechnol 102:847–856. doi: 10.1007/s00253-017-8635-4
24. Yamamoto T, Matsui H, Yamaji K et al. (2016) Narrow-spectrum inhibitors targeting an alternative menaquinone biosynthetic pathway of *Helicobacter pylori*. J Infect Chemother 22:587–592. doi: 10.1016/j.jiac.2016.05.012

Structure and biosynthesis of deoxy-polyamine in *X. bovienii*

Sebastian L. Wenski[1], Natalie Berghaus[1], Nadine Keller[1], Helge B. Bode[1,2,3,*]

[1] Molekulare Biotechnologie, Fachbereich Biowissenschaften, Goethe Universität Frankfurt, 60438 Frankfurt, Germany. E-mail: h.bode@bio.uni-frankfurt.de

[2] Buchmann Institute for Molecular Life Sciences (BMLS), Goethe Universität Frankfurt, 60438 Frankfurt, Germany.

[3] Senckenberg Gesellschaft für Naturforschung, 60325 Frankfurt, Germany

Material and methods

1. Strain cultivation

The strains were cultivated as described previously [15]: Briefly, *Xenorhabdus* or *E. coli* strains were cultivated on LB-agar plates or in liquid LB media at 30°C or 37°C. In general, LB-media was inoculated with an overnight grown pre-culture, production induced with 0.2 % L-arabinose and cultivated with constant shaking for 1-3 days at 30°C. For the HPLC-HRMS measurements of the polyamine production in *E. coli* and *X. bovienii* XPPM-media was used and after inoculation the cultures were incubated for 3 h at 30°C before 0.2% L-arabinose was added [2]. Kanamycin [50 µg/ml], chloramphenicol [34 µg/ml] or aminolevulinic acid (ALA) [50 µg/ml] were added if required.

2. Bioactivity assay

For the bioactivity assay the corresponding strains were inoculated with an OD_{600} of 0.1 without antibiotics, if appropriate induced with 0.2% L-arabinose and cultivated for 72 h with constant shaking (200 rpm) at 30°C. After centrifugation, the culture supernatant was heated for 10-15 min at 95°C and again centrifuged for 15 min and subsequent used as processed sample. Overnight cultures of the tested microbes were adjusted to a specific OD_{600} (*C. lusitaniae/ E. coli*: 0.5; *S. cerevisiae*: 1) and subsequent coated on agar-plates. Wells with a 12 mm diameter were perforated into the agar and filled with 200 µl processed sample (n=3), followed by cultivation for 2 d at 30°C. The inhibitory

activity was determined as the diameter of the inhibition zone deducting the diameter of the well in mm.

3. Generation of deletion and promoter exchange mutants

The generation of deletion or promoter exchange mutants was performed as described previously and corresponding oligonucleotides can be found in Table S2 [4, 15]: Promoter exchange vectors were generated via amplification of 300-1000 bp of the start of the corresponding gene and cloning it into the either PCR-amplified or digested vector pCEP_kan [1]. Deletion vectors were generated via amplification of approximately 1000 bp of the up- and downstream region of the corresponding gene and cloning it into the either PCR-amplified or digested vector pEB17 [2, 9]. *E. coli* S17 or ST18 were transformed with corresponding vectors and conjugated with the *Xenorhabdus* strain as described previously [9, 11, 12].

4. Heterologous polyamine production and addition/deletion of dehydratase domain

The cloning of the heterologous polyamine producing plasmids of *X. bovienii* and *X. hominickii* was performed as described previously and corresponding oligonucleotides can be found in Table S2 [15]: The polyamine responsible biosynthesis genes *fclCDEFGH* were amplified from the genome of the corresponding strain in 3 parts with overlaps for extension PCR and yeast homologous recombination (ExRec) [10]. For each construct the corresponding fragments and the EcoRI/SgsI digested plasmid pFF1 were transformed into yeast by the protocols by Gietz and Schiestl [3, 7, 8]. After isolation the plasmids were re-transformed into *E. coli* DH10B::*mtaA*. For the exchange of the polyamine in *X. szentirmaii*, its corresponding ∆*fclCDE*-mutant strain was transformed with the heterologous polyamine producing plasmids according to [15].

For the covalently addition or deletion of the dehydratase domain from *X. bovienii* (amino acid sequences are shown in Figure S7) the confirmed pFF1_*fclCDEFGH* vectors were restricted with two different enzymes to linearize the plasmids (*X. bovienii*: SgrAI/SwaI; *X. budapestensis*: BcuI/SmiI; *X. hominickii*: AleI-v2/SwaI). For the PKS-like DH domain deletion in the *X. bovienii* construct (pFF1_*fclC*(∆DH)*DEFGH*) the flanking regions of the DH domain were amplified from *X. bovienii* and cloned into the linearized pFF1_*fclCDEFGH* vector by a Hot fusion assembly and transformed into *E. coli*

DH10B::*mtaA* [5]. For the PKS-like DH domain addition constructs (pFF1_*fclC*(+DH)*DEFGH*) the flanking regions were amplified from the genome of *X. budapestensis* or *X. hominickii* and a third fragment, coding for the DH domain from *X. bovienii*, were cloned in between (direct after the YxAxK-motif). The three fragments were combined by Fusion PCR, cloned into the linearized pFF1_*fclCDEFGH* vector by a Hot fusion assembly and transformed into *E. coli* DH10B::*mtaA* [5]. The corresponding oligonucleotides for the deletion or addition of the DH domain can be found in Table S2.

5. Cloning of dehydratase domain from FclC *X. bovienii* and co-expression

For the co-production experiments we generated an inducible plasmid containing the separated PKS-like DH domain from *X. bovienii*. Therefore, the coding region of the DH domain (Start with an integrated methionine after the YxAxK-motif until the end of XBJ1_2953; amino acid sequences are shown in Figure S7) was amplified and cloned into the PCR-amplified vector plasmid pACYC_ara_tacI by Hot fusion assembly [5, 14]. The plasmid pACYC_ara_tacI_DH *X. bovienii* was transformed into electrocompetent *E. coli* DH10B::*mtaA*, which were already containing the pFF1_*fclCDEFGH* plasmid for the polyamine biosynthesis.

6. Matrix-assisted Laser Desorption/Ionization Mass Spectrometry

MALDI-MS measurements were performed as described previously [15, 16] : Briefly, 0.3 µl of a production culture (in LB-media) were spotted on a MALDI target and mixed with 0.25 µl 1:10 diluted ProteoMass Normal Mass Calibration Mix [ProteoMass™ MALDI Calibration Kit, Sigma-Aldrich] for internal calibration (only for high resolution measurements) and 0.9 µl α-cyano-4-hydroxycinnamic acid (CHCA) matrix [3 mg/ml in 75% acetonitrile, 0.1% trifluoroacetic acid]. The dried sample spot was coated with 5% formic acid in water. After the removal of the 5% formic acid solution the sample spot was mixed again with 0.6 µl CHCA. Cell MALDI measurements were performed with a MALDI LTQ Orbitrap XL [Thermo Fisher Scientific, Inc., Waltham, MA] instrument with a nitrogen laser at 337 nm in FTMS scan mode either with 60.000 or high resolution. Data analysis was performed with Qual Browser version 2.0.7 [Thermo Fisher Scientific].

7. High Resolution High Performance Liquid Chromatography Mass Spectrometry

For HPLC-HRMS measurements the heterologous production cultures (in XPPM-media) were incubated with equal volume of 2% formic acid in MeOH for 1 h at 30°C. The

X. szentirmaii cultures (in LB-media) were incubated with equal volume MeOH. If required production cultures were previously fivefold concentrated via lyophilization due to low signal intensities. Subsequent to centrifugation the supernatant was transferred and utilized as sample. A volume of 30 µl (20 µl for *X. szentirmaii* cultures) was injected into a Dionex Ultimate 3000 HPLC coupled to a Bruker Impact^{TM} II ESI-Q-OTOF instrument set to positive ionization mode. Separation was performed on a C18 [Waters, ACQUITY UPLC BEH, 50mm x 2.1 mm x 1.7 µm] column with acetonitrile [0.1% formic acid] in H_2O [0.1% formic acid] as solvent. The flow rate was 0.4 ml/min with the following gradient: 0-2 min 5 % ACN, 2-14 min 5-95 % ACN, 14-15 95 % ACN, 15-16 min 5 % ACN [3, 13]. The MS settings are described in detail in [13]. However, a mass range of m/z 100-800 was used. Data analysis was performed with the software DataAnalysis 4.3 [Bruker].

Supplementary Tables

Table S1. Strains used in this work. *E. coli*: *Escherichia coli*, *S. cerevisiae*: *Saccharomyces cerevisiae*, *C. lusitaniae*: *Candida lusitaniae*, *X. szentirmaii*: *Xenorhabdus szentirmaii*, *X. hominickii*: *Xenorhabdus hominickii*, *X. bovienii*: *Xenorhabdus bovienii*, DH: dehydratase domain, Fcl: full-length fabclavine; sFcl: shortened fabclavine; PolyA: polyamine.

Strain	Application	Description	Origin
E. coli S17 λ1-pir	Conjugation	-	[11]
E. coli ST18	Conjugation	-	[12]
S. cerevisiae CEN.PK 2-1C	Bioactivity assay and yeast cloning	-	Euroscarf
C. lusitaniae DSM 70102	Bioactivity assay	-	DSMZ
E. coli DH10B	Bioactivity assay	-	Invitrogen
X. szentirmaii DSM 16338 Δ*hfq*	Mutant in in Δ*hfq*-background	Deletion of *hfq*	[2]
X. szentirmaii DSM 16338 Δ*hfq* pCEP_*fcl*	Fcl/sFcl/PolyA-producer in Δ*hfq*-background	Deletion of *hfq* Promoter exchange in front of *fclC*	[2]
X. szentirmaii DSM 16338 Δ*hfq* Δ*fclI* pCEP_*fcl*	sFcl/PolyA-producer in Δ*hfq*-background	Deletion of *hfq* and *fclI* Promoterexchange in front of *fclC*	This work
X. szentirmaii DSM 16338 Δ*hfq* Δ*fclK* pCEP_*fcl*	PolyA-producer in Δ*hfq*-background	Deletion of *hfq* and *fclK* Promoter exchange in front of *fclC*	This work
KJ12.1 Δ*hfq* Δ*fclK* pCEP_*fcl*	PolyA-producer in Δ*hfq*-background	Deletion of *hfq* and *fclK* Promoter exchange in front of *fclC*	This work
X. hominickii DSM 17903 Δ*hfq* Δ*fclK* pCEP_*fcl*	PolyA-producer in Δ*hfq*-background	Deletion of *hfq* and *fclK* Promoter exchange in front of *fclC*	This work
X. bovienii SS-2004 pCEP_*fcl*	PolyA-producer	Promoter exchange in front of *fclC*	This work
E. coli DH10B::*mtaA*	Yeast cloning and heterologous PolyA production		[10]
E. coli DH10B::*mtaA* pFF1_*fclCDEFGH X. bovienii*	Heterologous PolyA production	Heterologous production of *X. bovienii fclCDEFGH*	This work
E. coli DH10B::*mtaA* pFF1_*fclC*(ΔDH)*DEFGH X. bovienii*	Heterologous PolyA production	Heterologous production of *X. bovienii fclCDEFGH* with deleted DH domain in *fclC*	This work
E. coli DH10B::*mtaA* pFF1_*fclC*(ΔDH)*DEFGH X. bovienii* pACYC_ara_tacI_DH *X. bovienii*	Heterologous PolyA production	Heterologous production of *X. bovienii fclCDEFGH* with deleted DH domain in *fclC* and plasmid-based co-expression of the DH domain of *fclC*	This work
E. coli DH10B::*mtaA* pFF1_*fclCDEFGH X. budapestensis*	Heterologous PolyA production	Heterologous production of *X. budapestensis fclCDEFGH*	[15]
E. coli DH10B::*mtaA* pFF1_*fclC*(+DH)*DEFGH X. budapestensis*	Heterologous PolyA production	Heterologous production of *X. budapestensis fclCDEFGH* with additional DH domain of *fclC* from *X. bovienii* integrated in *fclC X. budapestensis*	This work
E. coli DH10B::*mtaA* pFF1_*fclCDEFGH X. budapestensis* pACYC_ara_tacI_DH *X. bovienii*	Heterologous PolyA production	Heterologous production of *X. budapestensis fclCDEFGH* and plasmid-based co-expression of the DH domain of *fclC* from *X. bovienii*	This work
E. coli DH10B::*mtaA* pFF1_*fclCDEFGH X. hominickii*	Heterologous PolyA production	Heterologous production of *X. hominickii fclCDEFGH*	This work
E. coli DH10B::*mtaA* pFF1_*fclC*(+DH)*DEFGH X. hominickii*	Heterologous PolyA production	Heterologous production of *X. hominickii fclCDEFGH* with additional DH domain of *fclC* from *X. bovienii* integrated in *fclC X. hominickii*	This work
E. coli DH10B::*mtaA* pFF1_*fclCDEFGH X. hominickii* pACYC_ara_tacI_DH *X. bovienii*	Heterologous PolyA production	Heterologous production of *X. hominickii fclCDEFGH* and plasmid-based co-expression of the DH domain of *fclC* from *X. bovienii*	This work
X. szentirmaii DSM 16338 Δ*fclCDE*	PolyA exchange in *X. szentirmaii*	Deletion of *fclCDE* in *X. szentirmaii*	[15]

Table S1 (continued). Strains used in this work. *E. coli*: *Escherichia coli*, *S. cerevisiae*: *Saccharomyces cerevisiae*, *C. lusitaniae*: *Candida lusitaniae*, *X. szentirmaii*: *Xenorhabdus szentirmaii*, *X. hominickii*: *Xenorhabdus hominickii*, *X. bovienii*: *Xenorhabdus bovienii*, DH: dehydratase domain, Fcl: full-length fabclavine; sFcl: shortened fabclavine; PolyA: polyamine.

Strain	Application	Description	Origin
X. szentirmaii DSM 16338 Δ*fclCDE* pFF1_*fclCDEFGH X. bovienii*	PolyA exchange in *X. szentirmaii*	Deletion of *fclCDE* in *X. szentirmaii* and heterologous production of *fclCDEFGH* from *X. bovienii*	This work
X. szentirmaii DSM 16338 Δ*fclCDE* pFF1_*fclCDEFGH X. hominickii*	PolyA exchange in *X. szentirmaii*	Deletion of *fclCDE* in *X. szentirmaii* and heterologous production of *fclCDEFGH* from *X. hominickii*	This work
X. szentirmaii DSM 16338 Δ*fclK*	Influence of FclH	Deletion of *fclK* in *X. szentirmaii*	[15]
X. szentirmaii DSM 16338 Δ*fclK* Δ*fclH*	Influence of FclH	Deletion of *fclK* and *fclH* in *X. szentirmaii*	This work

Table S2. Plasmids and oligonucleotides and their origin.

Plasmid	Locus tag(s) of analyzed gene(s)	Oligonucleotide	Sequence 5'-3'
pCEP_*fcl* *X. szentirmaii*	Xsze_03745	[16]	[16]
Δ*fclI* *X. szentirmaii*	Xsze_03739	[15]	[15]
Δ*fclK* *X. szentirmaii*	Xsze_03737	[15]	[15]
Δ*fclH* *X. szentirmaii*	Xsze_03740	[15]	[15]
pCEP_*fcl* KJ12.1	Xekj_00388	[16]	[16]
Δ*hfq* KJ12.1	Xekj_01457	SW282_KJ12.1_LF_fw	CGATCCTCTAGAGTCGACCTGCAGCACTATCAATCGCTTTGCGTCAGC
		SW283_KJ12.1_LF_rv	TGTCAGGCATTATCACTGATTCTATATTTTCCTTATTTTGTTGTTTTTAACTAAGAACCC
		SW284_KJ12.1_RF_fw	CAAAATAAGGAAAATATAGAATCAGTGATAATGCCTGACATAAATAAAAACATAGG
		SW285_KJ12.1_RF_rv	GAGAGCTCAGATCTACGCGTTTCATATGCTTCCAGAACACTGTCCACTGC
Δ*fclK* KJ12.1	Xekj_00380	NB1_KJ_LF_fw	CGATCCTCTAGAGTCGACCTGCAGATCCTTGATAGCTTCCTCCATCC
		NB2_KJ_LF_rv	TATCAGGTTGTCCGGGATCCGTTATTCCTCATTCCC
		NB3_KJ_RF_ fw	GAGGAATAACGGATCCCGGACAACCTGATAGGC
		NB4_KJ_RF_rv	GAGAGCTCAGATCTACGCGTTTCATATGGGCTGTCCAGATTGACAGGC
pCEP_*fcl* *X. hominickii*	Xhom_02793	[16]	[16]
Δ*hfq* *X. hominickii*	Xhom_00479	SW290_Xhom_LF_fw	CGATCCTCTAGAGTCGACCTGCAGCTGCATTGATTTATCGTGGAATGGATATCGG
		SW291_Xhom_LF_rv	CGTCAGGTGTGGCCACTGATTCTATATTTTCCTTATTTTGTTGTTTTTAACTAAGAACCTATTGG
		SW292_Xhom_RF_fw	CAAAATAAGGAAAATATAGAATCAGTGGCCACACCTGACG
		SW293_Xhom_RF_rv	GAGAGCTCAGATCTACGCGTTTCATATGGGCAGCATAGACTTCAGCTGAGG
Δ*fclK* *X. hominickii*	Xhom_02785	SW329_Xhom_LF_fw	CGATCCTCTAGAGTCGACCTGCAGAAGGTACCAGTGTTCCCATCG
		SW330_Xhom_LF_rv	ATGGTTCTCCTGCGGGATCTGTTATCCCTTTTCCCTTACC
		SW331_Xhom_RF_fw	AAGGGATAACAGATCCCGCAGGAGAACCATGAAG
		SW332_Xhom_RF_rv	GAGAGCTCAGATCTACGCGTTTCATATGCTCACTACCCGGTTGTTCCC
pCEP_*fcl* *X. bov*ienii	XBJ1_2953	SW151_Xbov_fw	TTTGGGCTAACAGGAGGCTAGCATATGTCTGAGACATATTTTTTGCATGATAGG
		SW152_Xbov_rv	TCTGCAGAGCTCGAGCATGCACATCAACGCGACTTTCATCATAGACG
pFF1_*fclCDEFGH* *X. bovienii*	XBJ1_2948 -XBJ1_2953	SW361_Xb_F1_fw	TTATCGCAACTCTCTACTGTTTCTCCATACCCGTTTTTTTTGGGCTAACAGGAGGAATTCCATGTCTGAGACATATTTTTTGCATGATAGG
		SW362_Xb_F1_rv	CGATTAATTATTTTCGCTATTCACCCTGTTCGATAGTTGACTGAGGAAAGATAATTTCCTCTATTCAACAAACACGGTAAATTTTGC
		SW363_Xb_F2_fw	GAACAAGGCTATATTTATAGTCGGTTTCATAATGCAAAATTTACCGTGTTTGTTGAATAGAGGAAATTATCTTTCCTCAGTCAACTATCG
		SW364_Xb_F2_rv	CGTTAGCGGTAACGCTGTCAGTTGATGGTTCGATTGATTCACAGATAAGCGCTGACTCATTTTAAAGCTTCCTGTTTCAGTTCTGC
		SW365_Xb_F3_fw	ATACGAGCGACGCCAGCCACACCAGATCATGGCGGCAGAACTGAAACAGGAAGCTTTAAAATGAGTCAGCGCTTATCTGTG
		SW366_Xb_F3_rv	CTTCACCTTTGCTCATGAACTCGCCAGAACCAGCAGCGGAGCCAGCGGATCCGGCGCGCCTTAGGTATCATTTCCTAACACATCG
pFF1_*fclC*(ΔDH *)DEFGH* *X. bovienii*	XBJ1_2948 -XBJ1_2953	SW606	GCACCCACCCATCGTACGTCATCGCCGGTGGTGGATTATTCTGCTCTGGCCAAAGTG
		SW607	AATTTCCTCTATTCAACAAACTCTCCGATCCCCAACGCC
		SW608	AGGCGTTGGGGATCGGAGAGTTTGTTGAATAGAGGAAATTATCTTTCCTCAG
		SW609	CAATGCCTGCTCAGCAGAATAAATAGTCCATTTAAATAAATTATCCAGCGAATTTAATTCTTCTTCC
pFF1_*fclCDEFGH* *X. budapestensis*		[15]	[15]
pFF1_*fclC*(+DH)*DEFGH* *X. budapestensis*	Xbud_02634-02639 +partial XBJ1_2953	SW669	GCCATGCAGGTCAGTCCCCATGATGTACTAGTTGTGACAGGGGGAGCCC
		SW670	CCCAACGCCTTAACTGTTTTCGGAGCCATATAAGTTTTCCCTCC
		SW671	CTTATATGGCTCCGAAAACAGTTAAGGCGTTGGGG
		SW672	CGTAATTTATTAGGTATCGTTTTCACGGTAAATTTTGCATTATGAAACC
		SW673	TTCATAATGCAAAATTTACCGTGAAAACGATACCTAATAAATTACGTAATGTAATC
		SW674	ATGCCTGATCTGCTGCATAGATTGTCCATTTAAATAGATCATCCAGTGTATTTAATTCTTCTTC

Table S2 (continued). Plasmids and oligonucleotides and their origin.

Plasmid	Locus tag(s) of analyzed gene(s)	Oligonucleotide	Sequence 5‘-3‘
pFF1_*fclCDEFGH* *X. hominickii*	Xhom_02788 - Xhom_02793	SW420_Xh_F1_fw	TTATCGCAACTCTCTACTGTTTCTCCATACCCGTTTTTTTGGGCTAACAGGAGGAATTCCATGTCTGAGTCATATCTTTTACATGATGG
		SW421_Xh_F1_rv	TATTATTTATACCCGTTGTATTTCAAGTTGTCGCTTTATTTATTTCACTGCAACTGGATACAACC
		SW422_Xh_F2_fw	ATCCAATAATATTCAGGTTGTATCCAGTTGCAGTGAAATAAATAAAGCGACAACTTGAAATACAACGG
		SW423_Xh_F2_rv	GCCAATTGGCGGCCTGATTGATTCACCGATAAGCGCTGACTCATTTTGCTTCTTCCTGTTTCAGTTC
		SW424_Xh_F3_fw	GGCAGGTGCGACAGAACTGAAACAGGAAGAAGCAAAATGAGTCAGCGCTTATCGGTGAATCAATC
		SW425_Xh_F3_rv	CTTCACCTTTGCTCATGAACTCGCCAGAACCAGCAGCGGAGCCAGCGGATCCGGCGCGCCTTAATTCTTCAAAAGAAACGGATCTGCATC
pFF1_*fclC*(+DH)*DEFGH* *X. hominickii*	Xhom_02788 - Xhom_02793 + partial XBJ1_2953	SW652	CAATCTGTGGTGGGATATTCTGCCACCAACGTGGCACCATCAGCACCGATGACG
		SW653	CCCAACGCCTTAACTGTTTTGGGCGCTTTATAAGTTTCTCCGC
		SW654	CTTATAAAGCGCCCAAAACAGTTAAGGCGTTGGGG
		SW655	TTTCTGCTGATATTAGTTTTCACGGTAAATTTTGCATTATGAAACC
		SW656	ATAATGCAAAATTTACCGTGAAAACTAATATCAGCAGAAATAATAACAGG
		SW657	GCCTGTTCAGAGGCGTAAATACTCCATTTAAATAAGTTATCCAGTAAGTTCAATTCTTCTTC
pACYC_ara_tacI (empty)	/	[14]	[14]
pACYC_ara_tacI_DH *X. bovienii*	XBJ1_2953	SW667	CCATACCCGTTTTTTTGGGCTAACAGGAGGAATTCCATGACAGTTAAGGCGTTGGGG
		SW668	CGAGCCGATGATTAATTGTCAACAGCTCCTGCAGCTATTCAACAAACACGGTAAATTTTGC

Table S3. Occurrence of homologous dehydratase domains in the genus *Xenorhabdus* and further strains. FclC homologs were identified by a BlastP search. Only one representative strain of a genus is shown. FclC from *X. szentirmaii* is shown as reference protein without DH domain, representing FclC-homologs from other *Xenorhabdus* strains (Fig. S4) [16].

	Gene accession number	Protein size [Amino acids]	Identity [%]
***X. bovienii* subspecies**			
SS-2004	CBJ82077.1	2274	100
str. Jollieti	CDH27902.1	2274	100
str. puntauvense	CDG98370.1	2277	94
str. oregonense	CDH05851.1	2268	97
str. kraussei Quebec	CDH18916.1	2289	88
str. kraussei Becker Underwood	CDH23752.1	2290	94
str. Intermedium	CDH34284.1	2309	69
str. feltiae Moldova	CDH00683.1	2277	97
str. feltiae France	CDG88351.1	2277	94
str. feltiae Florida	CDG90959.1	2277	94
Further strains			
Fischerella thermalis CCMEE5201	PMB53690.1	2389	35
Dickeya zeae EC1	AJC65778.1	2332	41
Photorhabdus temperata subsp. temperata Meg1	KER04069.1	2218	49
Serratia plymuthica RVH1	CCM44330.1	2248	49
Agrobacterium tumefaciens	QCL88703.1	2373	37
Shewanella pneumatophori SCRC-2738	AAB81123.1	2756	24.8
FclC-reference without DH domain			
X. szentirmaii DSM 16338	PHM32993.1	1995	72

Table S4. Inhibitory activity of the fabclavine types from *X. szentirmaii* and polyamines from different strains. Testorganisms were *Saccharomyces cerevisiae* CEN.PK2 (*S. cerevisiae*), *Candida lusitaniae* DSM 70102 (*C. lusitaniae*) and *Escherichia coli* DH10B (*E. coli*) against processed samples of induced (ind) and non-induced (non ind) mutant strains of *Xenorhabdus szentirmaii* DSM 16338 (*X. sze.*), KJ12.1, *X. hominickii* DSM 17903 (*X. hom.*) and *X. bovienii* SS-2004 (*X. bov.*). Structures corresponding to the strain-specific fabclavine types a, b and c are shown in Figure 1 and 2. Strains without deletion in the *fcl* BGC are able to produce full-length (b) and shortened fabclavines (c) and the polyamine (a), while a deletion of *fclI* shows only production of a and c, and a deletion in *fclK* shows only production of a [15].

Analyzed strain	Fabclavine types	Inhibitory activity against tested microbe [mm]		
		S. cerevisiae	*C. lusitaniae*	*E. coli*
X. sze. Δ*hfq* pCEP_fcl (ind)	a, b, c	18.3	21.7	12.7
X. sze. Δ*hfq* pCEP_fcl (non ind)	-	0	0	0
X. sze. Δ*hfq* Δ*fclI* pCEP_fcl (ind)	a, c	4.3	3.7	0
X. sze. Δ*hfq* Δ*fclI* pCEP_fcl (non ind)	-	0	0	0
X. sze. Δ*hfq* Δ*fclK* pCEP_fcl (ind)	a	4	2.7	1
X. sze. Δ*hfq* Δ*fclK* pCEP_fcl (non ind)	-	0	0	0
KJ12.1 Δ*hfq* Δ*fclK* pCEP_fclC (ind)	a (**2**)	0	0	2
KJ12.1 Δ*hfq* Δ*fclK* pCEP_fclC (non ind)	-	0	0	0
X. hom. Δ*hfq* Δ*fclK* pCEP_fcl (ind)	a	0	1.3	2.7
X. hom. Δ*hfq* Δ*fclK* pCEP_fcl (non ind)	-	0	0	0
X.bov. pCEP_fclC (ind)	a (**1**, **2**)	8.3	10.3	10.3
X.bov. pCEP_fclC (non ind)	-	0	0	0

Supplementary Figures

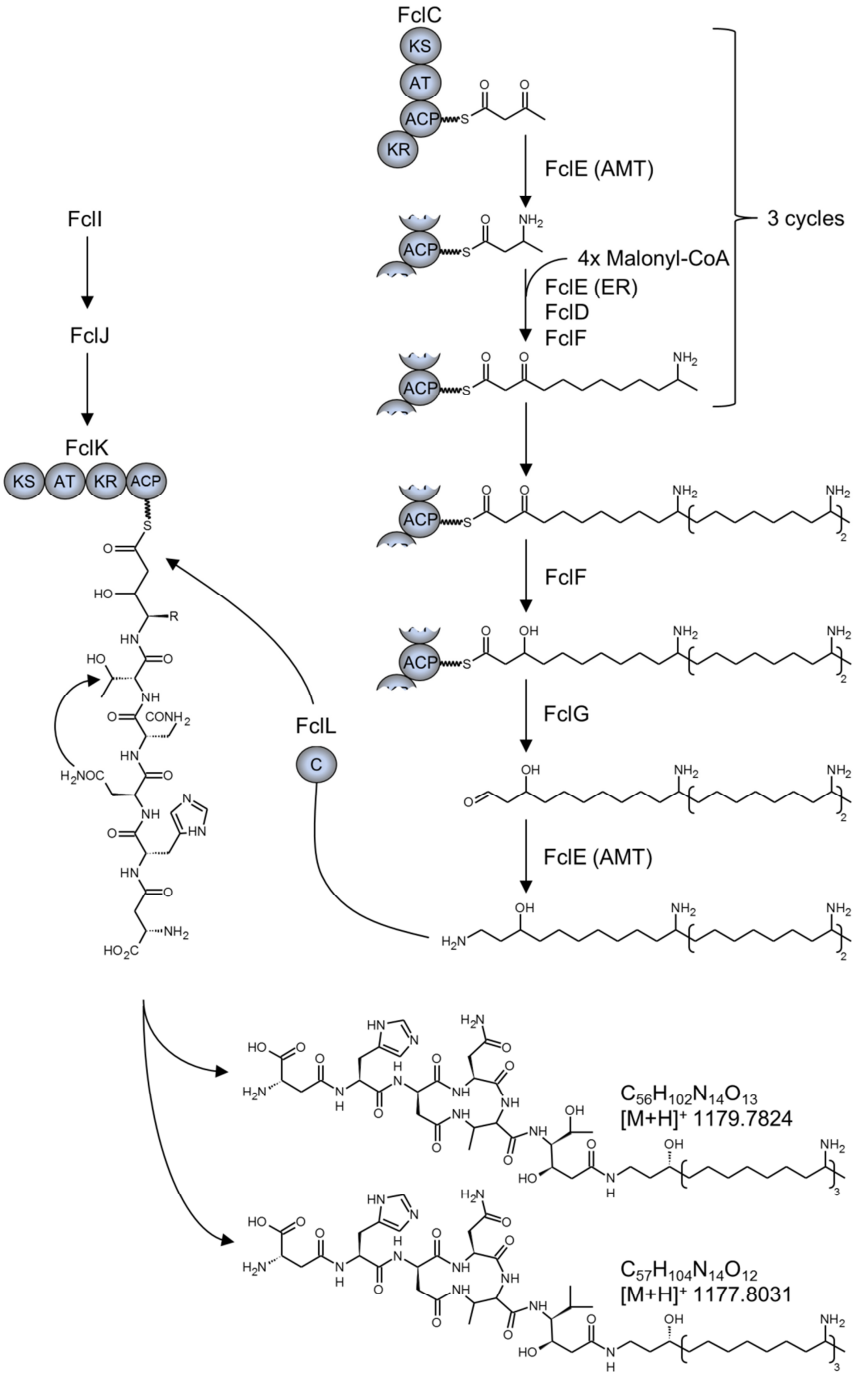

Figure S1. Fabclavine biosynthesis in *X. szentirmaii* (Modified from [15]). After the generation by the NRPS FclI, FclJ and the PKS FclK, the NRPS-PKS-part stays enzyme-bound until its condensation with the polyamine, catalyzed by FclL [15]. Abbreviations: C: condensation domain, KS: ketosynthase, AT: acyltransferase, ACP: acyl carrier protein, KR: ketoreductase.

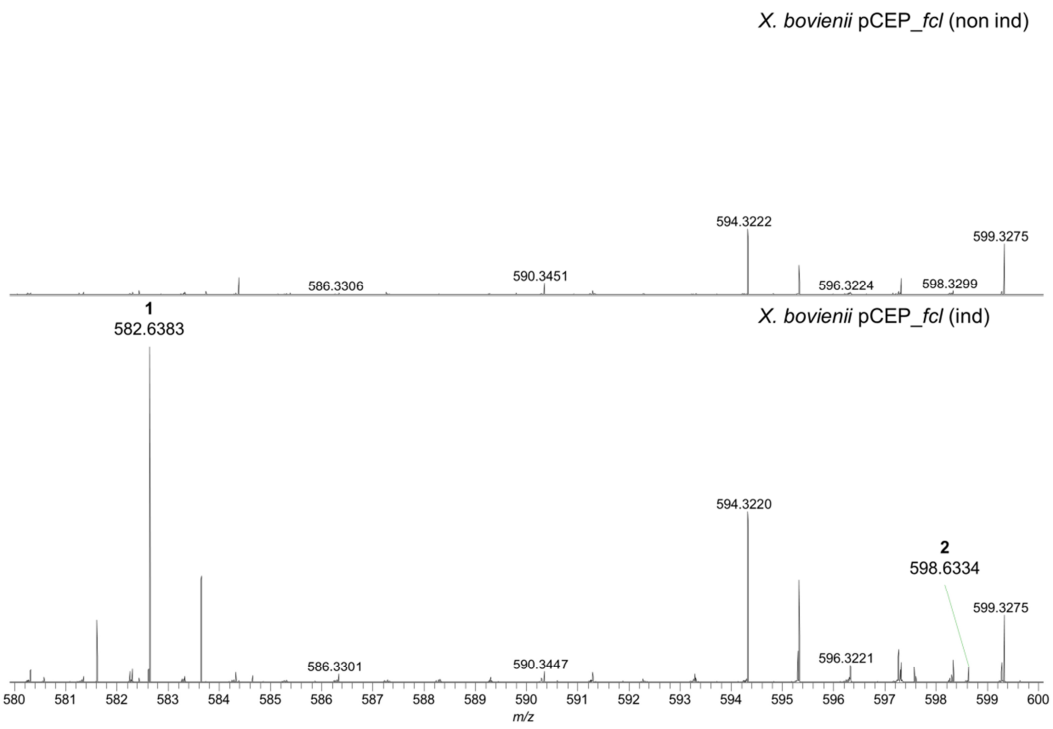

#	Sum formula	Calc. m/z	Det. m/z	Δppm
1	$C_{36}H_{79}N_5$	582.6408	582.6383	-4.332
2	$C_{36}H_{79}N_5O$	598.6357	598.6334	-3.990

Figure S2. MALDI-HRMS-spectra of *X. bovienii* pCEP*_fcl* mutant (induced and non-induced) with compounds **1** and **2.** Shown are sum formulas, calculated and detected masses and corresponding Δppm. Cultures were grown in LB media for 3 days with constant shaking at 30°C.

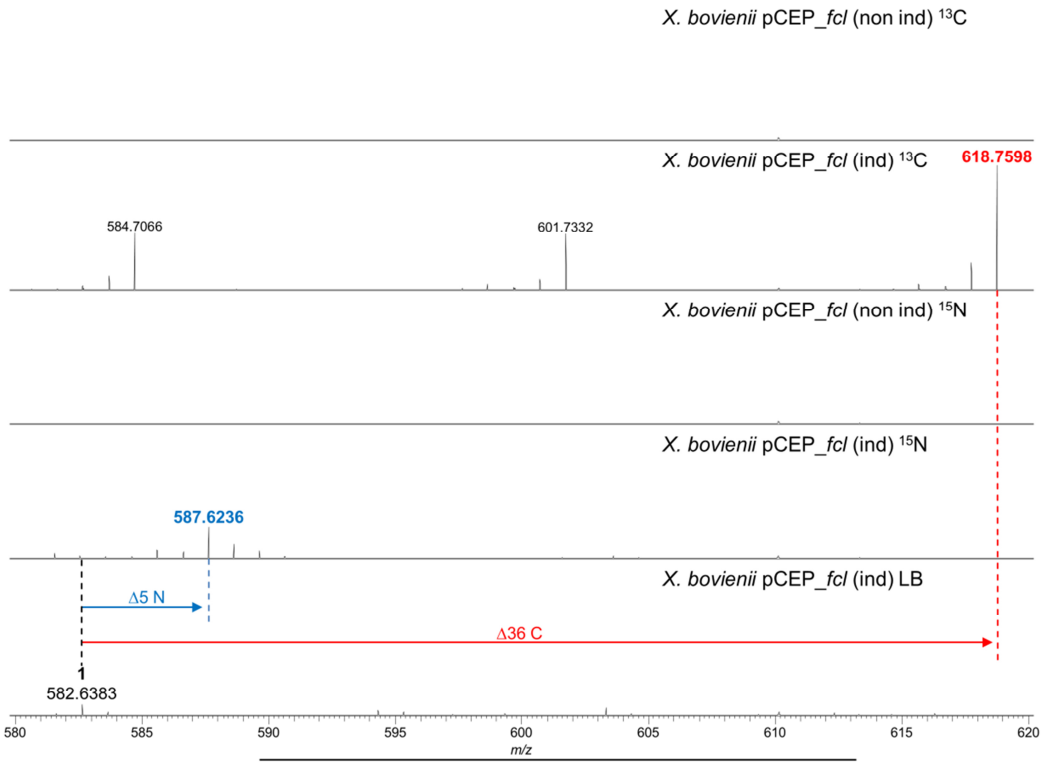

#	Sum formula	Calc. m/z	Det. m/z	Δppm
1	$C_{36}H_{79}N_5$	582.6408 (LB)	582.6383	-4.332
1	$C_{36}H_{79}N_5$	587.6266 (^{15}N)	587.6236	-5.003
1	$C_{36}H_{79}N_5$	618.7620 (^{13}C)	618.7598	-3.459

Figure S3. MALDI-HRMS-spectra of *X. bovienii* pCEP_*fcl* mutant (induced and non-induced) of isotope-labelling experiments compared to *X. bovienii* pCEP_*fcl* (ind) in LB to confirm the sum formula of compound **1**. Cultures in ^{15}N- or ^{13}C-media were grown for 2 days (LB: 3 days) with constant shaking at 30°C.

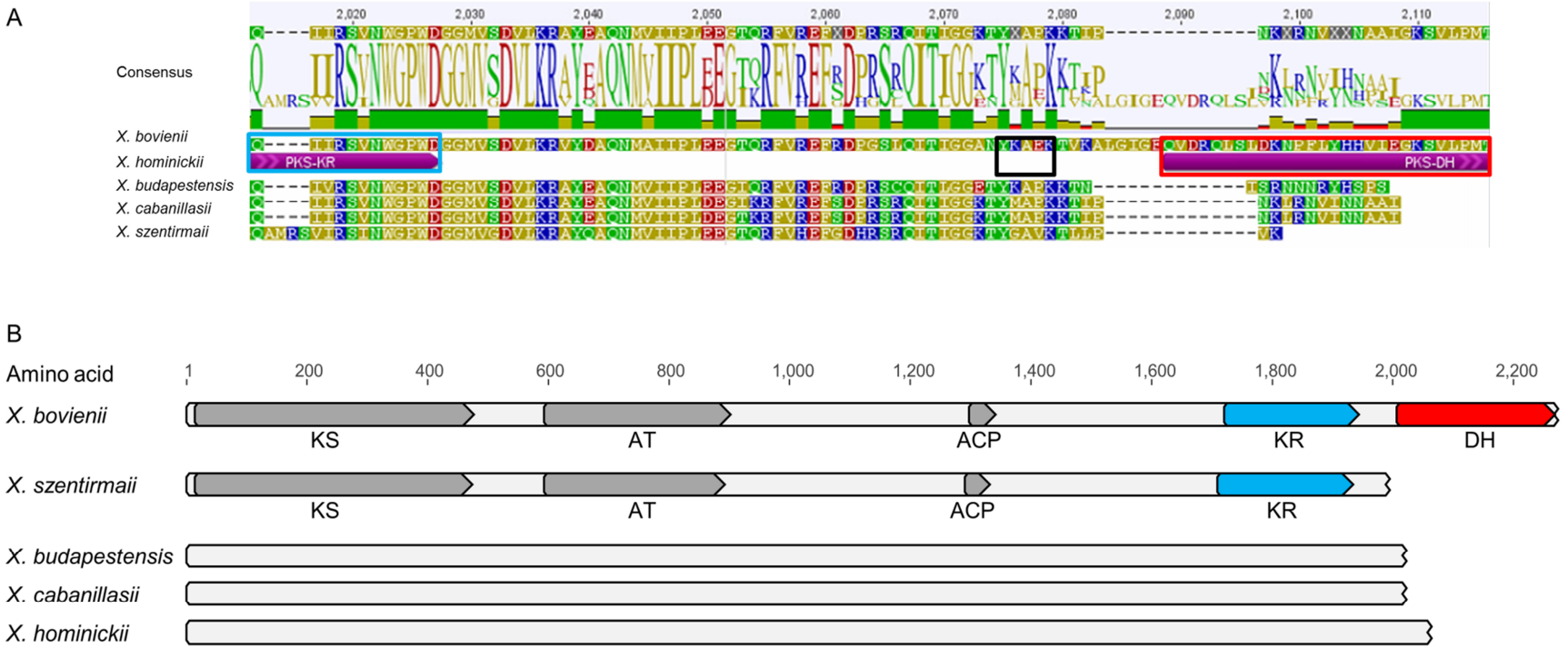

Figure S4. (A) Alignment of FclC homologues. Analyses were performed by ClustalW alignment with the CostMatrix BLOSUM in Geneious 6.1.8 [https://www.geneious.com]. Marked in light blue is the end of the ketoreductase domain, in red the start of the dehydratase domain and in black the YxAxK-motif. (B) Comparison of FclC from multiple *Xenorhabdus* strains. KS: ketosynthase, AT: acyltransferase, ACP: acyl carrier protein, KR: ketoreductase, DH: dehydratase

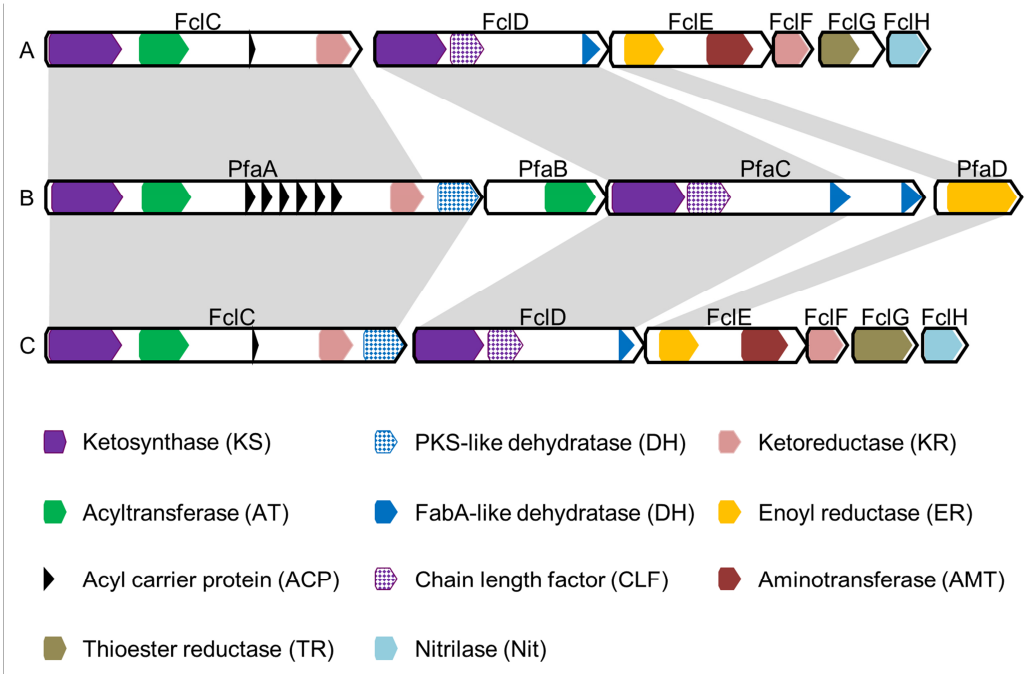

Figure S5. Domain organisation of the fabclavine polyamine biosynthesis in *X. szentirmaii* DSM 16338 (A) [NCBI accession number: NIBV00000000) and *X. bovienii* SS-2004 (C) [NCBI accession number: FN667741] in comparison with the EPA biosynthesis in *Shewanella pneumatophori* strain SCRC-2738 (B) [NCBI accession number: U73935.1]. Single proteins and domains were defined by BlastP, the online tool InterPro and corresponding literature [6, 15].

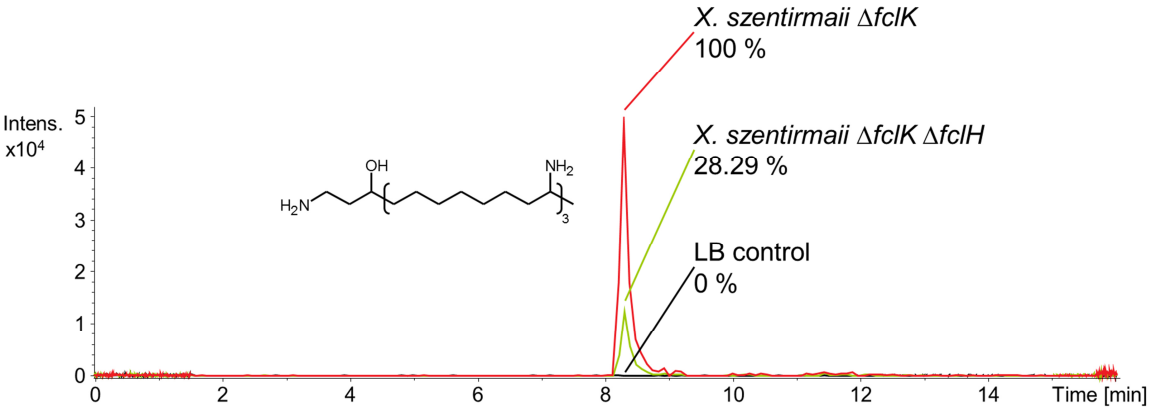

Figure S6. Influence of FclH on the production titer of the polyamine in *X. szentirmaii*. Production cultures in LB-media of the strains *X. szentirmaii* Δ*fclK* w/o Δ*fclH* and a LB control were measured in triplicates via HPLC-HRMS. The production titer was relatively quantified by comparing the average of the integrated peak area in the extracted ion chromatogram (EIC) of $C_{28}H_{62}N_4O$ $[M+H]^{2+}$.

```
   1 MSETYFLHDR KVRGDIAIVG MASHFPDAPD LYKFWENIIG KKDSLTDVST MLGDEYWQKE
  61 DFYDPNPAVA DKTYGHRAGF VPPIDFDPVE FKIPPAIIDS ISTAQLFALY VAKQAMLDAG
 121 LVGQENSRVD RDRIGVILGG AGNGNTSFSL ASRQQAPYLR KIMVKSGLSE KVANDIIERM
 181 HGMYLEWNED SFPGFLGNVA CGRIASYFDL GGTSYMVDAA CASSLAAIKA AIGELHSGSC
 241 DAVLTGGVNL ENSIFSFLCF SKTPALSKSN LSRPFDQSAD GMMLGDGVGM LVLKRLEDAE
 301 LDGDRIYAVI KSIEASSDGR AKSIFAPRLE GQAKALRRAY ASAGLSPNDI QLVEAHGTGT
 361 ASGDDTELKS LHTVFGEYQV PAKSVAIGSI KSQIGHTRCA AGAASMMKVA LALHHKVLPP
 421 TLNVDKPTNL LKAENSPFYV NSEARPWLRS FNSAPRRAAL SAFGFGGTNF HVILEEYEKH
 481 THGRYRLNES PWVMLFKGHN PAELLAQCEE ALTRFSGNLP DIAIRQHLEQ QDIDSLQPQQ
 541 ARVLFVSQSA EQTVELLSIA IKQLQQNSTH GWEHPRGIYY QPQGKMLDGK IVALFPGQGS
 601 QYVNMARDIA NDYPEMRQSL ETLDEVSISE LGHELSPVVY PVPTFSDDER QIHQQRLTDT
 661 ANAQPALGAI SAGYFNILKG MGFVPDFVAG HSYGEVTALW AAGVFSDKNF HRVSLARGWA
 721 AASASDHRGA DTDAGAMLAA SLNSAQRAQI LERYSGIIIA NDNSQQQVVF GGATPLIHQL
 781 HDELKKRDVH CRILPVSAAF HTAFIEPAYQ PYRERLAGIN FQSPQCRLFS SATAEPYGNS
 841 PQAIRELLAE QLIKPVQFRQ TIEAIYQEGG RLFVEVGPKG VLGKLVADIL KDKEHEVISV
 901 NPNDKGEDRL QFARAQAKLL AVGVKLREIN QHIRPQPMAE DKSKRLTFRM SGGFYLSQKN
 961 KARRQRALRD GDSAIVEQFI AESAPVPMAP VMPLHSQKEV NIKEEHSGKE VKPTQEVHPT
1021 QEVVVEKVEN KVEKIAENKT ISAQFIQQNM LTIIQRREST MEQNNQLSEN VDVNMLNGLL
1081 QAQQVMSQLH QQFQANQKDY IQLLGMLLDK QYTLLETCKD HQNLPSMLSS LSQSVQLLDK
1141 NLELYHSNHE HYFMAQQSLF QSGQVTPMIA PTHRTSSPVV DYSALAKVTT SATIASAPVS
1201 TPIPTPIPTT APAVKVDTAP VQAKPVDPIK EIEPVRSMMP EMPVMPSVVE EAVKPIVNDT
1261 PVSQPTPVVI ETKAKVLDPK VEKQFQILSQ ITEEKIVNQL ISIVSDRTGY PQDMITPEMD
1321 LEADLGIDSI KRLEIFGAMF DAFSANVGLY NEASRNKDLE NFEVDSLSNI SKMGVFFKQM
1381 LDDVMNDLLG NGGDEAVAEQ SPPSVETREH ENTKSNVVPD SGGATGKLQS LGFFTSTVTS
1441 PEADSVKKPL AEPQLIVPSV VQPVLKNEIV LNEEESFAGS PVSRFAVVKQ SLPMPDRLQG
1501 VFSSPKRWLV VDEGTTTVDD VVNALRQQGQ QVAVLMLKQN PAVMESEAAL DAALADIEQQ
1561 HGTIEGVIYL QTPKQSVKAL AEVFNEQDYR SVETTFLLAK RLQRSLNHDE QKTGYFMVIM
1621 RGDGELLTSG REHLSIVSAG LTGLTKSLNI EWKNVFCRTV DIDARVKDSD AAKMVVEELQ
1681 DSRTDMGEVG RGVNGERMTL ALTEENVLSA AFVNQVNAGD VLIVTGGARG ITAQCVIELA
1741 KQSQATFILL GRTDITEPLP EWAEGKTTQD ERKTAAMAYL KAQGIQLTPV KINGMLSRLT
1801 HLDEINGTLQ AIRQAGGRVM YLHCDITDLK QVKIALTKAQ QQLGQITGLI HGAGNLADKR
1861 IEKKTLADLH SVFNAKVKGL ENLCRELDFT SLRHIMLFSS VSGFFGNAGQ ADYSLANETL
1921 NKFIYLPFKG KNSQIIRSVN WGPWDGGMVS DVLKRVYDAQ NMAIIPLEEG TQRFVREFRD
1981 PGSLQITIGG ANYKAEKTVK ALGIGEQVDR QLSLDKNPFL YHHVIEGKSV LPMTAAIAWM
2041 ARICEDRFPG YKLETITDFK VLKGIVFDNT LAESYCVAWV PNTFDESGDG RLALDVVITS
2101 KRMKHYQATL ILSLQSREAQ HEVVGIDLNA EVPQTLPFYD GVGGEGILFH GESFHGVQKV
2161 VHVDDDNITL KCCVMPVQLE MQGQFSTRLF NLFINDIAFQ LPAIWFLQRN EMCLPNAIEK
2221 IEQYAELKFG QEFYASIEIK HQMSTEIIID IIFYDEQGYI YSRFHNAKFT VFVE
```

Figure S7. Sequence of FclC from *X. bovienii* SS-2004. Marked in red is the YxAxK-motif, crossed out is the removed sequence for pFF1_*fclC*(ΔDH)*DEFGH X. bovienii*, underlined is the sequence for the *X. bovienii* DH domain-integration into pFF1_*fclC*(+DH)*DEFGH X. budapestensis* and pFF1_*fclC*(+DH)*DEFGH X. hominickii*. For the co-expression plasmid pACYC_ara_tacI_DH *X. bovienii* the underlined sequence was used inclusive the three C-terminal residues FVE and an N-terminal M.

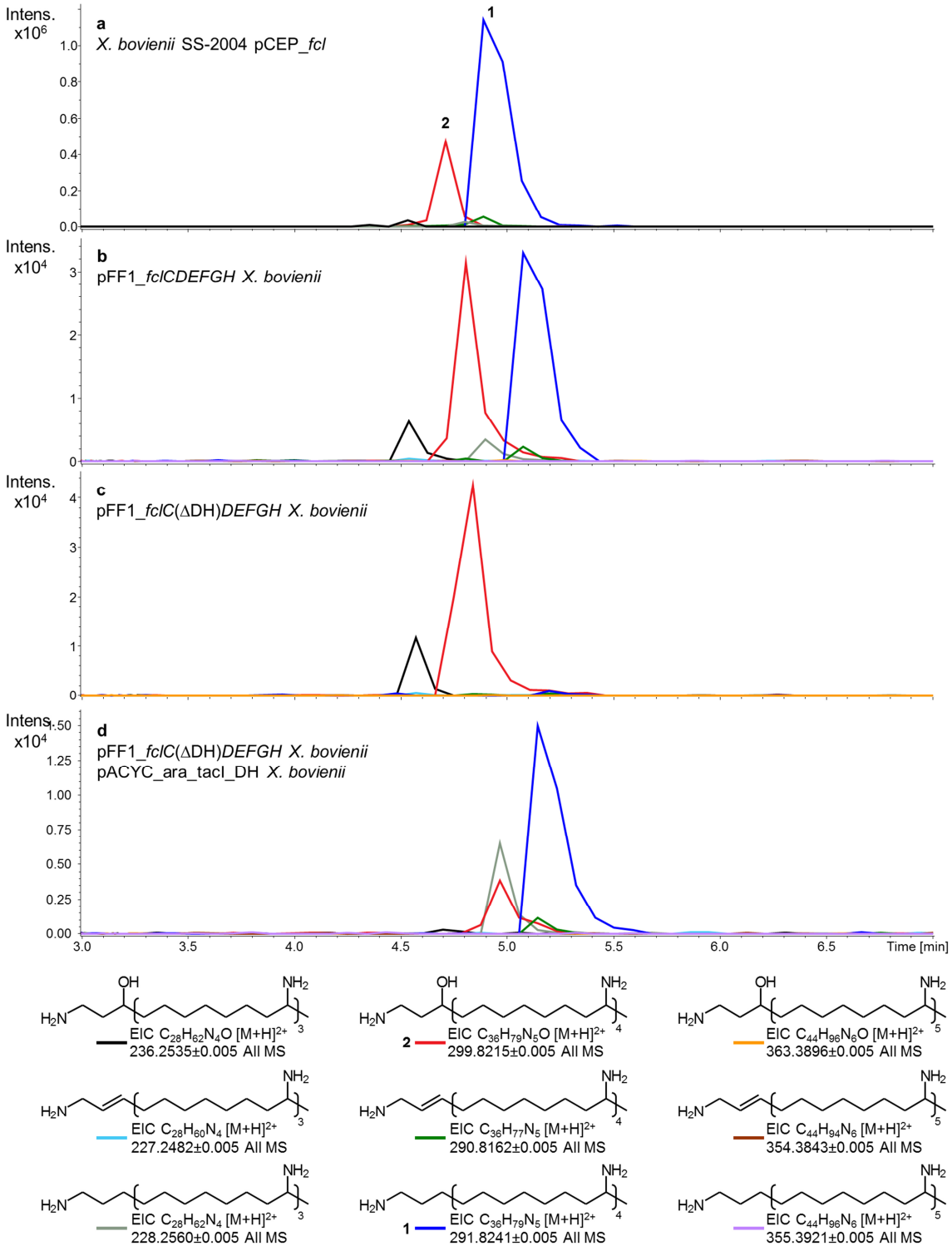

Figure S8. HPLC-HRMS analysis of *X. bovienii* pCEP_*fcl* (a) and the heterologous production of *fclCDEFGH* from *X. bovienii* in *E. coli* DH10B::*mtaA* (b-d). Shown are the extracted ion chromatograms (EIC) of the double charged masses. Sample numbers refer to Figure 3.

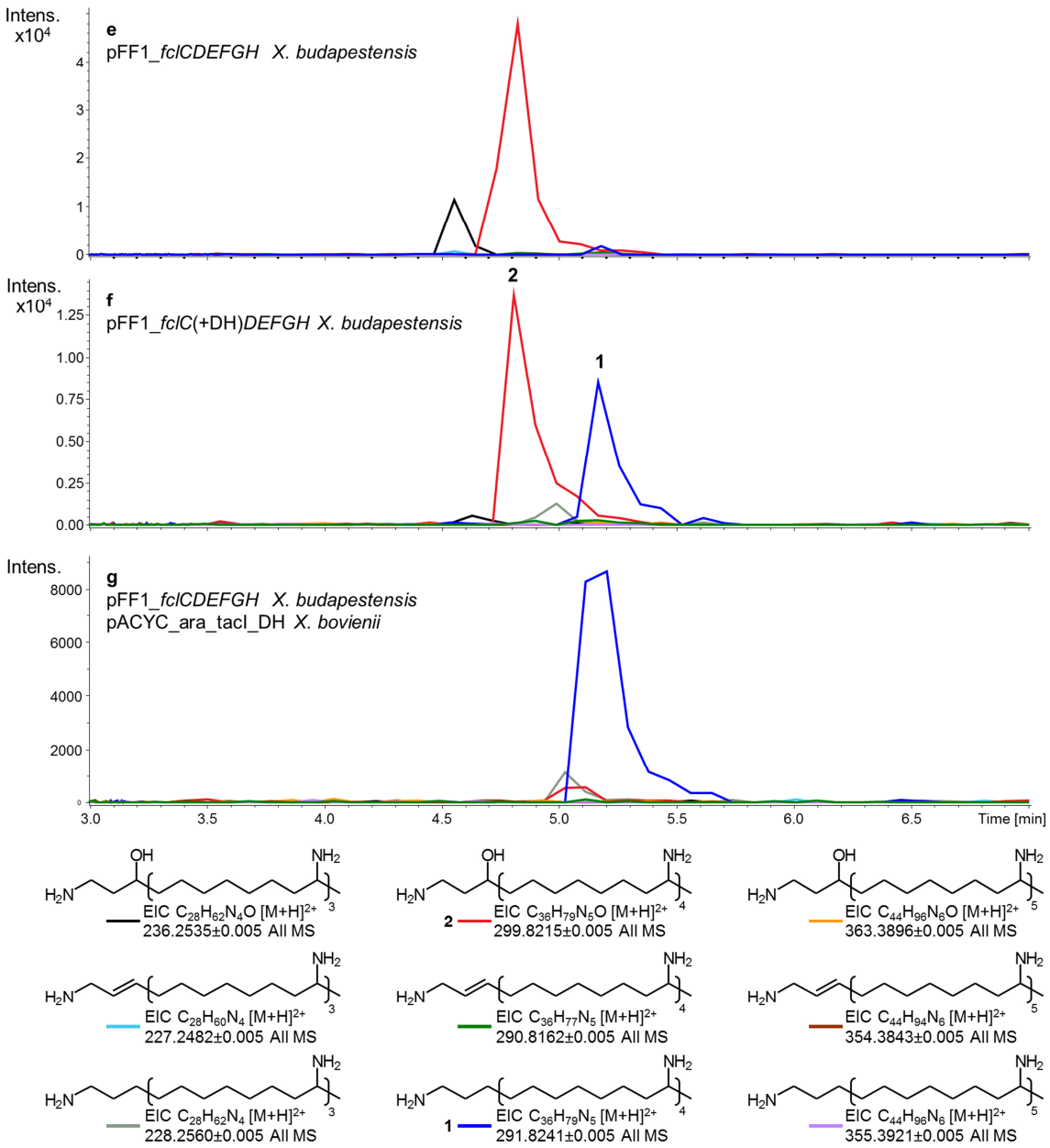

Figure S9. HPLC-HRMS analysis of the heterologous production of *fclCDEFGH* from *X. budapestensis* in *E. coli* DH10B::*mtaA*. Shown are the extracted ion chromatograms (EIC) of the double charged masses. The fused PKS-like DH domain from *X. bovienii* into FclC is marked as (+DH). Sample numbers refer to Figure 3.

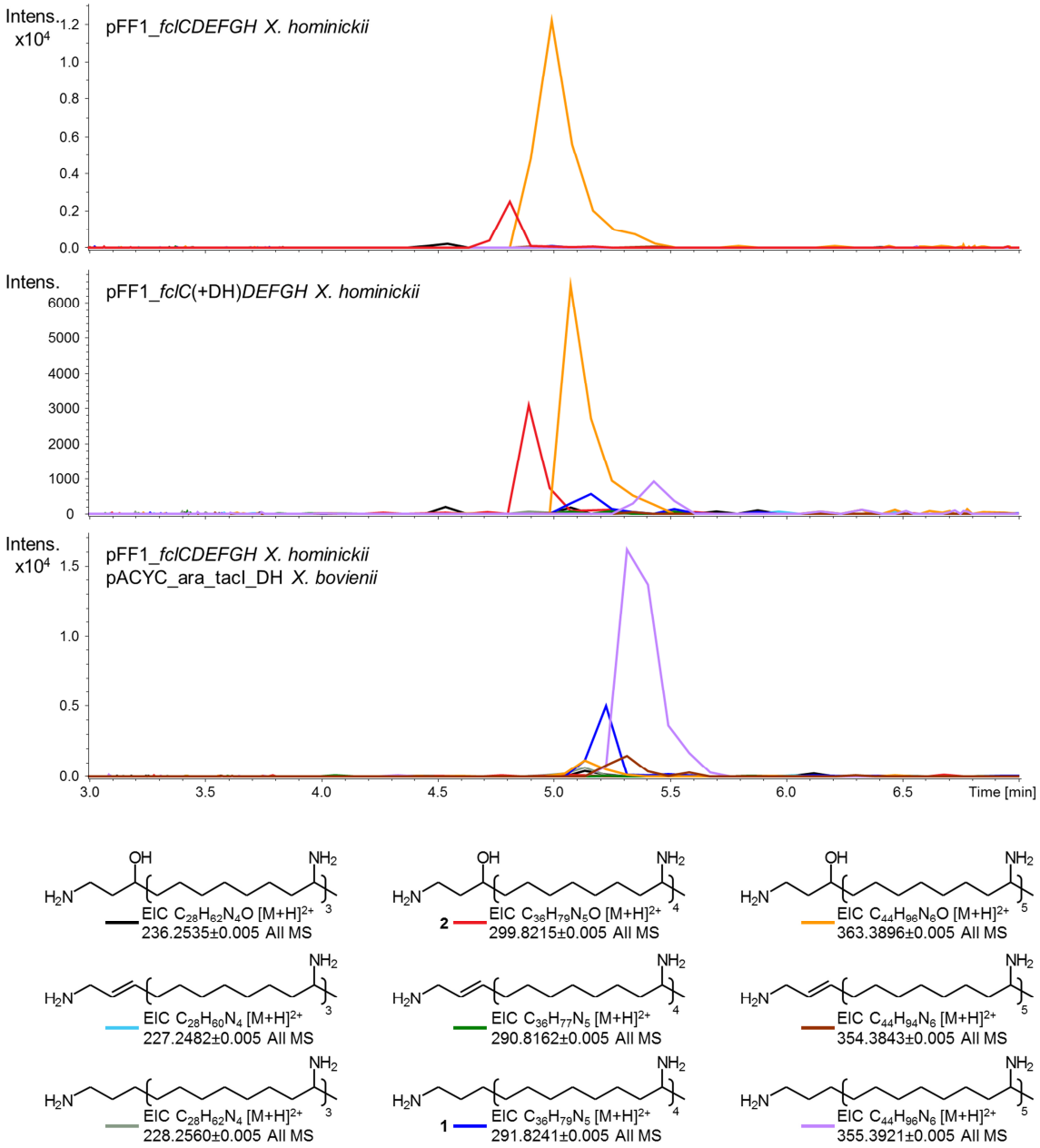

Figure S10. HPLC-HRMS analysis of the heterologous production of *fclCDEFGH* from *X. hominickii* in *E. coli* DH10B::*mtaA*. Shown are the extracted ion chromatograms (EIC) of the double charged masses. The fused PKS-like DH domain from *X. bovienii* into FclC is marked as (+DH). Samples were fivefold concentrated.

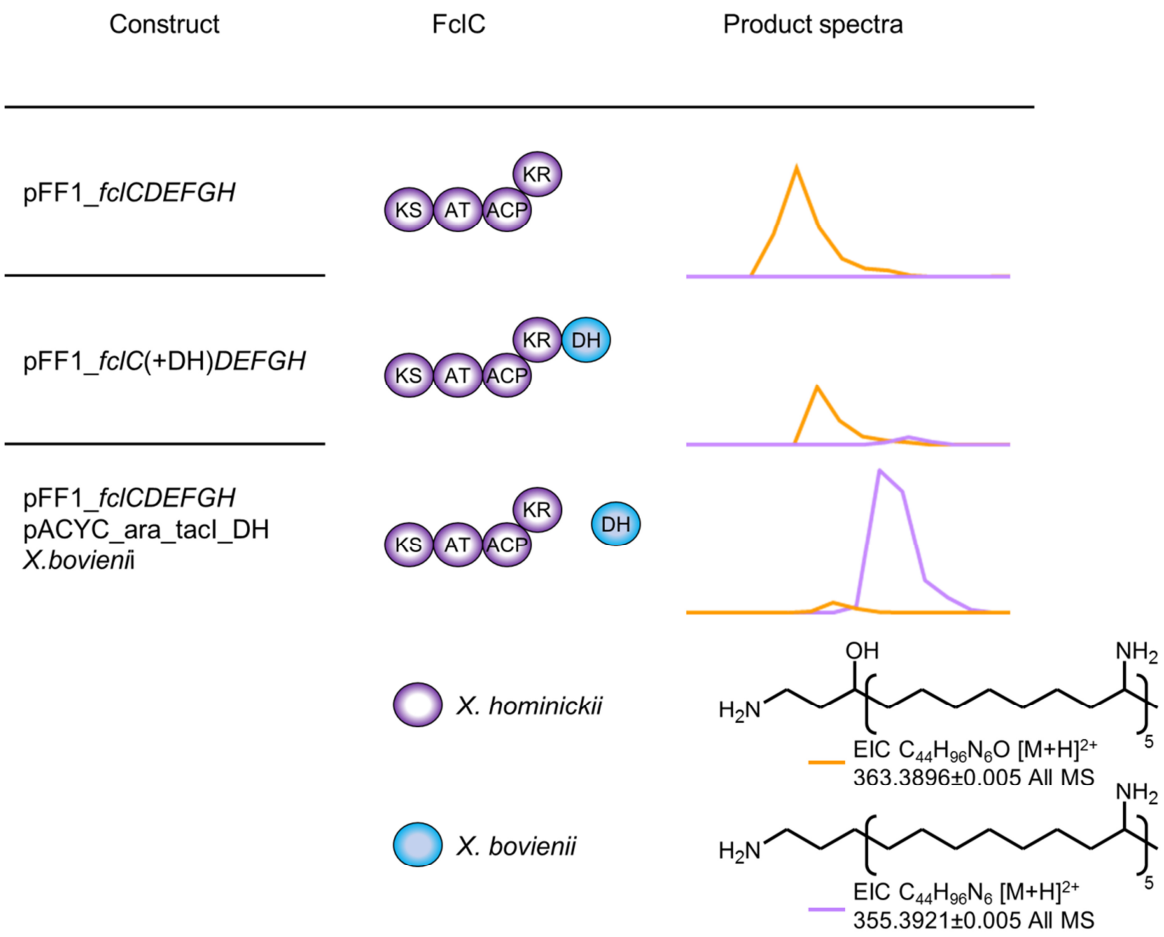

Figure S11. Manipulation of the polyamine biosynthesis of *X. hominickii*. The genes *fclCDEFGH* from *X. hominickii* were heterologously produced in *E. coli* DH10B::*mtaA*. The fused PKS-like DH domain from *X. bovienii* into FclC is marked as (+DH). Samples were fivefold concentrated.

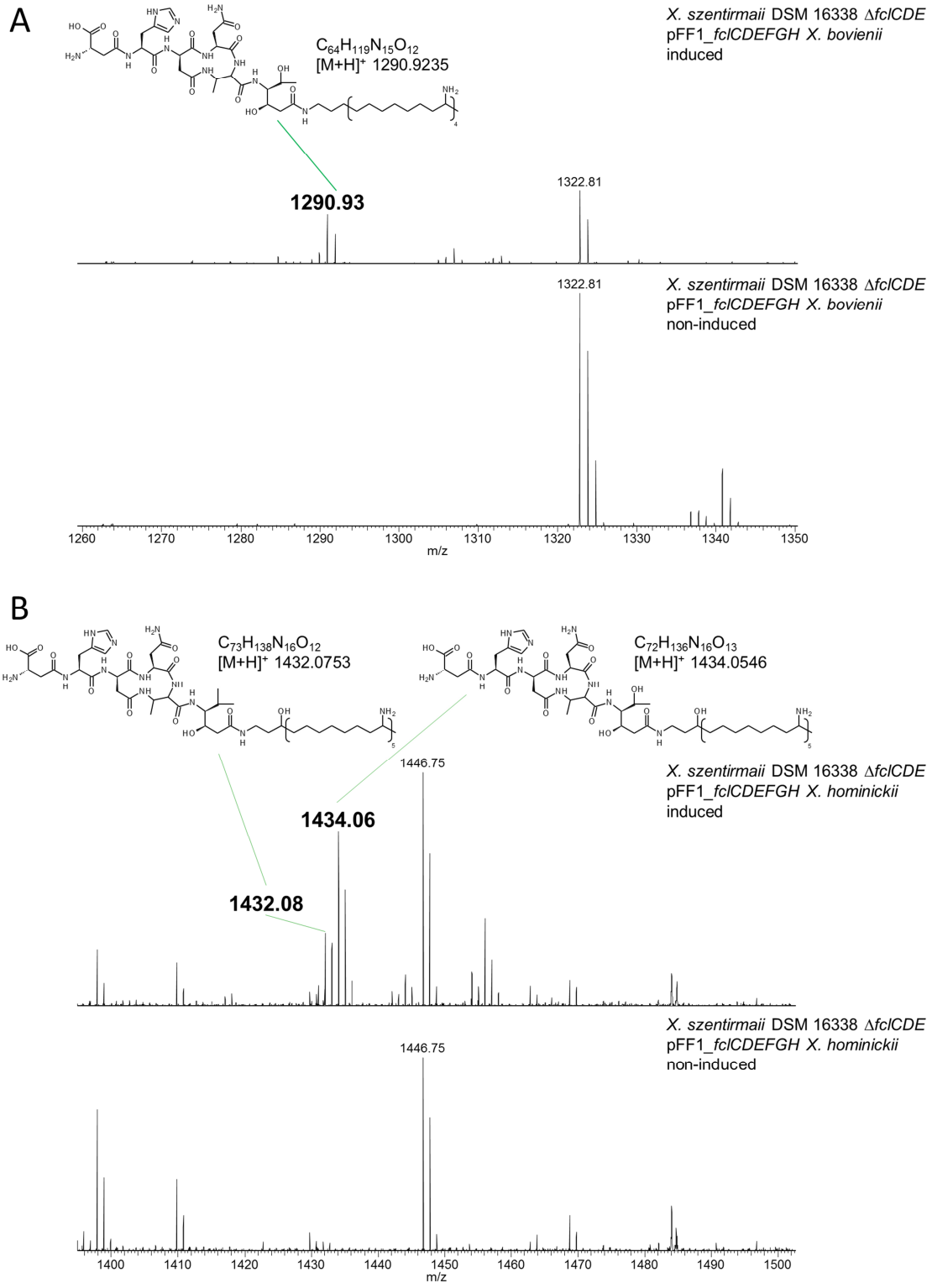

Figure S12. Exchange of the polyamine in the *X. szentirmaii* fabclavine biosynthesis. Shown are the MALDI-MS analysis of *X. szentirmaii* Δ*fclCDE* complemented with *fclCDEFGH* of *X. bovienii* (A) or *X. hominickii* (B) and corresponding fabclavine hybrids.

References

1. Bode E, Brachmann AO, Kegler C et al. (2015) Simple “on-demand” production of bioactive natural products. ChemBioChem 16:1115–1119. doi: 10.1002/cbic.201500094
2. Bode E, Heinrich AK, Hirschmann M et al. (2019) Promoter Activation in Δ hfq Mutants as an Efficient Tool for Specialized Metabolite Production Enabling Direct Bioactivity Testing. Angew Chem Int Ed 131:19133–19139. doi: 10.1002/anie.201910563
3. Bozhüyük KAJ, Fleischhacker F, Linck A et al. (2018) De novo design and engineering of non-ribosomal peptide synthetases. Nat Chem 10(3):275-281. doi: 10.1038/nchem.2890
4. Brachmann AO, Joyce SA, Jenke-Kodama H et al. (2007) A type II polyketide synthase is responsible for anthraquinone biosynthesis in *Photorhabdus luminescens*. ChemBioChem 8:1721–1728. doi: 10.1002/cbic.200700300
5. Fu C, Donovan WP, Shikapwashya-Hasser O et al. (2014) Hot Fusion: an efficient method to clone multiple DNA fragments as well as inverted repeats without ligase. PLoS ONE 9:e115318. doi: 10.1371/journal.pone.0115318
6. Gemperlein K, Rachid S, Garcia RO et al. (2014) Polyunsaturated fatty acid biosynthesis in myxobacteria: different PUFA synthases and their product diversity. Chem Sci 5:1733. doi: 10.1039/c3sc53163e
7. Gietz RD, Schiestl RH (2007) Frozen competent yeast cells that can be transformed with high efficiency using the LiAc/SS carrier DNA/PEG method. Nat Protoc 2:1–4. doi: 10.1038/nprot.2007.17
8. Gietz RD, Schiestl RH (2007) High-efficiency yeast transformation using the LiAc/SS carrier DNA/PEG method. Nat Protoc 2:31–34. doi: 10.1038/nprot.2007.13
9. Philippe N, Alcaraz J-P, Coursange E et al. (2004) Improvement of pCVD442, a suicide plasmid for gene allele exchange in bacteria. Plasmid 51:246–255. doi: 10.1016/j.plasmid.2004.02.003
10. Schimming O, Fleischhacker F, Nollmann FI et al. (2014) Yeast homologous recombination cloning leading to the novel peptides ambactin and xenolindicin. ChemBioChem 15:1290–1294. doi: 10.1002/cbic.201402065
11. Simon R, Priefer U, Pühler A (1983) A Broad Host Range Mobilization System for In Vivo Genetic Engineering: Transposon Mutagenesis in Gram Negative Bacteria. Bio/Technology 1:784 EP -. doi: 10.1038/nbt1183-784
12. Thoma S, Schobert M (2009) An improved *Escherichia coli* donor strain for diparental mating. FEMS Microbiol Lett 294:127–132. doi: 10.1111/j.1574-6968.2009.01556.x
13. Tobias NJ, Wolff H, Djahanschiri B et al. (2017) Natural product diversity associated with the nematode symbionts *Photorhabdus* and *Xenorhabdus*. Nat Microbiol 2:1676–1685. doi: 10.1038/s41564-017-0039-9
14. Tobias NJ, Heinrich AK, Eresmann H et al. (2017) *Photorhabdus*-nematode symbiosis is dependent on hfq-mediated regulation of secondary metabolites. Environ Microbiol 19:119–129. doi: 10.1111/1462-2920.13502
15. Wenski SL, Kolbert D, Grammbitter GLC et al. (2019) Fabclavine biosynthesis in *X. szentirmaii*: shortened derivatives and characterization of the thioester reductase FclG and the condensation domain-like protein FclL. J Ind Microbiol Biotechnol. doi: 10.1007/s10295-018-02124-8
16. Wenski SL, Cimen H, Berghaus N et al. (2020) Fabclavine diversity in *Xenorhabdus* bacteria. Beilstein J Org Chem 16:956–965. doi: 10.3762/bjoc.16.84

6.5 Additional results

6.5.1 Material and methods

Strain cultivation

Escherichia coli and *Xenorhabdus* strains were incubated on lysogeny broth (LB) agar plates at RT, 30°C or 37°C (only *E. coli*) depending on the incubation time. Usually, production cultures in LB-, terrific broth- or XPPM-media were inoculated with overnight grown pre-cultures and incubated at 30°C [147]. If appropriate kanamycin [50 µg/ml], chloramphenicol [34 µg/ml], L-arabinose [0.2%] or aminolevulinic acid [50 µg/ml] were added.

Generation of deletion mutants

The generation of deletion mutants was performed as described previously [122,168]: The upstream and downstream flanking regions of the corresponding gene (approximately 1000 bp) were amplified and cloned into the either PCR-amplified or digested vector pEB17 to generate deletion vectors [147]. After the Hot Fusion Assembly *E. coli* S17 or ST18 were transformed with the vectors, followed by conjugation with the corresponding *Xenorhabdus* strain as described previously [169–172].

Hetero- and homologous complementation plasmids

In general, the corresponding backbones pCOLA_ara_tacI or pACYC_ara_tacI were amplified with the oligonucleotides PEB_73 (5'-CTGCAGGAGCTGTTGACAATTA-3') und PEB_74 (5'- GGAATTCCTCCTGTTAGCCCAA-3') (a gift from Edna Bode). The coding region was amplified with the oligonucleotides listed in Table S2, cloned into the vector by Hot fusion assembly and transformed into *E. coli.*

NRPS-engineering plasmids

The pDD-constructs for engineering were based on the complementation plasmids pCOLA_ara_tacI_*fclJ* from *X. szentirmaii*, *X. budapestensis* or *X. hominickii*. Therefore, FclJ was subdivided into a first and a second part upstream of the last XU [49]. The vector and the last part of *fclJ* were together amplified with pEB74_rv and the

oligonucleotides (marked with a star) shown in Table S2. The first part of *fclJ* was amplified (oligonucleotides in Table S2), cloned into the prepared vector by Hot fusion assembly and transformed into *E. coli* (Figure S5).

Transformation of *X. szentirmaii*

Hetero- and homologous complementation as well as NRPS-engineering plasmids were transformed into the corresponding *X. szentirmaii* strain by heatshock transformation by an adapted protocol of Xu *et al*. as described previously [122,173].

Matrix-assisted laser desorption/ ionization mass spectrometry

In general, MALDI-MS experiments were performed as described previously [122,124]. In section 2.1 and 2.2 the conditions are described in detail. Different conditions for the results shown in section 3 are the mass range, which is adapted to expected products, the disuse of an internal calibration and a resolution of 60.000 instead of 100.000 (HR). Moreover, it is noteworthy, that measurements of the same experiments were partially performed on different times, with different sample preparations and/or cultures conditions. Finally, the production cultures of the heterologous FclJ complementation experiments (3.3) were incubated without antibiotics and after harvest they were heated and centrifuged.

Table S1. Used strains. *X. sz.*: *Xenorhabdus szentirmaii* DSM 16338; *X. hom.*: *Xenorhabdus hominickii* DSM 17903; *X. bov.*: *Xenorhabdus bovienii* SS-2004; *X. bud.*: *Xenorhabdus budapestensis* DSM 16342; *E. coli*::*mtaA*: *Escherichia coli* DH10B *mtaA*.[#]The strain *X. sz.* Δ*fclIJ* pDD5 was generated in cooperation with Janik Kranz.

Strain	Plasmid(s)	Reference section	Origin
X. sz. Δ*fclD*	-	Heterologous complementation of FclD	[122]
X. sz. Δ*fclD*	pCOLA_ara_tacI_*fclD X. sz.*	Heterologous complementation of FclD	This work
X. sz. Δ*fclD*	pCOLA_ara_tacI_*fclD X. bud.*	Heterologous complementation of FclD	This work
X. sz. Δ*fclD*	pCOLA_ara_tacI_*fclD X. hom.*	Heterologous complementation of FclD	This work
X. sz. Δ*fclD*	pCOLA_ara_tacI_*fclD X. bov.*	Heterologous complementation of FclD	This work
X. sz. Δ*fclD*	pCOLA_ara_tacI_*fclD* KJ12.1	Heterologous complementation of FclD	This work
X. sz. Δ*fclK*	-	Heterologous complementation of FclK	[122]
X. sz. Δ*fclK*	pCOLA_ara_tacI_*fclK X. sz.*	Heterologous complementation of FclK	This work
X. sz. Δ*fclK*	pCOLA_ara_tacI_*fclK* KJ12.1	Heterologous complementation of FclK	This work
X. sz. Δ*fclK*	pACYC_ara_tacI_*fclK X. bud.*	Heterologous complementation of FclK	This work
X. sz. Δ*fclK*	pACYC_ara_tacI_*fclK X. hom.*	Heterologous complementation of FclK	This work
X. sz. Δ*fclJ*	-	Heterologous complementation of FclJ	[122]
X. sz. Δ*fclJ*	pCOLA_ara_tacI_*fclJ X. sz.*	Heterologous complementation of FclJ	This work
X. sz. Δ*fclJ*	pCOLA_ara_tacI_*fclJ X. bud.*	Heterologous complementation of FclJ	This work
X. sz. Δ*fclJ*	pCOLA_ara_tacI_*fclJ X. hom.*	Heterologous complementation of FclJ	This work
X. sz. Δ*fclIJ*	-	NRPS engineering	This work
X. sz. Δ*fclIJ*	pCOLA_ara_tacI_*fclJ X. bud.*	NRPS engineering	This work
X. sz. Δ*fclIJ*	pCOLA_ara_tacI_*fclJ X. hom.*	NRPS engineering	This work
X. sz. Δ*fclIJ*	pCOLA_ara_tacI_*fclJ X. sz.*	NRPS engineering	This work
X. sz. Δ*fclIJ*	pDD3	NRPS engineering	This work
X. sz. Δ*fclIJ*	pDD4	NRPS engineering	This work
X. sz. Δ*fclIJ*	pDD5	NRPS engineering	This work[#]
X. sz. Δ*fclIJ*	pDD6	NRPS engineering	This work
X. sz. Δ*fclIJ*	pDD7	NRPS engineering	This work
X. sz. Δ*fclIJ*	pDD8	NRPS engineering	This work

Table S2. Used oligonucleotides. *X. sz.*: *Xenorhabdus szentirmaii* DSM 16338; *X. hom.*: *Xenorhabdus hominickii* DSM 17903; *X. bov.*: *Xenorhabdus bovienii* SS-2004; *X. bud.*: *Xenorhabdus budapestensis* DSM 16342. Oligonucleotides marked with a star were used in combination with pEB74_rv. Used templates were genomic DNA from *X. szentirmaii* DSM 16338, *X. budapestensis* DSM 16342, KJ12.1, *X. hominickii* DSM 17903 and *X. bovienii* SS-2004 as well as the plasmids pCOLA_ara_tacI_*fclJ* originated from *X. szentirmaii*, *X. budapestensis* or *X. hominickii*. [#]The plasmid pCOLA_ara_tacI_*fclK* KJ12.1 was a gift by Natalie Berghaus.

Construct	Primer	Sequence 5'-3'
pCOLA_ara_tacI_*fclD* *X. sz.*	SW436_XsD_KoL_fw	CCATACCCGTTTTTTTGGGCTAACAGGAGGAATTCCATGGAACATATTGCAATTGTTGGTGTTGG
	SW437_XsD_KoL_rv	CGAGCCGATGATTAATTGTCAACAGCTCCTGCAGTCATATTGAAGCTTCCTGTTTCTGCTCTGC
pCOLA_ara_tacI_*fclD* *X. bud.*	SW543_Xbud_KoD_fw	CCATACCCGTTTTTTTGGGCTAACAGGAGGAATTCCATGGAACATATTGCAATTATTGGGGTCGG
	SW544_Xbud_KoD_rv	CGAGCCGATGATTAATTGTCAACAGCTCCTGCAGTCATTTTGTGGCGTCCTGTTCCAATTCTG
pCOLA_ara_tacI_*fclD* *X. hom.*	SW545_Xhom_KoD_fw	CCATACCCGTTTTTTTGGGCTAACAGGAGGAATTCCATGGAACATATTGCCATTGTTGGGATGG
	SW546_Xhom_KoD_rv	CGAGCCGATGATTAATTGTCAACAGCTCCTGCAGTCATTTTGCTTCTTCCTGTTTCAGTTCTGTCG
pCOLA_ara_tacI_*fclD* *X. bov.*	SW549_Xbov_KoD_fw	CCATACCCGTTTTTTTGGGCTAACAGGAGGAATTCCATGGAAAATATTGCAATTATTGGGATGGGG
	SW550_Xbov_KoD_rv	CGAGCCGATGATTAATTGTCAACAGCTCCTGCAGTCATTTTAAAGCTTCCTGTTTCAGTTCTGC
pCOLA_ara_tacI_*fclD* KJ12.1	SW547_KJ12_KoD_fw	CCATACCCGTTTTTTTGGGCTAACAGGAGGAATTCCATGGAACATATTGCTATTGTTGGAGTCGG
	SW548_KJ12_KoD_rv	CGAGCCGATGATTAATTGTCAACAGCTCCTGCAGTCATTTTGCGGCTTCCTGTTCCG
pCOLA_ara_tacI_*fclK* *X. sz.*	SW343_Xsz_Ko_fw	GTTTTTTTGGGCTAACAGGAGGAATTCCATGAATAATACCGATGTCAATAATACCC
	SW344_Xsz_Ko_rv	GATGATTAATTGTCAACAGCTCCTGCAGTCATTGATCCCCCTTCCG
[#]pCOLA_ara_tacI_*fclK* KJ12.1	NB21_KJ_K_fw	CCATACCCGTTTTTTTGGGCTAACAGGAGGAATTCCATGAATAACACCGATGGTAATAACG
	NB22_KJ_k_rev	CGAGCCGATGATTAATTGTCAACAGCTCCTGCAGTCATCGCCTTTCCTCCG
pACYC_ara_tacI_*fclK* *X. bud.*	SW539_K_Xbud_fw	CCATACCCGTTTTTTTGGGCTAACAGGAGGAATTCCATGAATAACACCGAAGTTAATAAAGTTCAGG
	SW540_K_Xbud_rv	CGAGCCGATGATTAATTGTCAACAGCTCCTGCAGTCATTTCCTTCCCTCCGG
pACYC_ara_tacI_*fclK* *X. hom.*	SW535_K_Xhom_fw	CCATACCCGTTTTTTTGGGCTAACAGGAGGAATTCCATGAACAATGCAGAGTTAAATAAAGTCCAAGC
	SW536_K_Xhom_rv	CGAGCCGATGATTAATTGTCAACAGCTCCTGCAGTCATTTTCCCCCCTCCGGC
pCOLA_ara_tacI_*fclJ* *X. sz.*	SW440_XsJ_KoL_fw	CCATACCCGTTTTTTTGGGCTAACAGGAGGAATTCCATGCAGCAAGATACATTTAAATTTAAAGCATCCC
	SW441_XsJ_KoL_rv	CGAGCCGATGATTAATTGTCAACAGCTCCTGCAGTTACCCTTTGTGCTGCATTTTTTTCTGC
pCOLA_ara_tacI_*fclJ* *X. bud.*	SW478_XbudJ_fw	CCATACCCGTTTTTTTGGGCTAACAGGAGGAATTCCATGCAGGAAAATACATTTCAATTTAAGGC
	SW479_XbudJ_rv	CGAGCCGATGATTAATTGTCAACAGCTCCTGCAGCTATTCCTTTGCCTGTTTCTGCTGC
pCOLA_ara_tacI_*fclJ* *X. hom.*	SW480_XhomJ_fw	CCATACCCGTTTTTTTGGGCTAACAGGAGGAATTCCATGCAGGAAAACACATATAAATTCAAAGC
	SW481_Xhom_rv	CGAGCCGATGATTAATTGTCAACAGCTCCTGCAGTCATTGTTGCTGCATTTTTTTCTGC

Table S2 (continued). Used oligonucleotides. *X. sz.*: *Xenorhabdus szentirmaii* DSM 16338; *X. hom.*: *Xenorhabdus hominickii* DSM 17903; *X. bov.*: *Xenorhabdus bovienii* SS-2004; *X. bud.*: *Xenorhabdus budapestensis* DSM 16342. Oligonucleotides marked with a star were used in combination with pEB74_rv. Used templates were genomic DNA from *X. szentirmaii* DSM 16338, *X. budapestensis* DSM 16342, KJ12.1, *X. hominickii* DSM 17903 and *X. bovienii* SS-2004 as well as the plasmids pCOLA_ara_tacI_*fclJ* originated from *X. szentirmaii*, *X. budapestensis* or *X. hominickii*. #The plasmid pCOLA_ara_tacI_*fclK* KJ12.1 was a gift by Natalie Berghaus.

Construct	Primer	Sequence 5'-3'
pDD3	SW491	CCATACCCGTTTTTTTGGGCTAACAGGAGGAATTCCATGCAGGAAAATACATTTCAATTTAAGGC
	SW492	CCGGATGCCCCCTGACTGAAACTTTCAATCTTCCGTTGTTGGATTATCG
	SW493*	AACAACGGAAGATTGAAAGTTTCAGTCAGGGGGCATCCGG
pDD4	SW494	CCATACCCGTTTTTTTGGGCTAACAGGAGGAATTCCATGCAGGAAAACACATATAAATTCAAAGC
	SW495	CCGGATGCCCCCTGACTGAAACTCTCAATCAGCCGTTGTTGTG
	SW496*	AACAACGGCTGATTGAGAGTTTCAGTCAGGGGGCATCC
pDD5	SW497	CCATACCCGTTTTTTTGGGCTAACAGGAGGAATTCCATGCAGCAAGATACATTTAAATTTAAAGCATCCC
	SW498	CCCGGCGCTCCCTGATTGAAGGCTTCAATTTTCCGCTGCTGGG
	SW499*	AGCAGCGGAAAATTGAAGCCTTCAATCAGGGAGCGCCG
pDD6	SW500	CCATACCCGTTTTTTTGGGCTAACAGGAGGAATTCCATGCAGGAAAACACATATAAATTCAAAGC
	SW501	CCCGGCGCTCCCTGATTGAAACTCTCAATCAGCCGTTGTTGTG
	SW502/514*	AACAACGGCTGATTGAGAGTTTCAATCAGGGAGCGCCGG
pDD7	SW503	CCATACCCGTTTTTTTGGGCTAACAGGAGGAATTCCATGCAGCAAGATACATTTAAATTTAAAGCATCCC
	SW504	CCGGCTTCGCCATGACTGAAGGCTTCAATTTTCCGCTGCTGG
	SW505*	AGCAGCGGAAAATTGAAGCCTTCAGTCATGGCGAAGCCG
pDD8	SW506	CCATACCCGTTTTTTTGGGCTAACAGGAGGAATTCCATGCAGGAAAATACATTTCAATTTAAGGCATCCC
	SW507	CCGGCTTCGCCATGACTGAAACTTTCAATCTTCCGTTGTTGGATTATCGG
	SW508/509*	AACAACGGAAGATTGAAAGTTTCAGTCATGGCGAAGCCG
pEB17_Δ*fclJ* *X. szentirmaii*	SW112_I_LF_fw	CGATCCTCTAGAGTCGACCTGCAGCTATTTCAATTACTTGATTGAATGCGG [122]
	SW485_XszIJ_rv	AGCTCTGTTCCCTTTTCCCATAGCCATCATTCCTTCAATAAGAATTTATTACC
	SW486_XszIJ_fw	TATTGAAGGAATGATGGCTATGGGAAAAGGGAACAGAGC
	SW390_XszJ_RF_rv	GAGAGCTCAGATCTACGCGTTTCATATGGGTCGCTGTACCGTGTGC [122]

6.5.2 Supplementary informations

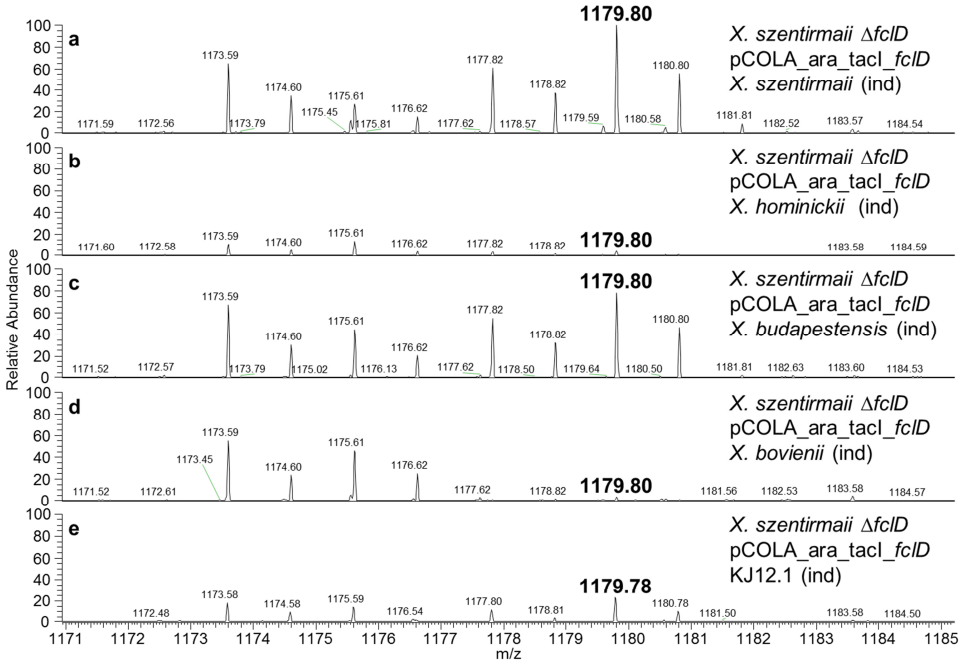

Figure S1. Heterologous complementation of FclD in *X. szentirmaii* Δ*fclD*. Induced and non-induced production cultures of the complementation mutants were analyzed for signals with m/z 1179.78 (m = 3), 1306.92 (m = 4) and 1434.05 (m = 5) [124].

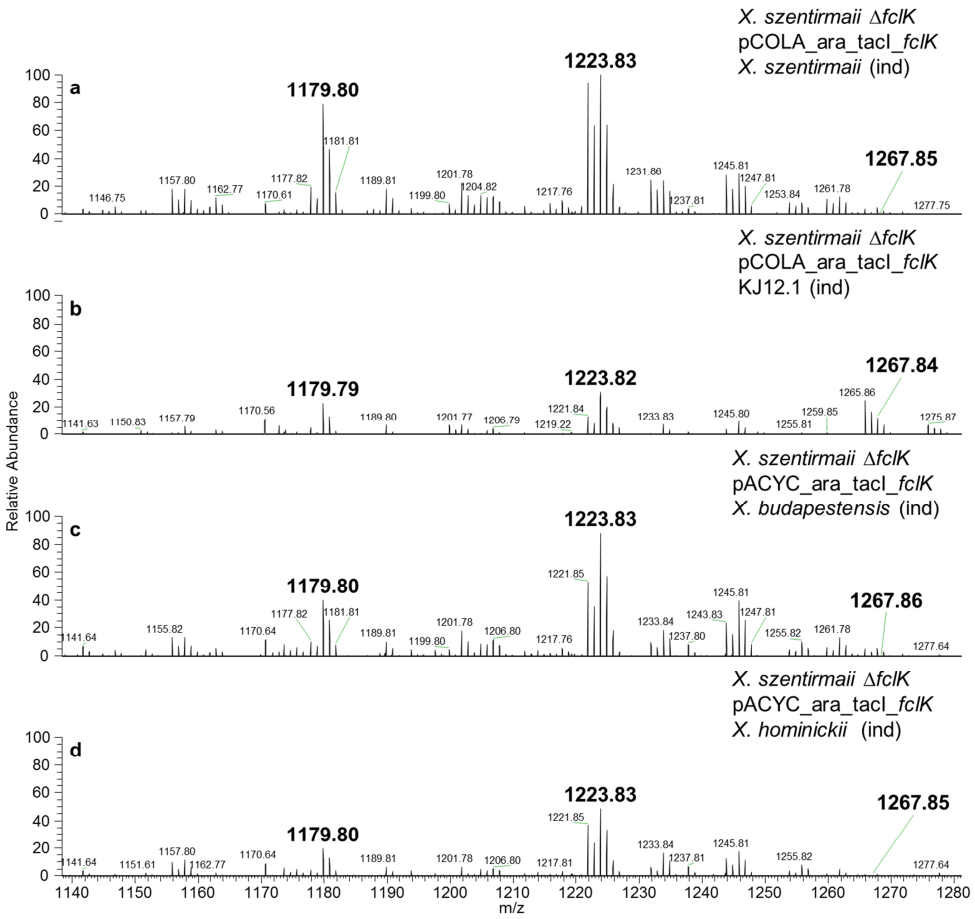

Figure S2. Heterologous complementation of FclK in *X. szentirmaii* Δ*fclK*. Induced and non-induced production cultures of the complementation mutants were analyzed for signals with m/z 1179.78 (n = 1), 1223.81 (n = 2) and 1267.83 (n = 3) [124].

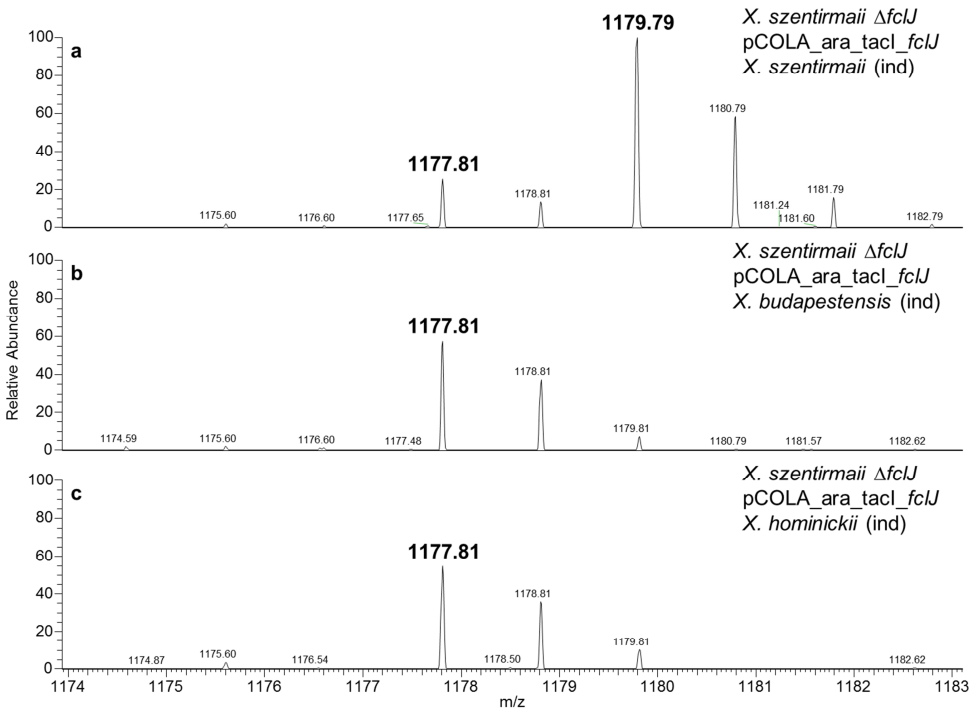

Figure S3. Heterologous complementation of FclJ in *X. szentirmaii* Δ*fclJ*. Induced and non-induced production cultures of the complementation mutants were analyzed for signals with m/z 1175.79 (proline-derivate), 1177.80 (valine-derivate) and 1179.78 (threonine-derivate) [124].

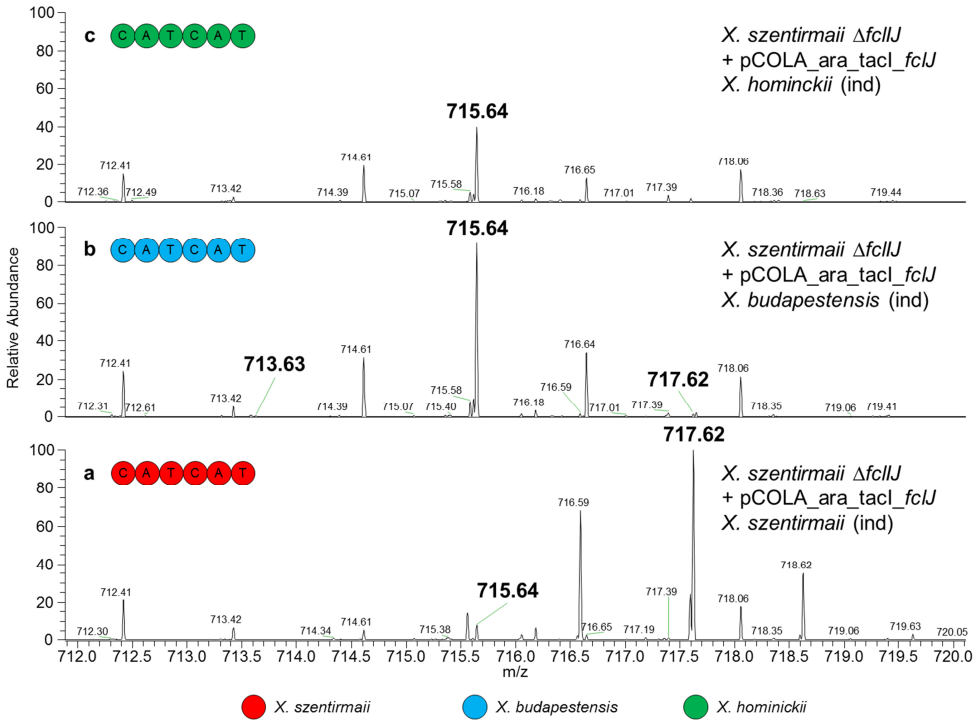

Figure S4. Heterologous complementation of FclJ in *X. szentirmaii* Δ*fclIJ*. Induced and non-induced production cultures of the complementation mutants were analyzed for signals with m/z 713.63 (proline-derivate), 715.64 (valine-derivate) and 717.62 (threonine-derivate) [124].

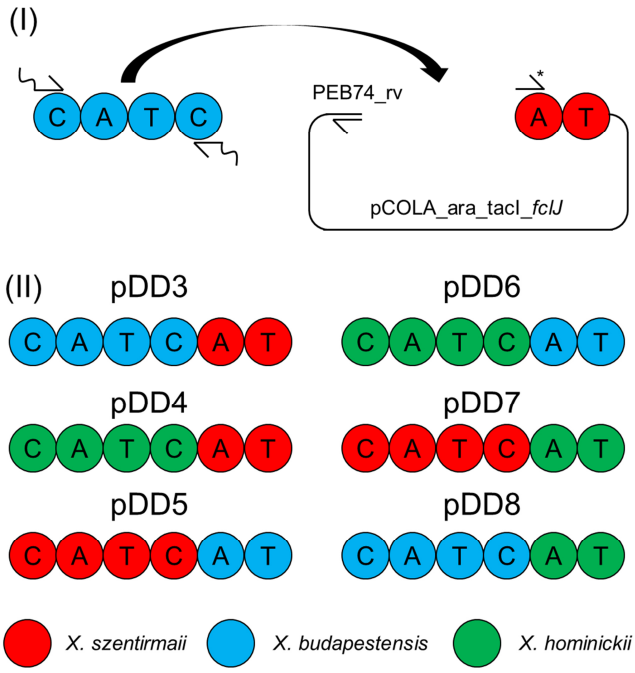

Figure S5. Construction of the NRPS-engineering constructs. (I) General cloning strategy. (II) Identities of the chimeric pDD-constructs.

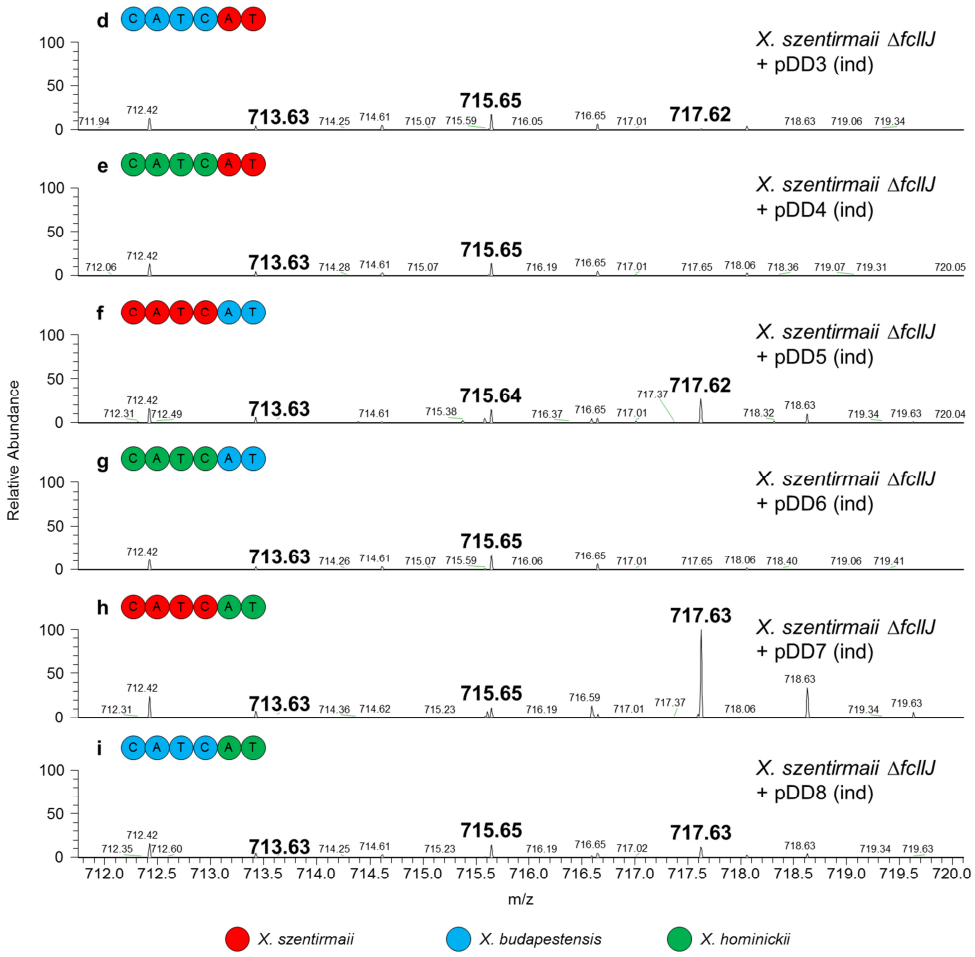

Figure S6. Chimeric NRPS constructs in *X. szentirmaii* Δ*fclIJ* mutant and resulting product spectra.Induced and non-induced production cultures of the complementation mutants were analyzed for signals with m/z 713.63 (proline-derivate), 715.64 (valine-derivate) and 717.62 (threonine-derivate) [124].

7 List of publications and manuscripts

Part of this thesis:

S.L. Wenski, D. Kolbert, G.L.C. Grammbitter, H.B. Bode, Fabclavine biosynthesis in *X. szentirmaii*: shortened derivatives and characterization of the thioester reductase FclG and the condensation domain-like protein FclL, *Journal of Industrial Microbiology & Biotechnology* 46 (**2019**) 565–572. https://doi.org/10.1007/s10295-018-02124-8

S.L. Wenski, H. Cimen, N. Berghaus, S.W. Fuchs, S. Hazir, H.B. Bode, Fabclavine diversity in *Xenorhabdus* bacteria, *Beilstein Journal of Organic Chemistry* 16 (**2020**) 956–965. https://doi.org/10.3762/bjoc.16.84

H. Donmez Ozkan, H. Cimen, D. Ulug, S. Wenski, S. Yigit Ozer, M. Telli, N. Aydin, H.B. Bode, S. Hazir, Nematode-Associated Bacteria: Production of Antimicrobial Agent as a Presumptive Nominee for Curing Endodontic Infections Caused by *Enterococcus faecalis*, *Frontiers in Microbiology* 10 (**2019**) 2672. https://doi.org/10.3389/fmicb.2019.02672

S.L. Wenski, N. Berghaus, N. Keller, H.B. Bode, Structure and biosynthesis of deoxy-polyamine in *X. bovienii* (submitted manuscript)

Not part of this thesis:

E. Bode, A.K. Heinrich, M. Hirschmann, D. Abebew, Y.-N. Shi, T.D. Vo, *et al*., Promoter Activation in Δ*hfq* Mutants as an Efficient Tool for Specialized Metabolite Production Enabling Direct Bioactivity Testing, *Angewandte Chemie International Edition* 58 (**2019**) 18957–18963. https://doi.org/10.1002/anie.201910563

8 Conference participation

Oral presentation

“Fabclavine biosynthesis: multiple mechanisms for natural product diversification in a peptide, polyketide, polyamine hybrid“
VAAM Workshop 31.08.-02.09.2018 Frankfurt am Main, Germany

Poster presentation

“*In vitro* characterization of the thioester reductase FclG in the fabclavine biosynthesis”
VAAM Jahrestagung 15.-18.04.2018 Wolfsburg, Germany

“Fabclavine Biosynthesis: Multiple mechanisms for natural product diversification in a peptide, polyketide, polyamine hybrid”
3rd European Conference on Natural Products (ECNP) 02.–05.09.2018 Frankfurt am Main, Germany

“Fabclavine derivatives in Xenorhabdus: How to create chemical diversity”
VAAM Workshop 15.-17.09.2019 Jena, Germany

9 Danksagung

Ein herzlicher Dank geht an meinen Doktorvater Prof. Dr. Helge B. Bode, der mir sowohl während meiner Masterthesis als auch Doktorthesis das Vertrauen schenkte. Dabei ermöglichte er mir einerseits viele Freiheiten, um meine wissenschaftliche Neugier umzusetzen, andererseits stand er mir immer zur Seite bei Rückschlägen und Problemen.

Darüber hinaus bedanke ich mich bei Prof. Dr. Eugen Proschak für die Übernahme meines Zweitgutachtens.

Ich bedanke mich bei unseren Kooperationspartnern Prof. Dr. Selcuk Hazir und Dr. Harun Cimen für die erfolgreiche Zusammenarbeit, sowie bei Prof. Dr. Michael Karas für die Nutzung des MALDI-Massenspektrometers und bei Matthias Brandl für zahlreiche Hilfestellungen.

Überaus dankbar bin ich Dr. Kenan Bozhüyük, Dr. Carsten Kegler, Dr. Gina Grammbitter und Svenja Badeck für das Korrekturlesen meiner Arbeit.

Eine tolle Erfahrung für mich war die Betreuung von Studenten und Studentinnen, was mir immer sehr viel Spaß gemacht hat, da ich nicht nur gelehrt habe, sondern auch viel gelernt habe. Besonders hervorzuheben sind hier Natalie Berghaus, Nadine Keller und Alexander Rill.

Der ganzen Arbeitsgruppe danke ich für das tolle Arbeitsklima und die produktive Atmosphäre. Mit Freude erinnere ich mich an das legendäre 2019er-Team „onlyhereforthebeer“-Volleyballteam und danke allen Mitgliedern sowie unseren beiden grandiosen Fans, ohne die der finale Triumph niemals möglich gewesen wäre.

Besonders bedanke ich mich bei Svenja Simonyi und Lukas Kreling, welche mir in schwierigen Zeiten der Promotion zur Seite gestanden haben. Vielen Dank auch an Andreas Tietze und Nick Neubacher für die gemeinsame Leidenszeit des Schreibens.

Meinen Eltern und meiner Lebensgefährtin Svenja Badeck danke ich für die jahrelange und bedingungslose Unterstützung während meines Studiums und meiner Doktorarbeit. Besonders hervorzuheben ist hier das „Home Office“ mit Svenja, was zumindest zu einer tollen Masterarbeit geführt hat.

10 Erklärung und Versicherung

Erklärung

Ich erkläre hiermit, dass ich mich bisher keiner Doktorprüfung im Mathematisch-Naturwissenschaftlichen Bereich unterzogen habe.

Frankfurt am Main, den ….....

Sebastian L. Wenski

Versicherung

Ich erkläre hiermit, dass ich die vorgelegte Dissertation über “Understanding the biosynthesis of fabclavines in entomopathogenic bacteria“ selbständig angefertigt und mich anderer Hilfsmittel als der in ihr angegebenen nicht bedient habe, insbesondere, dass alle Entlehnungen aus anderen Schriften mit Angabe der betreffenden Schrift gekennzeichnet sind.
Ich versichere, die Grundsätze der guten wissenschaftlichen Praxis beachtet, und nicht die Hilfe einer kommerziellen Promotionsvermittlung in Anspruch genommen zu haben.

Frankfurt am Main, den ….....

Sebastian L. Wenski

11 Curriculum vitae

Personal data

Name:	Sebastian Leonhard Wenski
Date of birth:	18.11.1990
Place of birth:	Frankfurt am Main
Nationality:	Germany
Contact:	Elsa-Brandström-Straße 13-15 65830 Kriftel Germany +49 152 34363199; sebastian_wenski@web.de

Professional experience

Since 11/2016	**Scientific assistant** and doctoral candidate in the working group Bode (Institute for molecular bioscience) at the Goethe-Universität Frankfurt am Main, Germany Supervisor: Prof. Dr. Helge B. Bode
11/2015-01/2016	**Internship** at AB Enzymes GmbH Darmstadt, Germany (Research & Development - Molecular biology) Supervisor: Dr. Thomas Haarmann
03/2015	**Working student** at Infraserv GmbH und Co. Höchst KG Frankfurt am Main, Germany (Microbiological analysis)

Education

10/2014-09/2016	**Master of Science** (Molecular biotechnology) at the Goethe-Universität Frankfurt am Main, Germany. Master thesis in the working group of Prof. Dr. Helge B. Bode.
04/2011-09/2014	**Bachelor of Science** (Molecular biology) at the Johannes Gutenberg-Universität in Mainz, Germany. Bachelor thesis in the working group of Prof. Dr. Harald Paulsen.
08/2010-01/2011	**Community service** at the GPR clinical center in Rüsselsheim, Germany
06/2010	**Abitur** at the Graf-Stauffenberg grammar school in Flörsheim am Main, Germany